Reliability and Maintenance of Structures under Severe Uncertainty

Thesis submitted in accordance

with the requirements of the University of Liverpool

for the degree of Doctor in Philosophy

by

David Akinyiwola Opeyemi

October 2016

Acknowledgements

This research work has been made possible with the support of the following individuals.

First and foremost, my profound gratitude, credit and acknowledgement go to my whole supervisory team: Dr. Edoardo Patelli and Professor Michael Beer. Their inspirational teaching, advise and motivational leadership role has been of immense support both in my personal life and in technical aspects which has given me impetus in researching on the area of risk and uncertainty in engineering.

Professor Sviatoslav A. Timashev offered me a collaborative opportunity, also as a foreign scholar to Ural Federal University through the friendship and connection of Professor Michael Beer. I am very grateful for his friendship, consultative advice and gains from his vast experience. His team in Russian Academy of Sciences, and Ural Federal University: Dr. Anna V. Bushinskaya and all the engineers are highly appreciated.

I am particularly grateful for the sponsorship received from Rufus Giwa Polytechnic (formerly Ondo State Polytechnic) Owo, and the Tertiary Education Trust Fund (TETFund) of the Federal Republic of Nigeria.

To my research group colleagues in the Institute for Risk and Uncertainty, School of Engineering, University of Liverpool; many thanks for the good atmosphere you afforded me both at the office and outside the office, and for the technical support. This has been a great encouragement for me.

Kudos to all my friends and family members (Wife – Blessing & Kids – Daniel, Joy, Favour and AanuOluwa), whose sacrifices, support and financial contribution have brought this great success.

Finally, unto the only wise God, who is certain and there is no risk in Him at all – nothing is certain except God and His Words!

David Opeyemi
Liverpool England, October 2016

Abstract

Reliability and Maintenance of Structures under Severe Uncertainty

By

David Akinyiwola Opeyemi

Maintenance of structures and infrastructures is of increasing importance in order to reach acceptable level of safety despite the unavoidable uncertainty, and the economic efforts have to be reasonable. These two goals represent competing objectives in an overall optimization of very complex system and structure, which involve significant uncertainties. In fact, all civil engineering structures and engineering systems are subjected to degradation by fatigue cracks and corrosion due to varying loads. When the cracks propagate or corrosion grows, the structural system accumulates damage thereby leading to serviceability loss and eventual collapse. These failures can be prevented by appropriate maintenance scheduling and repair, even in the presence of uncertainties of various nature and scale, leading to a reduction in fluctuations and changes of structural and environmental parameters and conditions in the models describing the processes involved in fatigue cracks and corrosion growth.

Degradation models used to predict the future state of components often involve simplifications and assumptions to compensate a lack of data, imprecision and vagueness, which cannot be ignored. To overcome these issues, the imprecise probabilities framework and markovian approach are proposed for performing reliability analysis, decision-making, and risk-based design and maintenance. It is shown how these approaches can improve the current practise based on models: B31G, Modified B31G, DNV-101 and Shell-92 failure pressure models. The reliability assessment is performed by taking into account the simultaneous action of many natural and technological loads. These loads are random by nature and can be adequately described only by stochastic processes; which are not performed due to lack of valid calculation methods. This methodology has been applied to study the reliability of arctic pipeline infrastructure.

Finally, a robust and efficient probabilistic framework for optimal inspection and maintenance schedule selection for corroded pipelines and fatigue cracks in bridges is presented. Optimal solution is obtained through only one reliability assessment removing huge computational cost of the reliability-base optimization approach and making the analysis of industrial size problem feasible.

List of Figures

List of Tables

List of Notations

The following list defines the main symbols appearing in the thesis.

a = crack length

a_0 = initial crack length

cdf = cumulative density function

CoV = coefficient of variation

C_T, C_I, C_R and C_F = expected total cost of operation, expected costs of inspection, repairs and failure respectively.

D = Diameter of pipe

d = depth of corrosion defect

da/dN = crack growth rate

E = Young's modulus

e = quality of inspection

$f_{X|\Theta}(X|\theta)$= conditional probability density function of X for a given θ

$f_{\Theta}(\theta)$ = joint probability density function of θ

$\overline{F}(x)$ = upper bound probability

$\underline{F}(x)$ = lower bound probability

$G(x)$ = limit state function

k = stress intensity factor

l = longitudinal length of corrosion defect

M = Folias' factor

$MAOP$ = Maximum Allowable Operating Pressure

N_I = number of inspection

O_p = Operating pressure

P_f = Probability of failure

p_f = failure pressure

pdf = probability density function

$P_{ij}(t)$ = transition probability of Markov process

PoD = probability of detection

r = radius of pipe

R = resistance variables

$R(t)$ = Reliability function

S = load variables

w_t = pipe wall thickness

x = basic random variables

t = time

v_d = radial corrosion rate

v_l = longitudinal corrosion rate

α = linear expansion coefficient of metal

β = reliability index

Φ = standard normal cumulative distribution function

λ_i = intensities of Birth

μ_i = intensities of Death

σ_f = flow stress

σ_y = material yield stress (SMYS)

σ_u = ultimate tensile strength (UTS)

χ = longitudinal curvature of bent pipe

Table of Contents

1. Introduction

Civil engineering structures and systems such as bridges, pipelines, aircrafts, etc. are subject to degradation by fatigue cracks and corrosion growth due to varying loads and impacts, thereby leading to serviceability loss or eventual collapse. These failures can be prevented by appropriate preventive maintenance actions and the effect of failure can be mitigated by corrective maintenances (i.e. repairs). Uncertainties of various nature and scale must be considered to ensure the faultless life of these structures and systems despite fluctuations and changes of structural and environmental parameters and conditions. These uncertainties must also be reduced in the models describing the processes involved in fatigue cracks and corrosion growth. Concise information on the actual state of the structure will increase the likelihood of meaningful application of repair activities.

Maintenance of structures and infrastructures assures acceptable level of safety but the economic efforts of maintenance have to be reasonable. These two goals are competing objectives in an overall optimization strategy. In addition, the optimization involves significant uncertainties.

Robust maintenance strategy for these engineering structures and systems subjected to uncertainty by fatigue must be considered. This can be achieved using reliability metrics redefined within the framework of imprecise probabilities in order to treat all forms of uncertainty: variability, imprecision, incompleteness, vagueness, ambiguity, dubiety, etc.

1.1 Background and Research Significance

The incentive to study reliability and maintenance of structures is very high as it plays an essential and integral role in preserving the intended load carrying capacity of the structures and ensures correct performance, continued safety throughout its service life and aesthetics. This is to be performed in a systematic way because it

has been proved to be the most economical. Without timely maintenance scheduling activities the structure will likely require more costly repairs compared to when it is properly maintained. The initial step towards good maintenance culture should be that all structures be designed and constructed with consideration of both capital expenditure and predictable maintenance cost. However, the reliability estimation and maintenance of engineered structures includes uncertainty and imprecision in parameters with different types of models. For instance, fatigue cracks and corrosion deterioration phenomena on structures are highly stochastic in nature. Uncertainty, variations and imprecision regarding the structural reliability and behaviour of the structures must be represented appropriately based on the available underlying empirical information. Then probabilistic models and stochastic simulation techniques need to be employed to properly capture the variability of the predicted output of interest.

The necessity of performing proper maintenance strategy is shown by the huge number of structures that requires maintenance. As an example, over two hundred million trips as daily routine are taken across deficient bridges in the US nation's 102 largest metropolitan regions. In total, one out of nine of the bridges are rated as structurally deficient, while the average age of the nation's 607,380 bridges is currently 42 years. The Federal Highway Administration (FHWA) estimates that to eliminate the nation's bridge deficient backlog by 2028, annual investment of $20.5 billion is needed, while only $12.8 billion is being spent currently. The challenge for federal, state, and local governments is to increase bridge investments by $8 billion annually to address the identified $76 billion in needs for deficient bridges across the United States (ASCE 2013 Report Card, 2014).

In a survey conducted by Committee on Fatigue and Fracture Reliability of the American Society of Civil Engineers (ASCE) in 1982, it has been discovered that the main causes of failure in steel structures is fatigue. A comprehensive study on the cost of fracture in the United States as reported indicated a $119 billion (in 1982 US Dollars) cost occurred in 1978, which is about 4% of the gross national product (GNP). This investigation further emphasized that the cost could be significantly

reduced by using proper and current fatigue design technology. Based on an independent study by Battelle, 1982; between 8 to 9 out of 10 structural failures occur due to fatigue. This results in an estimated annual cost of $1.5 Billion in the United States alone.

Considerable costs in terms of life, time and money are the direct implications of fatigue cracks in metallic structures. For example, 75 out of 100 of the US Air Force C-141 fleet presently are flying under flight restrictions owning to the effects of fatigue cracks, in which correction to the problem will come to a cost in the tune of millions USD in addition to the many years required for completion (Ramulu and Kobayashi, 2012).

Out of the 607,320 bridges in the USA about 34% are made out of steel (Bader, 2008; FOCUS, 2007). Field inspections of steel bridges found cracks, corrosion, delaminating steel, pack rust, and sectional loss. The numbers of deficient bridges for all the 50 states in US as of December 2007 are shown in Table 1.1.

Table 1.1: Deficient bridges across the entire United States (Bader, 2008)

	US Bridges	Structurally Deficient	Functional Obsolete	Total	% Deficient
National Highway System	116,145	6,160	17,149	23,309	20%
Non-National Highway System	483,621	66,364	62,643	129,007	27%
US Bridges	599,766	72,524	79,792	152,316	25%
% Deficient		12%	13%	25%	

Likewise, on corrosion, Velazquez et al., 2013 and the World Corrosion Organization (WCO) reports that the annual cost of corrosion worldwide is about 3 - 4% of the world's gross national product (GNP). For instance, in the case of the USA 1.5 million kilometres of oil and gas transportation pipelines the cost can exceed over $8.6 billion/year. Oil and gas companies, on the average, use 6% of their annual income to combat corrosion; according to African Review of Business and Technology, (ARBT, 2016). Other studies done in China, Japan, the United Kingdom, and Venezuela were similar to United States of America, and even more costly,

leading to an estimated worldwide direct cost exceeding $1.8 trillion (Schmitt et al., 2009).

Findings from a funded research (NACE, 2002) by the USA government as analysed on a number of sectors in industrial economy category, and annual corrosion cost to the Infrastructure sector are shown in Figures 1.1 and 1.2 respectively. Detailed analysis, released in 2002 by NACE International, was undertaken to establish costs within each sector and to calculate the cost to the US economy, resulting in the figure of 3.1%, which NACE calculates is applicable to all developed economies. Its applicability to some developed economies is shown in Table 1.2.

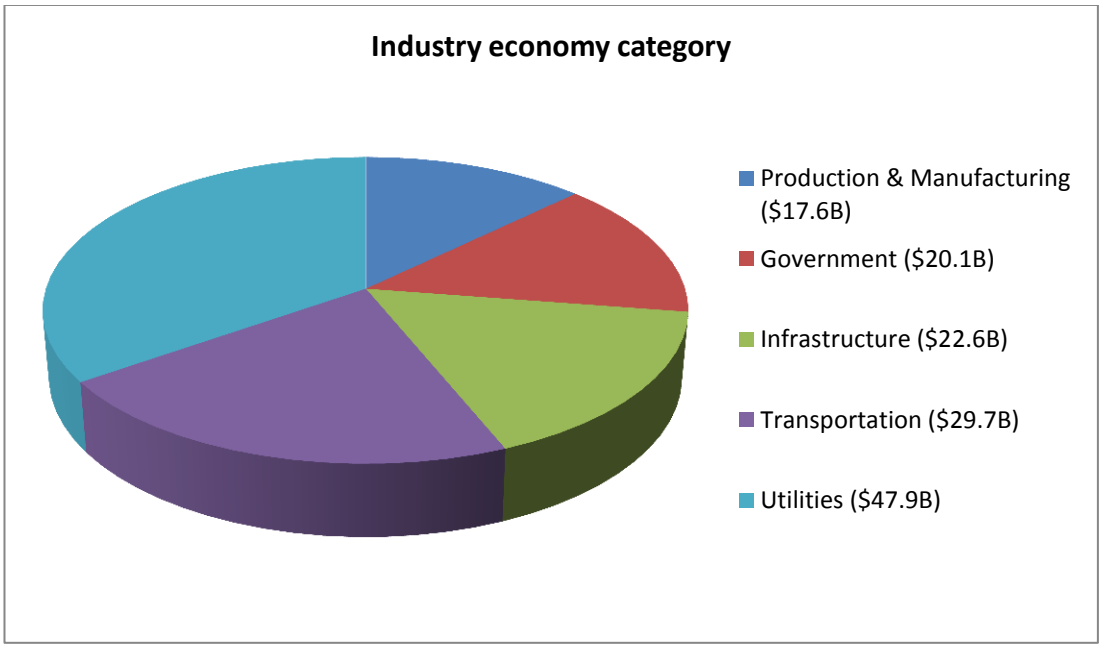

Figure 1.1: Corrosion cost in the industrial economy sectors of USA (see NACE, 2002)

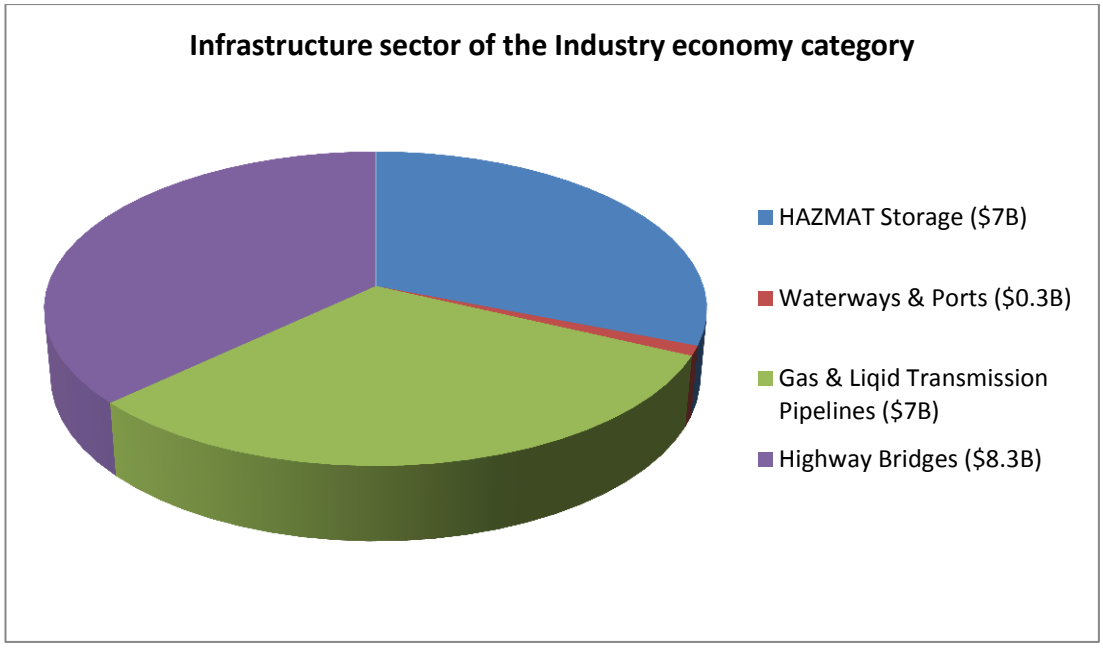

Figure 1.2: Annual corrosion cost to the Infrastructure sector in USA (Schmitt et al., 2009)

Table 1.2: Corrosion cost for industrial economy – see NACE International (NACE, 2002).

Country	Year	GDP (USD Billion)	Annual Corrosion Cost (USD Billion)
UK	2008	2,279	70.6
USA	2007	13,840	429
Australia	2009	920	70.6
Malaysia	2009	207.4	6.7

The costs on fatigue and fracture, and corrosion could be reduced significantly by proper design and maintenance. Battelle, 1982 states that structural failures as a result of fatigue mechanism could be reduced by 29% applying current fatigue technology (design and maintenance).

Structural reliability is related to safety of structures through design before service and through maintenance during service. For safety requirements of structures not to be compromised, the description of the objectives in an overall optimization of maintenance problem must reflect appropriately its nature and physics, and needs to be reasonably conservative, due to inherent uncertainties involved in the

maintenance activities. The deterministic description of the problem will definitely not lead to an acceptable level of safety that is to be ensured. Likewise, the effects of uncertainties not realistically accounted for will result in an unexpected maintenance costs that may sometimes equate or exceed the cost of new structure. All uncertainties inherent in maintenance scheduling activities of structures and infrastructures must be processed with numerically efficient techniques and be considered in a realistic manner to achieve proper quantification of the uncertainties.

1.1.1 Problem Statement

In solving engineering problems, it is extremely important to realistically take into consideration uncertainty and imprecision. This is a key issue in ensuring a faultless life of metallic structures and systems. When fatigue cracks propagate or corrosion grows due to the cyclic loading of metallic structures they accumulate damage, thereby leading to serviceability loss and eventual collapse. The main approach to mitigate this degradation or damage accumulation is maintenance realised by scheduling inspection followed by eventual repair.

Efforts have been made to quantify these uncertainties based on probability theory for the assessment of existing structural condition. However, robustness with respect to the probabilistic model choice has not yet been addressed. That is, results from available approaches that can be quite sensitive to assumptions and simplifications in the environment of vague information. Hence, the imprecise probabilities framework (Beer et al., 2013) provides a promising pathway towards a robust maintenance strategy.

1.1.2 Motivations

The most dominant form of degradation remains corrosion (Ahammed, 1998; Caleyo et al., 2002). Corrosion which leads to metal loss both in type and section (length and depth) is the most prevailing time dependent threat to the integrity, safe operation and cause of failure for oil and gas pipelines (Bazan and Beck, 2013).

Uncertainties such as in relation to operational data variation, randomness of environment and imperfect measurement of the tool; associated with pipeline geometry, material strength, operating pressure and inspection tool, in addition to aging of the pipeline make a complex scenario in reduction of the accuracy of pipeline remaining life estimation (Ahammed, 1998; Caleyo et al., 2002; Qian et al., 2011).

The remaining strength of a pipeline with corrosion defects can be assessed using one of the international design codes, viz: B31G, B31Gmod, Battelle, DNV-101, Shell-92, etc. The associated methods use deterministic values for load and resistance variables, thereby assuming no uncertainty. In the light of the existing inherent uncertainties in the corrosion process (such as defect dimensions and material properties) and in the operational conditions (e.g. operating pressure and human factors), the obtained results are obviously quite coarse approximations, which may significantly deviate from reality.

Most of the oil and gas transportation pipelines are placed above ground. These pipelines are required to resist a combination of loads such as dead load- weight of the pipe with insulation and fluid being pumped, operating pressure, wind load, and kinematic influence in the form of uneven vertical displacement of adjacent/closest vertical supports of the pipeline due to the frost upheaval/melting of the permafrost soil in case of an above ground arctic pipelines (Ahammed and Melchers 1997; Timashev, 1982). The modelling of various factors such as nonlinear material behaviour, corrosion geometry, large deformations and applied loading makes an accurate assessment of the integrity of a corroded pipe a complex and difficult task. Currently, simple analytical closed-form solutions for accurate evaluation of pipeline integrity are used. Studies on the behaviour of corroded pipelines under external pressure and/or combined loads are not so readily available; neither standardized (Bolzon et al., 2011). The guidelines in all the failure pressure models (e.g. B31G, Modified B31G, DNV-101, etc.) has been useful to pipeline operators in assessing the integrity of corroded pipelines, but one of the shortcomings of these codes is that they could give non-conservative failure predictions when combined

loading exists, particularly when only pressure loading is considered while bending and axial compression are neglected (Roy et al., 1997).

The prediction of future sizes of growing defects and the pipeline remaining life time are obtained by using consistent assessments of their corrosion rates (CRs). The best method for estimating corrosion rates of a pipeline according to industrial standards is by directly comparing measured wall thickness changes after a known time interval, such as excavation and examination, or in-line inspection. These CRs may be considered as deterministic, semi-probabilistic or fully stochastic values. So far, there is no comprehensive corrosion rate model available, which provides all the necessary information for a confident estimate of the corrosion rate of pipelines. In order to establish such a model, uncertainty needs to be considered in the failure pressure model used for predicting the remaining pressure strength of the corroded pipeline, in the defect size, and in the corrosion growth rate. On this basis, a realistic reliability analysis for the corroded pipeline can be performed. Efforts have been made to quantify these uncertainties based on probability theory for the assessment of existing pipelines condition. In this dissertation imprecise probabilities approach is utilized to propose a robust method for predicting the remaining strength of corroded pipelines by considering the corrosion growth rates as probabilistic values.

There is no general algorithm available to estimate the reliability of buried pipeline structural system (Khan and Tee, 2016). Corrosion can be detected by Magnetic flux leakage (MFL) or Ultrasonic (UTS) techniques. The scarcity of information associated with the condition of buried pipelines makes the maintenance of such system a challenging task. The inspection and monitoring of these pipelines is necessary in order to ensure their continued fitness for purpose, entails protection from any time-dependent degradation processes, such as corrosion, external interference and ground movement, either natural or man-made. This is necessary because pipeline failures have significant impact on the economic, environmental and social aspects of the society. Therefore, the proper assessment and maintenance of such structures are crucial; negligence will lead to serviceability loss and failure (Ahammed and Melchers, 1997). A challenging task is the identification

of optimal inspection interval time in order to reduce the overall inspection costs. For instance, areas needing repairs must be accurately pinpointed as to minimise excavations for verifications. This can be achieved in addition to non-destructive inspection tool that have the capability to deliver a consistently high-level of reporting pipeline features and defects (Caleyo et al., 2009; Hong, 1997). The information obtained from in-line inspection data are imprecise due to the imperfect measurement of defect dimensions and the limited resolution of non-destructive inspection tools. To capture the variability of the data, combination of imprecise probabilities framework with the concept and techniques from classical probability approach is employed in this research for robust reliability analysis of pipelines.

Scheduling of maintenance activities, even though very challenging is an effective means of reducing degradation, as the propagation of fatigue cracks is a highly uncertain phenomenon (Faber et al., 1999; Koutsourelakis et al., 2006; Valdebenito and Schuëller, 2010). Likewise, inspection activities are also uncertain, since inspection activities, based on the quality may assess the damage incorrectly or may not even detect any damage at all.

The monetary cost associated with the inspection and eventual repair compared to the cost to be expended as a result of failure in conjunction with the various nature and scale of uncertainties arising from fatigue crack propagation, inspection and repair activities has to be optimized with valuable tool for robust decisions (Stangenberg et al., 2009; Schuëller et al., 2001). Hence, a robust maintenance strategy for metallic structures under fatigue which works with reliability metrics redefined within the framework of imprecise probabilities (Beer et al., 2013), provides the means of evaluating optimal maintenance activities.

1.1.3 Scope

In this research, attention is restricted to: the quantification of uncertainties involved in the reliability and maintenance of structural steel pipelines subjected to corrosion in aboveground, buried, and arctic exposure conditions, and the quantification of uncertainties involved in the reliability and maintenance of

structural steel bridges subject to fatigue cracks in a welded connection between a web stiffener and girder's flange. A key challenge in this regard is the probabilistic modelling, which relies on substantial information and data that often does not exist, so that assumptions and simplifications cannot be justified completely. To solve this conflict, imprecise probabilities are utilized to realistically reflect the vagueness of the available information in the probabilistic model.

1.1.4 Research Significance

The following highlighted points are the scientific relevance of this research:

- Corrosion growth rates assessments and interpretation using probabilistic approaches and generalised methods for vague and imprecise information.
- Improvement on pipeline international design codes and standards - improvement on practice using B31G, Modified B31G, DNV-101 and Shell-92 failure pressure models.
- Availability of an applicable numerical approach to estimate the reliability of buried pipeline structural system.
- Accessibility to reliability estimation methods for reliability-based optimization that can determine a maintenance strategy which is robust with respect to uncertainties.
- Solving the problem of load combination in engineering structures and systems (e.g. pipeline) that has always been of great significance, by considering loads as having a stochastic nature.
- Method for assessing reliability of arctic pipelines in the space of loads.
- Modelling of initial fatigue crack lengths as variables with imprecise mean values for optimal maintenance strategy.

1.2 Objectives of the Research Work

Objectives

- The ultimate goal is an applicable numerical approach for comprehensive robust design and robust maintenance strategies for engineering structures and systems subject to varying loads under severe uncertainty – uncertainty

that contains model (often known as epistemic) uncertainty in addition to the ordinary stochastic variety.

- A reliability metrics based maintenance scheduling optimization method, which can treat various uncertainties described by classical probability theory, and, at the same time other forms of uncertainty - variability, imprecision, incompleteness, vagueness, ambiguity, dubiety, etc.
- The use of generalised probabilistic approaches to minimize the consequences of unexpected events, and decision margins for subsequent design revisions.

1.3 Outcome and Novelties of the Research

In a broader term, the research output is to contribute significantly to developments towards sustainability in engineering design. The focus is both on Civil Engineering structures and Engineering Systems, which can later be extended to further engineering fields as appropriate. Much more specifically, the immediate outcomes are outlined below:

- Improved use of international codes and generalised methods that will support the transferability of this research to multiple wide-ranging sectors/applications of fatigue.
- A new methodology of assessing reliability and residual life of pipe subjected to a vector of random function loads and environmental conditions. A methodology based on Markov description of the loads on the pipeline.
- Prediction of future sizes of growing defects and corrosion rates as semi-probabilistic or fully stochastic values, conduct and comparison of the results.
- The development of stochastic model for the reliability of the arctic above ground pipeline, that operates under impact of two loads from subsidence/frost upheaval of support and from corrosion defects. A mathematical model of the upheaval/subsidence phenomenon as a random function of time is created. By extension it is applicable as a sophisticated

model of upheaval/subsidence of the soil underneath any structure/infrastructure.

- Implementation of imprecise probability for reliability analysis and maintenance activities for robustness with respect to the probabilistic model choice. In order to make results from available approaches to be quite sensitive with respect to the assumptions and simplifications in the environment of vague information.
- Load models and its combination in engineering structures and systems (pipeline) as having a stochastic nature.

1.4 Computational Tool

Computational tool for uncertainty quantification and robustness assessment (i.e. robust maintenance strategy) employed in this research are approximate analytical methods, Markovian approaches, Monte Carlo simulation methods and generalised methods for vague and imprecise information. The proposed approach has been implemented in OpenCossan - the open source engine of COSSAN software for uncertainty quantification and risk management (Patelli et al., 2016). The latest version of COSSAN interacts with the commercial FE software to construct the basis of the program. The toolboxes implemented within COSSAN-X include the state-of-the-art algorithms, which build the engine of the software. The utilization of these advanced algorithms within specific solution sequences permits the analysis of problems of engineering interest, hence forming the Applications-layer, such as Uncertainty Quantification and Reliability Analysis.

1.5 Thesis Organisation

The thesis structure is represented schematically in Figure 1.3. A brief description of the thesis organisation is outlined. The introductory part of the thesis is in the first two Chapters (1 and 2). The background, problem statement, motivations, objectives and novelties of the research work has been presented in this chapter. Chapter 2 deals with the meanings and definitions of the keywords used in the work. This forms a basic foundation for quick familiarity and for readers to be in close proximity with the terms used in the thesis.

Chapter 3 presents the theoretical background and the computational framework for all the computational tools employed in the research. The numerical models for fatigue cracks, corrosion growths, and different load models applicable to metallic structures are presented in Chapter 4.

Chapter 5 presents the first application on the robust maintenance strategies for corroded pipelines. Chapter 6 shows the applicability on the reliability assessment of arctic pipelines. Lastly on applications, Chapter 7 presents the optimal maintenance strategy for metallic bridge with vague information, and reliability-based optimisation of inspection time interval for corroded buried pipelines.

Finally, Chapter 8 presents the concluding remarks and summary, recommendations, and suggested areas for future works.

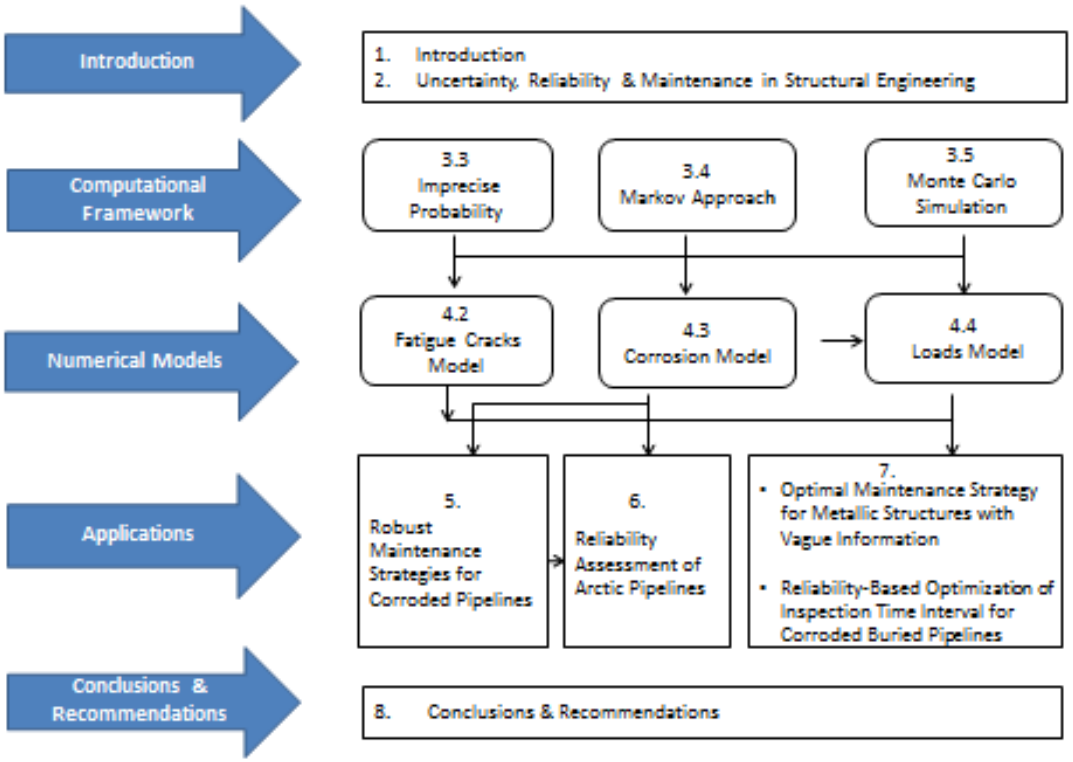

Figure 1.3: Schematic representation of the thesis organisation

2. Uncertainty, Reliability and Maintenance in Structural Engineering

2.1 Introduction

This chapter explains the definitions and meanings of the basic terms and keywords used in the research work. This is to acquaint the readers the foreknowledge and insight into the broader approaches and applications that will be encountered later on in the write up. The brief description and introduction is vital for the mind to comprehend and appreciate the importance of ensuring a faultless life of engineering structures and systems. It is possible to think about the proffered solution to the likely causes, problems and the challenges and thereafter adjudge its significance and applicability.

2.2 Uncertainty Quantification

2.2.1 What is uncertainty?

Uncertainty is the condition of not knowing everything necessary to choose the course of an action whose outcome is most preferred. In other words, it is the gap between what is presently known and certainty. It is the situation which involves imperfect and/or unknown information. It is the lack of certainty; a state of having limited knowledge where it is impossible to exactly describe the existing state, a future outcome, or more than one possible outcome. In engineering, uncertainty can be described as the phenomena whereby available information is very often imprecise, incomplete, vague, ambiguous, fluctuating, or dubious owning to an objective or subjective background, expert specification, or based on the data. The premise for this information is traditionally from codes and standards, measurements, expert knowledge, experiences, observations, drawings, plans, etc. Various nature and scale of uncertainties due to fluctuations and changes of structural and environmental parameters and conditions are to be considered realistically; which are the influences resulting from human errors and mistakes in

manufacturing, from the use and maintenance of the constructions, and from on-going changes in boundary and environmental conditions.

Structural engineering problems are brimful with uncertainties. Uncertainties in specifying material properties, geometric parameters, boundary conditions and applied loadings are unavoidable in describing real-life engineering structural systems. In engineering modelling for risk and reliability analyses, uncertainties are generally defined and categorized by two overall, broad types as either aleatory or epistemic (Melchers, 1999; Kiureghian and Ditlevsen, 2009; Bulleit, 2008; Moller and Beer, 2007; Zhang et al., 2010).

2.2.2 Types of uncertainty

Aleatory uncertainty: -- uncertainties that are irreducible variability or randomness inherent in nature. Sufficient data are available for characterizing the uncertainties. It is primarily associated with objectivity, modelled and processed appropriately with the aid of pure probabilistic methods. Probabilistic methods are commonly used for computing response distribution statistics based on input probability distribution specifications. It can be characterized statistically, and is often represented as a probability density function. Examples of aleatory uncertainty are such as in probability theory, these include the outcomes of drawing cards from a shuffled pack and/or tossing dice. In statistics, aleatory uncertainty is present in almost all data that we obtain, owing to random variability between the members of a population that we sample from, or to random measurement errors.

Epistemic uncertainty: -- uncertainties that are reducible resulting from a lack of knowledge (i.e. one that could in theory, be reduced by increasing the profession's knowledge about the area of interest). Data are generally too sparse to support objective probabilistic input descriptions, leading either to subjective probabilistic descriptions (such as Bayesian theory) or non-probabilistic methods based on interval specifications, fuzzy logic (i.e. imprecise probability). It is comprised of substantial amounts of both objectivity and subjectivity, either separately or simultaneously. An extension of probabilistic modelling to a particular class of epistemic uncertainty problems is achieved with the concept of subjective

probability including Bayesian theory. Quantification and characterization of epistemic uncertainty aims to better understand the underlying processes of the system and use non-traditional probabilistic methods. Examples of epistemic uncertainty are such as uncertainty about the atomic weight of aluminium, or about the population of the city of London. Looking in a suitable reference book could resolve the uncertainty in the given examples, to show that these uncertainties are potentially reducible by further investigation/knowledge.

2.2.3 Uncertainty quantification

Uncertainty quantification is the process of determining the effect of input uncertainties on response metrics of interest (Eldred et al., 2011). Subsuming what is known about the uncertainty into input parameters and variables used in optimization and simulation models can help in quantifying the uncertainty in the resulting model output or predictions. These input uncertainties may be characterized as either aleatory uncertainty, which are irreducible variability inherent in nature, or epistemic uncertainties, which are reducible uncertainties resulting from a lack of knowledge.

One of the main steps in structural reliability analysis is the modelling and quantification of various sources of uncertainty (Zhang et al., 2010; Bulleit, 2008). The design and construction of civil engineering structures and infrastructure is complicated by the various sources of uncertainties in structural resistance and loads, as well as in computational models. These uncertainties are treated as random variables when using established probabilistic methods for reliability analysis. But the probability distribution to describe a random phenomenon is generally imprecisely known. Highlighted below are the various sources of uncertainties (Kiureghian and Ditlevsen, 2009):

- Actual measurements: uncertainties attributed to measurements taken directly from load values and material properties as basic random variables.
- Model error: these uncertainties are as a result of selecting probabilistic and/or non-probabilistic model form used for the description of the basic random variables' distribution.

- Modelling error: uncertainties arising from the selection of the physical models used to describe the derived variables.
- Probabilistic model: the statistical uncertainties due to the estimation of the parameters of the probabilistic and/or non-probabilistic model.
- Physical model: the statistical uncertainties due to the estimation of the parameters of the physical model.
- Observatory measurements: uncertainties due to error involved in indirect measurement of observations on which the parameters of probabilistic and/or non-probabilistic model and physical model are measured.
- Computational errors: uncertainties resulting from numerical approximations, computation or truncations.
- Human error: uncertainties due to human decisions and activities; an example is undeliberate errors arising from design, modelling, operation and/or construction of a system or component.

Epistemic uncertainty is knowledge-based, and arises from imperfect modelling, simplification and limited availability of database. Its possible sources of uncertainty include model uncertainty and statistical uncertainty. Statistical uncertainty is a vital source of epistemic uncertainty - the standard deviation and mean, which are the statistical parameters, are usually estimated by statistical inference from sampled observational data with a point estimator used to approximate the exact parameter. Thus the distribution is itself subject to some uncertainty. Statistical uncertainty may be significant if only a limited sample of data is available. Model uncertainty which is another important source of epistemic uncertainty is related to the disparity between real structural behaviour and its simplified representation in mathematical models.

The numerical models and parameters must be specified according to the underlying nature in order to obtain reliable computation results. The uncertainty must be described by an appropriate mathematical model in accordance with the underlying real-world information and processed through numerical computations. Since the probability distribution to describe a random phenomenon is generally imprecisely known; this may lead to biased computational results with an

unrealistic accuracy and, in turn, lead to wrong decisions with the potential for associated serious consequences. The probabilistic modelling would have introduced unwarranted information in the form of a distribution function that is totally unjustified. According to Moller and Beer, 2007: it stated that the problem of selecting an appropriate uncertainty model can only be solved by analysing the sources of the uncertainty in each particular case, i.e. the underlying reality dictates the model. In the case of parameters, the knowledge about the fluctuations of the structural parameters is very limited so that a clear probabilistic specification of their associated uncertainty is impossible, and the capability for the development of reliable predictions, in terms of probability, is fundamentally limited. An uncertain parameter or quantity is that which a decision maker has uncertainty about. It is more general than a random variable because the uncertainty need not be represented using probability theory. One of the example applications in this research work presents a problematic issue which is the modelling of strongly non-stationary processes to predict exceptional environmental conditions of extreme wind loads that are affected by changes in global and local climate for arctic pipelines, as this defied a clear specification of future non stationarities.

Joint committee on structural safety (JCSS, 2000) states concerning model uncertainties that a numerical model is a physically based or an empirical relation between relevant variables, which are in general random variables $Y = f(X_1, X_2, ..., X_n)$. Here, Y and $f(\ )$ are the model output and function respectively, and X_i are the basic variables. The outcome Y can be predicted without error, if the values X_i are known, indicating that the model $f(\ )$ is probably complete or exact. But the reverse is always the case; in most cases the model will be incomplete and inexact. The difference between the model prediction and the real outcome of the problem or experiment can be written down as $Y = f'(X_1, X_2, ..., X_n, \theta_1, \theta_2, ..., \theta_m)$. θ_i are treated as random variables, and denote the parameters which contain the model uncertainties. Likewise, their statistical properties can be derived from observations, whereby the mean of these

parameters are obtained such that the calculation model correctly predicts the test results.

Overall, aleatory uncertainty in structural engineering problems can be fixed by employing classical probability methods, while epistemic uncertainty generally requires further specific models oriented to particular characteristics of the uncertainty associated with the available information. The problem of selecting an appropriate mathematical structure to represent epistemic uncertainties can be quite challenging. Some of the ways of representing epistemic uncertainty include probability theory, fuzzy sets, possibility theory, and imprecise probability. The uncertainty of the available information impedes the specification of certain models and precise parameter values without an artificial introduction of unwarranted information. These uncertainty models are constituted on a non-probabilistic or on a combination of probabilistic and non-probabilistic mathematical basis. One can clearly deduce from the afore-mentioned, that particular attention must be paid to the phenomenon of uncertainty. While traditional probabilistic methods are already well established and largely recognized as applicable to real world problems (see e.g. Schueller and Spanos, 2001; Deodatis and Spanos, 2004; Schenk and Schueller, 2005), approaches of non-traditional uncertainty modelling still appear scattered and scarce in engineering literature.

2.2.4 Consequences of uncertainties

Deterministic analysis and design is inadequate. This is mainly because the probability of failure is never zero; design codes and standards must include a rational safety reserve (i.e. too safe – too costly, otherwise – too many failures); and in actual fact, the factors of safety used in design codes and standards acknowledge the uncertainty in the design.

2.3 Structural Reliability

One of the major requirements for structures usually is to have a satisfactory performance in the expected lifetime, in other words, it is required that the structure does not collapse or becomes unsafe and that it fulfils certain functional requirements over its specified period of usage, and in an economic way. Reliability

is an efficient measure of the structural performance, the probability that the structure under consideration will perform its function during the predetermined lifetime. Reliability analysis methods provide a framework to account for numerous sources of uncertainties that should be considered in engineering design and problems in a rational and vigorous manner.

Structural analysis and design have been traditionally based on deterministic methods for decades, with the assumption and estimation that the strength of structural element is always exceeding the load with a certain margin. Contrary to this, uncertainties in the loads, strengths and in the modelling of the engineering systems require that probabilistic methods in a number of situations have to be used. In the traditional method, safety factor was defined as the ratio between the strength and the load, and in turn considered and taken as the measure of the reliability of the structure (Sorensen, 2004; Melchers, 1987; Madsen et al., 1986; Thoft-Christensen and Baker, 1982; Ditlevsen and Madsen, 1996). Furthermore, the traditional approach is based on specified minimum material properties, load intensities, and certain procedure for estimating stresses and deflections which are most of the time a deterministic prescription based on international standards and codes. It is widely accepted that the probabilistic approach seems to be well suitable for the measure of risk and reliability in structural reliability theory. It is an extension of traditional structural analysis as an art of formulating mathematical models as to how structure behaves when it's material and geometric properties, etc. and other actions are known.

2.3.1 Basic theory and methods of structural reliability

Structural reliability estimation methods are classified according to level, moment, order and exactness of calculation result in (Huyse, 2001). The theoretical methodologies are highlighted and briefly explained on in Table 2.1

Table 2.1: Structural reliability theoretical methods

Classification	Group/Type	Description
Level	I	Deterministic reliability methods. It uses only one characteristic value for each uncertain variable description.
	II	These reliability methods use two values to describe each uncertain variable (such as mean, variance, coefficient of variation). e.g. FOSM
	III	The joint probability density distribution of all the uncertain variables is used for description of each uncertain variable. Examples are - Numerical integration, approximate analytical method, FOSM, and simulation method.
	IV	This method makes a comparative analysis based on the principles of engineering economic under uncertainty between structural prospect and a reference prospect.
Moment and Order	Approximate methods: FOSM, SOSM, etc.	Reliability methods here are classified into approximate methods
Exactness of calculation result	Approximate methods	Examples are mean-value FOSM method, etc.
	Simulation methods	Monte Carlo method is an example.
	Direct integral method	Numerical integration.

Further classification in (Zang et al. 2002), shows that the reliability methods are roughly described and grouped into two major types, namely: mathematical-based reliability, and physics-based reliability as shown in Table 2.2.

Table 2.2: Summary and differences between two types of reliability (Zang et al. 2002)

Mathematical-based Reliability	Physics-based Reliability
Reliability is related to life- the time to failure.	Reliability is related to the limit state.
The state change is observed.	The state change can be mathematically modelled.
Reliability evaluation relies on testing or field data.	Reliability can be evaluated from physical equations (models).
The reliability is defined by expression: $R(t) = P(T > t)$: *T* is any future time	The reliability is defined by expression: $R = P[g(X) \geq 0]$
The reliability is time dependent.	The reliability may or may not be time dependent.
Typical methods include: ○ Fault tree analysis ○ Event tree analysis ○ Failure models, effects, and criticality analysis ○ Markov process ○ Monte Carlo simulation	Typical methods include: ○ First order second moment method ○ First order reliability method (FORM) ○ Second order reliability method (SORM) ○ Design of Experiment ○ Monte Carlo simulation

Followed by this brief description of the theoretical methods is the overview of the structural reliability estimations, which is equivalent to the calculation of the failure probability of the structure. Let an *n*-dimensional vector of basic variables with continuous joint density function $f_X(x)$ be associated with the existing structure, *G(X)* as the limit state function such that the limit state surface is *G(X)=0*, the safety region of the structure is denoted as *G(X)>0*, and the failure region is defined as *G(X)<0*. Then, the structural reliability is simply the calculation of the integral for estimating failure probability, P_f indicated (Rackwitz, 2001) as:

$$P_f = \int_{G(X)\leq 0} f_X(x)dx \tag{2.1}$$

Assuming that a probability preserving transformation $x = T(u)$ exists where u is an independent standard normal vector which transforms the probability integral into

$$P_f = \int_{G(x)\leq 0} f_X(x)dx = \int_{G(T(u))\leq 0} \varphi U(u)du \tag{2.2}$$

where $\varphi U(u)$ is the *n*-dimensional standard normal density with independent components. The simple result is Eq. (2.3).

$$P_f \approx \phi(-\beta) \tag{2.3}$$

The reliability of the structure *R*, which is the compliment $1 - P_f$ is defined as:

$$R = 1 - P_f \tag{2.4}$$

The reliability index, β is defined as:

$$\beta = -\Phi^{-1}(P_f) \tag{2.5}$$

Φ is the standard normal cumulative distribution function.

2.4 Maintenance of Structures

Maintenance in engineering structures is getting more attention as a research topic. Simply because of the ageing – a sudden or gradual decrease of strength - of the structures and infrastructures which are critical for the functionality of our environmental, societal and economical life. Breakdowns are the norm, and no structure operates flawless forever in non-ideal world that we live. Hence the need for proper approaches and measures to validate and ensure their safety and reliability. Maintenance helps in keeping components/systems in a good condition to enable the structure fulfil its functions. Explicit justification of all maintenance measures is required for higher societal availability of the structural engineering works. Other functional losses in structures are excess loads accrued to external

causes (such as extreme loads due to earthquakes, wind, terrorism, etc.), and human errors with regards to different stages in the structural lifetime ranging from design through execution, use, operation, management to maintenance of the structure. Uncertainties and complexity makes safety analysis and maintenance scheduling complicated, for example, conscientious inspection of an ageing structure may never guarantee the occurrence of non-functionality as a result of extreme loads and human errors at all stages in the life of the structure.

Brief mentions of some important facts and figures closely associated with structural engineering maintenance as reported in Dhillon, (2002) and other reviews are as follows: Over $300 billion are spent on plant maintenance and operations by U.S. industry annually, which comes to an approximate estimation of 80% (Latino, 1999). Report from a Ministry of Technology Working Party in Britain came up with an annual estimate of approximately £3000 million in 1970 for maintenance cost in the United Kingdom (Kelly, 1978; Working Party on Maintenance Engineering, 1970). In 1968, it was estimated that better maintenance practices in the United Kingdom could have saved approximately £300 million annually of lost production due to equipment unavailability (Kelly, 1984). The cost of maintaining a military jet aircraft annually is about $1.6 million; approximately 11% of the total operating cost (Kumar, 1999). Annually, the U.S. Department of Defence spends around $12 billion for depot maintenance of weapon systems and equipment: Navy (59%), Air Force (27%), Army (13%), and (1%) for others (Department of Defence, 1995). The operation and maintenance budget request of the U.S. Department of Defence for fiscal year 1997 was on the order of $79 billion (DOD Budget, 1996). In conclusion, the elimination of many of these persistent failures through effective maintenance can bring a reduction between 40 to 60% of the cost.

2.4.1 Maintenance strategies

A maintenance strategy may be defined as a decision rule which establishes the sequence of maintenance actions to be undertaken according to the degradation level of the structural system and with regard to the safety acceptable exploitation

thresholds (Riane et al., 2009). Each maintenance action consists of maintaining or restoring the structural system in a specified state using the appropriate resources. A cost and duration are incurred to execute each maintenance action. Maintenance strategies have witnessed a paradigm shift over the recent decades from breakdown maintenance to more sophisticated strategies like condition monitoring and Reliability Centred Maintenance (Garg and Deshmukh, 2006)

The maintenance objectives are summarized (Dekker, 1996) under four headings:

- To ensure system function – i.e. availability, efficiency and product quality,
- To ensure system life – which is asset management,
- To ensure safety, and
- To ensure human wellbeing.

Toorn, 1992 postulates that maintenance targets for the structure's functionality behaviour be distinguished into: reliability, availability, serviceability, durability, and presentability. Also that the basic maintenance strategies on the components level should be:

- Failure-based – i.e. maintenance activities are taken after failure has been noticed,
- Use-based – this involves maintenance activities taken after a certain use, and lastly,
- Condition-based - maintenance activities taken after a certain condition limit is exceeded and noticed, see Figure 2.1.

In general, the failure-based maintenance strategy will always lead to corrective maintenance and certain consequences of failure. In turn the use-based maintenance strategy will lead to preventive maintenance if the relationship between failure and use is known. Condition-based maintenance strategy can also lead to preventive maintenance if the condition is measurable.

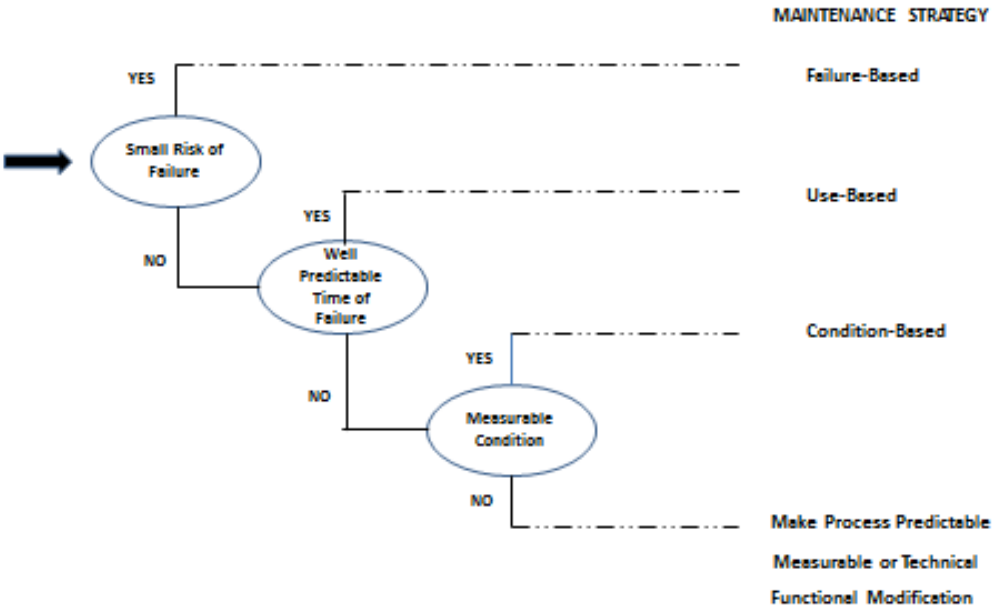

Figure 2.1: A qualitative decision-tree for maintenance strategies (adapted from Toorn, 1992)

The oldest, first generation and most common maintenance and repair strategy is the philosophical one of “fix it when it breaks”. The plea of this strategy is that no planning or analysis is required; the assumption was that downtime is not particularly important, since the industries are regarded as not highly mechanised; most of the equipment/components were taken to be simple, overdesigned, reliable and easy to repair. Hence, the only requirement is systematic maintenance. The shortcoming of this strategy is the occurrence of unscheduled downtime at times that may not be convenient, and of high consequences in applications that are very sensitive or critical, for example aircraft engines. (Kothamasu et al., 2006). With much concern and consideration over downtime and industrial mechanisation, the rationale to carry out maintenance before failure arises at pre-established intervals and with the notion that these failures could and should be prevented was reached. This strategy seems to provide relatively high equipment/ components reliability. The disadvantages are: failures are assumed to take place at

specific intervals, and there is increase in maintenance costs as a proportion of the total operation costs – higher scheduled downtimes leading to excessive costs.

Another strategy is the realisation of burn-in failure mode, where the incidence of failure over the life of equipment/components leads to the use of bath-tub curve, see Fig. 2.2. The rates of failure are low throughout the useful life of an equipment/component, but rises towards the end of life. The shortcomings of this bath-tub curve strategy are that the degradation progression of the system is assumed to be deterministic through a well-defined order of states. This does not capture the complexity in interactions between the system and their component as discrete systems, which is subject to function of the changes such as environmental effects and variations, etc. thereby causing seemingly random failure behaviour.

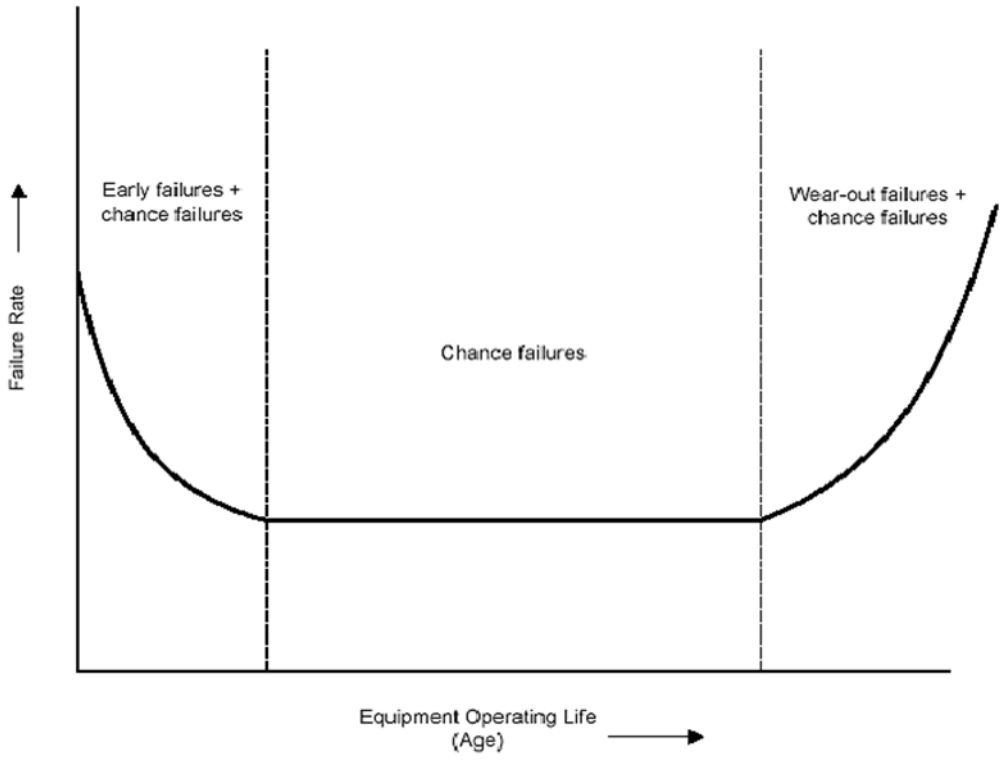

Figure 2.2: Bath-tub curve showing reliability in terms of equipment/components (after Stamatis, 1995; Kothamasu et al., 2006)

Lastly, is the third generation maintenance strategy, where the growth of mechanisation and automation increases focuses on plant availability and reliability. The safety regulations are tightened up as the effect of failures on health

and safety are held in high esteem, thereby raising the cost of maintenance. Eventually new techniques become available to collect data that would enable stakeholders or maintainers to predict failures (as predictive maintenance), and to optimise maintenance decisions (i.e. asset management).

The above outlined maintenance strategies involves various maintenance policies that can be classified as age replacement policy, periodic repair policy, block repair policy, failure limit policy, etc. each of which has different characteristics, advantages and disadvantages and requires extensive research (Garg and Deshmukh, 2006). Current maintenance policies are time oriented and are based on reliability models.

All the maintenance policies are governed by analytical models that make it possible to evaluate over an infinite horizon the associated performances under a series of hypothesis (Ait-Kadi et al., 2002). Also, these strategies differ from each other by the nature and the action sequel that they suggest, the selected performance criteria, the deterministic or stochastic character of the parameters that they take into account, and the fact that the system is considered as a sole entity or as a system constituted of many components which state may be known at all time or after inspection, etc.

Using an analytical formulation, one can model the considered maintenance strategy using its characteristic parameters and decision variables to describe the technical as well as the economic objectives to optimise. If one succeeds to solve to optimality of such analytical models, he can establish the existence and the uniqueness conditions of an optimal strategy.

The major inconvenience and shortcoming of such approaches is that one ends up with difficult models that are complex to solve, especially if one wants to consider other factors that have significant impact on the system's behaviour. This fact has brought us to explore simulation's possibilities in order to handle the situation and efficiently evaluate maintenance strategies.

Furthermore, one of the ways to minimise both maintenance and repair costs and probability of failure is the concise information on the inspections and the actual state of the structure which will increase the likelihood of meaningful application of repair activities. To mitigate the deterioration/degradation or damage accumulation in structures and infrastructures, one possible approach is maintenance activities, and the maintenance problem has been regarded as an optimization problem in this work.

2.4.2 Maintenance as an optimization problem

In the present world today, financial resources do not keep pace with the growing demand for maintenance of deteriorating structures and infrastructures. It is imperative that those stakeholders or maintainers responsible for maintenance decisions make the best possible use of limited financial resources. Decision makers also have to evaluate the expected life-cycle maintenance cost of deteriorating structures and use benefit/cost techniques for finding the optimal resource allocation (Kong and Frangopol, 2003).

A maintenance problem can be regarded as an optimization task, where the solution is a trade-off between the costs associated with inspection and repair activities and the benefits related to the faultless operation of the infrastructure. Maintenance as an optimization task aims at minimizing the total cost while adjusting some parameters, such as the number, time, and quality of inspections. Consequent to the unavoidable uncertainties, the expected cost of maintenance and failure can only be estimated by assessing the reliability of the system. The problem is therefore formulated as a time-variant reliability-based optimization, where both objective and constraint functions require the assessment of reliability with time (Dekker and Scarf, 1998; Valdebenito and Schuëller, 2010).

Maintenance optimization models can both be qualitative - includes techniques like total productive maintenance, reliability centred maintenance, etc., and quantitative - incorporates various deterministic/stochastic models like Markov

Decision, Bayesian models, etc. Furthermore, the models can be classified following after the degradation/deterioration modelling as deterministic or probabilistic models (Garg and Deshmukh, 2006). The maintenance optimisation consists mainly of mathematical models aimed at finding both the optimum balance between costs and benefits of maintenance and/or the most appropriate moment to execute maintenance. This is a well-established area as several reviews indicate (Dekker and Scarf, 1998; Valdebenito and Schuëller, 2010). But the major drawback is the complexity of these models, applications have become a bit difficult as data are often scarce and the models are not easy to apply. Hence, the needs for imprecise probabilities to both cater for scarce data and probabilistic model choice.

2.5 Summary

The main intention of this chapter is to allow readers to get acquainted with some keywords in the thesis. The brief introduction and definitions, basic interpretation and developments on uncertainty, reliability and maintenance of structure which are of particular interest and that will be often referred to in all the chapters. Even though very brief and introductory, the illustrations and explanations presented herein will provide appropriate and sufficient information to enable readers further appreciates discussions presented in the remaining content of this thesis.

The theoretical background that will serves as computational framework and proffer adequate solutions to some substantial level is now to be considered next, where a mention will be made on the concepts and computational tools for structural reliability estimations and reliability-based optimization for the maintenance activities. The use of Monte Carlo simulation as simulation strategy for uncertainty analysis and OpenCossan for numerical computational programs will be discussed.

3. Theoretical and Computational Frameworks

3.1 Introduction

This chapter presents theoretical and computational frameworks that provide the organization for the research study. It forms the bases that guide the research work and in the interpretations of its results. These theoretical frameworks provide a broad explanation of relationships that exists between the concepts used in the work, since the theoretical frameworks in principle start out as a conceptual framework and with much research developed into a research-based theoretical framework. Therefore the concepts of the research work relate back to the theory, thereby drawing out the importance of the theory which is dependent on the degree of research-based evidence and level of its theory development.

A brief mention is made on the concepts and computational tools for structural reliability estimations and reliability-based optimization; imprecise probabilities for reliability assessments- modeling imprecision using probability bounds analysis with p-boxes, and interval probabilities; and Markovian approaches. This chapter does not intend to discuss explicitly about the whole concepts and theoretical frameworks, but just the aspects that is related to this research work. The simulation strategy using Monte Carlo simulation as a methodology for uncertainty analysis, and OpenCossan for numerical computational programs are discussed but not in broad terms.

3.2 Structural Reliability Estimations

Reliability engineering provides the theoretical and practical analytical tools for measuring quantitatively the performance and integrity of the structural system. For an assurance of a desired level of structural performance, it requires the recognition and characterization of the variability in materials' responses to design and usage conditions. The variability in a material's behaviour response is not known beforehand but can be measured in experiments. Probabilistic and statistical

analytic techniques are universally applied. The traditional (deterministic) approach to structural design employs selected factors of safety multiplied by expected service loads and uses allowable working stresses. This approach is simple and easy to implement, but the shortcoming is that it lacks sufficient rigour to account quantitatively for design variables encountered in the design of critical structures.

3.2.1 Basic theory of reliability analysis

The load, geometry, and material parameters of structural systems subject to uncertainties can be represented by random variables – which are the simplest probabilistic characterization possible, even though in certain situations more advanced models might be required, (JCSS, 2000). In this case, the governing parameters of the problem are modelled as random variables. The basic random variables *S* and *R* represent sets of load and resistance variables respectively; and collectively represented by a random vector $X=(X_1, X_2, ..., X_n)$ in a space domain of the random variables. The safety margin is $M = R - S$. Structural reliability estimation can be simplified into calculating the failure probability of the structure. Failure here is a probabilistic event, with its probability of occurrence expressed as:

$$P_f = P[M \le 0] \tag{3.1}$$

$$P_f = P[g(X) \le 0] \tag{3.2}$$

where $M = g(X)$, *M* is the safety margin and a random variable. $g(X) = 0$ is the limit state function, such that: $g(X) > 0$ represent the safety region and $g(X) < 0$ the failure region.

The probability of failure can also be expressed in the form of an integral, as:

$$P_f = \int_{g(X)\le 0} \int f_X(x_1, x_2, .., x_n)\, dx_1 dx_2 ... dx_n \tag{3.3}$$

where $f_X(x_1, x_2, .., x_n)$ is the joint probability density function (PDF) of *X*.

The complement $1 - P_f$ is the reliability measure of the structure, and the corresponding reliability index, β is defined and derived from failure probability as:

$$P_f = \Phi(-\beta) = 1 - \Phi(\beta) \tag{3.4}$$

$$\beta = -\Phi^{-1}(P_f) = \Phi^{-1}(1 - P_f) \tag{3.5}$$

where Φ is the standard normal cumulative distribution function (CDF).

In structural engineering systems and applications where statistical and model uncertainties are conspicuously noticeable (JCSS, 2000); complete statistical information about the basic random variables *X*, and the mathematical model function $g(.)$ which represent the limit state is not available. The failure probability estimates from Equations 3.1, 3.2 and 3.3 is a point estimator for a particular set of assumptions regarding probabilistic model choice, and a particular mathematical model for $g(.)$. The limit state function can be written as $g(X, Q)$ when uncertainties associated with these models are represented in terms of a vector random parameters *Q*. Here, uncertainties in *X* cannot be influenced without changing the physics of the problem, but can be influenced in *Q* when alternative methods and additional data collection are employed.

Recasting Equation 3.3, to inculcate statistical and model uncertainties, the failure probability becomes:

$$P_f(\theta) = \int_{g(X,\theta)\le 0} f_{X|\Theta}(X|\theta) dX \tag{3.6}$$

where $P_f(\theta)$ is the conditional failure probability for a given set of values of the parameters θ and $f_{X|\Theta}(X|\theta)$ is the conditional probability density function of X for a given θ.

Expected value of the conditional failure probability can be estimated in order to account for the influence of parameter uncertainty on probability of failure, as:

$$\bar{P_f} = E[P_f(\theta)] = \int_\theta P_f(\theta) f_\Theta(\theta) d\theta \tag{3.7}$$

$f_\Theta(\theta)$ is the joint probability density function of θ.

The corresponding reliability index is evaluated as:

$$\bar{\beta} = -\Phi^{-1}\left(\bar{P}_f\right) \tag{3.8}$$

Table 3.1: Relationship between β and P_f (JCSS, 2000)

β	1.3	2.3	3.1	3.7	4.2	4.7	5.2
P_f	10^{-1}	10^{-2}	10^{-3}	10^{-4}	10^{-5}	10^{-6}	10^{-7}

Reliability analyses evaluate reliability index or probability of failure by replacing deterministic safety check with a probabilistic assessment of the safety of the structure; as its main target (Melchers, 1999; JCSS, 2000). Typical relationship between reliability and failure probability is shown in Table 3.1. In the like manner, reliability analysis methods offer the theoretical framework for considering uncertainties in a comprehensive decision scheme, and its main purpose is to evaluate the ability of systems or components to remain safe and operational during their lifecycle.

3.3 Imprecise Probability

Imprecision is the possible gap between the present state of information and a state of precise information. More specifically, it is the quality or state not being exactly or sharply defined or stated. This is directly opposite of the state of precise information of having acquired all information about a particular model of irreducible uncertainty available at any cost. Imprecise probabilities have emerged into several application fields in engineering with structured approaches. The largest application field appears as reliability assessment, where imprecise probabilities are implemented to address sensitivities of the failure probability with respect to the probabilistic model choice (Beer et al., 2013).

It is of great importance for probabilities to be regarded as imprecise in the presence of little information; while the extreme case of complete absence of relevant information concerning the possibility space should be modelled by vacuous probabilities which are maximally imprecise. When predicting the

reliability of engineering system and structures for realistic results, an appropriate quantification and modelling are prior requirements; else it will be difficult to capture the scenario. Modelling of imprecision includes the use of probability bounds analysis with p-boxes, fuzzy probabilities, interval probabilities, etc. Although it is not limited to the use of interval probabilities, an interval is a crude assertion of imprecision. When the value of a number is not exactly known, provision of exact bounds should be made on the number, thus specifying an interval for the parameter.

3.3.1 Interval Probabilities

An interval (Moore, 1979; Walley, 1991) is a closed bounded set of real numbers [a, b] = {x: a ≤ x ≤ b}. Suppose A is an interval, and its end points are $\underline{A}$ and $\overline{A}$, then $A = \left[\underline{A}, \overline{A}\right]$. So for n-dimensional interval vector, $\left(A_1, A_2, \ldots A_n\right)$ if A is a 2-dimensional interval vector, then $A = \left(A_1, A_2\right)$, and for some intervals $A_1 = \left[\underline{A_1}, \overline{A_1}\right]$ and $A_2 = \left[\underline{A_2}, \overline{A_2}\right]$ such that $\underline{A_1} \le a_1 \le \overline{A_1}$ and $\underline{A_2} \le a_2 \le \overline{A_2}$.

The following conditions hold for intervals and their corresponding endpoints:

- If real number *a* is in the interval *A*, $a \in A$. This also holds for a real vector $a = \left(a_1, a_2, \ldots, a_n\right)$ and $A = \left(A_1, A_2, \ldots A_n\right)$ the interval vector, $a \in A$ if $a_i \in A_i$ for $i = 1, 2, \ldots, n$.
- If two corresponding endpoints of two intervals are equal, such that $A = B$ if $\underline{A} = \underline{B}$ and $\overline{A} = \overline{B}$, the intervals are known as equal.
- The intersection of two intervals *A* and *B* is empty if either $\underline{A} > \overline{B}$ or $\underline{B} > \overline{A}$.
- If $A \cap B = \Phi$, then $\left(A \cap B\right) = \left[\max\left(\underline{A}, \underline{B}\right), \min\left(\overline{A}, \overline{B}\right)\right]$ is an interval.
- If the intersection of any of the corresponding components of two interval vector is empty, then their intersection is empty.
- If $A = \left(A_1, A_2, \ldots A_n\right)$ and $B = \left(B_1, B_2, \ldots B_n\right)$, then $A \cap B = \left(A_1 \cap B_1, \ldots, A_n \cap B_n\right)$ is an interval vector.

- If two intervals *A* and *B* have nonempty intersection, then $(A \cup B) = \left[\min\left(\underline{A}, \underline{B}\right), \max\left(\overline{A}, \overline{B}\right) \right]$ is an interval.
- Other extremely useful transitive order relation for intervals are < on the real line to interval and set inclusions:
  - $A < B$ If and only if $\overline{A} < \underline{B}$.
  - $A \subseteq B$ If and only if $\underline{B} \leq \underline{A}$ and $\overline{A} \leq \overline{B}$.

    Such that if $A = (A_1, A_2, \ldots A_n)$ and $B = (B_1, B_2, \ldots B_n)$ are interval vectors, then $A \subseteq B$ if $A_i \subseteq B_i$ for *i* = 1, 2, . . . , n.

    Where the width of an interval $A = [\underline{A}, \overline{A}]$ is $w(A) = \overline{A} - \underline{A}$

    The width of the interval vector is $w(A) = \max(w(A_1), \ldots, w(A_n))$

    Absolute value of an interval *A* is $|A| = \max\left(\left|\underline{A}\right|, \left|\overline{A}\right| \right)$, and

    The midpoint of an interval denoted by $m(A) = [\underline{A} + \overline{A}]/2$

An interval probability model (Beer et al., 2013) may be expressed as a mapping from the space of events to the space of intervals on [0, 1] and represented mathematically as:

$$\mathrm{I} = \{[a,b], a,b \in \Re | 0 \leq a \leq b \leq 1\} \tag{3.9}$$

If $P(A) = [a_1, a_2]$ and $P(B) = [b_1, b_2]$ (3.10)

Sure bounds on the logical intersection and union can be calculated as:

$$P(A \& B) = P(A \cap B) = [\max(0, a_1 + b_1), \min(a_2, b_2)] \tag{3.11}$$

$$P(A \vee B) = P(A \cup B) = [\max(a_1, b_1), \min(1, a_2 + b_2)] \tag{3.12}$$

Complementary to the analogous rules for intersection and union when events A and B are assumed to be independent

$$P(A \,\&\, B) = P(A \cap B) = [a_1 x b_1, a_2 x b_2] \tag{3.13}$$

$$P(A \vee B) = P(A \cup B) = [1-(1-a_1)(1-b_1), 1-(1-a_2)(1-b_2)] \tag{3.14}$$

While the rule for logical negation is:

$$P(A^C) = [1-a_2, 1-a_1] \tag{3.15}$$

3.3.2 Probability bound analysis with p-boxes

Uncertainty quantification approaches as part of the theory of imprecise probability include interval probabilities, probability bounds analysis with p-boxes, and fuzzy probabilities (Ferson et al., 2004; Beer et al., 2013). P-boxes are defined by left and right bounds on the cumulative probability distribution function of a quantity. It also gives additional information about the quantity's mean, variance and distributional shape. This bounding approach permits analysts to make calculations without requiring overly precise assumptions about parameter values, dependence among variables, or distribution shapes.

A p-box according to Beer et al. (2013) represents a class of probability distributions consistent with the highlighted constraints below. Let $\mathfrak{D}$ denote the space of distribution functions on the real numbers $\mathcal{R}$, that is $\mathfrak{D} = \{\mathrm{D} |\ \mathrm{D}: \mathcal{R} \rightarrow [0, 1], \mathrm{D}(\mathrm{x}) \leq \mathrm{D}(\mathrm{y})$ whenever $\mathrm{x} < \mathrm{y}$, for all $\mathrm{x}, \mathrm{y} \in \mathcal{R}\}$, and let $\mathcal{I}$ denote the space of real intervals, $\mathcal{I} = \{[\mathrm{i}_1, \mathrm{i}_2] \,|\mathrm{i}_1 \leq \mathrm{i}_2, \mathrm{i}_1, \mathrm{i}_2 \in \mathcal{R}\}$. Then a p-box is a quintuple $\langle \bar{F}, \underline{F}, \mathrm{m}, \upsilon, \mathcal{F} \rangle$, where $\bar{F}$, $\underline{F} \in \mathfrak{D}$, while $\mathrm{m}, \upsilon \in \mathcal{I}$, and $\mathcal{F} \subseteq \mathfrak{D}$. This quintuple denotes the set of distribution functions $\mathrm{F} \in \mathfrak{D}$ matching the following constraints:

$$\underline{F}(x) \leq F(x) \leq \bar{F}(x), \tag{3.16}$$

$$\int_{-\infty}^{\infty} x dF(x) = m, \tag{3.17}$$

$$\left(\int_{-\infty}^{\infty} x^2 dF(x)\right) - \left(\int_{-\infty}^{\infty} x dF(x)\right)^2 = v, \tag{3.18}$$

and

$F \in \mathcal{F}$. (3.19)

The constraints indicate that the distribution function F falls within prescribed bounds, the mean of the distribution (given by the Riemann–Stieltjes integral) is in the interval m, the variance of the distribution is in the interval v, and the distribution is within some admissible class of distributions $\mathcal{F}$. A p-box is minimally specified by its left and right bounds, in which case the other constraints are understood to be vacuous as $\langle \underline{F}, \bar{F}, [-\infty, \infty], [0, \infty), \mathfrak{D} \rangle$.

Most of the significant advantages of the use of p-boxes over a traditional probabilistic approach in risk analyses (Ferson and Long, 1995; Ferson, 2002; Ferson et. al., 2003; Beer et. al., 2013) are provision of convenient and comprehensive ways to handle several of the most practical serious problems faced by analysts, which includes:

- imprecisely specified distributions;
- poorly known or even unknown dependencies;
- non-negligible measurement uncertainty;
- non-detects or other censoring in measurements;
- small sample size;
- inconsistency in the quality of input data;
- model uncertainty; and
- non-constant distributions.

Likewise, if an analyst does not know the distribution family for some input, a distribution-free p-box can be used as bound to all possible distribution families consistent with the other information available about that variable. Also, if the nature of the stochastic dependence between two distributions is unknown, probability bounds analysis can be used as bound to all possible distributions that might arise as a function of the inputs whatever their interdependence might be.

The p-box is thus constructed as follows to characterize uncertain numbers (aleatory and epistemic uncertainties) involved in the quantitative uncertainty

modelling where numerical calculations must be performed: Suppose $\overline{F}$ and $\underline{F}$ are non-decreasing functions from the real line $\mathcal{R}$ into [0, 1] and $\overline{F}(x) \leq \underline{F}(x)$ for all x ϵ $\mathcal{R}$. Let $[\overline{F}, \underline{F}]$ denote the set of all non-decreasing functions *F* from the reals into [0, 1] such that $\overline{F}(x) \leq F(x) \leq \underline{F}(x)$. When the functions $\overline{F}$ and $\underline{F}$ circumscribe an imprecisely known probability distribution, we call $[\overline{F}, \underline{F}]$, specified by the pair of functions, a "probability box" or "p-box" (Ferson, 2002) for that distribution. This means that, if $[\overline{F}, \underline{F}]$ is a p-box for a random variable X whose distribution *F* is unknown except that it is within the p-box, then $\underline{F}(x)$ is a lower bound on *F(x)* which is the (imprecisely known) probability that the random variable X is smaller than x. Likewise, $\overline{F}(x)$ is an upper bound on the same probability. From a lower probability measure $\underline{P}$ for a random variable *X,* one can compute upper and lower bounds on distribution functions using (Walley, 1991)

$$\overline{F}_X(x) = 1 - \underline{P}(X > x) \tag{3.20}$$

$$\underline{F}_X(x) = \underline{P}(X \leq x) \tag{3.21}$$

A typical diagrammatic expression of a p-box for an uncertain number *x,* that consist of lower and upper bound on the probability distribution for *x* is shown in Fig. 3.1.

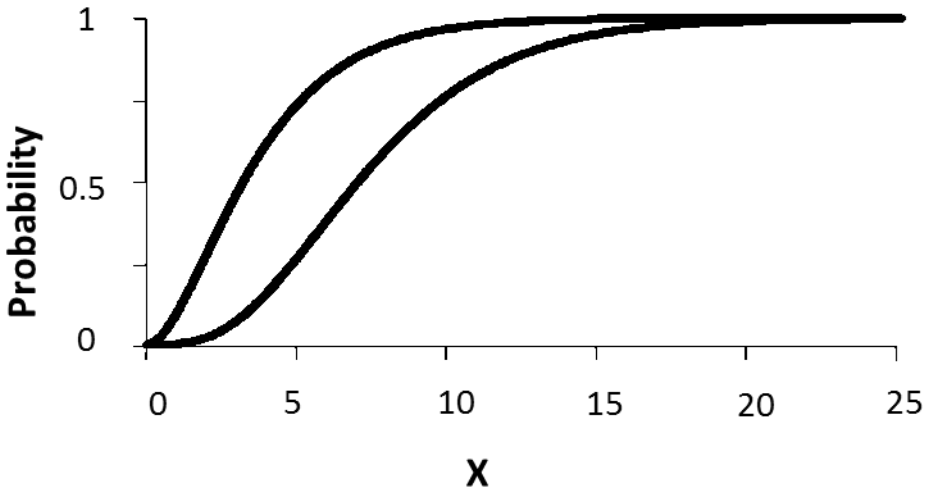

Figure 3.1: A typical probability box (p-box)

3.3.3 Probability plot

Probability plot is known as probability-probability plot and/or percent-percent plot. It is a graphical technique for comparing two data sets, either two sets of empirical observations, one empirical set against a theoretical set, (more rarely) two theoretical sets against each other, or whether or not a data set follows a given distribution (Chambers et al., 1983).

The data are plotted against a theoretical distribution in such a way that the points should form approximately a straight line. Any deviation/departures from this straight line imply deviation/departures from the specified distribution. Figure 3.2 shows a typical representation of probability-probability plot. The correlation coefficient associated with the linear fit to the data in the probability plot is a measure of the goodness of the fit. Estimates of the location and scale parameters of the distribution are given by the intercept and slope, which is one advantage of this method of computing probability plots. Probability plots can be generated for several competing distributions to see which provides the best fit, and the

probability plot generating the highest correlation coefficient is the best choice since it generates the straightest probability plot (Chambers et al., 1983).

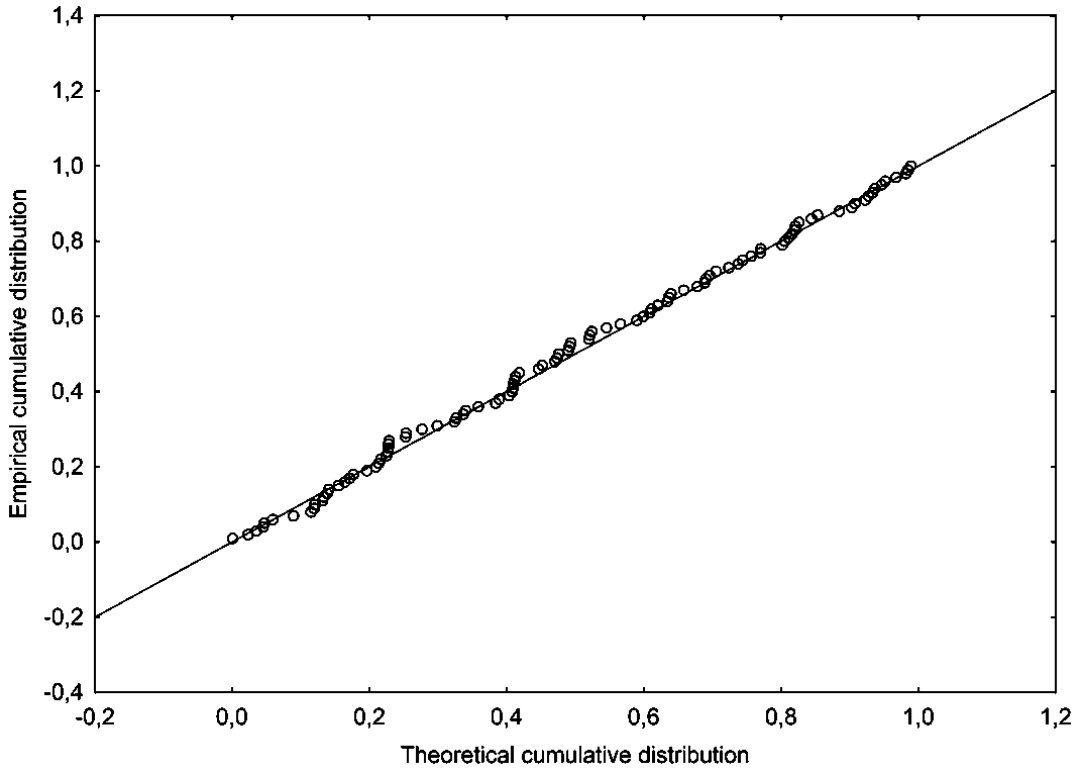

Figure 3.2: Typical representation of probability-probability plot

The interval estimation employed in the research work as a conceptual framework, particularly for reliability estimations of the structural systems is discussed fully with its applicability in Chapter 6.

In order to consider p-boxes from imprecise measurements view point, interval measurements have been used to generalize distributional estimates based on the maximum likelihood, which make shape assumptions for different distributions (Ferson et al., 2003). Even though the measurement uncertainty can be treated rigorously, the resulting distributional p-box generally will not be rigorous when it is a sample estimate based on only a subsample of the possible values. The fact that these calculations take account of the dependence between the parameters of the distribution, they will often yield tighter p-boxes.

3.4 Markovian Approach

3.4.1 Basic theorem

Suppose a structure is subject to a system of external loads $q_i(t), i=1,...,n$ described as non-differentiable random processes, the reliability analysis can be estimated by using Markovian processes theory.

Consider the reliability analysis of engineering structures and systems when it is subjected to two vector-type loads, which is regarded as combination of loads. The probabilities $P_{ij}(t)$ of a process dwelling in a fixed state, when the two vector-type loads are represented as independent markovian non-stationary homogeneous processes of Birth and Death type, can be calculated as a system of differential equations for the probability (Gnedenko et al., 1965; Timashev, 1982) as:

$$P_{ij} = P[q_1(t) = i; q_2(t) = j]$$

(3.22)

The systems of differential equations are of the form:

$$\begin{aligned} &\frac{d}{dt}P_{ij}(t) = -(\lambda_i + \mu_i + \lambda_j^{'} + \mu_j^{'})P_{ij}(t) + \\ &\lambda_{i-1}P_{i-1,j}(t) + \mu_{i+1}P_{i+1,j}(t) + \lambda_{j-1}^{'}P_{i,j-1}(t) + \mu_{j+1}^{'}P_{i,j+1}(t) \\ &i, j = 0.1,...; \lambda_{-1} = \mu_0 = 0; \lambda_{-1}^{'} = \mu_0^{'} = 0 \end{aligned} \tag{3.23}$$

The intensities of Birth λ_i and Death μ_i in this case depend only on the process $q_1(t)$, while the intensities $\lambda_j^{'}$ and $\mu_j^{'}$ depend on the process $q_2(t)$ only.

Subsequently, and without loss of generality, the initial conditions for the system in Eq. (3.22) may be taken as:

$$P_{0,0} = 1; P_{ij}(0) = 0; i, j = 1,2,... \tag{3.24}$$

Let's assume a region Ω with a boundary Γ is singled out in space $[q_1, q_2]$ and an auxiliary process $\bar{q}(t)$ is introduced such that $\bar{\lambda}_i = \lambda_i, \bar{\mu}_i = \mu_i, \bar{\lambda}_j^{'} = \lambda_j^{'}$ and $\bar{\mu}_j^{'} = \mu_j^{'}$ in points $(i, j) \in \Omega$ and $\bar{\lambda}_i = \bar{\mu}_i = \bar{\lambda}_j^{'} = \bar{\mu}_j^{'} = 0$ if points $(i, j) \in \Gamma$ which is the

boundary that is an absorbing one, then the probability of not leaving the region Ω by the process $\bar{q}(t)$ will be equal to :

$$R(t)=\sum_{i=0}^{m-1}\sum_{j=0}^{n}\bar{P}_{i,j}(t) \tag{3.25}$$

The system of differential equations satisfied by $\bar{P}_{i,j}(t)$ is written thus:

$$\begin{aligned}&\frac{d}{dt}\bar{P}_{ij}(t)=-\left(\bar{\lambda}_i+\bar{\mu}_i+\bar{\lambda}_j^{'}+\bar{\mu}_j^{'}\right)\bar{P}_{ij}(t)+\\&\bar{\lambda}_{i-1}\bar{P}_{i-1,j}(t)+\bar{\mu}_{i+1}\bar{P}_{i+1,j}(t)+\bar{\lambda}_{j-1}^{'}\bar{P}_{i,j-1}(t)+\bar{\mu}_{j+1}^{'}\bar{P}_{i,j+1}(t)\\&\bar{\lambda}_{-1}=\bar{\mu}_0=0;\bar{\lambda}_{-1}^{'}=\bar{\mu}_0^{'}=0\end{aligned} \tag{3.26}$$

The probability of the process $q(t)$ not leaving the region Ω is equal to the probability of the process $\bar{q}(t)$ staying within the region Ω at a moment of time t, is clearly reflected in Equation 3.25.

The probabilities of the process $q_1(t)[q_2(t)]$ at a moment of time t are in the $i(j)$ provided the state $m_j(n_i)$ is an absorbing one for it is denoted as:

$$P_i^{(m_j)}(t);i=0,1,\ldots,m_j;P_j^{(n_j)}(t);j=0,1,\ldots,n_i \tag{3.27}$$

Likewise, the corresponding systems of differential equations for estimating these probabilities are:

$$\left.\begin{aligned}&dP_i(t)/dt=-\left(\bar{\lambda}_i+\bar{\mu}_i\right)P_i(t)+\bar{\lambda}_{i-1}P_{i-1}(t)+\bar{\mu}_{i+1}P_{i+1}(t),\\&i=0,1,\ldots,m_j;\bar{\mu}_0=0,\bar{\mu}_i=\mu_i,\bar{\lambda}_i=\lambda_i;\\&i=0,1,\ldots,m_{j-1};\bar{\lambda}_{m_j}=\bar{\mu}_{m_j}=0;\\&P_0(0)=1;P_i(0)=0;i=1,2,\ldots,m_j.\end{aligned}\right\} \tag{3.28}$$

$$\left.\begin{aligned}
&\frac{d}{dt}P_j(t) = -\left(\bar{\lambda}_j + \bar{\mu}_j\right)P_j(t) + \bar{\lambda}_{j-1}P_{j-1}(t) + \bar{\mu}_{j+1}P_{j+1}(t),\\
&i = 0,1,\ldots,n_i;\ \bar{\mu}_0 = 0,\ \bar{\mu}_j = \mu_j;\ \bar{\lambda}_j = \lambda_j;\\
&j = 0,1,\ldots,n_{i-1};\ \bar{\lambda}_{n_i} = \bar{\mu}_{n_i} = 0;\\
&P_0(0) = 1, P_j(0) = 0,\ j = 1,2,\ldots,n_i.
\end{aligned}\right\} \quad (3.29)$$

Timashev, 1982 solved the problem of deriving a system of bilateral estimates for reliability function $R(t)$ on the basis of solutions of simplified systems of differential equations in Equations 3.23, 3.26, 3.28 and 3.29. Comprehensive details and notes on the markovian theories and approaches can be found in literatures.

Consider the following relation $\tilde{P}_{i,j} = P_i^{(m_j)}(t).P_j^{n_i}(t)$ in the light of an intermediate theorem as a proof (Lemma). For a region Ω which is such that $m_j \geq m_{j+1}; n_i \geq n_{i+1}; i = 0,1,\ldots,m_0 - 1;\ j = 0,1,\ldots,n_0 - 1$ and any moment of time $t > 0$

$$H(t) = \sum_{i=0}^{m_j - 1}\sum_{j=0}^{n_i - 1} h_{i,j}(t) \leq 0 \quad (3.30)$$

$h_{i,j}(t)$ are errors for an arbitrary point $(i, j) \in \Omega$ arising from substituting $\tilde{P}_{i,j} = P_i^{(m_j)}(t).P_j^{n_i}(t)$ into Eq. 3.25; calculated as:

$$\begin{aligned}
h_{i,j}(t) = {} & \bar{\lambda}_{i-1}P_{i-1}^{m_j}(t)\left[P_j^{n_i}(t) - P_j^{n_{i-1}}(t)\right] + \bar{\mu}_{i+1}P_{i+1}^{m_j}(t)\left[P_j^{n_i}(t) - P_j^{n_{i+1}}(t)\right] +\\
& \bar{\lambda}_{j-1}P_{j-1}^{n_j}(t)\left[P_i^{m_j}(t) - P_i^{m_{j+1}}(t)\right] + \bar{\mu}_{j+1}P_{j+1}^{n_i}(t)\left[P_i^{m_j}(t) - P_i^{m_{j+1}}(t)\right]
\end{aligned} \quad (3.31)$$

Based on the foregoing, the highlighted theorems below are true and hold based on the conditions of the lemma in permission of the construction of bilateral approximates for the reliability function.

For a region Ω, there exists a time T, finite or infinite and that $t < T$ such that $m_j \geq m_{j+1}; n_i \geq n_{i+1}; i = 0,1,\ldots,m_0 - 1;\ j = 0,1,\ldots,n_0 - 1.$ The reliability function $R_1(t)$ estimate can be calculated from the expression:

$$R_1(t) = \sum_{i=0}^{m_{j-}1} \sum_{j=0}^{n_{i-}1} P_i^{m_j}(t) P_j^{n_i}(t) = \sum_{i=0}^{m_{j-}1} \sum_{j=0}^{n_{i-}1} \tilde{P}_{i,j}(t) \tag{3.32}$$

This estimate is not larger than the true reliability function $R(t)$ i.e. $R_1(t) \leq R(t)$.

Following the conditions of the previous theorem above;

$R(t) \leq R_2(t)$ holds for any $t > 0$. $R(t)$ is the true reliability function, and $R_2(t)$ is thus estimated as:

$$R_2(t) = \sum_{i=0}^{m_{j-}1} \sum_{j=0}^{n_{i-}1} P_i^{m_0}(t) P_j^{n_0}(t) \tag{3.33}$$

In the condition where $R_3(t) \leq R_1(t)$, $R_1(t)$ is calculated using Equation 3.32, and $R_3(t)$ is estimated as:

$$R_3(t) = \sum_{i=0}^{m_0-1} P^{n_i}(t) \left[P^{n+1}(t) - P^i(t) \right] \tag{3.34}$$

Given that;

$$\left.\begin{aligned} P^{i+1}(t) &= \sum_{k=0}^{i} P_k^{i+1}(t) \\ P^{n_i}(t) &= \sum_{j=0}^{n_i-1} P_j^{n_i}(t) \end{aligned}\right\} \tag{3.35}$$

The probability $R_3(t)$ is the sum of the products of the probability that within the time t the $q_1(t)$ will at least once cross the level i but never cross the level $i+1$ by the probability that during the time t the process $q_2(t)$ will not cross the corresponding level n_i. In order to obtain $R_3(t)$, it will be sufficient if the probabilities that $q_1(t)$ and $q_2(t)$ processes will not cross the arbitrary levels are known. This information (Gnedenko et al., 1965; Barucha-Rheid, 1969) is made available through the distribution of maxima within the time t for the processes $q_1(t)$ and $q_2(t)$.

In the case of more than two vector-type loads, the results obtained from the first two theorems may be generalized. So for an *r*-dimensional load, the expressions for $R_1(t)$, $R_2(t)$ and $R_3(t)$ will assume the form:

$$R_1(t)=\sum_{i_1=0}^{n_i-1}\sum_{i_2=0}^{n_2-1}\ldots\sum_{i_r=0}^{n_r-1}P_{i_1}^{n_i}(t)P_{i_2}^{n_2}(t)\ldots P_{i_r}^{n_r}(t) \tag{3.36}$$

$$n_i=n_1(i_2,i_3,\ldots,i_r);n_2=n_2(i_2,i_3,\ldots,i_r);\ldots;n_r=n_r(i_2,i_3,\ldots,i_r);r=2,3,\ldots \tag{3.37}$$

The probability $P_{i_k}^{n_k}$ characterizes the component $x_k(t)$ of the process $\bar{z}(t)=[x_1(t),\ldots,x_r(t)]$.

$$R_1(t)=\sum_{i_1=0}^{n_1-1}\sum_{i_2=0}^{n_2-1}\ldots\sum_{i_r=0}^{n_r-1}P_{i_1}^{n_1^0}(t)P_{i_2}^{n_2^0}(t)\ldots P_{i_r}^{n_r^0}(t) \tag{3.38}$$

$$n_1^0=n_1(0,0,\ldots,0);n_2^0=n_2(0,0,\ldots,0);\ldots;n_r^0=n_r(0,0,\ldots,0) \tag{3.39}$$

$$R_3(t)=\sum_{i_1=0}^{n_1-1}\left\{\left[P^{i_1+1}(t)-P^{i_1}(t)\right]\left\{\sum_{i_2=0}^{n_2-1}\left[P^{i_2+1}(t)-P^{i_2}(t)\right]x\ldots x\sum_{i_{r-1}=0}^{n_{r-1}-1}\left\{\left[P^{i_r+1}(t)-P^{i_{r-1}}(t)\right]P^{n_r}(t)\right\}_{r-1}\right.\right.\{\ldots\} \tag{3.40}$$

$$n_2=n_2(i_1);n_3=n_3(i_1,i_2);\ldots;n_r=n_r(i_1,i_2,\ldots,i_{r-1}) \tag{3.41}$$

Similarly, $P^k(t)$ specifies $x^k(t)$.

Equation 3.36 can be modified for a specialized case, when the last *r*-th coordinate of the *r*- dimensional process is a Poisson process for which the probability $P_{i_r}^{n_r}(t)$ is independent of the absorbing state, to the form:

$$R_1(t)=\sum_{i_r=0}P_{i_r}(t)\sum_{i_1=0}^{n_i-1}\sum_{i_2=0}^{n_2-1}\ldots\sum_{i_r=0}^{n_r-1}P_{i_1}^{n_i}(t)P_{i_2}^{n_2}(t)\ldots P_{i_{r-1}}^{n_{r-1}}(t) \tag{3.42}$$

In practice when multidimensional random processes are encountered in which only some components are markovian Birth and Death processes; the reliability function $R(t)$ can be estimated by synthesizing Eqs. (3.36) and (3.40).

Let $z(t)=[x_1(t),...,x_r(t)]$ be an *r*-dimensional random process and K coordinates of the process $z(t)$ be markovian Birth and Death process. These components may be assumed to be $x_{r-k-1}(t),...,x_r(t)$, whereby the reliability function may be written as:

$$R(t)=P\left[Z(t)\in D^r \,|\, 0\le t\le T\right] \tag{3.43}$$

r is the dimension of the region *D.*

From Equations (3.36) and (3.40);

$$R(t)=\tilde{R}(t)=\sum_{i_1=0}^{n_1-1}\left\{\left[P^{i_1+1}(t)-P^{i_1}(t)\right]\right\}x\left\{\sum_{i_2=0}^{n_2-1}\left[P^{i_2+1}(t)-P^{i_2}(t)\right]\right\}...\left\{\sum_{i_{r-k}=0}^{n_{r-k}=0}\left[P^{i_{r-k}+1}(t)-P^{i_{r-k}}(t)\right]\right\}_{r-k-1}\{...\}x$$
$$P\left\{Z_k(t)\in D^k \,|\, 0\le t\le T\right\}$$

(3.44)

A *k*-dimensional markovian process is denoted by $Z_k(t)=[x_{r-k-1}(t),...,x_r(t)]$; $D^k=D^k_{i_1,...,i_k}$ is a K-dimensional quality space region depending on the values of $i_1,...,i_{r-k}$.

$$P\left\{Z_k(t)\in D^k \,|\, 0\le t\le T\right\} \tag{3.45}$$

Equation (3.45) is the probability that the *K*-dimensional markovian process will never extend beyond the region D^k within the time $t\in[0,T]$. This also can be calculated using Eq. (3.36). Estimate from the combination of Eqs. (3.36) and (3.40) is trivial/cumbersome compare to Eq. (3.40). Reliability function estimates from Eq. (3.44) is closer to the true value than the one obtained in Eq. (3.40).

3.5 Reliability assessment of structural systems subject to random vector of combined loads

The problem of load combination is of great significance in structural analysis, whereby the loads are traditionally considered as constants and probably because of safety, it is taken as the maximum values and this inputted in the design codes.

The loads are rather to be considered as having a stochastic nature. For example, Figures 3.3 and 3.4 are schematic illustrations of a continuous random load process and the potential exceedance of the deteriorating structural resistance; and typical outcrossing event in structural resistance space.

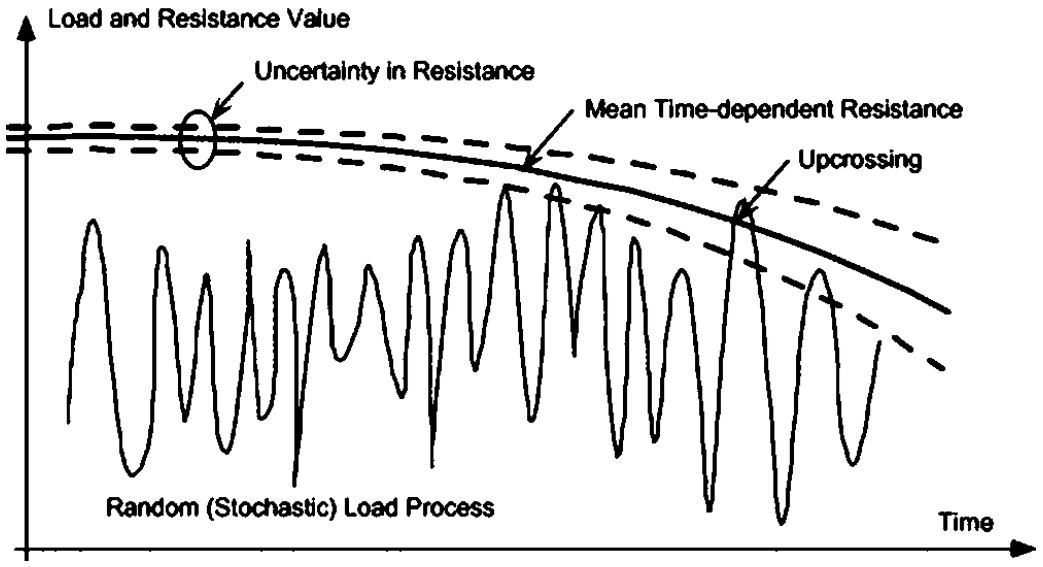

Figure 3.3: Realization of a continuous random load process Q(t) and the potential exceedance of the deteriorating structural resistance R(t) – Melchers, 2005.

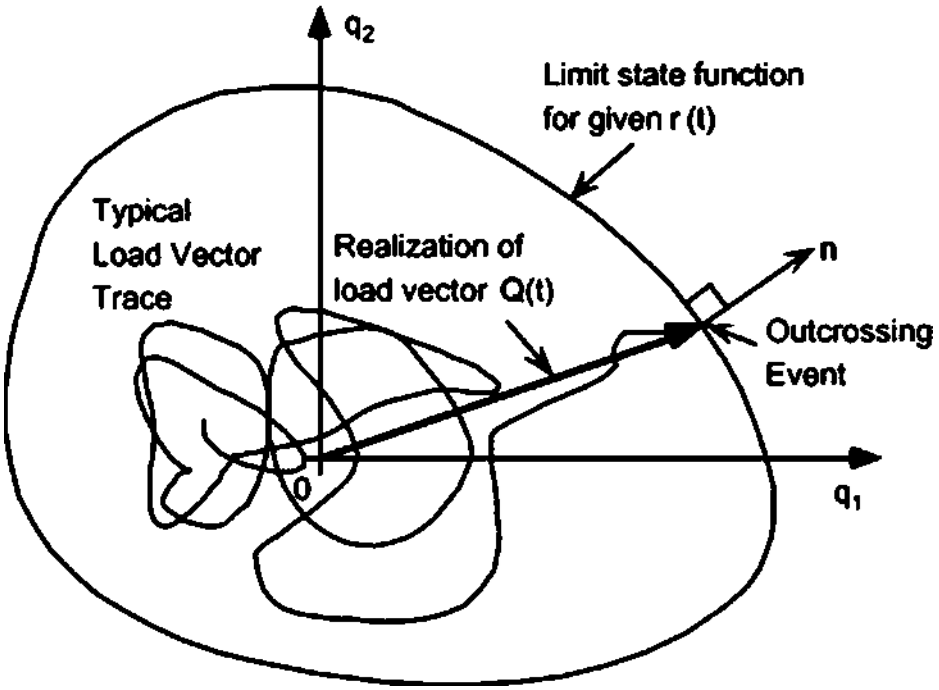

Figure 3.4: Typical outcrossing event in structural resistance space r(t) – Melchers, 2005.

Reliability analysis of structural (such as pipeline) systems subject to random vector of combined loads using Markovian approach is proposed in this work, where external forces are described by non-differentiable processes or when the problem requires calculations of the probabilities of processes up crossing low levels – such as when dealing with combination of random loads (Timashev, 1982). An advantage of this approach is that the essence of the problem is simple to interpret and dramatic. The structural engineer will be aware of the quality criteria that are the most stringent, and the elements that do not participate in the formation of the admissible regions; even before reliability function computation.

3.5.1 General case

In a general case, the reliability assessment of structural systems subject to random vector of combined loads can be estimated following the steps below:
Schematization of the structural (e.g. pipeline) system: selecting the input parameters space *Q* and the output parameter space *U*; such that introduction of system operator is inculcated as: $Lu = q; u \in U, q \in Q$

The elements are singled out in the operator: in operator L, the elements χ, χ_0, χ_S are singled out; where χ, χ_0 are the elements of K and K_0 spaces respectively of determinate properties of the system which are/are not subject to optimization; χ_S is the elements of space K_S of those properties of the system which are stochastic in nature

Solution of inverse problem of mechanics: the determination of the permissible subspace V in the space U, and the admissible region $\Omega_0(\chi_C)$ in the space Q

The system conditional reliability: estimation of the conditional reliability of the system, as:

$$R_C(t) = P[q(\tau) \in \Omega_C(\chi_C), 0 \le \tau \le t] \tag{3.46}$$

Finally, the total full reliability is calculated as:

$$R(t) = \int_{\chi_C} \ldots \int R_C(t) f(\chi_C) d\chi_0 \tag{3.47}$$

The admissible region of the reliability problem solved in the load space is constructed according to the equation

$$v_* = H(q, \chi_c) \tag{3.48}$$

v_* is the ultimate permissible value of the quality of vector of the system, H is the inverse to operator L.

3.6 Monte Carlo Simulation

This simulation process involves generating random variables and exhibits random behaviours, it has been named Monte Carlo simulation following after Monte Carlo city in Monaco which is well known for gambling such as dice, roulette, and slot machines. In uncertainty analysis methodology, it gives accurate solutions when enough samples are used, and can generate the complete distribution; when it comes to capability and accuracy. For efficiency, it needs a large number of function evaluations, especially when the probability is high. Monte Carlo simulation is very robust, and can always find the solution to classical optimization problems.

In a nutshell, Monte Carlo simulation performs random sampling and conducts a large number of experiments on computer. Three (3) major steps are taken into consideration in the simulation procedures viz:

Sampling on random input variables $X=(X_1,X_2,X_3,...,X_n)$ to generate samples that represent distributions of the input variable from their cdfs $F_{X_i}(x_i)(i=1,2,3,...,n)$ and in turn used as input to the simulation,

Evaluating model outputs Y are calculated through the performance function $Y=g(X)$ at the samples of input random variables, and

Statistical analyses on model output, e.g. mean variance, reliability, failure probability, cdf and pdf.

Suppose after generating N samples of each random variable, N sets of inputs $x_i=(x_{i1},x_{i2},x_{i3},...,x_{in}),i=1,2,3,...,N$ are formed from all the random variables samples and then inputted into the model $Y=g(X)$. The reliability of the structural system can be estimated, if the failure event is denoted by $g\le 0$. Then the failure probability is calculated as follows:

$$P_f=\frac{N_f}{N} \tag{3.49}$$

where N_f is the number of samples with $g\le 0$.

Finally, the reliability is estimated as $R=1-P_f$, which can be rewritten as:

$$R=\frac{N-N_f}{N} \tag{3.50}$$

Similarly, the other statistical outputs of the model such as mean, variance, cdf and pdf can be estimated by the following equations respectively:

$$\mu=\frac{1}{N}\sum_{i=1}^{N}y_i \tag{3.51}$$

$$\sigma^2=\frac{1}{N-1}\sum_{i=1}^{N}(y_i-\mu)^2 \tag{3.52}$$

$$F_Y(y)=\frac{1}{N}\sum_{i=1}^{N}I'(y_i) \tag{3.53}$$

Lastly, the pdf can be determined from the numerical differentiation of the cdf.

For many engineering problems, a performance function is expensive to evaluate, and approximate method – e.g. FORM and SORM may or may not be applicable for large scale problems, we have resort to Monte Carlo simulation based methods. Efficient Monte Carlo simulation strategy is required for analyzing complex real world problems.

Efficient Monte Carlo simulation is one of the most useful approaches to scientific computing due to its simplicity and general applicability. Monte Carlo techniques have proven very useful and powerful tool for providing optimal design, scheduling, and control of industrial-size systems, as well as offering new approaches to solve classical optimization problems. In many applications the complicated objective functions are deterministic, and randomness is introduced artificially in order to more efficiently search the domain of the objective function. It is also used to optimize noisy functions, where the function itself is random. In most cases, the Monte Carlo techniques have evolved directly from methods developed and designed for machines with a single processor. However, with the high performance computing, many processors running in parallel are used. While many Monte Carlo algorithms are inherently parallelizable, others cannot be easily adapted to this new computing demand. An efficient Monte Carlo technique that performs reliably (i.e. an effective random number generation technique for parallel computing) in the parallel processing framework is proposed to perform robust maintenance scheduling taking into account uncertainty and imprecision. It is applied for example in this research, to determine the optimal inspection interval and the repair strategy that would maintain adequate reliability level throughout the service life of the pipelines and bridges. The proposed reliability strategies are implemented in the general purpose software OpenCossan (Patelli, 2016).

3.7 Reliability-Based Optimization

In reliability-based optimization of structures, the total expected costs in relation to initial, maintenance and failure for the structure can be used as objective function

for optimal reliability-based inspection planning (see e.g. Enevoldsen and Sorensen, 1994). For example and in this work, the decision/design variables in inspection planning for fatigue cracks of individual critical points are usually the number of inspections in the remaining lifetime, time interval between inspections, qualities of inspection, and the number of repair actions based on the measured crack size possible.

The total cost of operation is formulated and adopted as a deterministic substitute optimization problem in Enevoldsen and Sorensen, 1994 as:

$$\min_{N_I,t,e,d} C_T\left(N_I,t,e,d\right)=C_I\left(N_I,t,e.d\right)+C_R\left(N_I,t.e.d\right)+C_F\left(N_I,t,e,d\right) \tag{3.54}$$

$$s.t. \qquad \beta\left(T_L,N_I,t,e,d\right)\geq\beta_{\min} \tag{3.55}$$

where N_I, t, e, and d denote the number of inspections in the remaining lifetime, time interval between inspections, qualities of inspection, and the number of repair actions based on the measured crack size possible; C_T, C_I, C_R and C_F are the expected total cost of operation, expected costs of inspection, repairs and failure respectively.

T_L is the expected lifetime and $\beta(T)$ is the generalized reliability index at the time T defined by:

$$\beta(T)=-\phi^{-1}\left(P_F(T)\right) \tag{3.56}$$

where $P_F(T)$ is the probability of failure in the time interval $[0,T]$ and ϕ^{-1} is the standardized normal distribution function.

The constraint on the minimum reliability Eq. (3.55) is somewhat unnecessary, as the reliability is already incorporated in the objective function through the expected cost of the failure term, but it is included to take account of prefixed code demands set up by authorities. Other constraints, for example on maximum of the individual costs or direct bounds on the optimization variables can be included in the problem, if necessary. Further, deterministic constraints may be needed to model limits of the inspection parameters. The optimization problem (Eq. 3.54) and (Eq. 3.55) is a general non-linear optimization problem with real, continuous and discrete variables.

The inspection cost represents the expenditures on performing non-destructive inspection. This inspection cost is an uncertain variable because of the possibility of structure, system or components failing before inspection. In this work it is assumed that failure before inspection is a rare event (i.e. failure not occurring very often), the probability of failure is far less than one ($P_F \ll 1$), hence it is deterministic and can be computed analytically. The expected inspection cost is calculated as the product of the unit inspection cost corrected by the discount rate and the probability that inspection takes place, e.g. Enevoldsen and Sorensen, 1994. This expected cost is expressed in mathematical form as:

$$\text{Inspection Cost, } C_I = \frac{c_I(q)}{(1+r)^{T_I}}\left(1-P_F^T\right) \qquad \left(P_F << 1\right) \tag{3.57}$$

where $c_I(q)$ is the unit cost of performing inspection of quality q, r is the discount rate and P_F^T is the probability that failure occurs before T_I.

The evaluation of the expected cost associated with repair is quite challenging, it is closely related with the evaluation of reliability; thus, methods of structural reliability have been applied in the literature in order to evaluate expected costs (Enevoldsen and Sorensen, 1994; Gasser and Schuëller, 1997; Valdebenito and Schuëller, 2010).

The expected repair costs are modelled as:

$$\text{Repair cost, } C_R = \sum_{i=1}^{N_I} C_{Ri}.P_{Ri}.\frac{1}{(1+r)^{T_I}} \tag{3.58}$$

where *i*th term represents the capitalized expected repair costs at the *i*th inspection; C_R, is the cost of a repair at the ith inspection and P_{Ri} is the probability of performing a repair after the *i*th inspection when failure has not occurred earlier.

The total capitalized expected costs due to failure are determined from Eq. (3.59), like the repair costs, it is the cost function associated with failure over the region of the corresponding demand functions with the first and second failure criterion, as a measure of uncertain parameters associated with the repair event.

$$C_F = \sum_{i=1}^{N_{I+1}} C_F(T_F).(P_F(T_F) - P_F(T_{F-1})).\frac{1}{(1+r)^{T_F}} \tag{3.59}$$

$C_F(T)$ is the cost of failure at the time T, and T_F is the time at which failure takes place.

3.8 Numerical Computation Programs

3.8.1 OpenCossan

COSSAN-X is a software package developed to make the concepts and technologies of uncertainty quantification and risk analysis available. One can perform realistic and reliable stochastic analysis of models, identify most critical components and optimize it, and many more using a simple graphical user interface.

The OpenCossan engine is an invaluable tool for uncertainty quantification and management representing the core of COSSAN software. All the algorithms and methods have been coded in a Matlab toolbox via Matlab command line interface allowing numerical analysis, reliability analysis, simulation, sensitivity, optimization, robust design and much more. This interaction method is especially offered to provide a high-level programming environment for advanced users. Using the command line interface, users and researchers can modify pre-written solution sequences, explore data, implement new algorithms, and more. This offers the ability to simply create custom tools, which enable the solution of specialised problems.

OpenCossan represents the computational core of the COSSAN project. It is an open and free toolbox for Uncertainty Quantification and Management and contains a collection of open source algorithms, methods and tools under continuous development at the Institute for Risk and Uncertainty, University of Liverpool, UK.

Most of the proposed approaches in this research work have been implemented in OpenCossan - the open source engine of COSSAN software for uncertainty quantification and risk management (Patelli et al., 2014; Patelli, 2016).

3.9 Summary

The theoretical frameworks presented in this chapter are the main concepts and approaches used in this thesis. Even though the theories and the methodologies are wide, the descriptions given here were simplified, made straight forward, and prepared intentionally to suit the content of the thesis.

Reliability analysis methods provide a framework to account for numerous sources of uncertainties that should be considered in engineering design and problems in a rational and vigorous manner. An overview of the use of imprecise probabilities (p-boxes and interval analysis) and Markovian approaches for reliability assessments and reliability-based optimization of structures has been presented. Likewise, the simulation process for uncertainty analysis using Monte Carlo simulation approaches, and the implementation of the same in OpenCossan - the open source engine of COSSAN software for uncertainty quantification and risk management is outlined.

Having the theoretical and practical analytical tools for measuring quantitatively the performance and integrity of the structural system; and to further consider realistically the uncertainties in ensuring faultless life of engineering structures and systems, models are needed. In many problems that involve modelling the behaviour of some systems, we lack sufficiently detailed information to determine how the system behaves, or the behaviour of the system is so complicated that an exact description of it becomes irrelevant or impossible. In that case, a probabilistic model is often useful.

To quantify these uncertainties, probabilistic model choice must be handy for robust maintenance strategy and this becomes the subject of the next chapter. Discussion on the modelling of the fatigue cracks, corrosion growth, and applied loads in structural metallic bridges and pipelines will be dealt with in chapter 4.

4. Numerical Models

4.1 Introduction

This chapter is concerned with the numerical modelling of fatigue cracks and corrosion deterioration, as the most important degradation mechanisms phenomena occurring in metallic structures. Under the background and research significance in Chapter 1 of this write up, it has been spelt out that the failures in metallic structures are fatigue, fracture, and corrosion related. These has formed the major scope and focus in this research to an extent in relation to uncertainty quantification. Part of the original work here consists of extension to the previous works through inclusion of imprecise mean values, interval analysis, probability bounds, and Markovian description on the modelling of these deterioration phenomena and loads.

Engineering modelling is the process of solving physical problems by appropriate simplification of reality, whereby fundamental scientific studies and exhaustive understanding of the physical phenomena has provided a reliable and set guideline. Numerical modelling has been adopted for nondestructive evaluation in this work.

The primary mission of uncertainty quantification is to find the probabilistic characteristics of model outputs (i.e. response variables). In other words, it is to find the probabilistic characteristics of a performance function given the distributions of random variables. This helps the engineers to understand how uncertainty of the model input impacts the uncertainty of the model output, so as to be able to manage and mitigate the effects of uncertainty by choosing appropriate design variables (model inputs) during the design/maintenance process.

In the numerical modelling of this research, all the variables that affect the deterioration mechanism phenomena are identified; reasonable assumptions and approximations are made after a careful study on the variables interdependency.

This further leads to formulating the problems mathematically and solved using proposed approaches in chapter 3 and results interpreted in chapters 5, 6 and 7.

4.2 Fatigue Cracks Model

4.2.1 Fatigue crack propagation

The presence of a crack in a component or structure can reduce its life significantly. The intention of this section therefore is to define and discuss on model describing the fatigue crack propagation dimensions at given times. A simple illustration of this analogy is described in Fig. 4.1 for a structural member or component subjected to repeated applied loading and/or unloading. The initial stage of the cyclic loading known as crack nucleation is when small cracks are formed, and this is often times at many locations in the structure or system. These cracks regarded as “small cracks” at the outset are too small to cause fracture, but later extend or propagates as time goes on under the repeated loading. The amalgamation of some of these cracks will continue to grow in a stable form to become a dominant crack that will in turn reach a size that can cause fracture.

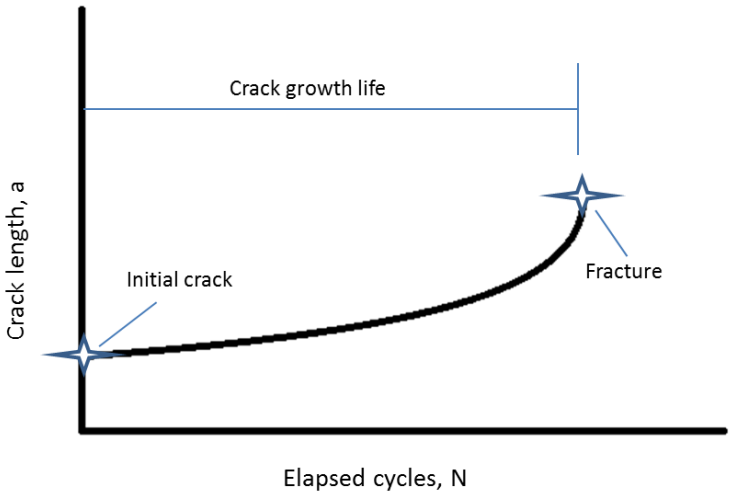

Figure 4.1: Schematic illustration of crack formation and propagation following a period of cycling loading.

For a given size of initial crack, the useful life to fracture is a function of the magnitude of the applied stress and the material's final fracture resistance. This final fracture resistance of the material also serves as a control for the critical crack size or final crack length. It is possible to estimate the number of cycles a structure or component can sustain before being replaced and scheduling the inspection interval from the curve in Fig. 4.1. The limitation is the uncertainty on this curve (about tens of percent as the level of uncertainty), therefore requiring regular intervals to validate or modify the life prediction.

For full details on fatigue crack propagation readers are referred to Anderson, 1991 and other literatures on fracture mechanics. This section is not aiming to provide detailed understanding of the processes of the subject, however, the crack propagation model's limitations and shortcomings will be discussed.

Considering crack growth due to fatigue, there are three modes describing crack displacement of structures and these are show in turn, see Fig. 4.2:

Mode I:

- Opening or tensile mode
- For most structures this mode is the dominant condition.
- Cracks tend to grow on the plane of maximum tensile stress.
- Other mode cracks, i.e. II and III, in combination with mode l cracks often turn into mode l cracks
- When stress intensity factor, K is used without a mode subscript, it normally refers to mode I

Mode II:

- Sliding or in-plane shear

Mode III:

- Tearing or anti-plane shear.
- It is associated with a pure shear condition, typical of a round notched bar loaded in torsion.

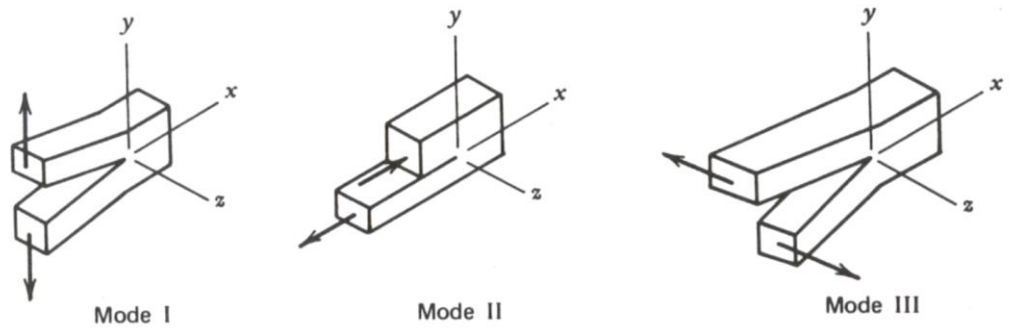

Figure 4.2: A schematic representation of each of these three modes.

Mode I crack displacement or extension is used in modelling fatigue degradation in this work because it is the most common one, and particularly the combination of modes II and III often turn into mode I cracks.

Crack propagation can only occur during the portion of the cycle when the crack is open. An effective stress intensity range should be employed to characterize the crack growth rate. The fatigue crack growth rate, da/dN, is simply the slope of crack length (a) against applied cycles (N) curve at a given crack length or given number of cycles as identified by da/dN. The damage due to fatigue is addressed using a fracture mechanics approach; this allows simulating the crack propagation phenomenon by integrating appropriate laws that describe the crack growth. Crack growth rate da/dN is obtained by applying Linear Elastic Fracture Mechanics (LEFM) concepts to a-N data, versus the applied stress intensity factor range, ΔK as shown in Fig. 4.3

The fatigue crack propagation behaviour of many materials can be divided into three regions as shown in Fig. 4.3.

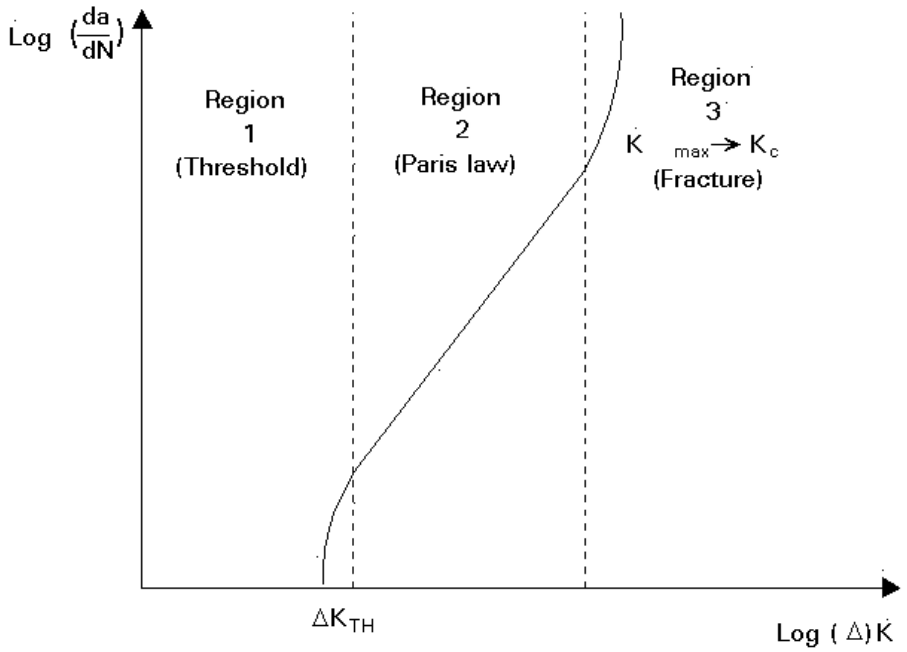

Figure 4.3: Typical fatigue crack propagation behaviour of many metallic materials in fracture mechanics

Region 1:

- This is near threshold region where crack growth rate is small, and threshold effects are important
- This is the initiation stage, and the threshold occurs at crack growth rates of the magnitude of 10^{-10} meters per cycle or less
- The Paris-Erdogan law cannot model this region of fatigue crack growth
- This region of crack growth is controlled mainly by the environment, microstructure and mean stress
- The stress intensity factor at the tip of the crack is too low to propagate a crack.

Region 2:

- The fatigue crack growth here is consistent and predictable, also corresponds to stable macroscopic crack growth

- In this region, mean stress and microstructure have less influence on fatigue crack growth
- The rate of crack growth changes roughly linearly with a change in stress intensity fluctuation.

Region 3:

- The fatigue crack growth rate here is very high, rapid and unstable
- Little fatigue crack growth life is involved, since it does not contribute significantly to the fatigue life, it is ignored
- Small increases in the stress intensity amplitude produce relatively large increases in crack growth rate since the material is nearing the point of unstable fracture.

The entire fatigue process involves the nucleation, growth of a crack or cracks (i.e. in stages I and II) to final fracture. In this research work, Region 2 is considered only, simply because the stress intensity factor at the tip of the crack is too low to propagate a crack as depicted in Region 1, and little fatigue crack growth life is involved in Region 3 since it does not contribute significantly to the fatigue life, it is ignored.

4.2.2 Failure and fracture

The ultimate cause of all fatigue failures is that a crack has grown to a point at which the remaining material can no longer tolerate the stresses or strains, and sudden fracture occurs. Fracture implies the last stage of the fatigue process; it is the separation of a component or structure into two or more parts. The fracture resistance of a material is characterised by its toughness, i.e. a quantity which can be a function of temperature and loading rate as well as geometric constrain to yield (could be specimen thickness for example).

Failure in the context of this work is not that of the ultimate cause of all fatigue failures where a crack has grown to a point at which the remaining material can no

longer tolerate the stresses or strains, and sudden fracture occurs. Neither is it fracture, the last stage of the fatigue process; which is the separation of a component or structure into two or more parts. Failure here is when bridges are closed or restricted due to repair actions or penalty charged to the owner (in case of private). When considering whether to restrict lanes, close bridges temporarily, or construct a detour bridge, but the only costs are those to conduct the actual work (not fees or penalties charged by the government, in case of public)

4.2.3 Stress intensity factors

Irwin, (1957) introduced the stress intensity factor which has been accepted as the basis of linear elastic fracture mechanics and of fatigue crack growth life predictions. The stress intensity factor K is the linear elastic fracture mechanics quantity that characterises the crack tip stress field which is the main parameter that controls fracture and subcritical crack growth rates. It relates remote load, crack size, and structural geometry. It is expressed in the form $K = \sigma\sqrt{\pi a\beta}$, where σ is the applied stress, a is the crack length, and β is a dimensionless factor which depends on the crack length and the component geometry.

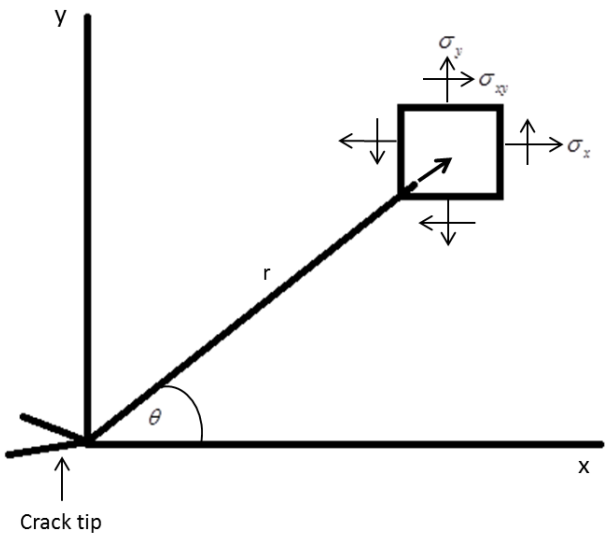

Figure 4.4: Crack tip stress schematic.

The stress intensity factors are based on the elastic stresses σ_i at a point (r,θ) near the crack tip as shown in Fig. 4.4. These are defined for modes I, II, and III in Fig. 4.2 as:

$$\left.\begin{aligned} K_{ModeI} &= \lim_{r\to 0}\sqrt{2\pi r}\,\sigma_y(\theta=0) \\ K_{ModeII} &= \lim_{r\to 0}\sqrt{2\pi r}\,\sigma_{xy}(\theta=0) \\ K_{ModeIII} &= \lim_{r\to 0}\sqrt{2\pi r}\,\sigma_{yz}(\theta=0) \end{aligned}\right\} \quad (4.1)$$

Crack growth theories have formed the bridge that links fatigue and fracture mechanics concepts (Su and Zheng, 2013; Newman Jr., 1998). The most important contribution is the establishment of the relationships between the crack growth rate d*a*/d*N* and the stress intensity factor. The most widely used fatigue crack growth model, commonly known as Paris law, was proposed by Paris and Erdogan, 1963. The Paris law connects the crack growth rate with the amplitude of stress intensity factors through a simple power function, which makes the engineering application more easily. After that, various modifications and extensions to Paris law have emerged, and different forms of modified crack growth equations have been offered by Forman et al. (1967); Elber (1970) and Walker (1970).

Analytical expressions for calculating stress intensity factors exist for very simple cases only, that usually involves a single crack or several symmetric cracks (Anderson, 1991). In more general cases, it is necessary to resort to numerical methods for calculating stress intensity factors, such as Finite Element Method (FEM) - Finite Element Alternating Method (FEAM), Extended Finite Element Method (XFEM); Boundary Element Method; Meshless methods, etc.

In this research work, the finite element method in which the global FEA (Finite Element Analysis) model, 2D FEA model, and 3D FEA model is applied in estimating stress intensity factors.

4.2.4 Fatigue crack growth rate models

Sophisticated fatigue crack growth models have been developed to correlate constant amplitude fatigue crack growth rates with various loading parameters

(Grandt, 2004). The proposed fatigue crack growth models are based on curve-fitting techniques and used primarily with computer programs to interpolate between experimental data obtained for various test conditions. Some of the models are listed here with their limitations.

- Paris equation (Paris and Erdogan, 1963)

$$\frac{da}{dN} = C\Delta K^{m} \tag{4.2}$$

- Forman equation (Forman et al., 1967)

$$\frac{da}{dN} = \frac{C\Delta K^{m}}{(1-R)K_c - \Delta K} \tag{4.3}$$

- Walker equation (Walker,1970)

$$\frac{da}{dN} = C\left\{K_{\max}(1-R)^{m}\right\}^{n} \tag{4.4}$$

- Collipriest equation (Forman and Hu, 1984)

$$\frac{da}{dN} = C(K_c\Delta K)^{n/2}\exp\left\{\ln\left(\frac{K_c}{\Delta K_0}\right)^{n/2}\arctan h\left(\frac{\ln\left[\Delta K^{2}/(1-R)K_c\Delta K_0\right]}{\ln\left[(1-R)K_c/\Delta K_0\right]}\right)\right\} \tag{4.5}$$

- NASGRO model (Forman et al., 1998)

$$\frac{da}{dN} = C\left\{\left(\frac{1-f}{1-R}\right)\Delta K\right\}^{n}\frac{(1-\Delta K_{th}/\Delta K)^{p}}{(1-K_{\max}/K_c)^{q}} \tag{4.6}$$

Where C, m, K_c, ΔK_0, n, p, and q are empirical constants. $\Delta K(\Delta K = K_{\max} - K_{\min})$ is either the sole load or two load variables, $R(R = \sigma_{\min}/\sigma_{\max})$ is the stress ratio, and f is the crack opening function.

The simple equation in Paris model is quite limited, it does not contain neither of the lower and upper asymptotes in the general sigmoidal $da/dN - \Delta K$ behaviour. It does not have a mean stress term. The possibility of a series of this equation could be used to fit various regions of the crack growth curve thereby providing a method to treat and estimate the asymptote case.

Walker model accounts for mean stress but does not provide the lower and upper asymptotes. Owing to the inverse hyperbolic tangent function in Collipriest model, even though it provides capability to estimate the lower and upper asymptotes, the

mathematical expressions used to correlate fatigue crack growth data is quite complex. In Forman equation, da/dN depends on R and yields an upper asymptote as the crack growth rate gets very large when $K_{\max}$ in ΔK approaches K_c. The description of the full sigmoidal nature of the fatigue crack growth rate curve is done in the NASGRO model.

4.2.5 Life estimation

Life estimations for fatigue crack growth and damage tolerance design are usually done by using the following important information: The stress intensity factor, the fracture toughness, the applicable fatigue crack growth rate expression, the initial crack size, and the final or critical crack size.

A provisional classification of the basic variants of the approaches for fatigue estimation is shown in Fig. 4.5. The methods become more exact and more demanding as it progresses.

Strength assessments are known as global approaches if they proceed directly from the external forces and moments or from nominal stresses in the critical cross-section. The global approaches use critical values of load or nominal stress which are related to global phenomena, like fully plastic yielding or total fracture of the specimen. On the other hand, strength assessments are termed local approaches if they proceed from local stress or strain parameters. The later take into consideration the local processes of damage by material fatigue, i.e. crack initiation, crack propagation and final fracture. Crack initiation is covered by the notch stress approach or notch strain approach which is based on the stresses or strains at the notch root/comparable regions of stress concentration. The crack propagation and final fracture is described by the crack propagation approach. The strength assessment in accordance to the complete local approach consists of notch stress or notch strain approach, and the crack propagation approach.

The most vital basic variants of the global and local approach as shown in Fig.4.5 have each variant characterised by the typical load, stress or strain parameter and the corresponding strength diagram (Radaj and Sonsino, 1998).

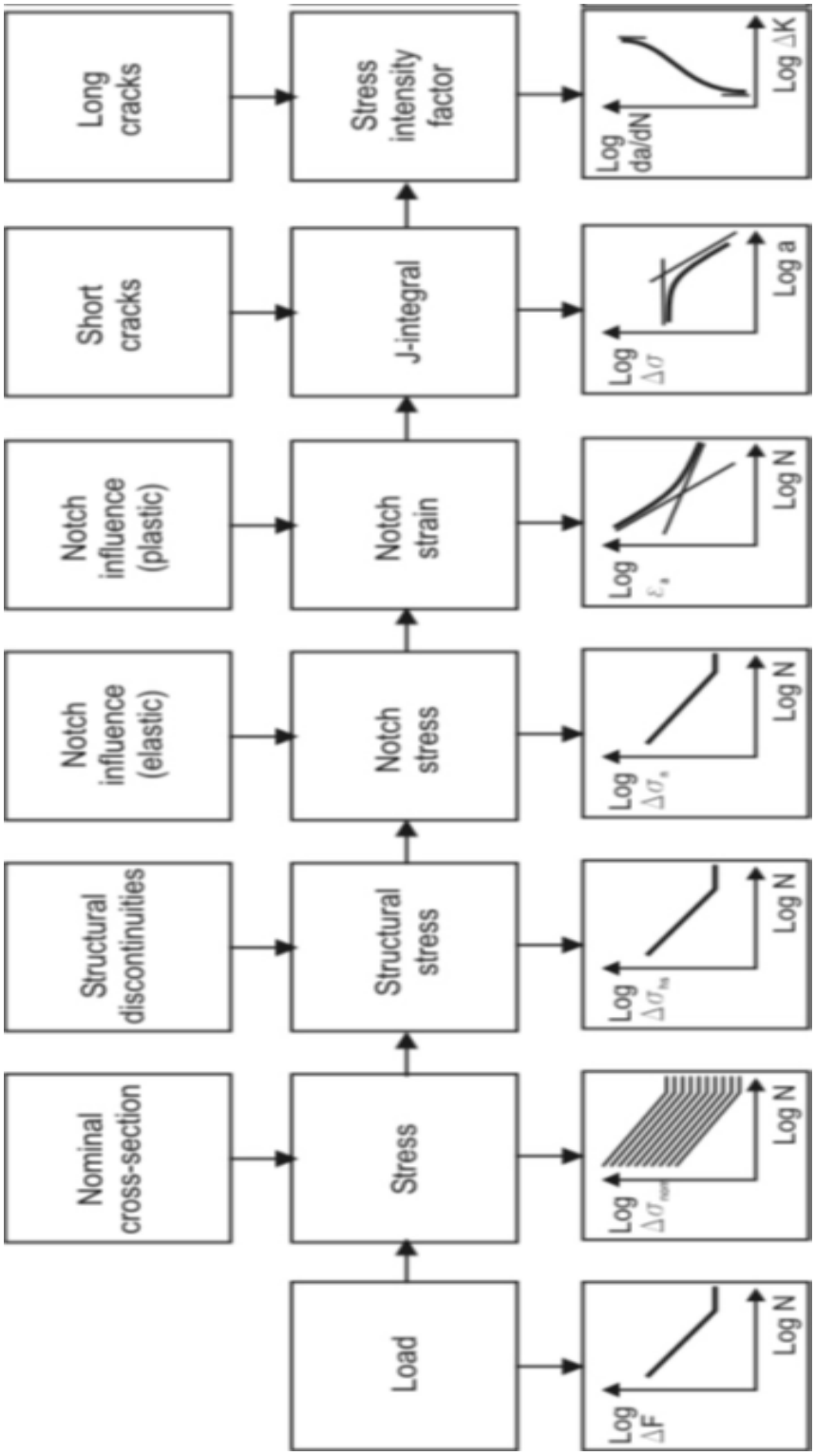

Figure 4.5: Various approaches for fatigue life evaluations (Radaj and Sonsino, 1998)

J-Integral has been proved to have several interesting features such as its definition for a nonlinear elastic body which made it a valid parameter in the deformation

theory of plasticity, and that the integral is path independent. The shortcomings of the J-Integral is that some mathematical rigour are lost when applied to crack growth, also analysis and test techniques can be quite complex for engineering applications.

The life estimation is made by adopting Paris-Erdogan's law as the applicable fatigue crack growth rate expression, and the stress intensity factors modified in Fisher et al., 1989 as follows:

Paris-Erdogan Law

$$\frac{da}{dN}=C\Delta K(a)^M \tag{4.7}$$

Where da/dN is crack growth rate, C and M are empirical constants of the material; N is the number of cycles and ΔK is the alternating stress intensity factor.

Stress Intensity Factor, K:

$$K=F_e.F_s.F_w.\sigma.\sqrt{\pi.a} \tag{4.8}$$

$$F_e=\sqrt{\frac{1}{\varphi(a)^2+0.5\frac{\Delta\sigma}{\sigma_{ys}}}} \tag{4.9}$$

$$\varphi(a)=\int_0^{\frac{\pi}{2}}\left[1-\left(\frac{c^2-a^2}{c^2}\right)\sin\theta i^2\right]^{\frac{1}{2}}d\theta \tag{4.10}$$

$$F_W=1.0+1.2\left(\frac{a}{t}-0.5\right) \tag{4.11}$$

Where a is the crack length, σ is the nominal tensile stress normal to the crack plane, F_e is a factor for crack shape, F_s is a factor to account for surface cracks = 1.12, F_w is a factor for a specimen with finite width, and F_g is a factor for non-uniform nominal stress.

The Fatigue Life (cycles) is expressed as:

$$N=\int_{a_i}^{a_f}\frac{1}{C(\Delta K(a))^M}da \tag{4.12}$$

$\Delta K = F_e F_s F_w \Delta\sigma\sqrt{\pi a}$; a_i is the initial crack length and $a_f = a_c$ the final or critical crack length. *C* and *M* are Paris Erdogan laws' constants.

The use of the Paris–Erdogan law does not imply a limitation in the robust maintenance strategy proposed in this work; rather it can be applied in principle and in conjunction with any appropriate crack propagation model.

The fatigue life of materials is an example of random variables that follow lognormal distribution (Ang and Tang, 1975), so the fatigue crack is modelled in this work as lognormal with mean imprecision values. Take for instance the initial crack length modelling as illustrated in the optimal maintenance strategies for metallic structures with vague information in chapter 5. The crack length is modelled as lognormal variable with mean value and standard deviation with mathematical expression in Eq. (4.13) and as shown in Fig. 4.6

$$p(a_0) = \frac{1}{a_0 \sigma\sqrt{2\pi}} e^{-\frac{(\ln a_0 - \mu)^2}{2\sigma^2}}, \; a_0 > 0 \qquad (4.13)$$

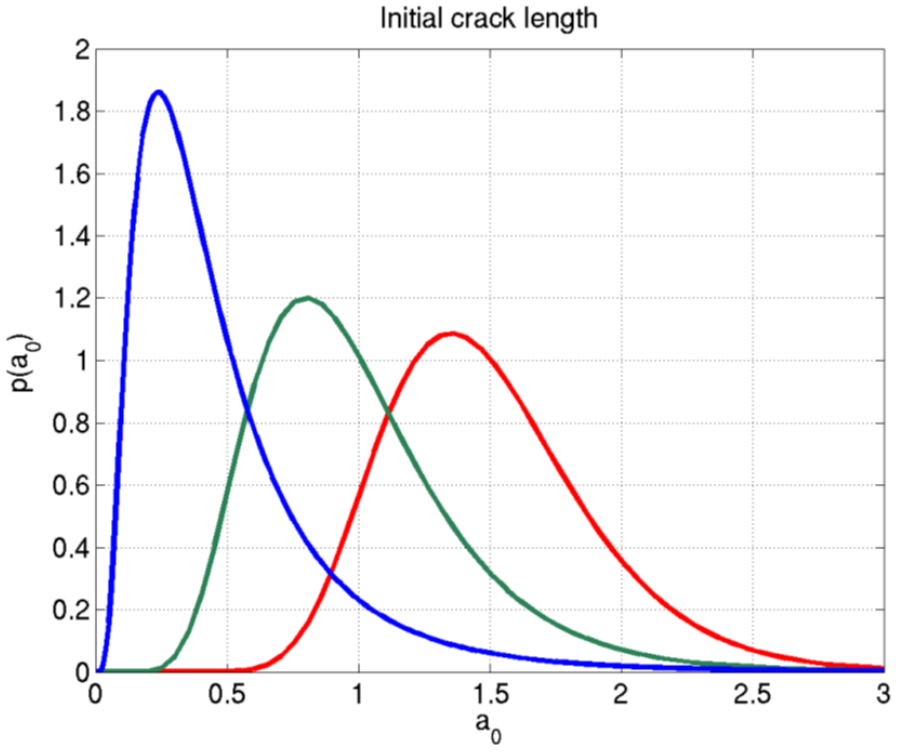

Figure 4.6: Model of the initial crack length as lognormal variable

Furthermore, the initial crack length is also taken to be an imprecise random variable with imprecision mean value when considering imprecision in the distribution parameters.

This is done by realistic consideration of uncertainties in the crack propagation phenomenon, inspection activities and imprecision of the input parameters employing fuzzy sets theory. A fuzzy set (Zadeh, 1965; McNeill and Freiberger, 1993; Beer, 2009) is completely characterized by its membership function. That is, the curve that defines how each point in the input space is mapped to a membership value (or degree of membership) usually between 0 and 1. The membership function may have different shapes like triangular, trapezoidal, Gaussian, etc. The triangular membership functions have been adopted in this work simply because it has been frequently used in many applications of fuzzy sets including fuzzy models, etc. The most obvious motivation behind their utilization stems from a striking simplicity of this form of the membership functions and a fairly limited availability of the pertinent information about the linguistic terms. It has been shown that under some weak assumptions, these specific triangular membership functions immediately comply with the relevant optimization criteria (Pedrycz, 1994). Since most fuzzy sets in use have a universe of discourse (input space) X consisting of the real line R, a more convenient and concise way to define a membership function is to express it as a mathematical formula. For triangular membership functions: The triangular curve is a function of a vector, x, and depends on three scalar parameters *a*, *b*, and *c*, as:

$$(x: a, b, c) = \begin{vmatrix} 0 & x < a \\ \frac{(x-a)}{(b-a)} & a \le x \le b \\ \frac{(c-x)}{(c-b)} & b \le x \le c \\ 0 & x > c \end{vmatrix} \tag{4.14}$$

Alternatively, could be expressed more compactly by:

$$(x: a, b, c) = \max\left(\min\left(\frac{x-a}{b-a}, \frac{c-x}{c-b} \right), 0 \right) \tag{4.15}$$

The parameters *a* and *c* locate the feet or base of the triangle and the parameter *b* locates the peak or height. The expected value of the initial crack length is modelled

as a fuzzy variable with a triangular membership function. This is shown in Fig. 4.7 based on the example application on metallic bridge described in chapter 7 of the thesis. The uncertainty in the length of the initial cracks is characterised by means of a lognormal distribution as indicated in Eq. (4.13) and Fig. 4.6. Several plots are obtained with various associated values (i.e. mean values and standard deviations); in which an expected mean value 1.5 mm and standard deviation 0.4 mm^2 are chosen. Furthermore, imprecision of the mean value of the initial crack length is estimated using fuzzy variable with a triangular membership function in Eq. (4.14) or Eq. (4.15). Fig. 4.7 describes how each point in the input space is mapped to a membership value (or degree of membership) usually between 0 and 1.

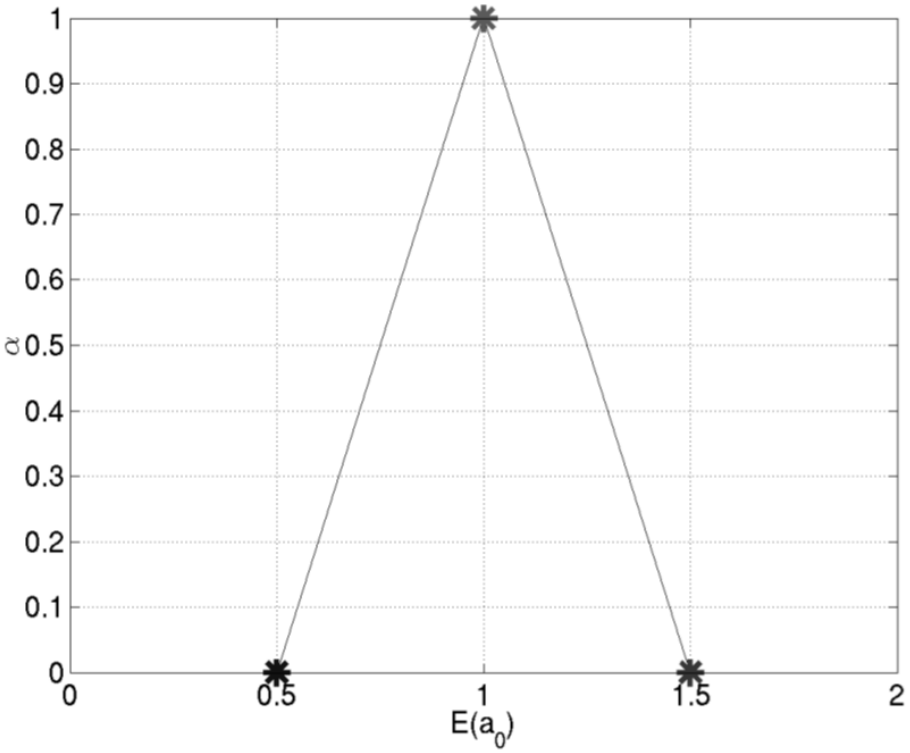

Figure 4.7: Model of the initial crack length as imprecise random variable

4.3 Corrosion Model

Corrosion is a naturally occurring phenomenon often defined as the deterioration or degradation of a metallic material or its properties because of a reaction with its environment (Schmitt et al., 2009). Corrosion is capable of weakening the structural integrity of a pipeline and makes it an unsafe medium for transporting potentially

hazardous materials, such as oil and gas resources. For more than a hundred and fifty years (150 years) studies on corrosion have been a major scientific subject.

Basically, corrosion classification are in two categories, namely: sweet corrosion – the deterioration of metal caused by contact with carbon dioxide (CO_2) in water (H_2O), and sour corrosion – the deterioration of metal caused by hydrogen sulphide (H_2S) or other acid gas. The corrosion defects in the pipelines considered in this work are mainly that of both sweet and sour corrosions which occurs and can be observed either or both at the internal and/or external side of the pipeline wall.

The different types of corrosion according to NACE are listed below:

- Generic: General or uniform corrosion is the one that occurs when the metal loss in structural system or component is uniform from the surface. This corrosion type is mostly made distinctive by high velocity fluid erosion with or without abrasives. The corrosion rate is usually assumed to be constant over the period of time. The corrosion length L and width W are greater than thrice the pipe wall thickness w_t (i.e. L and W > $3w_t$)
- Pitting: when the metal loss is randomly located on the surface, this is known as pitting corrosion. This corrosion type many a time combines with stationary fluid, or in contact with low fluid velocity areas. The wall thickness is reduced locally. L and W ≤ $3w_t$. Pitting corrosion is a localized form of corrosion by which cavities or holes are produced in the material. Pitting is considered to be more dangerous than uniform corrosion damage because it is more difficult to detect, predict and design against. Its mechanism is the dissolution of the passivating film and gradual acidification of the electrolyte caused by its insufficient aeration (oxygen penetration).
- Graphitic corrosion: this corrosion occurs particularly in cast irons, when its iron ore in acids or salt water are lost, thereby resulting in a soft weak metal after leaving the graphite in place.
- Crevice: similar to pitting corrosion in creation of pits, it only occurs where crevices exist; such as in cap joints, bolts, etc.

- Galvanic: when two metals with dissimilar electrode potentials are connected in a corrosive electrolytic environment, the result is galvanic corrosion. Deep pits in the surface are developed by the anodic metal. The concentration cell corrosion is the one that the metal surface is exposed to an electrolytic environment where there is variation in the concentration of the corrosive fluid or the dissolved oxygen. This corrosion type also, like pitting corrosion, combines with stationary fluid, or in contact with low fluid velocity areas.
- Microbiological induced corrosion: any biological growth in pipes and pipeline structural systems will definitely cause corrosion by providing an enabling environment for physical and chemical interactions to occur. This corrosion type is called microbiological induced corrosion.
- Others include intergranular, selective leaching, stress corrosion cracking, and velocity affected corrosions.

All engineering structures contain defects, without the exception of the pipelines. The prediction of future defects and the pipeline's remaining life time are obtained by using consistent assessments of corrosion rates. Assessed corrosion rate models have been outlined in (Caleyo et al., 2012; Valor et al., 2012) following National Association of Corrosion Engineers - NACE's recommendation (Race et al., 2007; RP 0169-92-NACE, 1992). This include the linear growth model; Markov model; time-independent generalized extreme value distribution (TI-GEVD) model; time-dependent generalized extreme value distribution (TD-GEVD) model; and single corrosion-rate value model (SVCR), following NACE's recommendation. It is a general consensus that no single approach provides all the necessary information for a confident estimate of the corrosion rate in the pipeline industry.

Some of the existing corrosion growth modelling in literature see e.g. (Caleyo et al., 2012; Valor et al., 2012) was designed to exclude the evolution of the corrosion defect lengths. The notion is that changes in the defect length do have little or no effect on the probability of failure estimation in association with the individual corrosion defects.

The corrosion model using linear growth is adopted in this work to include evolution of the corrosion defect lengths, measured maximum defect depth through the nominal wall thickness, and measured relative corrosion defect (ratio of defect depth to pipe wall thickness). This allows defining the failure criterion based on remaining pressure strength of corroded pipeline which depends on the length and depth of corrosion defects in addition with imprecision, rather than maximum defect depth only. This is to realistically reflect the vagueness of the available information in the probabilistic model by utilizing imprecise probabilities, and to address the robustness of the same. The traditional probabilistic methods are used in practice, it is also clear that the corresponding probabilities are only known imprecisely.

The idea of time dependence of the depth of a corrosion defect follows a power function has been widely accepted. Therefore, the corrosion rate for this type of defect is also time-dependent. With the power-type time dependence of defect growth, modelling the corrosion process would lead to a different corrosion rate distribution than obtained with the linear growth model. For structural engineering assessment and economical decision making, the estimate of the rate of deterioration with time is vital. The models for degradation/deterioration, e.g. corrosion of metallic structures currently available are of relatively poor quality, which is a great challenge. This is applicable to general (uniform) corrosion and for pitting corrosion as a function of time (Melchers, 2005).

So, for any type of analysis of the future state of a pipeline, such as failure probability, residual strength, etc., it is based on the predicted sizes of the defects which were detected during In-Line Inspection (ILI). The defect parameters at a given time, t for a linear rate of the length and depth of corrosion can be assessed (Timashev and Bushinskaya, 2010); Corrosion rates are assumed as constant values:

$$d(t) = d_0 + v_d t \tag{4.16}$$

$$l(t) = l_0 + v_l t \tag{4.17}$$

Where v_d and v_l are the CRs in the radial and longitudinal directions, respectively; d_0 and l_0 are ILI data for depth and length of defect respectively.

The most commonly used models for surface corrosion to account for a pitting corrosion process as to model the loss of wall thickness with the time of exposure are: power, two-phase and linear models (Lee et al., 2006; Ahammed and Melchers, 1997). These are expressed mathematically below. For this research, the power model commonly known as the power law is used for the analysis of the pipeline reliability and remaining life for corroded buried pipelines.

Power model:

$$d = kT^n \tag{4.18}$$

Two-phase model:

$$d = aT + b\left(1 - e^{-cT}\right) \tag{4.19}$$

Linear model:

$$d = \eta T \tag{4.20}$$

Where *d* is the depth of corrosion pit, *k* the multiplying constant, *T* is the exposure time, *n* the exponential constant, *a* is the final pitting rate constant, *b* the pitting depth scaling constant, *c* the corrosion rate inhibition constant, and η is the corrosion rate.

In Table 4.1, an overview of the metal corrosion rates in Western Europe based on the atmospheric environmental conditions with the corresponding annual rates for individual metallic materials is illustrated. This is to show the extent of damage to structural material by deterioration (steel in particular) due to corrosion rates.

Table 4.1: Metal corrosion rates in Western Europe (Bijen, 2003)

Atmospheric environment	Aluminium (μ m/yr)	Lead (μ m/yr)	Copper (μ m/yr)	Zinc (μ m/yr)	Steel (μ m/yr)
Industry	0.7	0.7	1.3	1-10	100-140
City	0.8	0.4	1.3	0.5-1	40-80
Maritime	0.7	0.5	1.4	1-5	150
Land	0.05	0.4	0.5	0.2-0.5	40-60

4.4 Load Models

4.4.1 Failure pressure models

The remaining strength of corroded pipelines can be evaluated using any of the international standards and codes in practice or industries. The failure mode is evaluated using a semi-empirical model based on fracture mechanics to determine the pressure at which the pipeline fails as a function of the size and geometry of the corrosion defect (Kiefener et al., 1973). This has been widely accepted and used till now for determining the remaining strength of corroded pipelines, as its been inculcated in codes and standards. The failure pressure models used to describe the reliability of corroded pipelines therefore originated from the mechanics of the circumferential stress or hoop stress acting on a pipeline. Some of these standards and codes (i.e. failure pressure models) are expressed mathematically in Eq. (4.21) to (4.35).

Four failure pressure models out of all the international standards and codes are used to compute the pipeline pressure failure, namely; Shell-92, B31G, DNV-101 and Modified B31G. All these models are used as deterministic and probabilistic values, while DNV-101 model is used alone in addition to deterministic and probabilistic values as semi-probabilistic values. Some of the failure pressure models are highlighted below.

Battelle (Leis and Stephens, 1997)

$$p_f = \frac{2\sigma_u w_t}{D}\left(1-\frac{d}{w_t}M\right) \tag{4.21}$$

$$M = 1-\exp\left(-0.157\frac{L}{\sqrt{D(w_t-d)/2}}\right) \tag{4.22}$$

B31G Code (ASME-B31G, 1991)

$$p_f = 1.11\frac{2\sigma_y w_t}{D}\left(\frac{1-\frac{2d}{3w_t}}{1-\frac{2d}{3w_t}M^{-1}}\right) \text{ for G<4} \tag{4.23}$$

$$p_f = 1.11\frac{2\sigma_y w_t}{D}\left(1-\frac{d}{w_t}\right) \text{ for } G \geq 4 \tag{4.24}$$

$$G = 0.893\frac{L}{\sqrt{Dw_t}},\quad M = \sqrt{1+0.893\frac{L^2}{Dw_t}} \tag{4.25}$$

Modified B31G Code (ASME-B31G, 1995)

$$p_f = \frac{2\left(\sigma_y + 68.95\right)w_t}{D}\left(\frac{1-0.85\frac{d}{w_t}}{1-0.85\frac{d}{w_t}M^{-1}}\right) \tag{4.26}$$

$$M = \sqrt{1+0.6275\frac{L^2}{Dw_t}-0.003375\frac{L^4}{D^2 {w_t}^2}} \tag{4.27}$$

for $L^2/Dw_t \leq 50$

$$M = 0.032\frac{L^2}{Dw_t}+3.3 \text{ for } L^2/Dw_t > 50 \tag{4.28}$$

DNV-101Code (DNV, 1999)

$$p_f = \frac{2\sigma_u w_t}{D-w_t}\left(\frac{1-\frac{d}{w_t}}{1-\frac{d}{w_t}M^{-1}}\right) \tag{4.29}$$

$$M = \sqrt{1+0.31\frac{L^2}{Dw_t}} \tag{4.30}$$

$$p_f = \frac{\gamma_m 2w_t\sigma_u\left(1-\gamma_d\left(d/w_t\right)^*\right)}{\left(D-w_t\right)\left(1-\gamma_d\left(d/w_t\right)^* M^{-1}\right)} \geq MAOP \tag{4.31}$$

$$\left(d/w_t\right)^* = \left(d/w_t\right)_{measured} + \varepsilon_d .StDev\left(d/w_t\right) \tag{4.32}$$

$$StDev\left[d/w_t\right]_T = \sqrt{\left(StDev\left[d/w_t\right]_0\right)^2 + \frac{T^2}{{w_t}^2}StDev\left[cr\right]^2} \tag{4.33}$$

Shell-92 (Klever and Stewart, 1995)

$$p_f = \frac{1.8\sigma_u w_t}{D}\left(\frac{1-\frac{d}{w_t}}{1-\frac{d}{w_t}M^{-1}}\right) \tag{4.34}$$

$$M = \sqrt{1+0.805\frac{L^2}{Dw_t}} \tag{4.35}$$

Where p_f is the failure pressure, d the defect depth, D is the outside diameter of pipe, and w_t the wall thickness of the pipe. L is the longitudinal length of defect, σ_y the material yield stress, σ_u the ultimate tensile strength. M is Folias' factor, γ_d is the partial safety for the defect, γ_m the partial safety factor for inspection method, ε_d the fractile factor value, and $(d/w_t)_{measured}$ the measured relative corrosion defect. $StDev(d/w_t)$ is the standard deviation for measurement (d/w_t) ratio and $MAOP$ the maximum allowable operating pressure. $StDev\ [d/t]_T$ the standard deviation of inspection tool in future, $StDev[d/w_t]_0$ is the standard deviation of inspection tool in the first year of assessment, $Std[cr]$ the standard deviation of corrosion, and T the prediction interval time.

The assumption and limitation of these models (Cosham et al., 2007; Mustaffa, 2014) are reflected on the individual flow stresses – which is the measure of the strength of steel in the presence of a defect. Failure is assumed to be as a result of the flow stress, defined by yield strength (for example in B31G and Modified B31G codes) or ultimate tensile strength (in DNV-101 and Shell-92) as their tensile properties. Then further consideration and assumption on different shapes and areas of corrosion defect; and different Folias' factors- the geometry correction factor - to account for the stress concentration due to radial deflection of the pipe surrounding a defect.

For instance, the B31G and the Modified B31G failure pressure models provide a simple representation of short longitudinal corrosion defect as parabolic in shape with corresponding area. Possibly, a long corrosion defect could be made more comprehensible as a rectangular shape. In B31G and DNV-101 pressure models, the failure of corroded pipelines take into account both the defect size and the flow

stress of the material. In the DNV-101 pressure model, the assessment of single and interacting defects and complex shaped defects are inclusive. The DNV- 101 pressure model finds its best application when considering defects subjected to both operating pressure loading only and/or operating pressure loading combined with longitudinal compressive stresses; while the B31G is limited to defect subjected to operating pressure only.

4.4.2 Failure modes

The dominating failure criteria of corroded pipelines are based on operating pressure, and compressive longitudinal stresses due to axial, bending and temperature loads. Others include combination of operating pressure with bending load and/or tensile longitudinal loads; deflection, wall thrust, bending stress and buckling. Typical representations of some of the failure criteria in pipes are shown in Table 4.2.

Table 4.2: Failure criterion in pipes

Mode of deformation	Diagrammatical representation
Longitudinal force	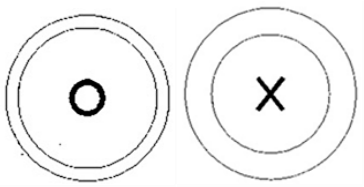
Pressure	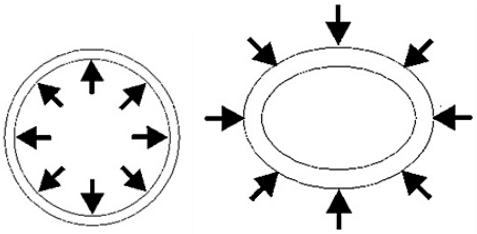
Bending	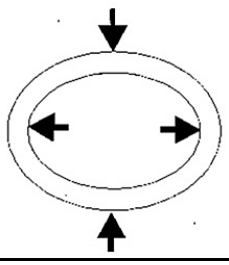

Basically, metallic pipelines vulnerable to corrosion defect may fail by small leak, burst, or rupture. When the corrosion defects perforate the pipe wall, it is regarded as small leak. But when there is plastic collapse due to operating pressure in the pipe wall at the defect location before its being perforated, this failure mode is known as burst. Furthermore, a burst can be classified as rupture where the through wall defect arising from burst is long enough to undergo an unstable axial extension. Lastly, burst can also be classified as a large leak when a burst without unstable axial extension of the resulting through wall defect occurs.

4.5 Assessment of the Stress State of the Above Ground Pipeline

The general stress state of the oil pipeline is comprised of following components:

Stresses due to the operating pressure;

Stresses which depend on the oil pipeline temperature; and

Stresses defined by external forces and influences.

4.5.1 Stresses due to the operating pressure

The internal operating pressure in the pipe induces circumferential stresses σ_c, which are calculated according to formula (SNIP, 2000; Ahammed and Melchers, 1997)

$$\sigma_c = \frac{P_{op}\left(D - 2w_t\right)}{2w_t} \tag{4.36}$$

where D is the pipe outer diameter; w_t is the pipe wall thickness; P_{op} is operating pressure.

4.5.2 Stresses which depend on the oil pipeline temperature

According to (Aynbinder and Kamershteyn, 1982; STO, 2007) the longitudinal axial stresses σ_p in the pipeline due to operating pressure OP and temperature σ_t will be:

- In the case when the temperature deformation is compensated

$$\sigma_l^* = \sigma_p = 0.5\sigma_c, \tag{4.37}$$

- In the case when the temperature deformations are not compensated

$$\sigma_l^* = \sigma_p + \sigma_t = \mu\sigma_c - E\alpha\Delta t, \quad (4.38)$$

where α is the linear expansion coefficient of the metal; *E* is the Young modulus; Δt is the design temperature differential, equal to the difference of temperatures during its layout and when operating; μ is the Poisson coefficient.

4.5.3 Stresses defined by external forces and influences

The elastic bending of the pipeline in the vertical and horizontal planes induces longitudinal bending stresses, which depend on the influence of different external forces. The bending stresses in the pipeline are calculated using formulas from (Aynbinder and Kamershteyn, 1982; STO, 2007; Kuzbozhev et al., 2013)

$$\sigma_u = \frac{M}{W}, \quad (4.39)$$

where *M* is the bending moment; *W* is the axial resistance moment of the pipe cross section (defined as for a thin wall ring)

$$W = \frac{\pi(D - 2w_t)^2 w_t}{4} \quad (4.40)$$

Hence, the overall axial stresses in the pipeline are defined using formula (STO, 2007; Kuzbozhev, et al. 2013):

$$\sigma_l = \sigma_l^* \pm \sigma_u. \quad (4.41)$$

The equivalent stresses in the oil pipeline are calculated according to the energy theory of strength (Aynbinder and Kamershteyn, 1982):

$$\sigma_e = \sqrt{\sigma_c^2 + \sigma_l^2 - \sigma_c\sigma_l}\ . \quad (4.42)$$

For any above ground pipeline compression stresses are hazards, as they may lead to pipeline loss of stability, as well as the extension stresses, which may lead to rupture of the pipe. At this point in each cross section of the pipe both types of stresses (compression and extension) may be present simultaneously, as in the case considered here of bending due to the settlement of pipe supports. Hence, when designing a pipeline, four types of stresses should be considered:

- Maximal circumferential stress;

- Minimal longitudinal stress taking into account its sign;
- Maximal longitudinal stress taking into account its sign;
- Maximal equivalent stress.

4.6 Assessment of the Extra Stresses Induced by Surface Corrosion Defects

According to the references (Aynbinder and Kamershteyn, 1982; Kuzbozhev et al., 2013), the connection of the design failure pressure P_f with the geometric parameters of a single surface corrosion defect has the form:

$$p_f = \frac{2w_t\sigma_f}{D-w_t}\frac{\left(1-\frac{d}{w_t}\right)}{\left(1-\frac{d}{w_t M}\right)} \tag{4.43}$$

The Folias factor M is assessed using formula

$$M = \sqrt{1+0.31\frac{l^2}{D-w_t}} \tag{4.44}$$

where *d* is the maximal depth of the corrosion defect; *M* is the Folias coefficient (factor) for the defect depth; σ_f is the flow stress, and *l* is the maximal length of the corrosion defect.

In order to assess the ultimate sizes of defects it is necessary to define the ultimate circumferential stresses:

$$\begin{aligned} &a_1 = \left(1-\mu+\mu^2\right);\ b_1 = E\alpha\Delta t\left(1-2\mu\right)-\sigma_u(1-2\mu);\\ &c_1 = \left(E\alpha\Delta t-\sigma_u\right)^2-\left[\sigma\right]^2;\ D_1 = b_1^2-4a_1c_1;\\ &\sigma_c^{(1,2)} = \frac{-b_1\pm\sqrt{D_1}}{2a_1}; \end{aligned} \tag{4.45}$$

$$\begin{aligned} &a_2 = \left(1-\mu+\mu^2\right);\ b_2 = E\alpha\Delta t\left(1-2\mu\right)+\sigma_u(1-2\mu);\\ &c_2 = \left(E\alpha\Delta t+\sigma_u\right)^2-\left[\sigma\right]^2;\ D_2 = b_2^2-4a_2c_2;\\ &\sigma_c^{(3,4)} = \frac{-b_2\pm\sqrt{D_2}}{2a_2}. \end{aligned} \tag{4.46}$$

Only two values, $\sigma_{c,1}$ and $\sigma_{c,2}$, out of four values $\sigma_c^{(1,2)}, \sigma_c^{(3,4)}$ are positive (as defined during calculations). Then the ultimate value of circumferential stresses at which the limit state is reached will be the maximal value:

$$\sigma_{c,\lim} = \max\left\{\sigma_{c,1}; \sigma_{c,2}\right\}. \tag{4.47}$$

The ultimate value of total longitudinal stresses is calculated using formula:

$$\sigma_{l,\lim} = \frac{\sigma_c \pm \sqrt{4[\sigma]^2 - 3\sigma_c^2}}{2}. \tag{4.48}$$

The ultimate circumferential stresses in the pipeline are reached at a pressure equal to

$$p_{\lim} = \frac{2\sigma_{c,\lim} w_t}{D - 2w_t} \tag{4.49}$$

Inserting the ultimate value of circumferential stresses at which the limit state is reached in Eq. (4.47) into Eq. (4.43), the obtained value of $p_{\lim}$ instead of the failure pressure P_f gives the possibility of assessing the ultimate sizes of the defects.

4.7 Assessment of the Longitudinal Bending Stresses in an Above Ground Pipeline

4.7.1 Assessment of the bending stresses due to wind load

The linear parts of the above ground oil pipelines on their supports are treated as continuous beams on hinge supports. The design is conducted by taking into account the influence of the transverse dead load/wind load. Calculations also take into account the vertical displacement of supports.

Design of a continuous beam with constant cross section on hinge supports section is conducted using the three-moment equation, which for the case of uniformly distributed transverse load takes the following form:

$$M_{n-1}L_n + 2M_n\left(L_n + L_{n+1}\right) + M_{n+1}L_{n+1} = -0.25q\left(L_n^3 + L_{n+1}^3\right), \tag{4.50}$$

where M_{n-1}, M_n, M_{n+1} are, correspondingly, bending moments on the supports $n-1$, n, $n+1$; L_n is the span between the supports $n-1$ and n; L_{n+1} is the span between the supports n and $n+1$; q is the load intensity of the transverse uniformly distributed load.

If the ends of the pipeline segments are rigidly fixed, then, in order to assess the values of the bending moments at the ends of the pipeline segment, an extra bay of zero length is introduced at the very ends of the segment (Kuzbozhev et al., 2013).

The three-moment equation is composed and solved for each vertical support of the pipeline segment. When the number of spans is k, we have the system of $k-1$ linear equations

$$\begin{cases} 2M_1\left(L_1+L_2\right)+M_2L_2=c_1; \\ M_1L_2+2M_2\left(L_2+L_3\right)+M_3L_3=c_2; \\ \ldots\ldots, \\ M_{k-2}L_{k-1}+2M_{k-1}\left(L_{k-1}+L_k\right)=c_{k-1}, \end{cases} \tag{4.51}$$

where $c_i=-0.25q\left(L_i^3+L_{i+1}^3\right), i=1,2,\ldots,k-1$ are the coefficients which indicate the right side of Eq. (4.51).

It can be proved that

$$M_{k-1}=\frac{\sum_{i=1}^{k-1}c_ia_i}{L_{k-1}a_{k-2}+2\left(L_{k-1}+L_k\right)a_{k-1}}, \tag{4.52}$$

Where $a_1=1;\ \ a_2=-2\left(\frac{L_1}{L_2}+1\right);\ a_i=-2a_{i-1}\left(\frac{L_{i-1}}{L_i}+1\right)-a_{i-2}\frac{L_i-1}{L_i}.$

After determining the value of M_{k-1}, it is substituted into the last equation of the system (Eq. 4.51) the values of M_{k-2} are calculated. Thus, all values of unknown bending moments on the supports are determined sequentially.

When the wind load is acting in the horizontal plane, the bending moments are found from Eq. (4.51) and (4.52) considering the wind load as being transverse.

When both bending moments in the vertical and horizontal planes are present, the design moment should be assessed as follows (Aynbinder and Kamershteyn, 1982)

$$M = \sqrt{M_v^2 + M_h^2}, \tag{4.53}$$

M_v, M_h are the bending moments from the vertical and horizontal loads, correspondingly.

To estimate the limit values of the wind load at a fixed vertical transverse load we define the limit bending stresses. Since the total longitudinal stress (Eq. 4.41) has two values (for tension and compression areas), there are two limit states:

$$\begin{aligned} &\sigma_c^2 + \left(\sigma_l^* + \sigma_u\right)^2 - \sigma_c\left(\sigma_l^* + \sigma_u\right) = \left[\sigma\right]^2; \\ &\sigma_c^2 + \left(\sigma_l^* - \sigma_u\right)^2 - \sigma_c\left(\sigma_l^* - \sigma_u\right) = \left[\sigma\right]^2, \end{aligned} \tag{4.54}$$

$\left[\sigma\right]$ is the yield strength of the pipe material.

From Eq. (4.54) we have

$$\begin{aligned} &b_1 = 2\sigma_l^* - \sigma_c;\ c = \sigma_c^2 + \sigma_l^{*2} - \sigma_c\sigma_l^* - \left[\sigma\right]^2;\ D_1 = b_1^2 - 4c; \\ &\sigma_u^{(1,2)} = \frac{-b_1 \pm \sqrt{D_1}}{2}; \\ &b_2 = \sigma_c - 2\sigma_l^*;\ D_2 = b_2^2 - 4c; \\ &\sigma_u^{(2,3)} = \frac{-b_2 \pm \sqrt{D_2}}{2}. \end{aligned} \tag{4.55}$$

Thus, we have four roots of the two limit state equations, which are pairwise equal to each other but are opposite in signs. Therefore, from two roots of one limit state (e.g. first one) we need to select the minimum value of the absolute value, i.e., the bending stress, which is created by the minimal ultimate bending moment*:*

$$\begin{aligned} &\sigma_{u,\lim} = \min\left\{\left|\sigma_u^{(1)}\right|, \left|\sigma_u^{(2)}\right|\right\}; \\ &M_{\lim} = \sigma_{u,\lim} W. \end{aligned} \tag{4.56}$$

Further, knowing the bending moment from the vertical load, we assess, using Eq. (4.53), the ultimate moment from the horizontal transverse (wind) load.

4.7.2 Assessment of the bending stresses due to wind load based on normative wind load model

Wind speed is usually caused by air moving from high pressure to low pressure, due to changes in temperature. It is of great significance to consider and analyse the static and dynamic effects of high winds on above ground pipelines, because high winds can be very dangerous and destructive. Its loads are randomly applied and dynamic; the velocity of wind varies at various distances from ground, and increases with structural heights. Wind speed is most uncertain and unpredictable when it is closer to the ground. This makes accurate wind load calculations difficult; for reliability analysis of arctic pipelines, an account of the global change of temperatures using wind loads should be taken into cognisance.

The normative wind load q_w, (N/m) on a metre span (1m) of the arctic pipeline length should be determined by formula (Aynbinder and Kamershteyn 1982):

$$q_w = (q_n^c + q_n^d) D_{in}, \tag{4.57}$$

where q_n^c is the normative value of the static component of wind load, N/m^2, determined according to (SP 20, 2011); q_n^d is the normative value of the dynamic component of wind load (N/m^2), determined according to (SP 20, 2011) as well as for buildings with a uniformly distributed mass and constant stiffness; and D_{in} is outer pipeline diameter, in meter, with the insulating cover and the lining.

For simplicity, we consider only the static component of wind load. The normative value of the static (average) component wind load $q_{\mathrm{n}}^{\mathrm{c}}$ is calculated (SP 20, 2011) as:

$$q_n^c = w_0 k\left(z_e\right) c, \tag{4.58}$$

where w_0 is the normative value of wind pressure; $k(z_e)$ is the coefficient that takes into account the change of wind pressure at height z_e; and c is the aerodynamic coefficient.

Normative value w_0 of wind pressure is chosen from Table 4.3 depending on the wind area. Normative value of wind pressure may be determined in accordance with established procedure on the basis of the Roshydromet meteorological stations data. In the latter case the w_0 (Pa), should be determined by formula (SP 20, 2011)

$$w_0 = 0,43v_{50}^2 , \quad (4.59)$$

where v_{50}^2 is the wind pressure corresponding to the wind speed (m/s), at 10 m above the ground level for terrain type A, which is determined by averaging measurements made in 10-minute intervals and is exceeded once in 50 years.

Table 4.3: Normative value of wind pressure, depending on the wind region (adopted on map 3 (SP 20, 2011))

Wind areas	Ia	I	II	III	IV	V	VI	VII
w_0 , kPa	0.17	0.23	0.30	0.38	0.48	0.60	0.73	0.85

Equivalent height $z_e = z_g + d/2$, where d, m, is the pipeline diameter; z_g is the distance from the ground to the pipeline, see Fig. 4.8.

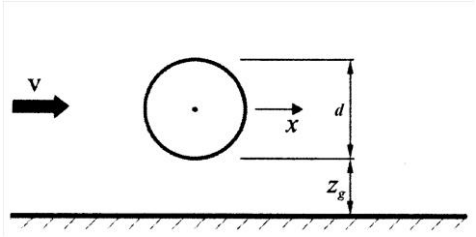

Figure 4.8: The distance of the pipeline from the ground, z_g.

Coefficient $k(z_e)$ is determined by Table 4.4 or Eq. (4.60).

Table 4.4: Coefficient $k(z_e)$ (SP 20, 2011)

Height	Coefficient *k* for terrain types		
z_e, m	A	B	C
5	0.75	0.5	0.4
10	1.0	0.65	0.4
20	1.25	0.85	0.55
40	1.5	1.1	0.8
60	1.7	1.3	1.0
80	1.85	1.45	1.15
100	2.0	1.6	1.25
150	2.25	1.9	1.55
200	2.45	2.1	1.8
250	2.65	2.3	2.0
300	2.75	2.5	2.2
350	2.75	2.75	2.35
480	2.75	2.75	2.75

In Table 4.4:-

A represents open coastal seas, lakes and water reservoirs, countrysides, including buildings with a height of less than 10 m, deserts, steppes, forest steppes, tundra; B considers urban areas, forests and other areas, which are uniformly covered with obstacles greater than 10 m in height; and C the urban areas with dense buildings higher than 25 m.

The construction is considered to be located in an area of given type, if this area is on the windward side of buildings at distance $30h$ (at the height of buildings h to 60 m and at distance 2 km) and at $h > 60$ m.

Note - The types of terrain can be different for different calculated wind directions.

$$k(z_e) = k_{10}(z_e/10)^{2\alpha}. \qquad (4.60)$$

The aerodynamic drag coefficient $c = 0.5$. Parameter values k_{10} and α for different types of terrain are listed in Table 4.5.

Table 4.5: Parameter values k_{10} and α for different types of terrain according to (SP 20, 2011)

Parameter	Types of terrain		
	A	B	C
α	0.15	0.20	0.25
k_{10}	1.0	0.65	0.4

4.7.3 Assessment of the bending stresses due to wind load based on traditional (Deterministic) method for wind loads

Traditionally, the design wind load is estimated using ASCE 7-05 (ASCE, 2006) as:

$$F = q_z G C_f A_f \tag{4.61}$$

The design wind load is the summation of the velocity pressure, gust-effect factor, force coefficients and projected area normal to the wind; their estimations are highlighted in turn below.

The velocity pressure also can be evaluated as:

$$q_z = 0.613 K_z K_{zt} K_d V^2 I \tag{4.62}$$

When the Gust-effect factor is computed as:

$$G = 0.925\left(\frac{\left(1+1.7 g_Q I_{\bar{z}} Q\right)}{1+1.7 g_v I_{\bar{z}}}\right) \tag{4.63}$$

The Intensity of turbulence at height $\bar{z}$ is defined as

$$I_{\bar{z}} = c\left(\frac{10}{\bar{z}}\right)^{\frac{1}{6}} \tag{4.64}$$

The Background response *Q* is given by:

$$Q = \sqrt{\frac{1}{1+0.63\left(\frac{B+h}{L_{\bar{z}}}\right)^{0.63}}} \tag{4.65}$$

Integral length scale of turbulence at the equivalent height is:

$$L_{\bar{z}} = l\left(\frac{\bar{z}}{10}\right)^{\bar{\varepsilon}} \tag{4.66}$$

where q_z is the velocity pressure evaluated at height *z; G* the gust-effect factor; C_f is the force coefficients and A_f the projected area normal to the wind. K_z is the velocity pressure exposure coefficient; K_{zt} the topographic factor; K_d the wind directional factor; and V is the wind speed (m/s). I is the importance factor; $\bar{z}$ the equivalent height of the structure defined as 0.6h, but not less than z_{min}; g_Q and g_v taken as 3.4; c and z_{min} are listed for each exposure in ASCE 7-05 Table 6-2. B is the horizontal dimension of building/structure measured normal to wind direction (m); h the height of building /other structure (m); *l* and $\bar{\varepsilon}$ are constants listed at ASCE 7-05 Table 6-2.

4.7.4 Assessment of the bending stresses due to wind load based on probabilistic wind load models

Longitudinal wind speed is assumed (Kareem, 1990; Kareem, 1999; Wang and Kareem, 2004) to be a stationary random process in the traditional analysis of wind effects on structures. The variation of current wind speed over time can be presented as the sum of the mean wind speed and the fluctuations caused by the turbulence, as expressed in Eq. (4.67).

$$U(t) = \bar{U} + u(t) \tag{4.67}$$

Also, non-stationary wind speed is modelled as the sum of a deterministic time-varying wind speed and a zero-mean stationary random process as fluctuating component. These are expressed mathematically respectively as:

$$U(t) = \bar{U}(t) + u'(t) \tag{4.68}$$

For non-stationary wind speed time history with time-dependent mean, the turbulence intensity of non-stationary wind speed is proposed to be given by the expected value of the time-dependent turbulence intensity over the time interval T, as:

$$I_{u'}, T = E\left[\frac{\sigma_{u',T}}{\bar{U}_T(t)}\right] \tag{4.69}$$

Turbulence is also characterised by its intensity which is defined as the ratio of the standard deviation of the wind speed fluctuations to the mean wind speed.

The gust factor is defined as the maximum ratio of time-varying mean wind speed over time t_1 to the corresponding hourly time-varying mean wind speed:

$$G(t_1) = \max\left[\frac{\bar{U}_{t_1}(t)}{\bar{U}_{3600}(t)}\right] \tag{4.70}$$

The integral length scale in the direction of the flow is defined as

$$L_{u'} = \bar{U}(t)\int_0^{\infty}\frac{R_{u'}(\tau)}{\sigma^2_{u'}}d\tau = \frac{\bar{U}(t)}{4\sigma^2_{u'}}S_{u'}(0) \tag{4.71a}$$

Utilizing the calculated length scale of longitudinal wind speed fluctuations, the commonly used von Karman spectrum is recast as:

$$\frac{nS_{u'}(n)}{\sigma^2_{u'}} = \frac{4nL_{u'}/\bar{U}(t)}{\left[1+70.8\left(nL_{u'}/\bar{U}(t)^2\right)\right]^{5/6}} \tag{4.71b}$$

where $\bar{U}$ is the constant mean wind speed, $u(t)$ the longitudinal fluctuating wind speed component. $\bar{U}(t)$ is the temporal trend of wind speed and $u'(t)$ is the fluctuating component which can be taken as a zero-mean stationary process. $E[\ ]$ is the expected value over the time interval *T*; $\sigma_{u'}, T$ represents the standard deviation of the fluctuating wind speed over the time interval T. $R_{u'}(\tau)$ the autocorrelation function of $u'(t)$, and $S_{u'}$ represents its Fourier transform.

For probabilistic analysis, the turbulence intensity, gust-effect factor, and integral length scale of turbulence are modelled using Eq. (4.69), (4.70) and (4.71) and substituted in the place of its equivalence in the traditional method in Eq. (4.64), (4.63) and (4.66) respectively; and used to calculate the wind load in Eq. (4.61).

4.8 Assessment of Combined Loadings for Buried Pipelines

When the residual ultimate strength of a buried pipeline is exceeded, breakage becomes imminent and the overall reliability of the pipe is reduced. The failure criteria adopted here are due to loss of structural strength of pipelines by corrosion through reduction of the pipe wall thickness, which then leads to pipe failure by a

vector of random function loads and environmental conditions. The deformation of the pipe wall can normally occur under loading conditions that may be idealized as combinations of variable internal pressure, compressive axial load, transverse load, and moment. This load at times is mainly due to differential ground displacement caused by adjacent excavation and construction work, traffic, pipe bursting, swelling and/or shrinking of soil, piling and ground subsidence, etc. Hence, the need to determine the performance required to ensure that the pipelines would not fail when subjected to different loading conditions.

Oil and gas pipelines are required to withstand circumferential and longitudinal stresses produced by operating pressure, external forces and influences, and differences in installation and operating temperature.

The circumferential stress due to internal/operating fluid pressure σ_{co} is estimated (Ahammed and Melchers, 1997; Timashev, 1982) as:

$$\sigma_{co} = \frac{P_{op}\left(D - 2w_t\right)}{2w_t} \tag{4.72}$$

P_{op} = operating pressure, D = pipe outside diameter and w_t = pipe wall thickness.

For buried pipelines under combined loadings, assuming the pipeline does not pass under roadway, railway, or airplane traffic, but the loading on the pipe wall is purely overlying soil; the circumferential bending stress is:

$$\sigma_{cbs} = \frac{6k_m C_d \gamma B_d^2 E w_t r}{E w_t^{\,3} + 24 k_d P_{op} r^3} \tag{4.73}$$

σ_{cbs} is the circumferential bending stress; B_d is width of ditch at the pipe top level; C_d is coefficient of earth pressure; k_d is deflection coefficient; γ is soil density; r is internal pipe radius ($r = \frac{\left(D - 2w_t\right)}{2}$); and E is the Young's modulus of elasticity.

The interest of the pipeline industry for long has being evaluating the effects of external loading due to fill and surface loads, like excavation equipment, on buried pipes. This interest stems not only from the initial design of pipeline systems, but also from the need to evaluate changing loading conditions over the life of the

pipeline. Variations in loading conditions may arise due to the construction of roads and railroads over the pipeline; and one-time or continuous events in which, may be, heavy equipment must cross the pipeline. If the pipeline passed under roadway, railway, or airplane traffic; the circumferential bending stress produced in the pipe wall due to the external effects of the traffic loads is estimated as:

$$\sigma_{cbt} = \frac{6k_m I_c C_t F E w_t r}{L_e\left(E w_t^{\,3} + 24 K_d P_{op} r^3\right)} \tag{4.74}$$

L_e is the pipe effective length on which load is computed; I_c is the impact factor; C_t is the surface load coefficient; and F is the surface wheel load magnitude.

The width of the trench depends on the dual side fills of the soil. If the cross sections of the buried pipelines are close to the circle configuration, then the width of the trench should be limited to twice the diameter of the buried pipelines. Based on this, the compressive stress produced on the pipe wall is:

$$\sigma_{cc} = \frac{\mathrm{Pr}}{w_t} \tag{4.75}$$

σ_{cc} is the compressive stress in the pipe wall; P is the compression ($P = P_l + P_d$), where: P_l is the surface live load, and P_d is the pressure dead load.

For longitudinal stresses that are induced as a result of the pipeline operating pressure and temperature - these are the effects of Poisson's ratio from outward radial action of the operating pressure of the fluid, in addition to the temperature deformations resulting from the differences in operation and installation temperatures, and elastic bending of the pipeline causing longitudinal bending stresses due to the influence of external forces cumulates into longitudinal stresses of the pipeline.

A longitudinal tensile stress produced due to Poisson's ratio effect from the outward radial action of the internal fluid pressure is:

$$\sigma_{lf} = \frac{\mu P_{op}\left(D - 2w_t\right)}{2w_t} \tag{4.76}$$

σ_{lf} is the longitudinal tensile stress; and μ is the Poisson coefficient.

Temperature differential, which is difference of temperatures during its layout and when operating can lead to longitudinal thermal differences; and may be estimated as:

$$\sigma_{lt} = \alpha E \Delta T \tag{4.77}$$

α is the linear expansion coefficient of the metal; and ΔT is the design temperature differential.

Unevenness and/or settlement of the pipeline bedding may cause bending deformation of the pipelines sections. So, the maximum longitudinal bending stress can be calculated as:

$$\sigma_{lb} = Er\chi \tag{4.78}$$

σ_{lb} is the maximum longitudinal bending stress; and χ is longitudinal curvature of the bent pipe.

A maximum value of the circumferential stress can be determined by adding the hoop stress and the wall-bending stress. If the circumferential stress and its Poisson contribution to the longitudinal stress are used to calculate the Von Mises stress, the resulting equations can be solved to determine the minimum acceptable wall thickness ratio as a function of internal pipe pressure. The combinations of the circumferential σ_{cs} and longitudinal σ_{ls} stresses produced in the pipeline are expressed mathematically as:

$$\sigma_{cs} = \sigma_{cc} + \sigma_{cbs} + \sigma_{cbt} + \sigma_{co} \tag{4.79}$$

$$\sigma_{ls} = \sigma_{lb} + \sigma_{lt} + \sigma_{lf} \tag{4.80}$$

The equivalent stresses σ_{es} in the buried pipelines are calculated according to the energy theory of strength, this is the combination of both longitudinal and circumferential stresses and these are described as a function of the applied load with the aid of a mechanical model using von Mises equivalent stress expression:

$$\sigma_{es} = \left(\sigma_{cs}^2 + \sigma_{ls}^2 - \sigma_{cs}\sigma_{ls}\right)^{0.5} \tag{4.81}$$

where σ_{cs} and σ_{ls} are circumferential stress and longitudinal stress respectively.

To make allowance for corrosion losses, it is very crucial to consider the net wall thickness rather than the original wall thickness of the pipeline in the stresses estimation. The corrosion losses are accounted for by inserting ($w_t - kT^n$) in the place of (wt) in Eq. (4.72), (4.73), (4.74) and (4.76) to be in the form of Eq. (4.82), (4.83), (4.84) and (4.85).

$$\sigma_{co} = \frac{P_{op} r}{w_t - kT^n} \tag{4.82}$$

$$\sigma_{cbs} = \frac{6k_m C_d \gamma B_d^2 E\left(w_t - kT^n\right) r}{E\left(w_t - kT^n\right)^3 + 24k_d P_{op} r^3} \tag{4.83}$$

$$\sigma_{cbt} = \frac{6k_m I_c C_t F E\left(w_t - kT^n\right) r}{L_e\left[E\left(w_t - kT^n\right)^3 + 24k_d P_{op} r^3\right]} \tag{4.84}$$

$$\sigma_{lf} = \mu \frac{P_{op} r}{w_t - kT^n} \tag{4.85}$$

The limit state function G(x) is defined as the difference between the yield stress of the pipe material (SMYS) and the equivalent stresses σ_{es} , expressed mathematically as:

$$G(x) = SMYS - \sigma_{es} \tag{4.86}$$

The probability of failure P_f for the pipeline is written as:

$$P_f = P\left(G(x) \le 0\right) \tag{4.87}$$

4.9 Loads and Impacts Acting on Arctic Pipelines

The actual loads and impacts in the form of random variables are rare and can be considered as a certain idealization of the actual loads. Many wearing impacts (friction, erosion, cavitation, corrosion and so on) and shock loads are adequately described by the model of the second group. Meteorological loads - snow, wind (static component) are described by the model of discrete Markov processes,

diffusion and semi-Markov models. Loads of near and far acoustic field, atmospheric turbulence and turbulence in the boundary layer, wave pressure and seismic impacts are most aptly described by the differentiable random processes and fields (the latter in conjunction with the second group of models).

Loads and impacts acting on the arctic pipelines generally are random processes. To solve the problems of arctic pipelines reliability under the action of combinations of random loads and impacts one needs to have, as initial data, their models.

Adequate interpretation of these loads is possible in different ways, depending on the type and degree of completeness of primary statistical data, aims and objectives of research and the required presentation forms of the final results.

In solving problems of arctic pipelines reliability we need:

- load models as random processes, which adequately account for all their basic physical properties; and
- possibility to calculate easily enough the probability of staying of these loads on arbitrary, including low levels.

4.9.1 Description of load models as a pure birth or pure death Markov process

The development of any stochastic model for a real process is always a compromise between the desired level of detail describing the process and feasibility of achieving it. One of the most simple and at the same time available model for the description of such processes is Markov process of the “birth and death” type.

Considering the calculation of the reliability of the Arctic pipeline where it operates under impact of two loads from subsidence/frost upheaval of support and from corrosion defects as presented below.

4.9.1.1 Presentation of the load from the subsidence/heave of support in the form of a homogeneous pure birth (death) Markov process.

Consider one calendar year as a cycle of process of subsidence-heave support. Conditionally this cycle can be divided into the two periods: winter (when the process of frost heaving) and summer (the period when the process of support subsidence on seasonal thawing soils). Visually it is demonstrated in Fig. 4.9.

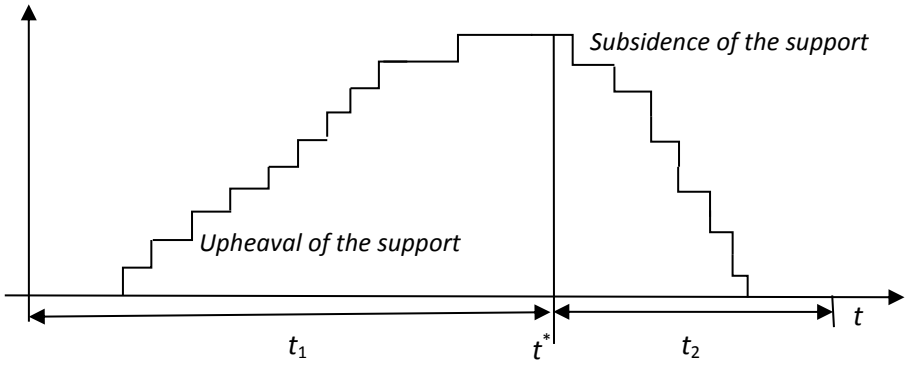

Figure 4.9: One cycle of upheaval-subsidence process of arctic pipeline support

Obviously, the time period for winter t_1 and for summer t_2 and time t^* are random variables. Moreover, $T = t_1 + t_2$ = 365 days.

Thus, the process of heaving-subsidence support can be considered as two of the Markov process: when frost heave - pure birth Markov process; at the subsidence of support - pure death Markov process.

In fact, there is a case where the support subsidence occurs by an amount greater than the one which started the process of frost heaving. Visually, this case is shown in Fig. 4.10.

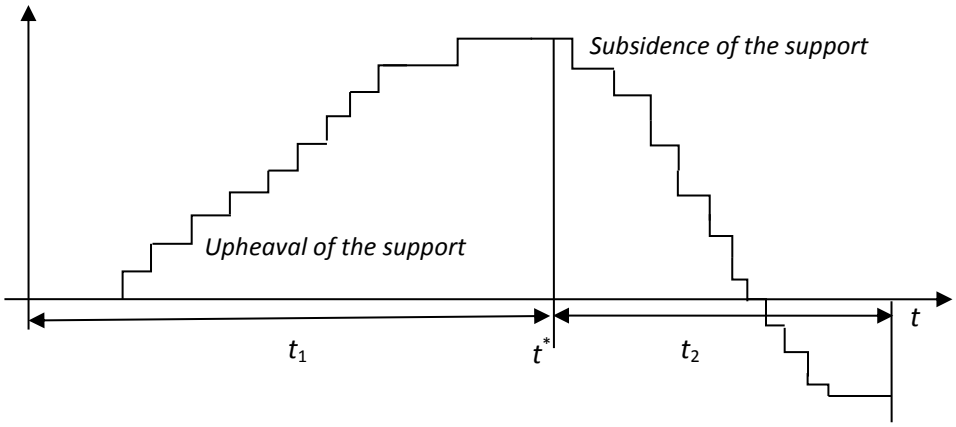

Figure 4.10: One cycle of upheaval-subsidence of the support process for the case where the value of subsidence of the support does not match the magnitude with which began the process of frost upheaval

In this case, the process is below the level of the beginning of the process of frost heaving must be considered separately. And, in the next cycle, the process of frost heaving begins with level of subsidence support.

We divide the range of the possible values of the considered load on *M* disjoint intervals (states). If the possible values of the load on the arctic pipeline can only increase or decrease in time, and at random time moments can transit from the *i*–th state only to the (*i* + 1)-th state or (*i* -- 1)-th, then such a transition process can be described by a pure birth or death Markov process.

The system of differential equations that describes this process is

$$\begin{cases} \dfrac{dP_1(t)}{dt} = -\lambda_1 P_1(t); \\ \dfrac{dP_i(t)}{dt} = \lambda_{i-1} P_{i-1}(t) - \lambda_i P_i(t), \ i = 2,..,M-1; \\ \dfrac{dP_M(t)}{dt} = \lambda_{M-1} P_{M-1}(t), \end{cases} \tag{4.88}$$

where $P_i(t)$ is the probability that the load value is in the i-th state at the moment of time *t*, $\lambda_i(t)$ is the transition intensity form *i*-th state to the (*i* + 1)-th state. For pure death process the intensity $\lambda_i(t)$ replaced by the transition intensity $\mu_i(t)$ from *i*-th state to the (*i* -- 1)-th state.

If at the initial time t_0 load value is in a first state, the solution of system of differential equations in Eq. (4.88) has the form:

$$P_i(t) = \sum_{j=1}^{i} \eta_{ij} \exp\left[-\lambda_j t\right], \quad i = 1,2,..,M, \tag{4.89}$$

where:

$$\eta_{ij}=\begin{cases}\eta_{11}=1;\\ \eta_{i-1,j}\cdot\dfrac{\lambda_{i-1}}{\lambda_i-\lambda_j}, \quad j\neq i, i=2,....M,\ j=1,2...,(i-1);\\ -\sum\limits_{q=1}^{i-1}\eta_{iq}, \quad j=i, i=2,...,M,\end{cases} \tag{4.90}$$

4.9.1.2 Description of the influence of the arctic pipeline defects on failure (burst) pressure as a homogeneous pure death Markov process

Divide the possible range of change of the burst pressure of a pipeline defective cross section $\left(P_{op}; P_f(0)\right]$ into *M*-1 non-overlapping equal interval $I_i\left(i=M-1,..,1\right)$. Here $P_f(0)$ is the defect failure pressure at initial time *t* = 0. The last interval (conditional failure state) I_M which includes the lowest values of failure pressure is taken as (0; P_{op}).

The failure pressure $P_f(t)$ of the defective cross section can only monotonically decrease over time, i.e., transit at random moments of time from the *i*-th state only to the (*i* + 1)- th state, where state is one of the intervals $I_i\ \left(i=1,..,M\right)$.

The system of differential equations, that describes this process, has the form

$$\begin{cases}\dfrac{dP_1(t)}{dt}=-\mu_1(t)P_1(t),\\ \dfrac{dP_i(t)}{dt}=\mu_{i-1}(t)P_{i-1}(t)-\mu_i(t)P_i(t),\ (i=2,..,M-1),\\ \dfrac{dP_M(t)}{dt}=\mu_{M-1}(t)P_{M-1}(t),\end{cases} \tag{4.91}$$

where $P_i(t)$ is the probability that the failure (burst) pressure $P_f(t)$ of defective cross section is in the *i*-th state at time *t*, $\mu_i(t)$ is the intensity of transition from the *i*- th state to the (*i* + 1)-th.

The quantity $\mu(t)$ may be associated with the rate of change of random variables $P_f(t)$ as follows:

$$\mu(t)=-\frac{P_f'(t)}{\Delta I}, \tag{4.92}$$

where ΔI is the interval length, $P_f'(t)$ is the derivative of the function $P_f(t)$ with respect to time at time *t*. The minus sign in this formula is due to the fact that the derivative of monotonously decreasing function has negative values in the whole domain of its definition.

Now the system of differential equations in Eq. (4.91) can be rewritten as

$$\begin{cases} \dfrac{dP_1(t)}{dt} = -\mu(t)P_1(t), \\ \dfrac{dP_i(t)}{dt} = \mu(t)P_{i-1}(t) - \mu(t)P_i(t), \ (i = 2,..,M-1), \\ \dfrac{dP_M(t)}{dt} = \mu(t)P_{M-1}(t), \end{cases} \tag{4.93}$$

It is obvious that at the initial moment of time *t* = 0 the random variables $P_f(0) \in I_1$, Hence, the initial conditions for the system of differential equations in Eq. (4.93) will be:

$$P_1(0) = 1,\ P_i(0) = 0,\ (i = 2,..,M).$$

The general solution of system of differential equations in Eq. (4.93) will be as follows:

$$\begin{cases} P_i(t) = \dfrac{\rho^{i-1}(t)}{(i-1)!} \cdot \exp\{-\rho(t)\},\ i = 1,..,M-1, \\ P_M(t) = 1 - \left[\exp\{-\rho(t)\} + \sum\limits_{i=2}^{M-1} \dfrac{\rho^{i-1}(t)}{(i-1)!} \cdot \exp\{-\rho(t)\} \right], \end{cases} \tag{4.94}$$

where $P_i(t)$ is the probability that the failure (burst) pressure of defective cross section is in the *i*-th state at the moment of time *t*, $\rho(t)$ is calculated using formula:

$$\rho(t) = \int_0^t \mu(\tau)\,d\tau - \int_0^t \frac{P_f'(\tau)}{\Delta I}\,d\tau = \frac{P_f(t) - P_f(0)}{\Delta I}. \tag{4.95}$$

4.10 Summary

An explicit description of the numerical models used in this research work has been outlined and explained in details in this chapter. These numerical modelling which employ the theoretical and computational frameworks in Chapter 3 forms the major approaches for the solutions to the problem statement of the need for reliability and maintenance of structures under severe uncertainty as a key issue in ensuring a faultless life of engineering structures and systems despite fluctuations and changes of structural and environmental parameters and conditions. Extension to the previous works through inclusion of imprecise mean values, interval analysis, probability bounds, and Markovian description on the modelling of these deterioration phenomena and loads has been reported. Through scientific studies and understanding of the phenomena (fatigue cracks and corrosion) provision for a reliable and set guideline has been outlined by appropriating simplification of reality.

This has further led to formulation of the problems in mathematical form and solved using proposed theoretical approaches in Chapter 3. The application of these numerical approaches for reliability assessment of metallic structures is the subject of next discussion in Chapters 5, 6 and 7.

5. Robust Maintenance Strategies for Corroded Pipelines

5.1 Introduction

Pipeline load carrying capacity and safety are often reduced by corrosion and associated damage. The prediction of future defects and the pipeline's remaining life time are obtained by using consistent assessments of corrosion rates. However, its modelling often involves simplifications and assumptions to compensate a lack of data, imprecision and vagueness, which cannot be justified completely and may, thus lead to biased results. To overcome these issues, an imprecise probabilities approach is proposed for reliability analysis, decision-making, risk-based design and maintenance. It is shown how this approach can improve the practise using B31G, Modified B31G, DNV-101 and Shell-92 failure pressure models. In addition, a robust and efficient probabilistic framework for optimal inspection and maintenance schedule selection for corroded pipelines is proposed. Optimal solution is obtained through only one reliability assessment removing huge computational cost of reliability-base optimization and generalised probabilistic methods and in turn, making the analysis of industrial size problem feasible.

One of the most important degradation/deterioration mechanisms that affect the long-term reliability and integrity of metallic pipelines is corrosion (Ahammed, 1998; Bazan and Beck, 2013). Corrosion which leads to metal loss both in type and section (length and depth) is the most prevailing time dependent threat to the integrity, safe operation and cause of failure for oil and gas pipelines (Caleyo et al., 2002). Unavoidable uncertainties make the assessment of pipelines a complex and challenging task (Ahammed, 1998; Bazan and Beck, 2013; Qian et al., 2011). These uncertainties appear, such as in relation to operational data variation, as randomness of the environment, in form of imperfect measurement pipeline geometry, in the material strength, operating pressure and inspection tools, and in aging processes of the pipeline.

The remaining strength of a pipeline with corrosion defects can be assessed using one or all of the international design codes viz: B31G (ASME, 1991), B31Gmod (ASME, 1995), Battelle (Leis and Stephens, 1997), DNV-101(DNV, 1999) and Shell-92 (Klever and Stewart, 1995). The associated methods use deterministic values for load and resistance variables, thereby assuming no uncertainty. In the light of the existing inherent uncertainties in the corrosion process, the obtained results are obviously quite coarse approximations, which may deviate from reality significantly. A key challenge in this regard is the probabilistic modelling, which relies on substantial information and data required to define parameter distributions. However the amount of data required to define univocally those distributions might not be available in practice, assumptions and simplifications are applied that cannot be justified completely. To solve this conflict, the use of imprecise probabilities (Beer et al., 2013) is proposed to realistically reflect the vagueness of the available information in the probabilistic model. In fact, since these assumptions and simplifications can be quite decisive, an imprecise probabilities approach provides a promising pathway towards a robust maintenance strategy. This work therefore proposes the use of a novel reliability metrics redefined within the framework of imprecise probabilities.

Another challenging task is the identification of optimal inspection interval time in order to reduce the overall costs of pipelines including cost of inspection, repair and failure. For instance, areas needing repairs should be accurately pinpointed as to minimise excavations for verifications. Likewise, early observations of failure mechanisms, and determination of the likelihood of failure in association with the pipeline must be handy. The identification of optimal maintenance scheduling requires in turn the evolution of the model reliability that can be computational expensive to evaluate. Approximate methods – e.g. FORM may not be sufficiently accurate or applicable for large scale problems, and we have to resort to Monte Carlo simulation based methods. Efficient Monte Carlo simulation is one of the most useful approaches to scientific computing due to its simplicity and general applicability; required for analyzing complex real world problems. In this work, an efficient computational technique is proposed for the identification of a robust

maintenance scheduling taking into account uncertainty and imprecision. More specifically, the proposed approach allows determining the optimal inspection interval and the repair strategy that would maintain adequate reliability level throughout the service life of the pipeline obtained through only one reliability assessment. Hence, the proposed approach is applicable to the analysis of industrial size problem. The proposed reliability strategies are implemented in the general purpose software OpenCossan (Patelli, 2012; Patelli, 2016).

Applications and numerical examples are presented to show the applicability of the proposed strategies.

5.2 Modelling of the Pipeline Corrosion Defect

One of the significant potential threats to existing structures and infrastructures is corrosion. Metal losses due to corrosion affect the ultimate resistance, safety and serviceability of the structure and cause changes in its elastic and dynamic properties. These are major concerns in structural reliability assessment of existing structures and infrastructures, also in the prediction of the safe and serviceable life for both new and existing structures.

The prediction of future defects and the pipeline's remaining life time are obtained by using consistent assessments of corrosion rates. Assessed corrosion rate models has been outlined in (Caleyo et al., 2012; Valor et al., 2012) following National Association of Corrosion Engineers - NACE's recommendation (Race et al., 2007). It is a general consensus that no single approach provides all the necessary information for a confident estimate of the corrosion rate in the pipeline industry.

Some of the existing corrosion growth modelling in literature (see e.g. Caleyo et al., 2012; Valor et al., 2012) was designed to exclude the evolution of the corrosion defect lengths. The notion is that changes in the defect length do have little or no effect on the probability of failure estimation in association with the individual corrosion defects.

The corrosion model using linear growth is adopted in this research to include evolution of the corrosion defect lengths, measured maximum defect depth through the nominal wall thickness, and measured relative corrosion defect (ratio of defect depth to pipe wall thickness). This allows defining the failure criterion based on remaining pressure strength of corroded pipeline which depends on the length and depth of corrosion defects in addition with imprecise numbers, rather than maximum defect depth only. This is to realistically reflect the vagueness of the available information in the probabilistic model by utilizing imprecise probabilities, and to address the robustness of the same. The traditional probabilistic methods are used in practice, it is also clear that the corresponding probabilities are only known imprecisely.

For instance, corrosion growth rates are presumed traditionally to be constant values. The analysis of the future state of pipelines, such as failure probability, residual strength, etc., is based on the predicted sizes of the defects which were detected during in line inspection. The defect parameters at a given time t, for a linear growth rate of the length and depth of corrosion are assessed. From Section 4.3 of Chapter 4, the corrosion rates are expressed mathematically in Eq. (4.16) and (4.17) as

$$d(t) = d_0 + v_d t$$

$$l(t) = l_0 + v_l t$$

The failure modes adopted here are the loss of structural strength of pipelines through reduction of the remaining pressure strength, and pipe wall thickness caused by corrosion defects. The failure pressure of the pipeline with corrosion defects at different elapsed times are assessed using four international design codes: Shell-92, B31G, DNV-101 and Modified B31G models. The summary of all the failure pressure models is shown in Table 5.1.

In Table 5.1, p_f , *d*, and *D* are the failure pressure, defect depth, and outside diameter of pipe respectively. While w_t is the pipe wall thickness; *L* the longitudinal

length of defect, σ_y is material yield stress, σ_u the ultimate tensile strength and M is the Folias' factor.

Table 5.1: Failure pressure models used for computing pipeline failure pressure (Bjornoy et al., 1997; Cosham et al., 2007)

Failure pressure Model	Flow stress	Folias' factor	Shape of defect	Area of defect	Failure pressure expression
B31G	1.1 SMYS	$M = \sqrt{1+0.893\frac{L^2}{Dw_t}}$	Parabolic	A= 2/3dL	$p_f = 1.11\frac{2\sigma_y w_t}{D}\left(\frac{1-\frac{2d}{3w_t}}{1-\frac{2d}{3w_t}M^{-1}}\right)$
Mod B31G	SMYS + 68.95 MPa	$M = \sqrt{1+0.6275\frac{L^2}{Dw_t}-0.003375\frac{L^4}{D^2 w_t{}^2}}$	Arbitrary	A= 0.85dL	$p_f = \frac{2(\sigma_y+68.95)w_t}{D}\left(\frac{1-0.85\frac{d}{w_t}}{1-0.85\frac{d}{w_t}M^{-1}}\right)$
DNV-101	SMTS	$M = \sqrt{1+0.31\frac{L^2}{Dw_t}}$	Rectangle	A= dL	$p_f = \frac{2\sigma_u w_t}{D-w_t}\left(\frac{1-\frac{d}{w_t}}{1-\frac{d}{w_t}M^{-1}}\right)$
Shell-92	SMTS	$M = \sqrt{1+0.893\frac{L^2}{Dw_t}}$	Rectangle	A= dL	$p_f = \frac{1.8\sigma_u w_t}{D}\left(\frac{1-\frac{d}{w_t}}{1-\frac{d}{w_t}M^{-1}}\right)$

The assumption and limitation of these models are reflected on the individual flow stresses – which is the measure of the strength of steel in the presence of a defect. Failure is assumed to be as a result of the flow stress, defined by yield strength (in B31G and Modified B31G codes) or ultimate tensile strength (in DNV-101 and Shell-92) as their tensile properties. Then further consideration and assumption on different shapes and areas of corrosion defect; and different Folias' factors- the geometry correction factor - to account for the stress concentration due to radial deflection of the pipe surrounding a defect. These lead to variations in the obtained results based on different modifications.

5.3 Pipeline Reliability Assessments

Reliability is the probability of a structural system performing its intended function over its specified period of usage and under specified operating conditions. It is the

measure of the probability of failure. The failure probabilities of the pipeline can be obtained from the models shown in Table 5.1.

5.3.1 Deterministic analysis

The level I analysis (also known as deterministic approach) is based on safety factors. Based on these developed capacity equations or codes presented in Table 5.1, deterministic procedures are straight forward. The major advantage of deterministic approach is the easy assessment of pipeline current condition when prediction capabilities are lacking. In all these failure pressure models, the safety factor is considered to be 1 (unity), so that only the real failure pressure model is considered. Deterministic approaches do not model explicitly the uncertainties that might have occurred and increased over the years of the pipeline service. The effects of the uncertainty are considered in terms of safety margins and factors. Worst-case scenario is used for loads and capacity of the structural system and in turn, this might leads to greater safety/reliability but also to huge costs associated with the overdesign of pipelines. Prediction of pipeline integrity using deterministic assessment is not able to achieve optimal design required by the operators. In addition, since deterministic methods do not provide realistic predictions the operators have to inspect their pipelines frequently in order to obtain accurate information on pipeline conditions. Deterministic analysis aims at demonstrating that the pipeline is tolerant to identified faults/defects that are within the design basis, thereby defining the limits of safe operation. The associated calculations are straightforward, it can be carried out with comparatively little effort, and the analysis and decision making process is relatively clear and simple.

5.3.2 Semi-probabilistic analysis

Level II analysis (or Semi-probabilistic approach) represents the probabilistic element within deterministic equations. It is based on partial safety factors and considers only the first and second moment of the parameter distributions. For instance, DNV-101 code uses analytical expression to derive the values of standard deviation of relative corrosion defect, and the failure pressure. The safety factors take care of uncertainties for defect depth and failure pressure (burst) capacity. To

predict the remaining future pressure, the inherent uncertainties in corrosion rate, materials and environmental properties are taken into account. This is reflected by the increment of the partial safety factors as a function of time to represent the influence by these uncertainties. Then, the standard deviation of the inspection tool as a function of the pipeline operation time was obtained (DNV, 1999) from Eq. (5.3).

The expressions for DNV-101 failure pressure model, describing the chosen semi-probabilistic values for probabilistic element within the deterministic equation of the code are:

$$p_f = \frac{\gamma_m 2 w_t \sigma_u \left(1-\gamma_d \left(d(t)/w_t\right)^*\right)}{\left(D-w_t\right)\left(1-\gamma_d \left(d(t)/w_t\right)^* M^{-1}\right)} \geq MAOP \tag{5.1}$$

$$\left(d(t)/w_t\right)^* = \left(d(t)/w_t\right)_{measured} + \varepsilon_d . \sigma\left(d(t)/w_t\right) \tag{5.2}$$

$$\sigma\left[d/w_t\right]_T = \sqrt{\left(\sigma\left[d/w_t\right]_0\right)^2 + \frac{t^2}{w_t^2}\sigma[cr]^2} \tag{5.3}$$

In addition to parameters defined in Table 5.1, γ_d is the defect partial safety, γ_m the inspection method partial safety factor. ε_d the fractile factor value, $(d/w_t)_{measured}$ the measured relative corrosion defect, $\sigma\ (d/w_t)$ is the standard deviation for measurement (d/w_t) ratio and the maximum allowable operating pressure is *MAOP*. t is the prediction time interval, $\sigma\ [d/w_t]_T$, represents the standard deviation of inspection tool in future, $\sigma\ [d/w_t]_0$ is the standard deviation of inspection tool in the first year of assessment, and finally $\sigma\ [cr]$ is the standard deviation of corrosion process.

The advantage of the semi-probabilistic approach is the realization of a consistent reliability level for various combinations of material properties, pipe geometries and corrosion defects configurations. It accounts directly for the accuracy in sizing the corrosion defect, but limited as it is not a full probabilistic method.

5.3.3 Probabilistic analysis

In the level III analysis (or full probabilistic approach), the pipeline assessment has been modified with the integration of probabilistic values into the existing failure pressure models through the use of limit state function equations as shown in Eq. (5.4).

The limit state function g is defined as the difference between the failure pressure, p_f of the pipeline and the operating pressure, O_p, expressed mathematically as:

$$g = p_f - O_p \tag{5.4}$$

The probability of failure, P_f for the pipeline is defined as:

$$P_f = P(g \le 0) = \int_{g(\theta)\le 0} f(\theta)d\theta \tag{5.5}$$

θ represents the vector of uncertainty and in realistic cases it might be composed of a large number of variables. Hence, analytical and approximate like FORM and SORM methods result to be inadequate for solving Eq. (5.4). Simulation methods are required. Monte Carlo simulation based methods are well known techniques that can be used to evaluate the integral of Eq. (5.4). When dealing with rare case events, plain Monte Carlo simulation might become infeasible due to the large number of the samples required to achieve a specific level of accuracy. To overcome this limitation, advanced Monte Carlo techniques such as Line Sampling (Pradlwarter et al., 2007) and Subset simulations (Au and Beck, 2001) can be adopted for analyzing complex real world problems. Line Sampling is applicable to cases where important directions can be evaluated, and for weakly nonlinear reliability problems. Subset simulations compute small failure probabilities encountered in reliability analysis of engineering systems.

Probabilistic approach aims at providing a realistic estimation of the risk presented by the pipeline system. This can also be used to confirm the validity of the deterministic safety assessment. The major advantage of the probabilistic approach is the integrative and quantitative approach which allows explicit consideration and treatment of all types of uncertainties. Furthermore, it enhances safety and

operational management; results and decisions can be communicated on a clearly defined basis.

5.3.4 Imprecise analysis

Imprecise probability is a powerful tool to take into account imprecision and vagueness, also to address sensitivities of the failure probability with respect to the probabilistic model choice and the imprecision on the characterisation of the input parameters (Beer et al., 2013). It provides another set of tools for analysing computational error, verifying sufficient conditions for existence and convergence, constructing upper and lower bounds on sets of solutions, and in providing natural stopping criteria for iterative methods. More specifically, the effect of imprecision on the most common models used to predict the effect of corrosion are analysed in section 5.6.1.

Imprecise analysis is helpful in identifying low-probability but high-consequence events for risk analysis. It controls modelling accuracy with high degree of flexibility in uncertainty quantification; improves design, performance and reliability of structures. For a defined confidence level, interval bounds may be easier to specify or to control than moments of the parameter distributions.

5.4 Robust Maintenance Strategy

Inspection and monitoring of pipelines is necessary in order to ensure their continued fitness for purpose, which entails protection from any time-dependent degradation processes, such as corrosion. Also, pipeline failures have significant impact on the economic, environmental and social aspects of the society. Therefore, the proper assessment and maintenance of such structures are crucial; negligence will lead to serviceability loss, failure and might lead to catastrophic environmental and financial consequences (Ahammed and Melchers, 1997). On the other hand, maintenance is an expensive activity and the availability of robust maintenance scheduling is of paramount importance. The premise for these decisions is supplied by reliability estimation inculcating the impact of inspection scheduling and reparation activities over the pipeline's service life.

5.4.1 Optimization problem

In reliability-based optimization of structures, the total expected costs in relation to maintenance and failure for the structure is the objective function that needs to be minimised (Enevoldsen and Sorensen, 1994). The time of inspection represents the design variable of the optimization problem. The monetary cost associated with the inspection, the cost of the repair and the expected cost of failure form the objective function that can be formulated as:

$$\arg\min_{N_I,e,t_i} C_T(N_I,e,t_i) = C_I(N_I,e,t_i) + C_R(N_I,e,t_i) + C_F(N_I,e,t_i) \tag{5.6}$$

where N_I, e, and t_i denote the number of inspections, the qualities of inspection, and the time of inspection; C_T, C_I, C_R and C_F are the expected total cost of operation, expected costs of inspection, repairs and failure respectively. In addition, the optimisation problem must satisfy some constraints. For instance, it might be necessary to guarantee a minimum level of reliability:

$$\beta = 1 - P_f(t) \tag{5.7}$$

where $P_f(t)$ is the probability of failure at the expected lifetime.

Hence, the robust maintenance strategy is closely related to the evaluation of reliability and methods of structural reliability have been applied in the literature in order to evaluate expected costs (Enevoldsen and Sorensen, 1994; Valdebenito and Schuëller, 2010; Schuëller et al., 2001).

The probability of failure is calculated by evaluating the integral of Eq. (5.5).

Following an inspection, if a defect is detected, it can be repaired or not. A defect is repaired immediately after an inspection if the pipe defects are lower than the threshold based on the sizing of the inspection method (the pipeline has to be excavated and repaired). On the other hand when the pipe defects are above a predefined threshold the pipe will be left unrepaired, this indicates that the processed data collected from in-line inspection to identify defects are not critical to the pipeline integrity. The threshold is a typical value $1.25 \leq SF_{Fp} \leq 1.5$ (see Eq.

5.8) where SF_{Fp} is the failure pressure safety factor often that defines the repair criterion (Pandey, 1998).

$$SF_{Fp} = \frac{p_f}{MAOP} \tag{5.8}$$

p_f is the failure pressure as defined in Table 5.1 and *MAOP* is the Maximum Allowable Operating Pressure.

This value is in agreement for the level of integrity established by actual pipeline hydro testing, and corresponds with the repair factor for a class 2 pipeline in Canadian code (CSA Z662-07) as its safety factor adopted in design.

The expected inspection cost is calculated as the product of the unit inspection cost, C_I, corrected by the discount rate, *r*, and the probability that inspection takes place (Enevoldsen and Sorensen, 1994). This expected cost is expressed in mathematical form as:

$$C_I = \sum_i \frac{c_I(q)}{(1+r)^{t_i}} .\left(1 - P_f^{t_i}\right) \tag{5.9}$$

The unit cost of performing inspection depends on the quality of inspection *q*, and P_f^t is the probability that failure occurs before the time of inspection t_i.

The evaluation of the expected cost associated with repair is quite challenging and depends on the probability of detection (i.e. the probability to detect a defect).

The expected repair costs are modelled as:

$$C_R = \sum_{i=1}^{N_I} C_{R_i} . P_{R_i} . \frac{1}{(1+r)^{t_i}} \tag{5.10}$$

Where i-th term represents the capitalized expected repair costs at the i-th inspection; C_{Ri}, is the cost of a repair at the i-th inspection and P_{Ri} is the probability of performing a repair after the i-th inspection when failure has not occurred earlier.

The most common tools for metal loss and crack inspection are based on the Magnetic Flux Leakage or Ultrasonic techniques (Pipeline Operators' Forum, version 2009). Pigging data is gathered through in-line inspection activities using Magnetic Flux Leakage (MFL) intelligent pig, whereby the values of parameters in the model

is as a result of the operations and inspection histories of the pipeline. Geometry tools are available for detecting and sizing of deformations and mapping tools for localization of a pipeline and/or pipeline features (Pipeline Operators' Forum, version 2009). The inspection activities may assess the damage incorrectly or may not even detect any damage at all based on the quality. Hence, a probability of detection (PoD) associated with the non-destructive inspection techniques is assigned. The probability of detection (Pandey, 1998) is:

$$PoD = 1 - \exp^{-qd} \tag{5.11}$$

where *d* represents the defect depth and *q* the quality of inspection.

The typical minimal detectable depth of a high resolution Magnetic Flux Leakage (MFL) tool for uniform corrosion is 0.*1wt* with a PoD of 0.9 (POF, version 2009) as illustrated in Fig. 5.1. Using these values, and a typical value of the pipeline wall thickness w_t = 9.52mm the quality of inspection can be estimated as q = 2.42.

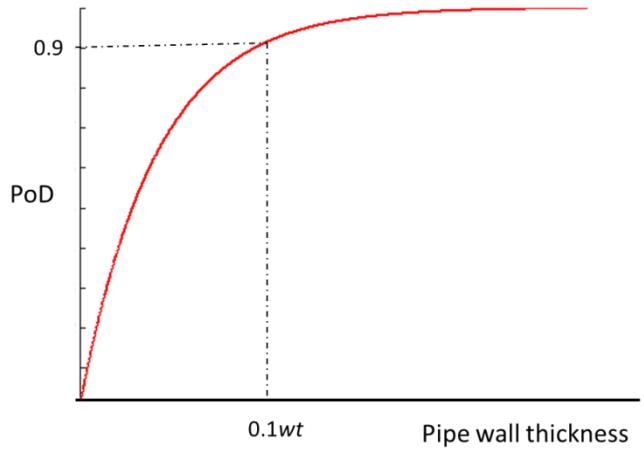

Figure 5.1: The PoD for minimal detectable for uniform corrosion using MFL tool.

The total capitalized expected costs due to failure are determined from Eq. (5.12). It is the cost function associated with failure over the region of the corresponding demand functions (i.e. threshold based on the sizing of the inspection method) with the first, t_{i-1} and second failure criterion, t_i .

$$C_F = \sum_{i=1}^{N_{I+1}} C_F(t_i).\left(P_f(t_i) - P_f(t_{i-1})\right).\frac{1}{(1+r)^{t_i}} \tag{5.12}$$

5.5 Computational Strategy

The estimation of the probability of failure requires in general significant computation effort, in particular for highly reliable pipelines. In fact, the number of model evaluations increases with the reliability of the pipeline and they easily exceed the computational resources available. For this reason, the Line Sampling method is adopted to estimate the probability of failure. Line Sampling (Pradlwarter et al., 2007) proved to be quite robust and efficient for high dimensional problems particularly where an important direction towards the failure domain could be estimated. Line sampling employs lines instead of points in order to collect information about the probability content of the failure domain. It was shown that it always outperforms direct Monte Carlo (Pradlwarter et al., 2007). The variance of the respective estimator depends on the deviation of the limiting hyper-surface from a hyper-plane; i.e., a single line suffices to obtain the exact value of the probability content of the failure domain. Likewise, the limit state functions which are far from plain can be accounted for in an efficient manner.

In addition, the presence of imprecision adds another level of complexity. The estimation of the bounds requires an optimization approach making the required computational cost quite challenge. Further, the identification of the optimal maintenance strategy requires a second optimization approach, making the analysis unfeasible. In order to overcome these computational issues the adoption of Advanced Line Sampling is suggested for the calculation of the reliability and a novel optimisation strategy is proposed for the solving the maintenance approach. The Advanced Line Sampling (de Angelis et al., 2015), increases the efficiency of reliability analyses and the efficiency to estimate lower and upper bounds of the failure probability. It makes the computation of failure probabilities much faster compared with direct Monte Carlo, and most importantly because it eases the search procedure for lower and upper failure probabilities; it allows changing the important direction without re-evaluating the performance function along the processed lines.

The robust maintenance is computed adopting a novel computational strategy that allows computing the reliability of the model only once. The idea is to first simulate

the evolution of the pipelines without considering inspections and repairs by performing a Monte Carlo simulation of the model evolution (i.e. solving the equations in Table 5.1) till the time of interest. Then the solution of the optimisation problem formulated in Eq. (5.6) and (5.7) is performed within the OpenCossan software environment by simply combining all the algorithms.

5.6 Example Application

In order to demonstrate the usefulness and applicability of the approach discussed in this work, a real life above ground oil pipeline with corrosion defects is analysed. First, the effect of parameter uncertainty and model uncertainty are analysed and then a robust maintenance scheduling is performed. The pipeline characteristics are shown in Table 5.2. The evaluation of remaining strength and reliability assessment of the pipeline with defect is carried out using both DNV-101 code for semi-probabilistic values and Shell-92, B31G and B31Gmod codes for full probabilistic analysis.

The corrosion defects were assigned an interval of 150 – 250 mm and 0 - 100% as defect length and measured defect depth through the nominal wall thickness based on professional judgements, respectively. In addition, imprecise values are added to the mean values of the parameters. The quality of inspection associated with PoD is 2.42 (from Eq. 5.11). Monte Carlo simulation is employed to simulate the evolution of the system over the time considering inspections and reparation. Simulations were completed using line sampling with 20 lines, varying the number of inspections from 1 to 25 in a time period of 25 years.

Table 5.2: The pipeline characteristics

Transported substance	Crude oil
Pipe outlay	Above ground
Outside Diameter	609.6mm
Pipe material	Class X52: UTS 496MPa, SMYS 358MPa, and MAOP 4.96MPa.
Pipe nominal wall thickness	9.52mm

Table 5.3: Stochastic model used for the corroded pipeline (Ahammed, 1998; Caleyo et al., 2002)

Variable	Symbol	Unit	pdf	Mean	CoV
Diameter	D	mm	N	609.6	0.02
Defect depth	d	mm	N	3	0.1
Wall thickness	w_t	mm	N	9.52	0.02
Ultimate Tensile Strength (Quian et al., 2011)	σ_u	MPa	LN	496	0.07
Pipe Yield Stress	σ_y	MPa	N	358	0.07
Defect length	l	mm	N	200	0.1
Operating Pressure (Quian et al., 2011)	O_p	MPa	LN	4.96	0.1
Radial corrosion rate (Zhou,2010)	v_d	mm/yr	LN	0.5	0.10
Long. Corrosion rate (Zhou,2010)	v_l	mm/yr	LN	0.5	0.10

The random variables involved in the analysis and their statistical parameters in Table 5.3 are numerical values based on practice and have been obtained from Spangler and Handy (1982) and Melchers (1987). The normal distribution has been adopted for some of the variables since only means and variances are available in this literature.

Table 5.4: The monetary unit cost for operation (multiplicative factor) - Gomes & Beck, 2014.

Cost of Inspection	0.018
Cost of Repairs	0.243
Cost of Failure	36.55
Discount Rate	0.05

The monetary unit costs for operation in the form of multiplicative factors in Table 5.4 are estimated based on the summary of unit costs presented in Table A–1.1 in the Appendix.

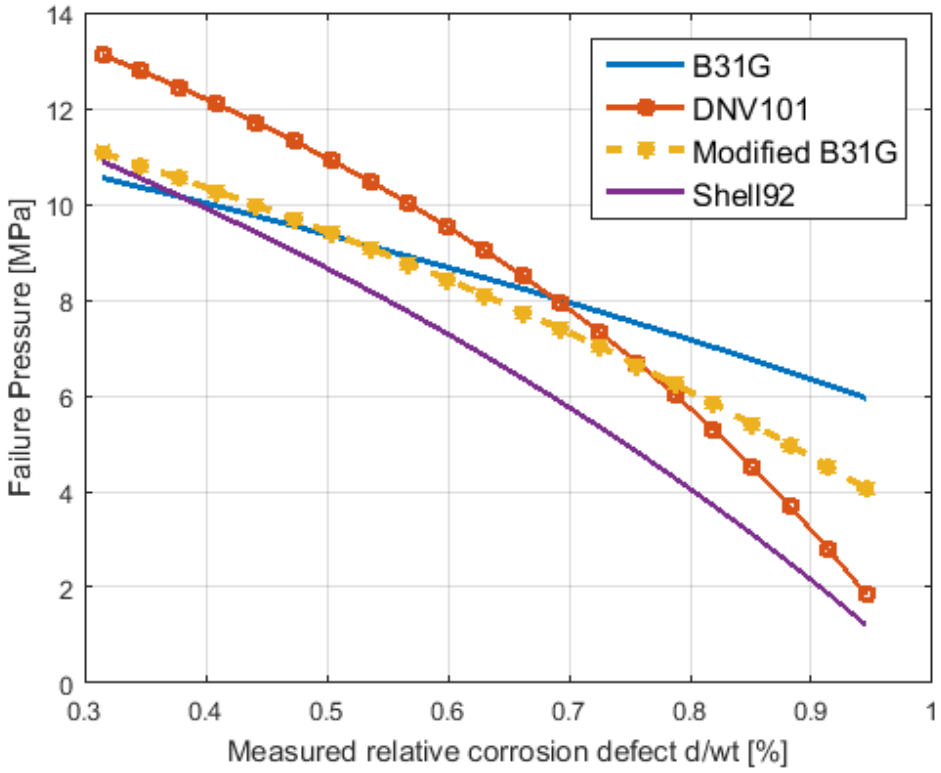

Figure 5.2: Failure pressure of the corroded pipeline in accordance with B31G, DNV-101, Shell-92, and Modified B31G codes as deterministic values.

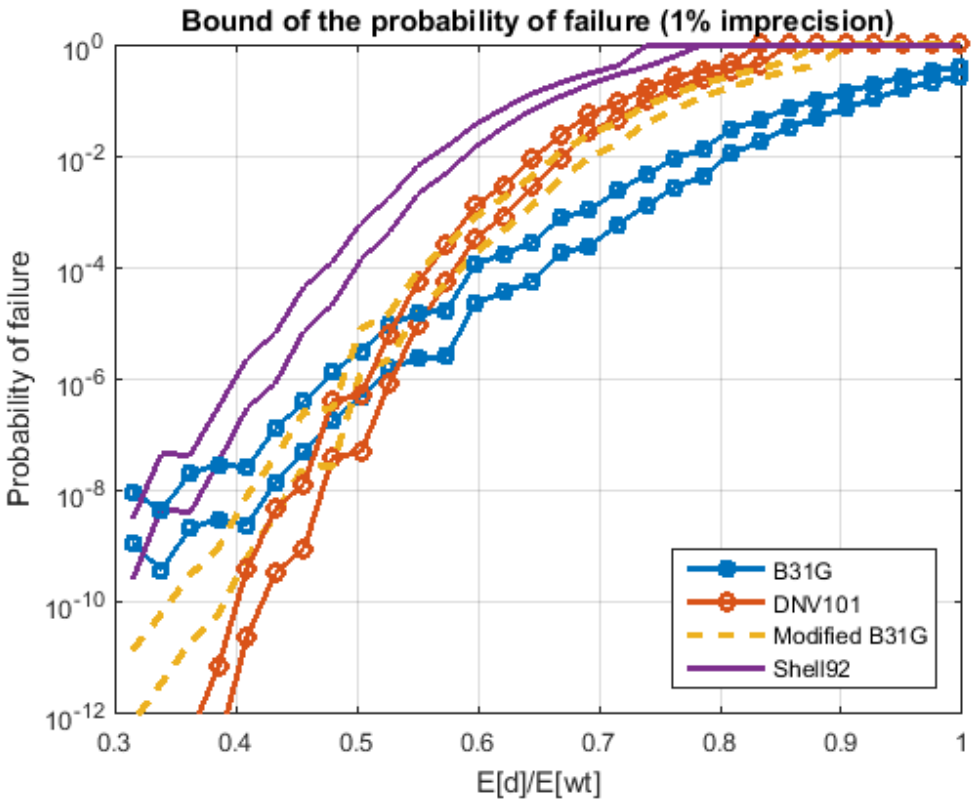

Figure 5.3: Lower and upper bounds of the probability of failure of a pipeline as a function of assigned 1% imprecision on the variables using Shell-92, B31G, Modified B31G and DNV-101 failure pressure models.

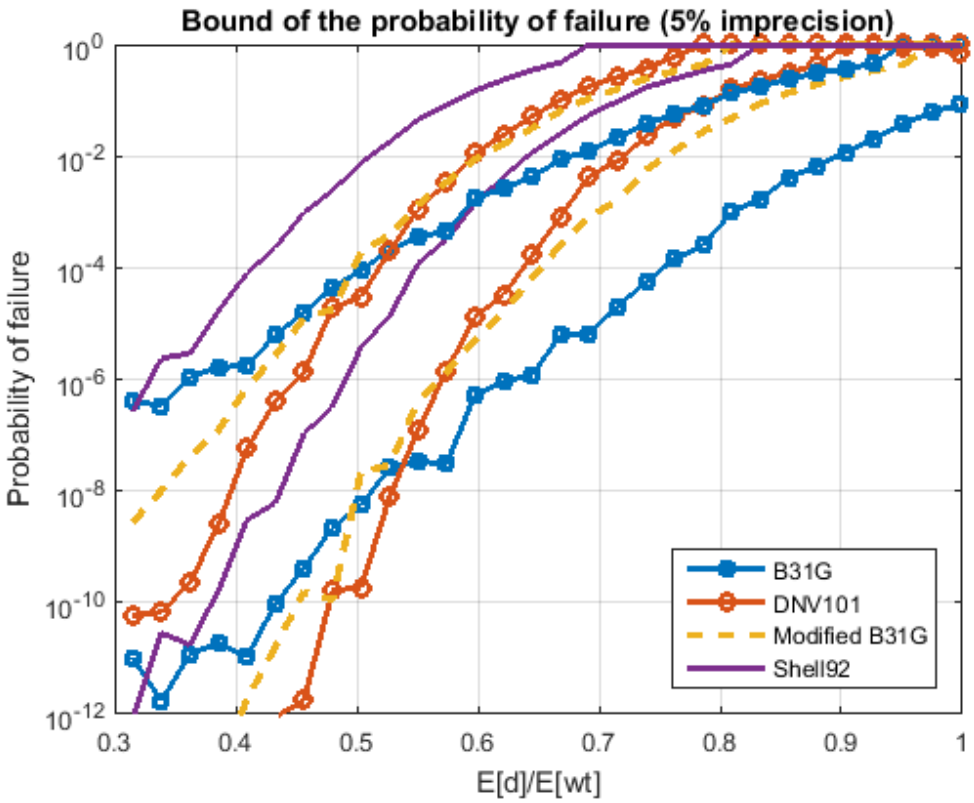

Figure 5.4: Lower and upper bounds of the probability of failure as a function of assigned 5% imprecision on the variables using Shell-92, B31G, Modified B31G and DNV-101 failure pressure models.

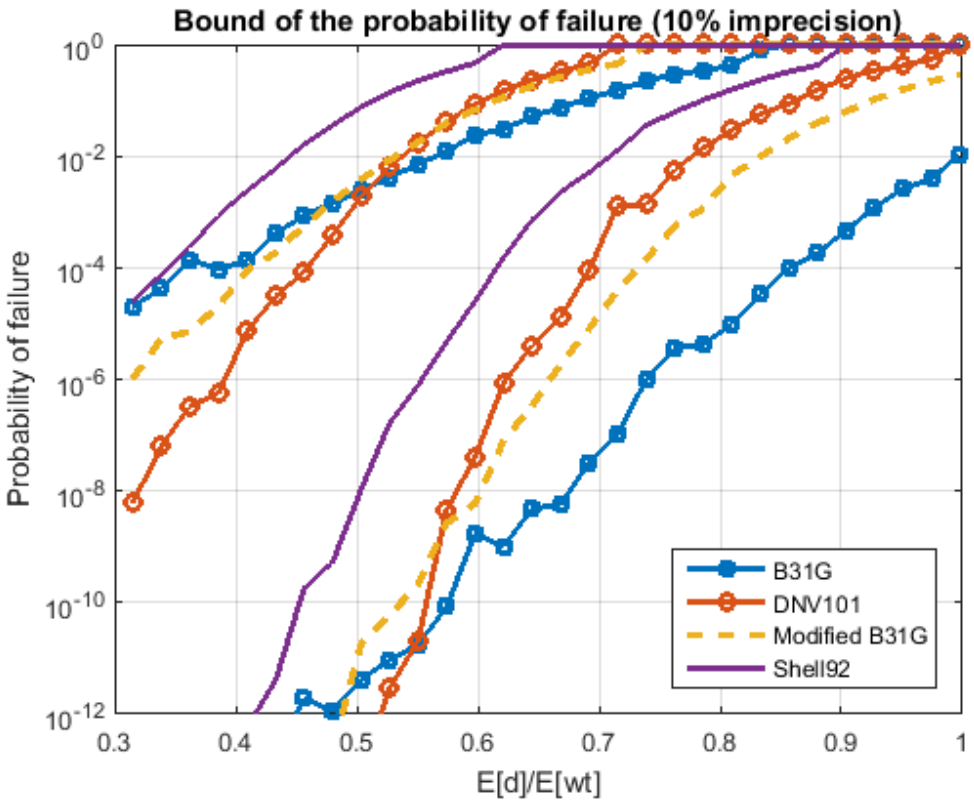

Figure 5.5: Lower and upper bounds of the probability of failure as a function of assigned 10% imprecision on the variables using Shell-92, B31G, Modified B31G and DNV-101 failure pressure models.

5.6.1 Model and parameter uncertainty

Figure 5.2 shows the model uncertainty and the corresponding variations in the failure pressure as a function of the relative corrosion defect. The failure pressure is calculated by the deterministic methods based on the Shell-92, B31G, Modified B31G and DNV-101 models. It can be seen that DNV-101 and Modified B31G models are the more conservative models, followed by the B31G model, while the Shell-92 model gives the most non-conservative result for the corroded pipeline. The reason behind the conservatism is because of the removal of several conservative simplifications (e.g. Folias' bulging factor, flow stress particularly in the Modified B31G model) in an effort to be a bit more accurate. Generally, and it is obvious that the failure pressure decreases with increasing measured relative corrosion defects for all the deterministic analyses.

In Figures 5.3 and 5.4, the probability of failure as a function of the expected values of the relative corrosion defect ($E[d]/E[w_t]$) is shown. The probability of failure has been calculated using the parameters shown in Table 5.3. Advanced Line Sampling simulation is adopted with 20 lines resulting in 120 model evaluations for each reliability analysis but independently of the reliability level. As expected, the probability of failure of the corroded pipeline increases with increase in measured relative corrosion defect. It is highly conservative in the Shell-92 and the DNV-101 models followed by Modified B31G model and the least in the B31G model. Considering a small level of imprecision in the parameter values (1%) the results in Fig. 5.3 show that the Shell-92 and the B31G models give the highest and the lowest failure probabilities (for a relative corrosion level greater than 0.6) respectively; and this is in accordance with obtained results from literature (Qian et al., 2011; Caleyo et al., 2002).

The results in Caleyo et al. (2002) show that the failure pressure models used to predict failure pressure give similar pipeline failure probabilities for relatively short service time. For longer service times, the Shell-92 gives the highest failure probabilities while B31G gives the smallest. This is in agreement with the results obtained here in this study without considering imprecision in the model parameters.

In order to understand the effect of imprecision on the probabilistic model, imprecision has been included. The first moments of the distribution have been assumed to be known with a degree of imprecision. More specifically, a 1%, 5%, and 10% of variation around the mean values have been considered. The analysis is shown in Table 5.5.

Table 5.5: Imprecise values on the probabilistic model

Safety Level	Bounds (%)	B31G		DNV-101		ModB31G		Shell-92	
		Upper	Lower	Upper	Lower	Upper	Lower	Upper	Lower
1e-3	1	0.7389	0.6918	0.6447	0.5977	0.6447	0.6212	0.556	0.5270
1e-4		0.6683	0.5977	0.5977	0.5741	0.5977	0.5741	0.5035	0.4799
1e-5		0.5977	0.5506	0.5741	0.5506	0.5506	0.5270	0.4799	0.4564
1e-6		0.5270	0.4799	0.5506	0.5270	0.5035	0.5035	0.4564	0.4093
1e-7		0.4799	0.4328	0.5270	0.4799	0.5035	0.4564	0.4093	0.3858
1e-3	5	0.8331	0.5977	0.6918	0.5506	0.7154	0.5506	0.5977	0.4799
1e-4		0.7625	0.5270	0.6447	0.5270	0.6683	0.5035	0.5506	0.4328
1e-5		0.7154	0.4564	0.5977	0.4799	0.6212	0.4564	0.5270	0.3858
1e-6		0.6447	0.3622	0.5741	0.4564	0.5741	0.4328	0.5035	0.3387
1e-7		0.5977	0.3151	0.5506	0.4328	0.5506	0.3858	0.4564	0.3151
1e-3	10	0.9273	0.4799	0.7389	0.5035	0.7860	0.4799	0.6683	0.4093
1e-4		0.8566	0.4093	0.7154	0.4564	0.7389	0.4328	0.6212	0.3622
1e-5		0.8095	0.3151	0.6683	0.4328	0.7154	0.3858	0.5977	0.3151
1e-6		0.7625	0.3151	0.6447	0.4093	0.6683	0.3151	0.5741	0.3151
1e-7		0.7154	0.3151	0.6212	0.3622	0.6212	0.3151	0.5270	0.3151

The uncertainty in the output predictions is dominated by the model uncertainty. While for an imprecision level of 5% in the parameter values, the uncertainty due to the model parameters become comparable with the model uncertainty, in particular for small relative corrosion level. For imprecision of 10%, in a relative corrosion level of 0.6; the B31G model (lower bounds) and the Shell-92 (upper bounds) give the lowest and the highest failure probabilities respectively. DNV-101 and Modified B3iG models give the same levels of failure probabilities both for lower and upper bounds of imprecise values (see Fig. 5.5).

Considering the lower and upper probability bounds, DNV-101 and Modified B31G models could be quite relevant when dealing with unnecessary pipe repairs and for greater safe operating pressure in the pipelines. It will provide the operator with several options to manage both the present and future integrity of the pipeline at a minimum acceptable reliability level with limited resources.

To summarise, the probabilistic procedures are required to evaluate pipeline integrity because of the inherent uncertainties associated with corrosion growth rate, inspection tools, pipeline geometry, material properties and operating pressure. Considering the effect of imprecision is of paramount importance. First, it allows accounting for the effect of such imprecision on the quantity of interest and

secondly can allow identifying the maximum level of imprecision that can be tolerated. In fact, this has overcome the drawbacks in classical probabilistic methods with the consideration of an entire set of probabilistic models in one analysis; thereby making imprecise probabilities framework provide mathematical basis for dealing with problems which involve both probabilistic and non-probabilistic information.

The safety level of imprecision and uncertainty that can be tolerated according to this result, for a meaningful outcome or performance on the measured defect depth through the nominal wall thickness has been outlined. After having analysed the pipeline probability a robust maintenance scheduling is performed in order to get an optimal solution as to remove huge computational cost of reliability-base optimization and making the analysis of industrial size problem feasible.

5.6.2 Robust maintenance

Optimal maintenance strategy for the remaining life time of the pipeline is assessed using the failure pressure models in Table 5.1 and performed adopting a very efficient procedure requiring performing only a single reliability analysis.

Fig. 5.6 shows the results of the application of the imprecise probability to compute the pipeline failure probability at mission time against the number of inspection using the failure pressure models in Table 5.1. A mission time interval of 25 years from the last in-line inspection time was considered with numbers of inspections ranging from 1 to 10.

Considering imprecision in the failure pressure models, results in Fig. 5.6 show that the failure probability is lowest with the upper bound of imprecision in B31G model and highest with the lower bound of imprecision in Modified B31G model. Probability of failure increases with lesser numbers of inspections for a specified mission time, but decreases with large numbers of inspections within the same mission time.

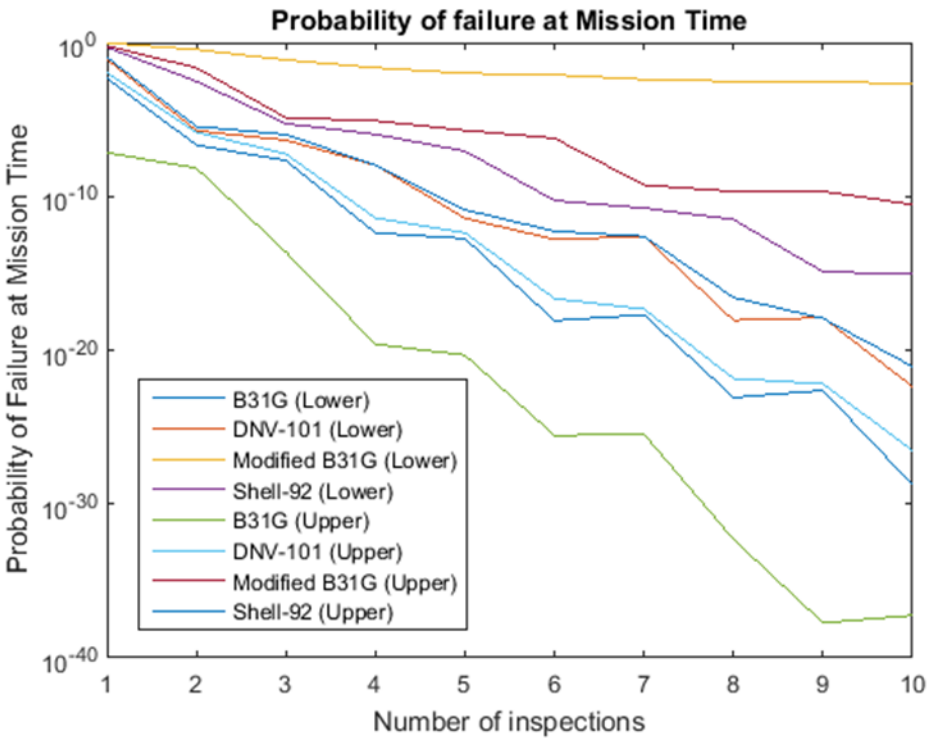

Figure 5.6: Pipeline probability of failure at mission time as a function of the number of inspection using Shell-92, B31G, Modified B31G and DNV-101 failure pressure models.

The expected number of total repairs action is shown in Fig. 5.7. The lower bound of imprecision in Modified B31G model predicts the lowest number of repair actions and highest was in the lower bounds of imprecision in B31G, DNV-101 and upper bounds of imprecision in Shell-92, DNV-101, and B31G models. The increase in expected number of repairs with an increase in the inspection numbers signifies that increase in numbers of inspection increases the chances of failures to be detected, in addition to the possible damage to the system during each inspection thereby increasing the total cost of operation.

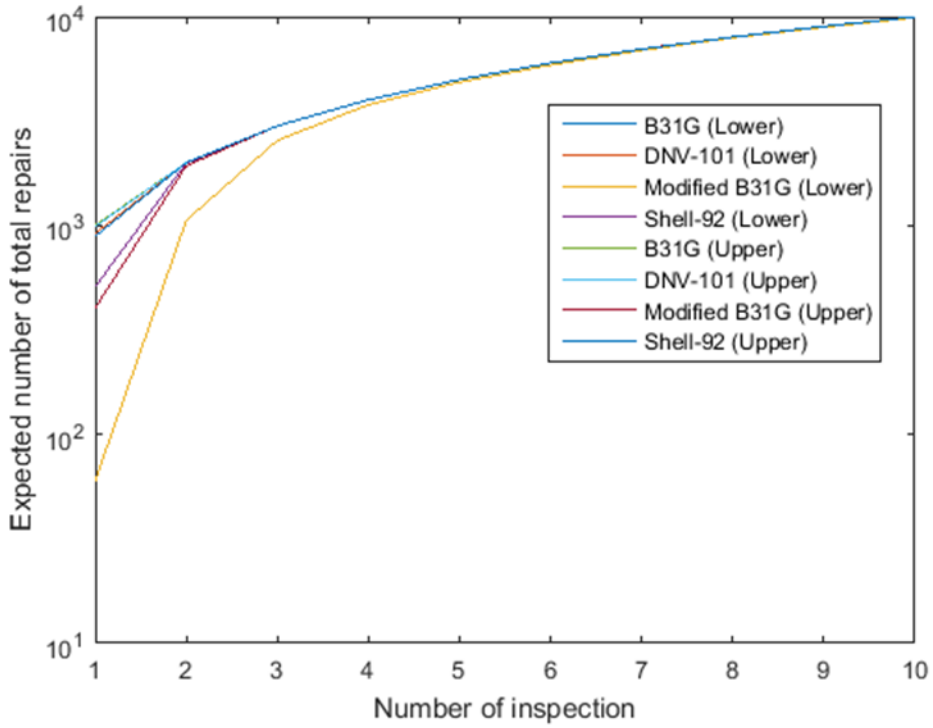

Figure 5.7: The expected number of total repairs as a function of the number of inspection using Shell-92, B31G, Modified B31G and DNV-101 failure pressure models.

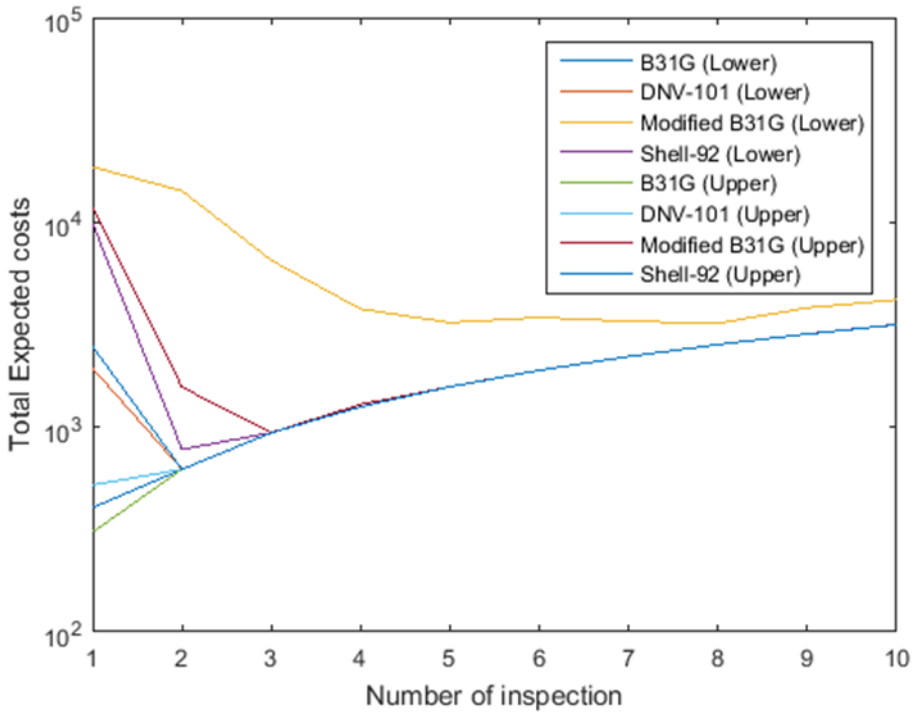

Figure 5.8: Pipeline expected costs as a function of the number of inspection using Shell-92, B31G, Modified B31G and DNV-101 failure pressure models.

The optimal inspection time is usually between when inspections are performed too early (e.g. for 10 inspections carried out in a mission time of 25 years, i.e. every 2.5 years an inspection is carried out), and when inspections are undertaken too late (e.g. for 1 inspection carried out in a mission time of 25 years, i.e. only one inspection in 25 years). Almost no damage will be found and no repair will take place for early inspections resulting in marginal or no improvement in the pipeline reliability. While for too late inspections, in relation to the level of defect damage, the detection probability will be large. In this case, it is most likely that the pipeline system will have failed already.

In Fig. 5.8, the total expected costs as a function of the number of inspections with eventual repairs shows similar results for all the failure pressure models (particularly from 3 to 10 numbers of inspections), and only the lower bound in Modified B31G differs notably from the rest. It can be deduced here also that the optimal inspection time for both lower and upper bound of imprecision in all the failure pressure models is 3 inspections with eventual repairs (i.e. about 8 years), with the exception of the lower bound in Modified B31G. Furthermore, the optimal solution is dependent on the number of inspections for different mission times.

Other results on cost details for total costs of operation, inspections, repairs and failure using all the failure pressure models either separately or collectively considering 1 to 10 inspections in mission times of 20 years and 50 years are shown in the appendix: Figs. A- 2.1, A- 2.2, A- 2.15 and A- 2.16. Expected total number of repairs for all the failure pressure models considering 1 to 10 inspections in mission times of 20 years and 50 years in Figs. A- 2.3 and A- 2.4 respectively. Pipeline probability of failure at mission time as a function of the number of inspection using Shell-92, B31G, Modified B31G and DNV-101 failure pressure models are shown in Figs. A- 2.5 to A- 2.14.

5.7 Concluding Summary

In this work the importance of the model uncertainty on a proper characterisation of uncertainty has been shown. The proposed imprecise probabilities approach can

be applied for the design of new systems as well as for assessing existing pipelines in operation, its inspection and repair for scheduling maintenance. It has been shown how this approach can improve the practise using B31G, Modified B31G, DNV-101 and Shell-92 failure pressure models.

In addition, an efficient numerical approach for robust optimal pipeline inspection time has been proposed. The procedure allows minimization of expenditures incurred when conducting maintenance activities, and at the same time keeping the pipeline in safe operation mode. The probabilistic framework presented is well suited for use to determine the optimal inspection interval and the repair strategy that would maintain adequate reliability throughout pipeline service life due to its simplicity, general applicability and singular reliability estimation for the whole optimization procedures.

6. Reliability Assessment of Arctic Pipelines

6.1 Introduction

This chapter presents an application of the imprecise probabilities (p-boxes) for reliability analysis of above ground arctic oil pipelines with surface corrosion defects, subjected to a combination of loads. The effect of wind load is one of the main components of the pipeline design in this setting, which depends on climate change, and it is modelled with imprecise probability framework. The primary concern is the uncertainty characterization of the wind load and its influence on the overall pipeline reliability. The other combinations of simultaneous loads are the pipe weight, and oil or gas pressure. The pipeline probability of failure is defined as ultimate permissible moments, and it is reached when the equivalent stresses in pipe wall reach the yield stress of pipe material. Since the structural system reliability depends on the parameters of the probability model; probability bounds concept is introduced into the conventional reliability theory and proposed to deal with error in parameter estimation and, in turn, with error in resulting probability. The advantages of using the proposed approach are discussed. Results obtained for typical pipelines are presented to show the feasibility of the proposed approach.

Studies on the behaviour of corroded pipelines under external pressure and/or combined loads are not readily available or standardized (Bolzon et al., 2011). Reliability analysis techniques have been adopted in several contributions in the literature, as to make allowance for the uncertainties of the design variables on pipelines. Hence, a probabilistic method of remaining life estimation which is more robust than deterministic analyses, which can be used to evaluate the pipeline's current reliability and the time-dependent change in reliability, is widely accepted (Ahammed and Melchers, 1997; Melchers, 1999; Caleyo et al., 2002; Qian et al., 2011; Bazan and Beck, 2013; Timashev and Bushinskaya, 2010). The problem of load combination is of great significance in structural analysis, whereby the loads are traditionally considered as constants due to safety concern, they are taken as

the maximum values in the design codes. The loads here are considered as having a stochastic nature.

The modelling of various factors such as nonlinear material behaviour, corrosion geometry (i.e. the size and shape), large deformations and applied loading made an accurate assessment of the integrity of a corroded pipe very complex and difficult; which leads to development of simple analytical closed-form solutions for accurate evaluation of pipeline integrity. The guidelines in all the failure pressure models e.g. (ASME-B31G, 1991; ASME-B31G, 1995; DNV, 1999), etc. have been useful to pipeline operators in assessing the integrity of corroded pipelines. One of the possible shortcomings of these codes is that they could give non-conservative failure predictions when combined loading exists, particularly when only pressure loading is considered while bending and axial compression are neglected (Roy et al., 1997).To quantify these uncertainties, probability theory has been applied in assessing existing pipeline conditions. But beyond classical probability theorem in dealing with uncertainties associated with pipelines reliability and maintenance, inspection time interval, and cost of operations; imprecision should be added to these uncertainties for a robust maintenance strategy. Imprecise probabilities have emerged in several application fields in structural engineering (Walley, 1991). The largest application field appears as reliability assessment, where imprecise probabilities are implemented to address sensitivities of the failure probability with respect to the probabilistic model choice (Beer et al., 2013). Limitations in engineering practice can be quite substantial, due to poor quality and limited available data. Information is not often available in the form of precise models and parameter values, but as imprecise, vague or incomplete.

This contribution proposes a robust method for predicting remaining strength for corroded pipeline subject to combined loadings, which works with reliability metric redefined within the framework of imprecise probabilities. The novelty of the proposed approach is the combination of the classical probability theory (probabilistic methodology) with non-classical probability theory (probability bounds analysis with p-boxes), to determine the bounds of pipeline's structural

reliability taking cognisance of the wind parameters, which evolve in time due to global climate change.

In this work, a description is given of the first stage of assessing reliability of a pipeline subject to a combination of loads described as random Markov processes. This method, developed by Timashev in (Timashev, 1982), assumes the ability of constructing admissible areas in this load space with respect to different limit states. The method is applied to a segment of an above ground arctic oil pipeline with surface corrosion type defects, subjected to a combination (simultaneous action) of four loads: 1) dead weight of the pipe with insulation and oil being pumped, 2) operating pressure, 3) wind load, and 4) exposure to a uniform wall thickness thinning. The pipeline is considered as a continuous multi-bay thin wall cylindrical beam. The pipeline design is performed according to the (conditional) limit state which is reached when the equivalent stresses in pipe wall reach the yield stress of pipe material.

As the final result, we obtain two-sided estimate of the reliability/probability of failure of the pipeline. These estimates also as functions of time form a corridor and have the same shape as the permissible wind pressure.

The advantage of the developed approach is the visibility and ease of interpretation of problem essence. Indeed, even before calculating the reliability function for the engineer it is clear what quality criteria are the most severe, and which elements are not involved in the formation of the admissible region. It allows selecting elements with redundant reliability and outlining constructive measures to reduce its reliability to the level, which does not affect the overall system reliability.

6.2 Model of the Arctic Pipelines

Arctic pipelines are located north of the 60th parallel. The main factors that characterize features of such pipelines are the climatic conditions in their areas of installation. Arctic pipeline routes pass through tundra with dwarf vegetation, marshes, and large areas with permafrost lenses, in watery and swampy areas with

unique geological and hydrological conditions. The absolute difference of temperatures ranges from -56 degrees Centigrade in winter to 34 Centigrade in summer; and strong winds with speed over 40 m/s. Under these conditions, reliability and safety assessment of pipelines is associated with many principal difficulties, one of which is the need to take into account the simultaneous action (a combination) of many natural and technological loads on the pipeline infrastructure, which are random by nature and can be adequately described only by stochastic processes. Currently, reliability assessment of such systems is not performed due to lack of valid calculation methods.

The main purpose of the presented work is reliability assessment of arctic pipeline in the space of load (impacts). At this the dead load of the pipeline structure is considered to be deterministic. The influence of the wind load, uniform corrosion, and operating pressure are considered to be variables. For them the permissible region is constructed using the above limit state.

Wind pressure in the Arctic zone, due to the fact of climate change is a non-stationary random process. Currently we know too little about it, and do not fit into any of the classic forms of probabilistic description of uncertainty. Therefore, we describe it using a time series of measured wind speeds, using the interval probabilities method (Opeyemi et al., 2015a; Opeyemi et al., 2015b).

In this work we estimate the arctic pipeline reliability through the probability of finding the vector of loads and impacts on a system in the admissible area, which is constructed using the limit state function (see e.g. SNIP 2.05.06-85*). The boundary of this area is found by solving a series of inverse problems at fixed values of the deterministic values and several values of the random variables, which cover the whole area of their existence. From physics and mechanics of the process it is clear that the maximum allowable wind pressure is at the initial time (start of the system operation) when the whole pipe is brand new. At a fixed corrosion rate for each subsequent moment of time the coordinate x of the parabola y is the maximum permissible wind pressure on the pipe, i.e., the pressure at which the limit state is

realized in at least one of the points of pipeline cross-section. In this case the limit state equations and the actual wall thickness as related to the considered moment of time *x*, is used. It is clear that, over time, with the pipe wall thickness thinning, the maximum wind pressure that the pipe can bear will be decreasing. Now, for each such point (through which the permissible level of wind pressure y) we need to find an interval estimate of the probability that this pressure is exceeded, using interval estimates method.

6.2.1 Stress state of the above ground pipelines

The general stress state of the oil pipeline has been extensively discussed in Section 4.5 of Chapter 4. This is comprised of stresses due to the operating pressure; stresses which depend on the oil pipeline temperature; and stresses defined by external forces and influences. The models for estimating all these are stated in Eq. (4.36) to (4.42) of Sections 4.5.1 to 4.5.3.

6.2.2 Longitudinal bending stresses in an above ground pipelines

Consider the linear segment of an arctic above ground pipeline as continuous beams on hinge supports, and taking into account the kinematic influence of the transverse dead load/wind load. The vertical displacement of its supports can be estimated using the three-moment equation. All the values of unknown bending moments on the supports are determined in a sequence. To estimate the limit values of the wind load at a fixed vertical transverse load, we defined the limit bending stresses. Then we selected the minimum value of the absolute value (i.e., the bending stress), which is created by the minimal ultimate bending moment. These have been outlined in the assessment of the bending stresses due to wind load (see Section 4.7.1), and the numerical modelling stated in Eq. (4.50) to (4.56).

6.2.3 Assessment of the bending stresses due to wind load based on normative wind load model

Knowing the bending moment from the vertical load, we can assess, using Eq. (4.53) the ultimate moment from the horizontal transverse (wind) load.

$$M = \sqrt{M_v^2 + M_h^2}$$

The normative wind load q_w, (N/m) on a metre span (1m) of the arctic pipeline length is determined using Eq. (4.57)

$$q_w = (q_n^c + q_n^d) D_{in},$$

Only static component of wind load is considered here for simplicity. That is, only the wind blow is taken into consideration and not the gust and turbulence components. So the normative value of the static (average) component wind load q_{n}^{c} is calculated by Eq. (4.58) as:

$$q_n^c = w_0 k(z_e) c,$$

Normative value w_0 of wind pressure is chosen from Table 4.3 depending on the wind area. Normative value of wind pressure may be determined in accordance with established procedure on the basis of the RosHydromet meteorological stations data (RosHydromet, 2008). In the latter case the w_0 (Pa), should be determined by Eq. (4.59)

$$w_0 = 0,43 v_{50}^2 ,$$

where v_{50}^2 is the wind pressure corresponding to the wind speed, m/s, at 10 m above the ground level for terrain type A, which is determined by averaging measurements made in 10-minute intervals and is exceeded once in 50 years.

Equivalent height $z_e = z_g + d/2$, where d, in meters, is the pipeline diameter; z_g is the distance from the ground to the pipeline in Fig. 4.8 as shown below.

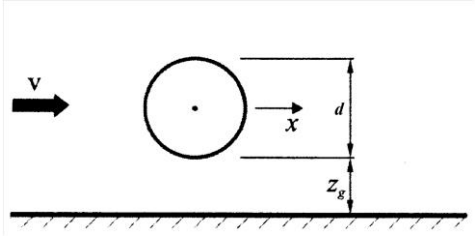

Figure 4.8: The distance of the pipeline from the ground, z_g

The coefficient $k(z_e)$ can either be determined by Eq. (4.60) or Table 4.4.

$k(z_e) = k_{10}(z_e/10)^{2\alpha}$.

The aerodynamic drag coefficient c = 0.5. Table 4.5 shows parameter values k_{10} and α for different types of terrain.

6.3 Uncertainty Characterization in the Wind Parameter

Set models of wind loads were created, by analysing the distribution of the maxima annual values of the wind speed. The maxima measured wind speeds over a given period of 25 years (1990 – 2014) were taken, i.e. 25 data points were taken over 25 years from Svalbard airport, Spitsbergen Norway station. The values are presented in Fig. 6.1. Analysis is made considering wind loads as imprecise values for the Svalbard airport stations.

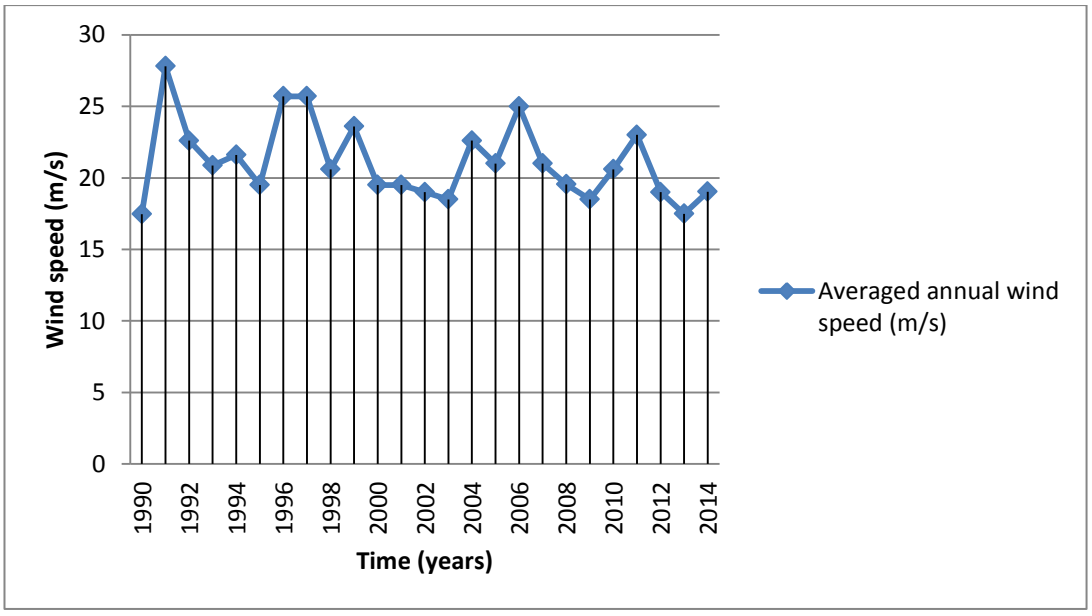

Figure 6.1: Maximum measured wind speed over a period of 25 years - Svalbard, 1990 – 2014 (WeatherSpark, 2015)

In this work, the maximum likelihood estimate was employed to get the two parameters in the type 1 Gumbel distribution. The statistics of such extremes of natural phenomena are of great significance, since extreme value distributions are widely used in reliability analysis to model a variety of extreme phenomena like

wind temperature in a changing climate, failures under stress, flood data, etc.; maximum or minimum are of importance in science and engineering.

Suppose X is a random variable with the pdf f_X and the cdf F_X. Let $X_1,...,X_n$ be i.i.d random variables, $X_1 \sim f_X$ ("population"). Our point of interest is $Y_1 = \min\{X_1,...,X_n\}$, and/or $Y_n = \max\{X_1,...,X_n\}$. Then,

The cdf of $Y_n = F_{Y_n}(y) = [F_X(y)]^n$ (6.1)

The pdf of $Y_n = f_{Y_n}(y) = n[F_X(y)]^{n-1} f_X(y)$ (6.2)

The parameters of the distributions are calculated using maximum likelihood estimates for the sets of the wind data. Maximum likelihood was employed as a method of point estimation (see e.g. Forbes et al., 2010). Given a random variable X with pdf f (x; θ) and sample size n; the most likely value of θ that will produce the particular set of observations.

So, for a sample of size n, with sample values $X_1,...,X_n$, the likelihood function $\ell(.)$ is given by:

$$\ell(X_1,...,X_n;\theta) = f(X_1;\theta)f(X_2;\theta),...,f(X_n;\theta) \quad (6.3)$$

Define the maximum likelihood estimator as $\hat{\theta}$ that maximizes $\ell(.)$. First procedure was differentiating the likelihood function

$$\frac{\partial \ell(X_1,...,X_n;\theta)}{\partial \theta} = 0 \quad (6.4)$$

Since the likelihood function is a product, it is possible to work with the logarithm. As the logarithm is monotonic, it does not affect the result of the optimisation procedure.

$$\frac{\partial \log \ell(X_1,...,X_n;\theta)}{\partial \theta} = 0 \quad (6.5)$$

For pdfs defined by more than one parameter, the procedure is analogous:

$$\ell(X_1,...,X_n;\theta_1,...,\theta_m)=\prod_{i=1}^{n} f(X_1;\theta_1,...,\theta_m) \tag{6.6}$$

$$\partial \log \ell\left(\frac{(X_1,...,X_n;\theta_1,...,\theta_m)}{\partial\theta_j}\right)=0 \tag{6.7}$$

The intention initially was to use the more generalized extreme value distribution (GEV) for this distribution modelling, but the shape parameter of the GEV ξ equals zero. Then, as a rule following this condition, Gumbel distribution "type I extreme value distribution" was used. The parameter fitting using maximum likelihood estimation (MLE) of a Gumbel distribution is performed as follows:

The type 1 Gumbel distribution's CDF is

$$F_X(x)=\exp\left(-\exp\left(-\frac{x-\mu}{\sigma}\right)\right), \text{ x } \epsilon\ \mathcal{R} \tag{6.8}$$

Its PDF is given by expression

$$f_X(x)=\frac{1}{\sigma}\exp\left(-\frac{x-\mu}{\sigma}\right).\exp\left\{-\exp\left(-\frac{x-\mu}{\sigma}\right)\right\}, \ \mu \in \mathcal{R} \text{ and } \sigma > 0 \tag{6.9}$$

The inverse cdf for probability *p* is given by

$$Q(p)=\mu-\mu.\log(-\log(p)) \tag{6.10}$$

The parameter estimation is obtained following the procedure below.

Given that $X_1,...,X_n$ are i.i.d variables following a Gumbel distribution, the log-likelihood is

$$\mathcal{L}(\mu,\sigma)=-n\log(\sigma)-\sum_{i=1}^{n}\left(\frac{x_i-\mu}{\sigma}\right)-\sum\exp\left\{-\left(\frac{x_i-\mu}{\sigma}\right)\right\} \tag{6.11}$$

The log-likelihood can be maximized using standard numerical optimization algorithms.

Forbes in (Forbes et al., 2010) provides the MLE estimates for μ and σ. namely, the estimators $\hat{\mu}$, $\hat{\sigma}$ as the solutions of equations;

$$\hat{\mu} = -\hat{\sigma} \log\left[\frac{1}{n}\sum_{i=1}^{n} \exp\left(-\frac{x_i}{\hat{\sigma}}\right)\right] \tag{6.12}$$

$$\hat{\sigma} = \bar{x} - \frac{\sum_{i-1}^{n} x_i \exp\left(-\frac{x_i}{\hat{\sigma}}\right)}{\sum_{i=1}^{n} \exp\left(-\frac{x_i}{\hat{\sigma}}\right)} \tag{6.13}$$

Where $\bar{x}$ denotes the sample mean.

In order to better understand these wind speed data we mimicked its variability with a bootstrap, as an alternative to the traditional statistical technique of assuming a particular probability distribution (Burn Statistics). This bootstrap is a procedure of sampling from the empirical distribution of the data, under an assumption that the bootstrapped data are independent and identically distributed. Bootstrapping is a nonparametric method and comes in handy when there is doubt that the usual distributional assumptions and asymptotic results are valid and accurate. Bootstrapping permits computation of estimated standard errors, confidence intervals and hypothesis testing (Burn Statistics). In our case one bootstrap sample is 25 randomly sampled annual returns. This sampling is with replacement, so some of the years will be in the bootstrap sample multiple times and other years will not appear at all. A thousand (1000) bootstrap samples were created. In a nutshell, the steps involve: 1) resampling a given data set a specified number of times; 2) calculating a specific statistic from each sample; and 3) finding the standard deviation of the distribution of that statistic.

Intervals of the location and scaling parameters of the type 1 extreme value distribution were created and the maximum and minimum values across all the sample values of the distribution were obtained. A lower and upper probability for

the wind speed is obtained by constructing a p-box to characterize uncertainty in wind parameter, Fig. 6.2 – this is to cater for incertitude and variability. All simulations are implemented in OpenCossan - the open source engine of COSSAN software for uncertainty quantification and risk management (Patelli et al., 2014; Patelli, 2016). The COSSAN software has been validated on NASA Langley multidisciplinary uncertainty quantification challenge, where limitations and ranges of applicability of existing uncertainty quantification methodologies were determined, new discipline-independent uncertainty quantification methods relevant to engineering applications developed, and the advancement of the state of the practice in uncertainty quantification problems of direct interest to NASA (Patelli, 2016).

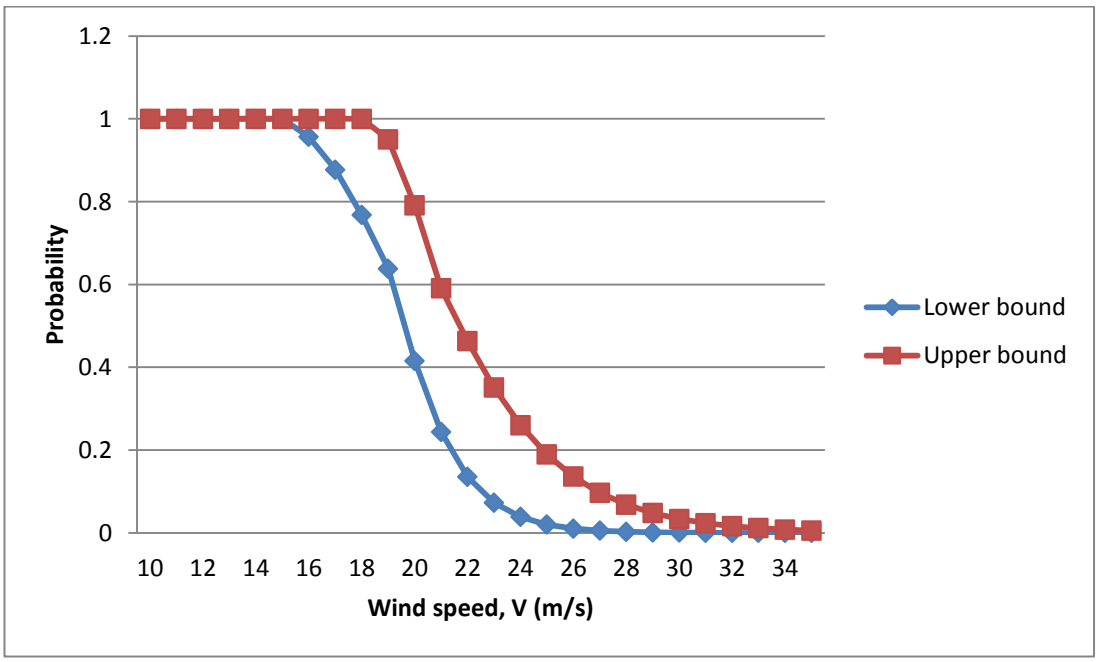

Figure 6.2: Probability box for wind speed - Svalbard, 1990 – 2014 (WeatherSpark, 2015)

The construction of the p-box is described in Section 3.3.2. Recall that, if $[\overline{F}, \underline{F}]$ is a p-box for a random variable X whose distribution *F* is unknown except that it is within the p-box, then $\underline{F}$ (x) is a lower bound on *F(x)* which is the (imprecisely known) probability that the random variable X is smaller than x. Likewise, $\overline{F}$ (x) is

an upper bound on the same probability. From a lower probability measure $\underline{P}$ for a random variable *X,* one can compute upper and lower bounds on distribution functions using Eq. (3.20) and (3.21)

$$\overline{F}_X(x) = 1 - \underline{P}(X > x)$$

$$\underline{F}_X(x) = \underline{P}(X \leq x)$$

A plot of the minimum and maximum values (p-box) was constructed and creation of empirical cumulative distribution function ecdf to compare with the p-box. When the information about a distribution is very good, the bounds on the distribution will be very tight, approximating the precise distribution that is used in a Monte Carlo simulation. When the information is very poor, the bounds will tend to be much wider, representing weaker confidence about the specification of this distribution. This bounding approach permits analysts making calculations without requiring overly precise assumptions about parameter values, dependence among variables, or distribution shapes. In principle, this approach allows the analyst to decide which assumptions are reasonable and which are not.

The summary of the interval estimation in a nutshell is highlighted below:

Probability Plots (p-p plots)

- Get a set of data - Take some wind data (maximum measured wind velocity over a given period). Here, 25 data points taken over 25 years
- Form an empirical cdf (ecdf)
- Produce a most likely cumulative probability function for this set of data (e.g. Gumbel type 1 in this case) on vertical axis. Use maximum likelihood estimate to get the two parameters of the Gumbel distribution
- Plot the data (sorted) against this new axis
- Compare Normal, Lognormal, Exponential, Weibull, Rayleigh and Extreme value distributions probability plots
- Compare looking at cdfs
- Compare other error measures

Probability Box (p-box)

- Get a set of data.
- Create a function to evaluate the parameters using maximum likelihood estimates
- Resample from the existing samples using bootstrap
- Give intervals of the location parameters
- Give intervals of the scaling parameters
- Obtain maximum and minimum values across all the sample values of the distribution
- Plot the minimum and maximum values (p-box)
- Create ecdf to compare with the p-box.

There are two interpretations of the p-box. Firstly, as bounds on the cumulative probability associated with any wind speed value - In Fig. 6.2 for example, the probability that the wind speed value will be 25m/s or more is between 2% and 19%. Secondly, as bounds on the wind speed value at any particular probability level- here also in the p-box, the 95th percentile is sure to be between 16m/s and 19m/s.

6.4 Example Application – case 1

Consider a segment of a real above ground arctic oil field collection pipeline, parameters of which are given in Table 6.1.

Table 6.1: Initial design parameters of the oil pipeline

Transported substance	Crude oil
Oil density	863.7 kg/m^3
Pipe outlay	Above ground
Outside Diameter of Pipe	325 mm
Pipe material	Steel grade: 20, SMYS: 245MPa
Steel density	7.85x10^3 kg/m^3
Pipe wall thickness	9 mm
Operating Pressure	6.4MPa
Design temperature	+20^{o}C
Temperature at pipeline outlay	– 32^{o}C
Insulation	Epoxy anticorrosion insulation, spiral zinc coated folded pipe insulation shell 1.5 mm thick. The insulation proper thickness is 100 mm
Young modulus	2.06 x10^5 MPa
Linear expansion coefficient	1.2x10^{-5} 1/^{o}C
Poisson coefficient: a) for elastic performance of metal b) for plastic performance of metal	 0.3 0.5

The considered segment has 6 spans which lengths are: L_1 = 4m, L_2 = 5m, L_3 = 4m, L_4 = 5m, L_5 = 3m, and L_6 = 5m. For simplicity sake it is assumed that both ends of the oil pipeline segment are rigidly fixed (which creates an error in pipe strength assessment on the safe side). The oil pipeline scheme is given in Fig. 6.3.

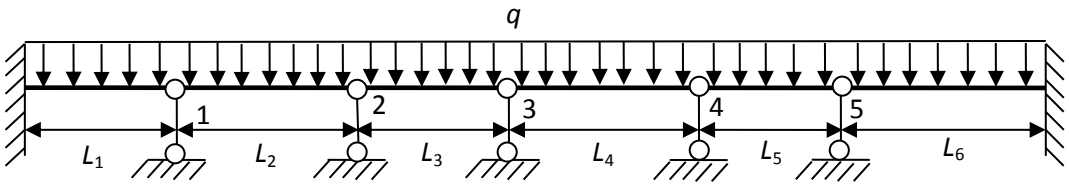

Figure 6.3: Design scheme of the oil pipeline segment

6.4.1 Results and discussion

To calculate the linear load, Weight w_p (N/m) of a meter span (1m) of pipe length we use Eq. (6.14):

$$w_p = g\rho S \tag{6.14}$$

where g is the gravity acceleration, m/s^2; ρ is the steel density, kg/m^2; $S = \frac{\pi\left(D^2 - D_{in}^2\right)}{4}$ is the cross-sectional area of the pipe, m^2.

Therefore the weight of 1m of the pipe estimated from Eq. (6.14) is

$$w_p = 9.8x7850x3.14\left(0.325^2 - \left(0.325 - 2x0.009\right)^2\right)/4 = 686.99 \text{ N/m}$$

Weight of transported oil w_{oil} (N/m) in 1 m of pipeline is determined by Eq. (6.15)

$$w_{oil} = g\rho_{oil}\frac{\pi D_{in}^{\ 2}}{4}, \tag{6.15}$$

where ρ_{oil} is oil density, kg/m^3.

In this example application case:

$$w_{oil} = 9.8x863.7\frac{3.14\left(0.325 - 2x0.009\right)^2}{4} = 626.23 \text{ N/m}$$

Mass of the pipe hydro/heat insulating shell of 1 m of pipe length is approximately equal to 69.41 kg or 680.22 N/m.

Thus, the total vertical transverse load on the arctic pipeline is

$$q = 686.99 + 626.23 + 680.22 = 1993.45 \text{ N/m}$$

The bending moments at which the arctic pipeline limiting state is achieved are found depending on the corrosion rate and different values of operating pressure P_{op}. Consider the pipe wall thinning rate is linear and equal to 0.2 mm/yr. Then for each moment of time (corresponding pipe wall thickness) and operating pressure according to Eq. (4.56) the ultimate bending moment is calculated. The results are shown in Figs. 6.4 and 6.5. Wind loads corresponding to these ultimate bending moments are shown in Fig. 6.6 and 6.7.

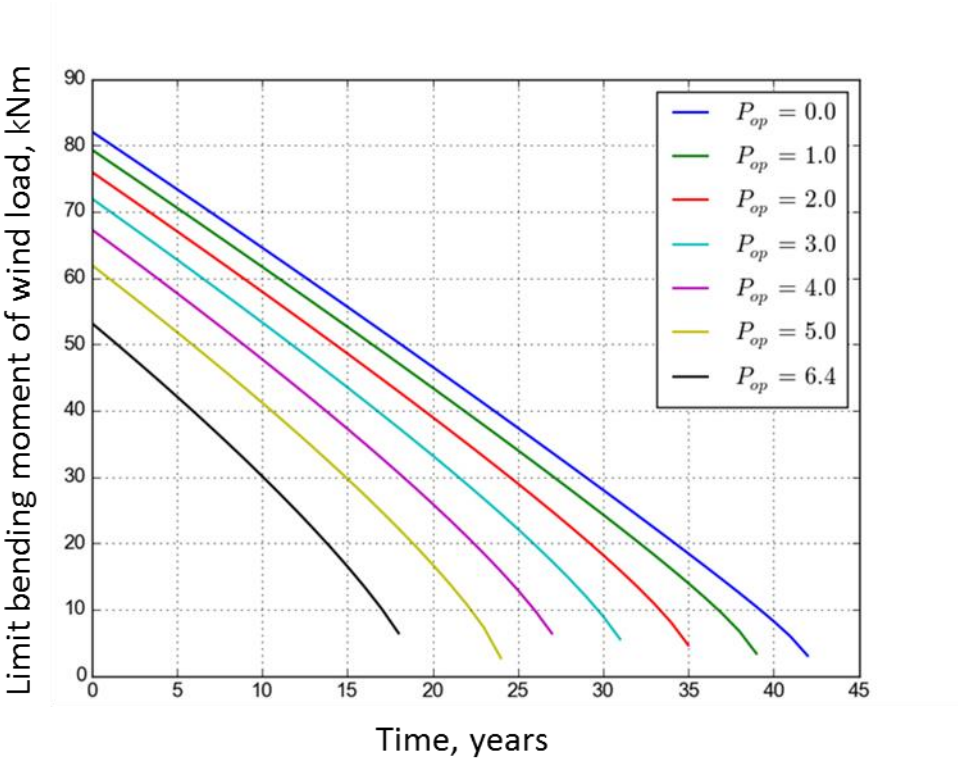

Figure 6.4: Ultimate permissible bending moment of horizontal wind load against time

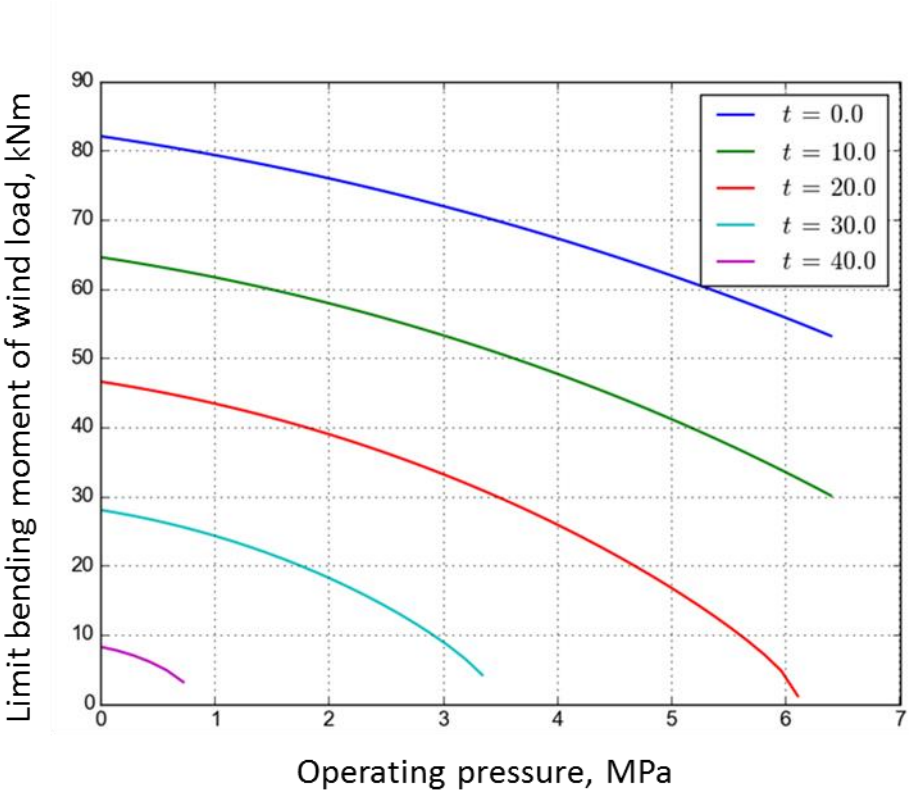

Figure 6.5: Ultimate permissible bending moment of horizontal wind pressure versus operating pressure

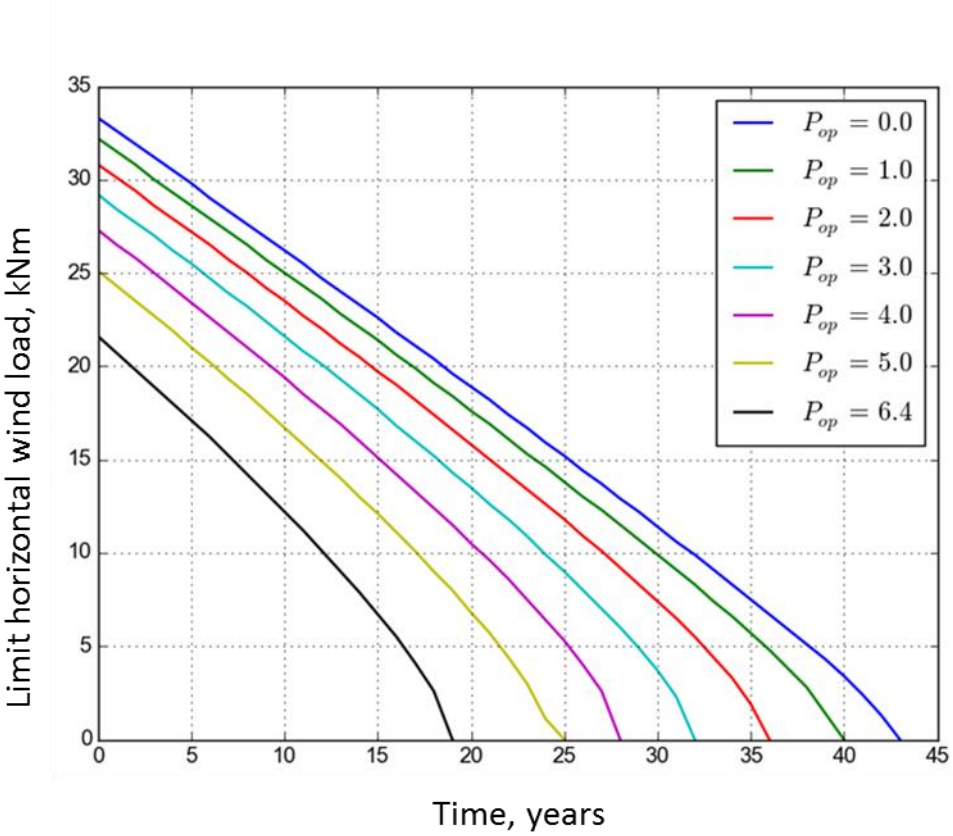

Figure 6.6: Ultimate permissible horizontal wind load against time

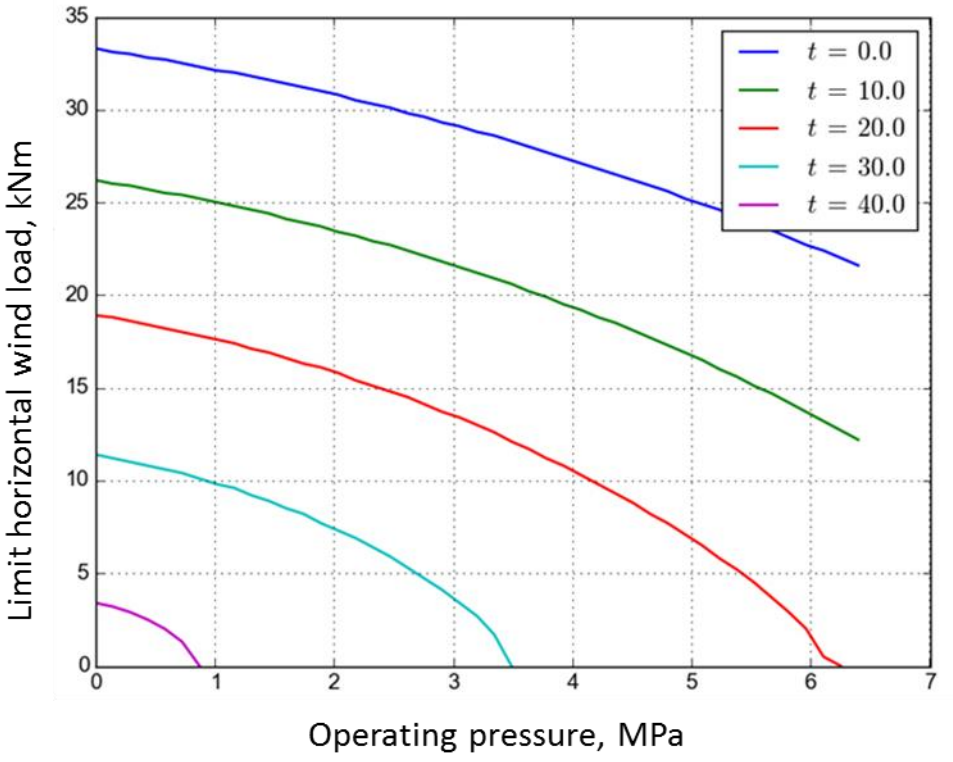

Figure 6.7: Ultimate horizontal wind load versus operating pressure

We calculate the ultimate values for wind speed using Eq. (4.57) and (4.58). For simplicity, we do not take into account the dynamic component of wind load. Consider section of the arctic pipeline which is 2 m above the ground, and the type of terrain is A. The equivalent height z_e = 2 + 0.350/2 = 2.175 m. From Eq. (4.60):

$$k\left(z_e\right) = 1.0 \cdot (2.175/10)^{2 \cdot 0.15} = 0.633\,\text{m}.$$

According to the Russian building code and regulation (SNIP 2.05.06-85*), and Vasilyev et al. (2007), the aerodynamic coefficient c = 0.5.

From Eq. (4.57) without taking into account the dynamic component, it follows that

$$q_w = 0.43 v_{50}^2 k\left(z_e\right) c D_{in}, \tag{6.16}$$

It can be deduced from this Eq. (6.16) that the wind speed that can occur once in 50 years could be estimated by:

$$v_{50} = \sqrt{\frac{q_w}{0.43 k\left(z_e\right) c D_{in}}}, \tag{6.17}$$

Let time t = 10 years and the operating pressure P_{op} = 5.4 MPa. Substituting q_w into the Eq. (6.17) from Eq. (6.16) we obtain the ultimate limit values of wind load, and the ultimate permissible wind speed values. The results are shown in Fig. 6.8 and 6.9.

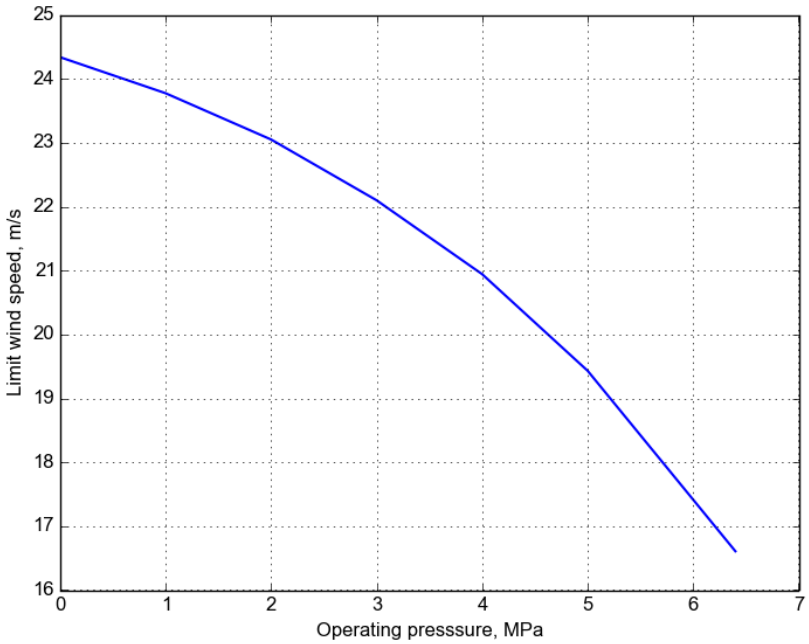

Figure 6.8: Ultimate permissible wind speed at time t = 10 years, depending on the operating pressure

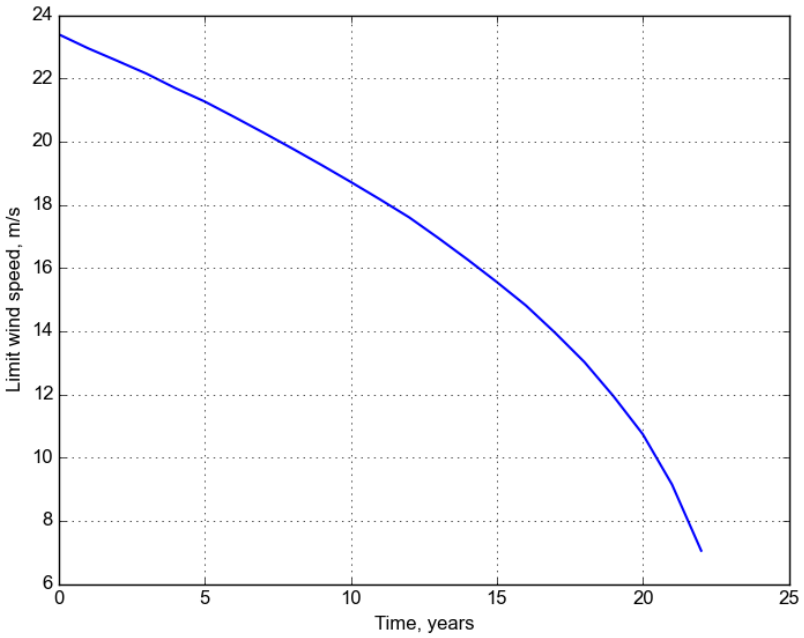

Figure 6.9: Ultimate permissible wind speed at operating pressure P_{op} = 5.4 MPa, depending on the time (corrosion rate)

In accordance to Fig. 6.9, at t = 10 years and P_{op} = 5.4 MPa, the ultimate wind speed is equal to 18.7 m/sec. In Fig. 6.2, the interval probability of occurrence of such wind speed value is equal to [0.64; 0.95]. Hence, the point wise pipeline reliability

(Rpl) in this particular case will be 0.64 ≤ Rpl ≤ 0.95. Integrating the whole curve of Fig. 6.9, gives the overall interval of pipeline reliability.

6.5 The two-sided estimate of the true reliability function of arctic pipeline at the combination of the two loads

Consider the calculation of the reliability of the arctic pipeline where it operates under impact of two loads from subsidence / frost upheaval of support and from corrosion defects. The model is described under loads and impacts acting on arctic pipelines in section 4.9 of chapter 4.

Assume that the load of the subsidence (upheaval) of the support is described by pure death Markov process or pure birth Markov process $q_1(t)$ with intensities of transition λ_i, $i=1,2,..,M_1$, and load from the arctic pipeline defectiveness - by means pure death Markov process $q_2(t)$ with intensities of transition μ_j, $j=1,2,..,M_2$; moreover, $q_1(t), q_2(t)$ are independent processes. Refer to the model on loads and impacts acting on arctic pipelines in section 4.9 of chapter 4.

Let $z(t)=\{q_1(t), q_2(t)\}$ be a two-dimensional process. Then the system of differential equations of this process is:

$$\begin{cases} \dfrac{dP_{1,1}(t)}{dt} = -(\lambda_1+\mu_1)P_{1,1}(t); \\ \dfrac{dP_{i,j}(t)}{dt} = -(\lambda_i+\mu_j)P_{i,j}(t)+\lambda_{i-1}P_{i-1,j}(t)+\mu_{j-1}P_{i,j-1}(t),\ i,j=2,3,.. \end{cases} \tag{6.18}$$

The relative probabilities are:

$$P_{i,j}(t)=P\{q_1(t)=i,\ q_2(t)=j\}. \tag{6.19}$$

The initial conditions for the system of differential equations in Equation (6.18) have the form

$$P_{1,1}(t)=1,\ P_{i,j}(t)=0,\ i,j=2,3,...$$

If we select an area Ω in space with boundary Γ and introduce the auxiliary process $\bar{z}(t)$ so that $\bar{\lambda}_i=\lambda_i, \bar{\mu}_j=\mu_j$ if the point $(i,j)\in\Omega$ and $\bar{\lambda}_i=0, \bar{\mu}_j=0$, if

$(i, j) \in \Gamma$, that is, the boundary is absorbing. Then the probability of non-way out of the process $z(t)$ from area Ω will be calculated by the formula

$$P(t) = \sum_{i=1}^{m_j - 1} \sum_{j=1}^{n_i - 1} \bar{P}_{i,j}(t), \tag{6.20}$$

Where $\bar{P}_{i,j}(t)$ satisfies the following system of differential equations:

$$\begin{cases} \dfrac{d\bar{P}_{1,1}(t)}{dt} = -\left(\bar{\lambda}_1 + \bar{\mu}_1\right)\bar{P}_{1,1}(t); \\ \dfrac{d\bar{P}_{i,j}(t)}{dt} = -\left(\bar{\lambda}_i + \bar{\mu}_j\right)\bar{P}_{i,j}(t) + \bar{\lambda}_{i-1}\bar{P}_{i-1,j}(t) + \bar{\mu}_{j-1}\bar{P}_{i,j-1}(t),\ i, j = 2,3,.. \end{cases} \tag{6.21}$$

Equation (6.20) reflects the fact that the probability of non-way out of the process $z(t)$ from area Ω is equal to the probability of finding the process $\bar{z}(t)$ inside the area Ω at time *t*.

The probability estimation using Eq. (6.20) is the true function of arctic pipeline reliability at influence on its two considered loads.

Considering the probabilities, we construct a two-sided estimate of this function:

$$P_i^{(m_j)}(t),\ i = 1,2,..,m_j;\ P_j^{(n_i)}(t),\ j = 1,2,..,n_i; \tag{6.22}$$

This is the expression of the probability that at time *t* the process $q_1(t)\left[q_2(t)\right]$ is in a state *i*(*j*) on the condition that the state $m_j\left(n_i\right)$ is absorbing. These probabilities are determined by solving the following system of differential equations:

$$\begin{cases} \dfrac{dP_1(t)}{dt} = -\lambda_1 P_1(t); \\ \dfrac{dP_i(t)}{dt} = \lambda_{i-1} P_{i-1}(t) - \lambda_i P_i(t), \ \ i = 2,..., m_j - 1; \\ \dfrac{dP_{m_j}(t)}{dt} = \lambda_{m_j-1} P_{m_j-1}(t); \\ P_1(0) = 1, \ P_i(0) = 0, \ i = 2,..., m_j. \end{cases} \tag{6.23}$$

$$\begin{cases} \dfrac{dP_1(t)}{dt} = -\mu_1 P_1(t); \\ \dfrac{dP_j(t)}{dt} = \mu_{j-1} P_{j-1}(t) - \mu_j P_j(t), \ \ j = 2,..., n_i - 1; \\ \dfrac{dP_{n_i}(t)}{dt} = \mu_{n_i-1} P_{n_i-1}(t); \\ P_1(0) = 1, \ P_j(0) = 0, \ j = 2,..., n_i. \end{cases}$$

The solutions to these systems of differential equations are determined from the Equation (6.24) or (6.26).

$$P_i(t) = \sum_{j=1}^{i} \eta_{ij} \exp\left[-\lambda_j t\right], \quad i = 1, 2, .., M, \tag{6.24}$$

where:

$$\eta_{ij} = \begin{cases} \eta_{11} = 1; \\ \begin{cases} \eta_{i-1,j} \cdot \dfrac{\lambda_{i-1}}{\lambda_i - \lambda_j}, \quad j \neq i, i = 2, ...M, \ j = 1, 2..., (i-1); \\ -\sum\limits_{q=1}^{i-1} \eta_{iq}, \quad j = i, i = 2, ..., M, \end{cases} \end{cases} \tag{6.25}$$

$$\begin{cases} P_i(t) = \dfrac{\rho^{i-1}(t)}{(i-1)!} \cdot \exp\{-\rho(t)\}, \ i = 1, .., M-1, \\ P_M(t) = 1 - \left[\exp\{-\rho(t)\} + \sum\limits_{i=2}^{M-1} \dfrac{\rho^{i-1}(t)}{(i-1)!} \cdot \exp\{-\rho(t)\} \right], \end{cases} \tag{6.26}$$

where $P_i(t)$ is the probability that the failure (burst) pressure of defective cross section is in the *i*-th state at the moment of time *t*, $\rho(t)$ is calculated using formula:

$$\rho(t)=\int_0^t \mu(\tau)\,d\tau-\int_0^t \frac{P_f'(\tau)}{\Delta I}\,d\tau=\frac{P_f(t)-P_f(0)}{\Delta I}. \tag{6.27}$$

The two-sided estimate of the true reliability function $R(t)$ of arctic pipeline at the combination of the two loads is given by (see e.g. Timashev, 1982):

$$R_1 \le R(t) \le R_2(t), \tag{6.28}$$

where:

$$\begin{aligned} R_1(t)&=\sum_{i=1}^{m_j-1}\sum_{j=1}^{n_i-1} P_i^{(m_j)}(t)\,P_j^{(n_i)}(t),\\ R_2(t)&=\sum_{i=1}^{m_j-1}\sum_{j=1}^{n_i-1} P_i^{(m_1)}(t)\,P_j^{(n_1)}(t). \end{aligned} \tag{6.29}$$

We have plotted the marginal wind velocity on the operating pressure (see Fig. 6.8). Considering the limiting wind speed as a random discrete value can build a cumulative distribution function, i.e. the probability of failure against limit wind speed. The resulting function is shown in Fig. 6.10. Two-sided reliability assessment of pipeline probability of failure depending on the limit wind speed is shown in Figs. 6.11 and 6.12.

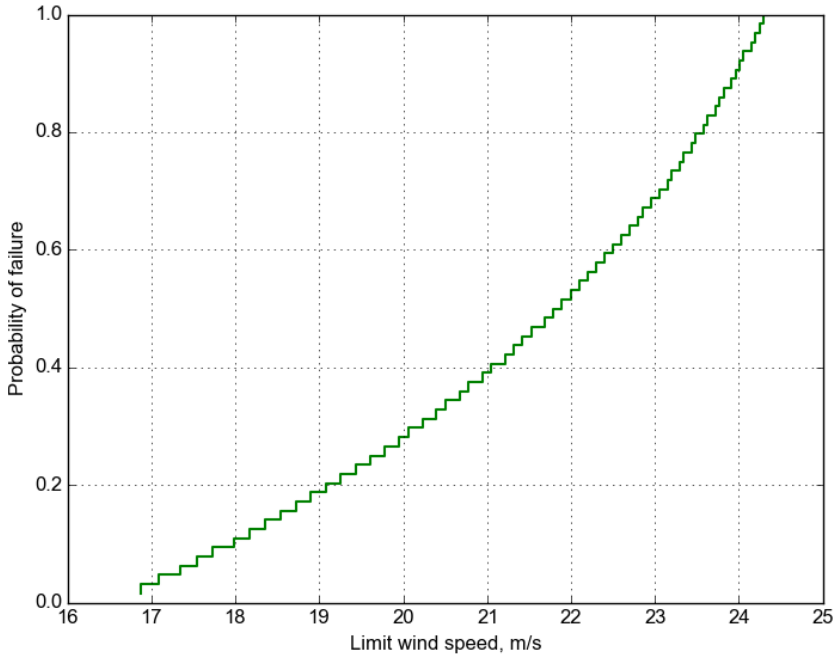

Figure 6.10: The probability of failure of the pipeline depending on the wind speed limit

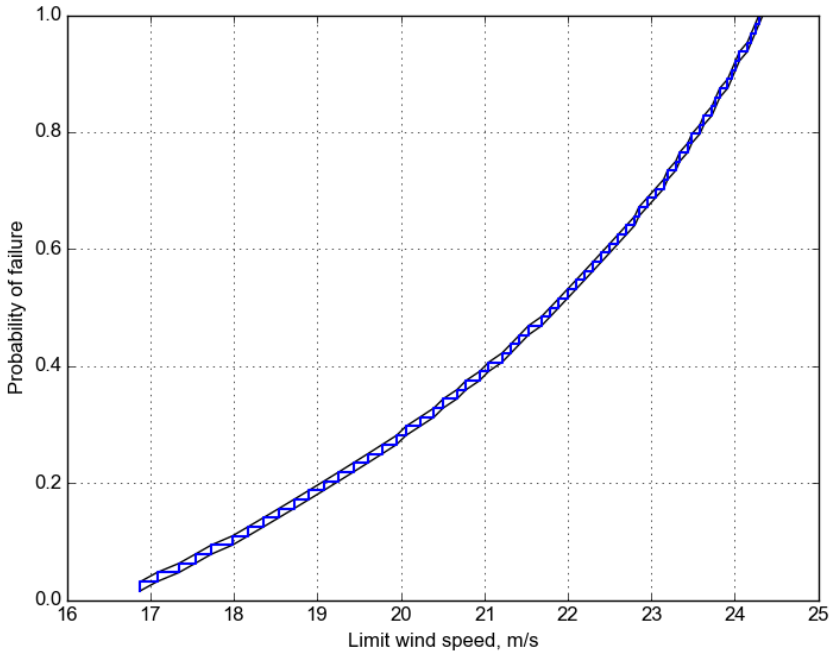

Figure 6.11: Two-sided reliability assessment of pipeline failure probability depending on the limit wind speed

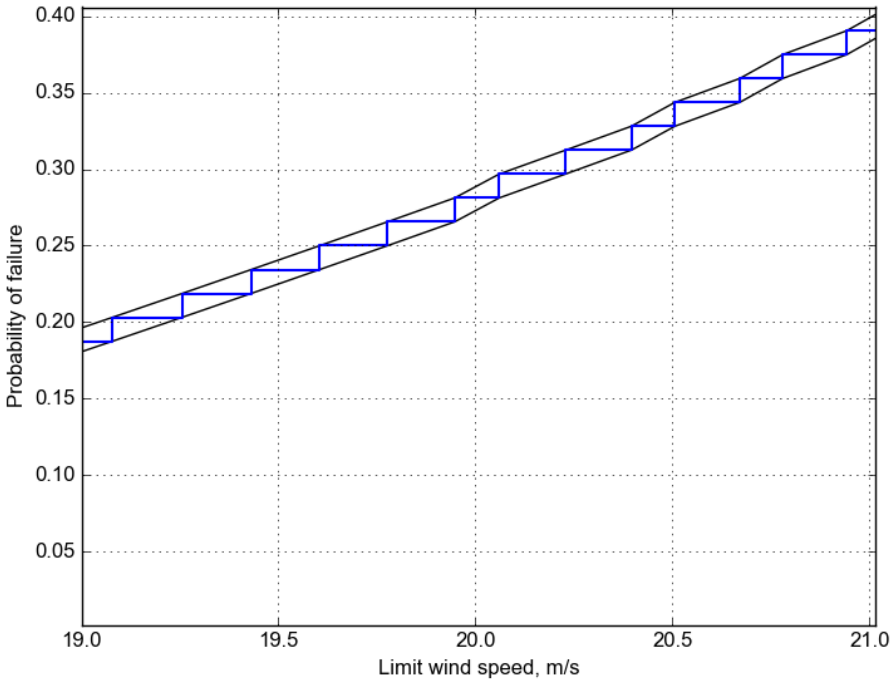

Figure 6.12: Two-sided reliability assessment of pipeline failure probability depending on the limit wind speed from 19 to 21 m/s (magnified).

6.6 Example Application – case 2

Consider a segment of a real above ground arctic oil main pipeline, parameters of which are given in Table 6.2.

Table 6.2: Design parameters of an oil pipeline

Transported substance	Crude oil
Oil density	863.7 kg/m^3
Pipe outlay	Above ground
Outside Diameter of Pipe	1.020 m
Pipe material	Class X60: UTS = 590MPa and SMYS = 460MPa
Steel density	7.85x10^3 kg/m^3
Pipe wall thickness	0.016 m
Operating Pressure	7.5MPa
Design temperature	+20^{o}C
Temperature at pipeline outlay	– 32^{o}C
Insulation	Epoxy anti corrosion insulation, spiral zinc coated folded pipe insulation shell 1.5mm thick. The insulation proper thickness is 100mm
Young modulus	2.06x10^5 MPa
Linear expansion coefficient	1.2x10^{-5} 1/^{o}C
Poisson coefficient: a) for elastic performance of metal b) for plastic performance of metal	 0.3 0.5

The considered segment has six (6) spans which lengths are: L_1 = 17m, L_2 = 18m, L_3 = 16m, L_4 = 18m, L_5 = 15m, and L_6 = 18m. For simplicity sake it is assumed that both ends of the oil pipeline segment are rigidly fixed (which creates an error in pipe strength assessment on the safe side). The oil pipeline scheme is given in Fig. 6.13.

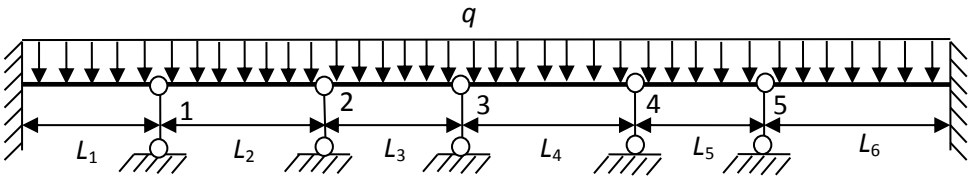

Figure 6.13: Design scheme of the oil pipeline segment #2

From Eq. (4.45), $\sigma_{c,\lim} = \max\left\{\sigma_{c,1}; \sigma_{c,2}\right\}$. these stresses are reached when the bending stresses are:

In the extension zones of the oil pipeline segment:

$\sigma_u = 588.84$ MPa; and

In the compressed zones of the oil pipeline segment:

$\sigma_u = 239.12$ MPa.

The ultimate values of the sum of axial stresses from Eq. (4.46) $\sigma_{l,\lim} = \dfrac{\sigma_c \pm \sqrt{4[\sigma]^2 - 3\sigma_c^2}}{2}$. are:

$\sigma_{l,\lim}^{+} = 529.76$ MPa

$\sigma_{l,\lim}^{-} = -298.20$ MPa

Thus, we have four roots of the two limit state equations, which are pairwise equal to each other but are opposite in signs. Therefore, from two roots of one limit state (e.g. first one) we need to select the minimum value of the absolute value, i.e., the bending stress, which is created by the minimal ultimate bending moment*:*

From Eq. (4.40)

$\sigma_{u,\lim} = \min\left\{\left|\sigma_u^{(1)}\right|, \left|\sigma_u^{(2)}\right|\right\};$

$M_{\lim} = \sigma_{u,\lim} W.$

The moments which correspond to these bending stresses are correspondingly equal to 7458.92 kNm and 3029.07 kNm. Then the ultimate bending moment is equal to the minimal moment, M_{lim} = 3029.07 kNm.

The ultimate permissible displacement of the support 3 is found to be 16.5 cm. In constructing the admissible region in the load space for arctic pipelines, the region in reality is physically intrinsic property of the design pipe. In this case, upheaval will be allowed up to 16.5cm as the ultimate permissible displacement of the support.

Several curves of moments related to the displacement of support 3 equal to $\Delta = 0,\ 5,\ 10,\ 15,\ 16.5$ cm are given in Fig. 6.14

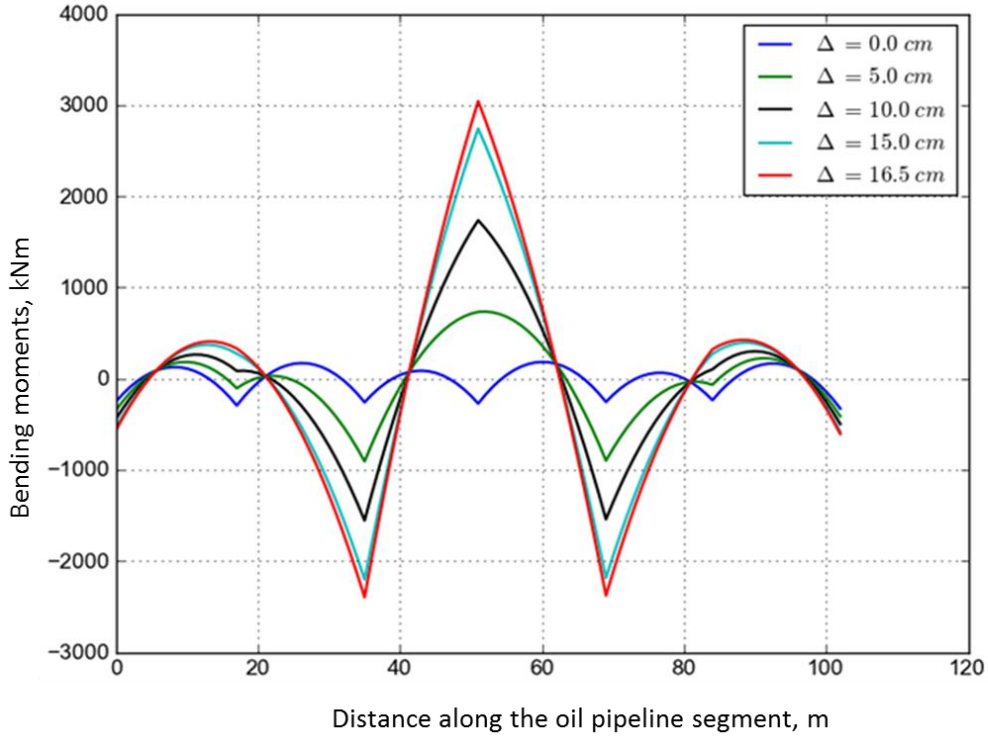

Figure 6.14: Bending moments for the oil pipeline segment

For each value of support displacement the ultimate defect depths were calculated taking into account their lengths (5 ultimate curves, shown in Fig. 6.15). According to this figure when the support displacement is equal to 15 cm and 16.5 cm the curves practically coincide, hence, in Fig. 6.15 they overlap.

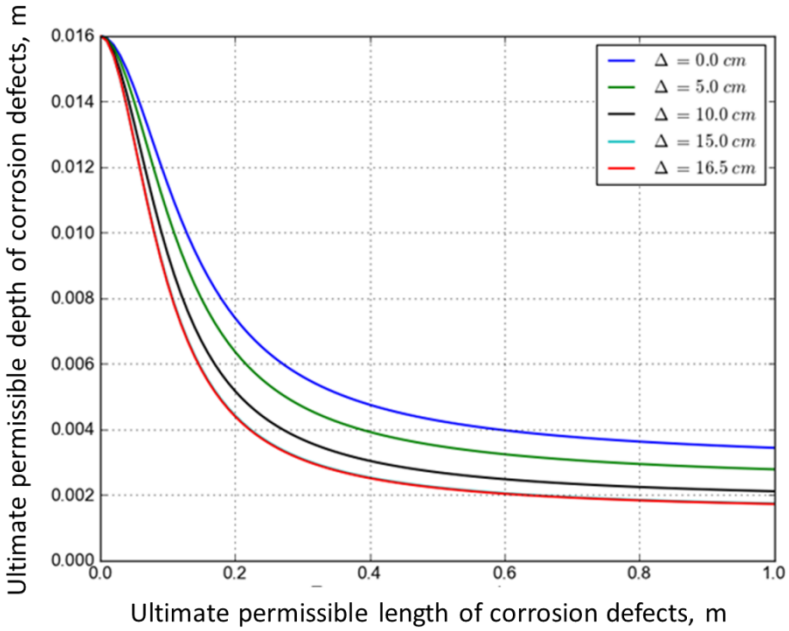

Figure 6.15: Ultimate permissible sizes of corrosion defects of the pipeline segment depending on the value of support displacement

The ultimate bending moments for the wind load, depending on the displacement of support 3 are given in Fig. 6.16. The values of the horizontal wind load, at which ultimate value of the bending moment is reached, depending on the value of the displacement of the support 3, are shown in Fig. 6.17.

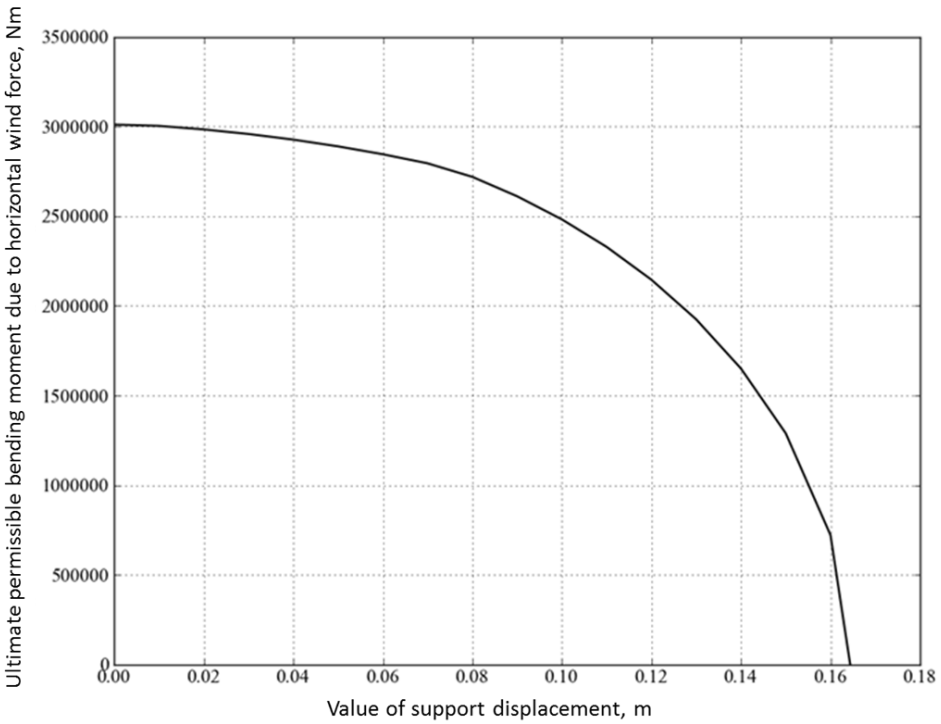

Figure 6.16: Ultimate permissible moment due to horizontal wind force depending on the value of support displacement

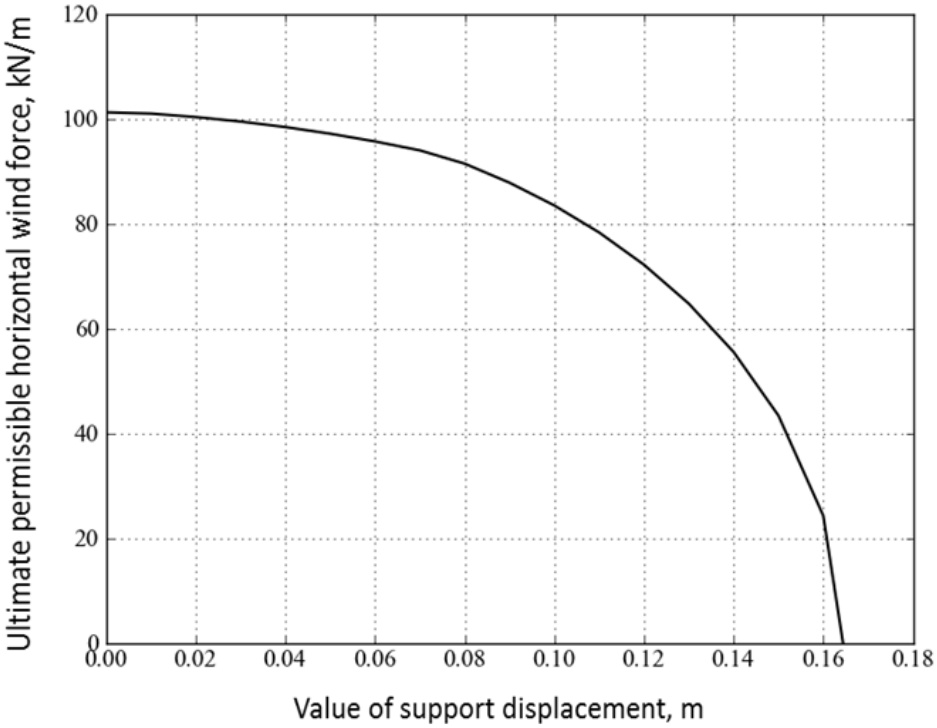

Figure 6.17: Ultimate sizes of defects of a pipeline segment depending on the value of support displacement

6.6.1 Assessment of the bending stresses due to wind load based on probabilistic wind load model.

From the analysis of the sets of wind speed data above (Section 6.3), the reliability assessment of the present example application above ground arctic oil main pipeline with pitting surface corrosion type defects subjected to a combination (simultaneous action) of loads with random variables is estimated. The statistical data of the parameters are shown in Table 6.3. The assessment and modelling of combined loadings for the above ground pipelines have been outlined in chapter 4 section 4.5. Also, the assessment of the bending stresses due to wind load based on traditional (deterministic) and probabilistic approaches for wind loads estimation are employed in this analysis (Sections 4.7.3 and 4.7.4).

We now consider the effect of wind load as one of the main components of the pipeline design, and several values of load intensity q in the absence of support displacements, i.e. the analysis here does not explore kinematic influence in the form of uneven vertical displacement of adjacent/closest vertical supports of the pipeline due to the frost upheaval/melting of the permafrost soil.

Table 6.3: Probabilistic model

Variable	Symbol	Unit	Probability distribution	Mean	Coefficient of variation
Young Modulus	E	MPa	LN	2.06×10^5	0.0327
SMYS	σ	MPa	LN	460	0.035
Pipe wall thickness	w_t	m	N	0.016	0.06
Operating pressure	P_{op}	MPa	Gumbel	7.5	0.007
Diameter	D	m	N	1.020	0.03
Poisson coefficient	μ	-	LN	0.3	0.023
Linear expansion coefficient	α	$1/^oC$	N	1.2×10^{-5}	0.01
Temperature differential	Δt	^oC	N	12	0.15
Moment	M	Nm	LN	4×10^6	0.15
Multiplying constant	k	-	N	0.3	0.3
Exponential constant	n	-	N	0.6	0.2

The internal operating pressure in the pipe induces circumferential stresses σ_{cs}, which are calculated according to Eq. (4.36)

$$\sigma_{cs} = \frac{P_{op}(D - 2wt)}{2wt} \tag{6.30}$$

P_{op} = operating pressure, D = pipe outside diameter, and wt = pipe wall thickness.

The longitudinal axial stresses σ_{ls} in the pipeline due to operating pressure and temperature; and the bending stresses σ_{bs} in the pipeline are estimated (see Eq. 4.38, 4.39 and 3.40) as:

$$\sigma_{ls} = \mu\sigma_{cs} - \alpha E\Delta t + \sigma_{bs} \tag{6.31}$$

where $\sigma_{bs} = \frac{M}{W}$, and $W = \frac{\pi(D - wt)^2 wt}{4}$.

The above ground pipelines are subjected to both longitudinal and circumferential stresses and these are described as a function of the applied load with the aid of a mechanical model using von Mises equivalent stress expression in Eq. (4.42):

$$\sigma_{es} = \left(\sigma_{cs}^2 + \sigma_{ls}^2 - \sigma_{cs}\sigma_{ls}\right)^{\frac{1}{2}}$$

σ_{es} , σ_{cs} and σ_{ls} are von Mises equivalent stress, circumferential stress and longitudinal stress respectively.

The assessment of the extra stresses induced by the surface corrosion defects in connection with the design failure pressure for the geometric parameters of a single surface corrosion defect is estimated using the DNV-101 failure pressure model:

$$p_f = \frac{2w_t\sigma_f}{(D - w_t)} \tag{6.32}$$

p_f is the failure pressure, D is the pipe outside diameter, σ_f the flow stress, and wt is the pipe wall thickness.

The power model also known as the power law was used for the analysis of the pipeline reliability and remaining life due to pitting corrosion process, as to model the loss of wall thickness with the time of exposure (see Eq. 4.18).

$$d = kT^n$$

The net wall thickness was used instead of the original wall thickness in accounting for corrosion losses in the pipeline's stresses estimation. This is inculcated in Eq. (6.30) and (6.31) by inserting ($w_t - kT^n$) in place of (w_t) in σ_{cs} and σ_{ls} .

The limit state function $G(x)$ is defined as the difference between the yield stress of the pipe material (SMYS) and the equivalent stresses σ_{es} , expressed mathematically as (from Eq. 4.86):

$$G(x) = SMYS - \sigma_{es}$$

And the probability of failure P_f for the pipeline is written as (from Eq. 4.87):

$$P_f = P(G(x) \leq 0)$$

Analytical methods are inadequate for solving Eq. (4.87) due to its complexity; Monte Carlo simulation is employed to calculate the probability of failure. Large number (10^5) of realizations are generated according to probabilistic model (see Table 6.3), the reliability estimation and Monte Carlo simulations have been performed adopting OpenCossan - the open source engine of COSSAN software for uncertainty quantification and risk management (Patelli et al., 2014).

The reliability assessment of the pipeline using probabilistic approach is done representing each variable as random, with an estimated mean and variation and assigning the appropriate probability density function. The corrosion defect depth as one of the most important variables in the reliability analysis is assigned an interval of 0 to 100% (the net wall thickness rather than the original wall thickness of the pipeline in the stresses estimation) as measured defect depth through the nominal wall thickness, and $1x10^6$ to $6x10^6$ N/m as combined load intensity on the pipeline; representing epistemic uncertainty in the probabilistic procedures. Simulations were run and the bounds of the defect depth calculated and repeated for different level of uncertainty using the corrosion model. The probabilities of

failure as a function of ultimate permissible moments, and elapsed life of pipeline were also determined.

The bounds on the wind speed for estimating of the pipeline reliability are made possible by considering them as bounds on the cumulative probability associated with any wind speed value in the p-box. Take for example, the probability that the wind speed value will be 25m/s or more is between 2% and 19% (in Fig. 6.2). In another part, consideration as bounds on the wind speed value at any particular probability level. The 95th percentile is sure to be between 16m/s and 19m/s (see Fig. 6.2). Using the 95^{th} percentile, we have an interval of 16m/s and 19m/s to represent the lower and upper probability levels. Hence, the wind pressure is calculated using Eq. (4.62), and the design wind load from Eq. (4.61), after inculcating the probabilistic values in the deterministic equation.

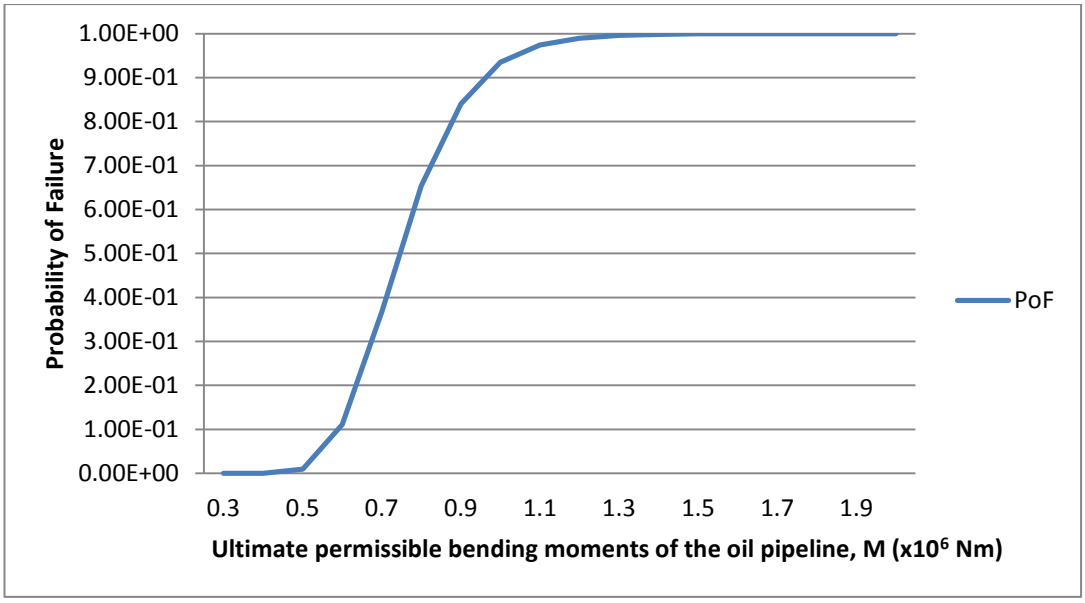

Figure 6.18: Probability of failure of the pipeline as a function of ultimate permissible bending moments

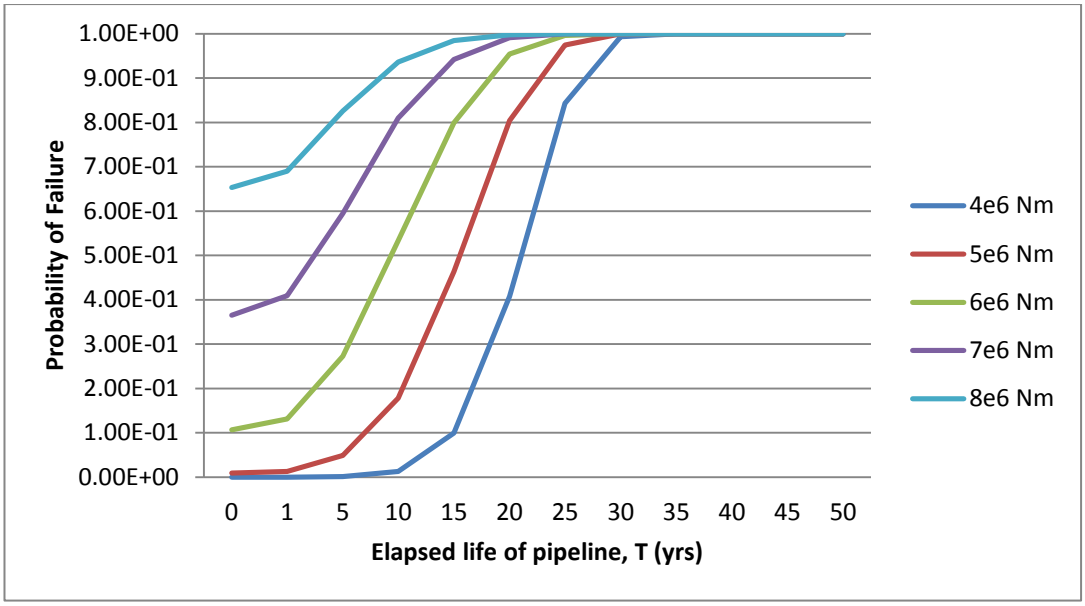

Figure 6.19: Probability of failure as a function of elapsed life of pipeline and the resulting moments from loading

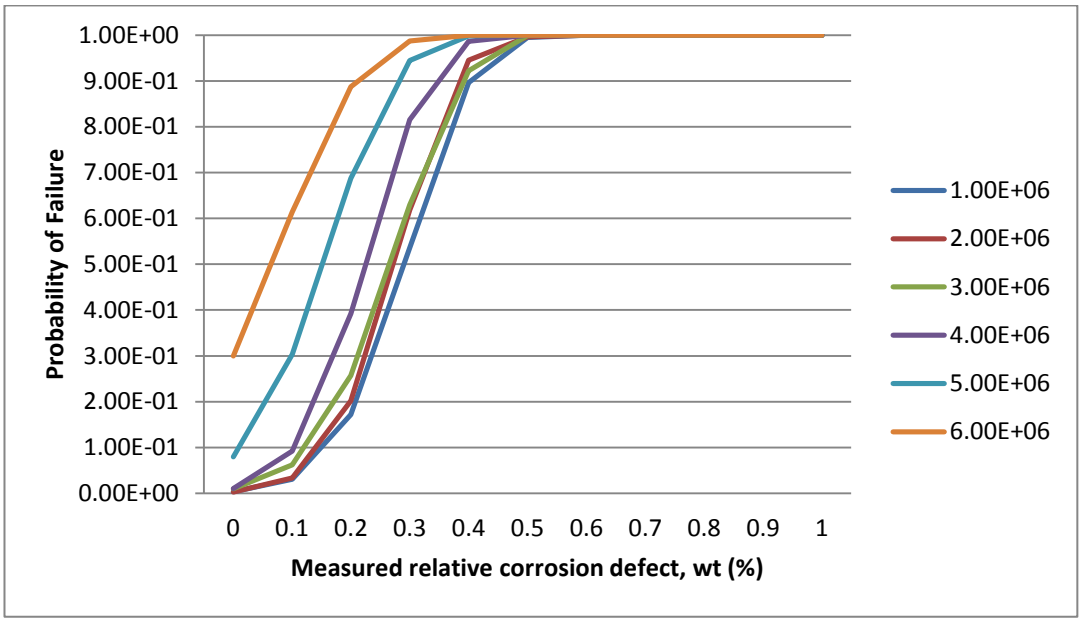

Figure 6.20: Probability of failure as a function of assigned epistemic uncertainty on load intensity (N/m) and measured relative corrosion defect variable

6.6.2 Results and discussion

The reliability analysis and remaining life of an oil pipeline subject to combined loading was determined using a combination of probabilistic and non-probabilistic approach.

It is seen from Fig. 6.18 that the pipeline probability of failure increases with an increase in the bending moment as expected. As the combination of the loads increase, failure probability also increases. For instance, when the bending moment is $0.6x10^6$ Nm, the failure probability is 0.1; while at $1.2x10^7$Nm, the failure probability is 0.99. The range of safety and reliability could be assessed based on this plot.

Figure 6.19 depicts further investigation on the effects of increment of time on probability of failure as its value was varied from 1 to 50 years, then an interval of $4x10^6$ to $8x10^6$ Nm as resultant moments from the combined loading was assigned. The result shows that both the probability of failure and rate of change of probability of failure increases with time.

Finally, Fig. 6.20 deals with the consideration of intervals of load intensities but with varying measured relative corrosion defect when net wall thickness ($w_t - kT^n$) were utilized instead of original wall thickness (w_t) of pipeline during stress estimation. The load intensities $5x10^6$ and $6x10^6$ show the most conservative implications on elapsed life of the pipeline.

6.7 Concluding Summary

The method of assessing reliability of arctic above-ground oil field collection and main pipelines is presented. The application of the imprecise probabilities (p-boxes) for reliability analysis of above ground arctic oil pipelines with surface corrosion defects, subjected to a combination of loads has been employed. The advantage of this approach is in that it allows an easy visualization and interpretation of the essence of the problem in consideration. Indeed, even before starting solving the reliability problem it is clear for the engineer which pipeline quality criteria are the most restrictive, and which elements of the system are not participating in constructing the admissible region in the space of loads. This permits singling out elements with excessive reliability, and to formulate structural means for decreasing their reliability to the level, which does not impede the overall reliability of the system as a whole.

The specifics of the developed approach are that it splits the task of evaluating the reliability into two independent tasks: 1) constructing admissible areas in load space 2) assessment the probability of escape of the vector load from the admissible region. In this formulation, the dimension of the problem is not the product of the number of defects on the number of loads in combination, but just the number of loads, which allows overcoming the curse of dimensionality.

Further conclusions include:

- When designing new arctic pipelines or reassessing the “future” reliability of existing pipeline systems, the necessity to modify design wind loads due to global climate change has to be taken into direct consideration.
- In order to modify design wind loads, a quantitative analysis of the trend of the wind speed in time has to be performed, its goal being finding the change of the climate mean and variance of the wind extremes for a particular geographic region.
- As it is shown in the work, one of the most convenient ways to achieve this goal is by using the imprecise probabilistic approach.
- Its application to study wind speed evolution in long term calendar time due to climate change as related to the above ground pipeline reliability by using a set of wind load models is given in Section 6.3. Results of this study vividly show the utility of the imprecise probabilistic approach and provided the much needed robustness with respect to the probabilistic model choice.
- As one of the generalized methods, the imprecise probabilistic approach permits overcoming the simplifications and assumptions, which cannot be justified, to compensate for lack of data, imprecision and vagueness in modelling.
- The results of this contribution could help engineers and pipeline operators in achieving a better design of future pipelines, more accurate risk analysis and providing a better pipeline life cycle cost estimate.

- The imprecise probabilistic approach could also be useful in planning the next inspection and repair time interval when scheduling pipeline maintenance, when drafting the life cycle of arctic pipelines.

7. Optimal Maintenance Scheduling

7.1 Introduction

This chapter presents optimal maintenance scheduling due to fatigue cracks in bridges as a metallic structure with vague information, and the reliability based optimization of inspection time interval for corroded buried pipelines. This is another direct example application of the computational framework and models presented in Chapters 3 and 4.

7.2 Optimal Maintenance Strategy for Metallic Structures with Vague Information

Fatigue failures occur in every field of engineering. Examples are bridges in civil engineering, aircraft in aeronautic engineering, and thermal and/or mechanical fatigue failure in electrical circuit board in electrical engineering, also farm tractors in agricultural engineering. Others include nuclear piping in nuclear engineering, pressure vessels in chemical engineering, automobiles in mechanical engineering, and heart valve implants in biomedical engineering. Bridges for example, in general are susceptible to deterioration. They are often exposed to harsh environments, rain, snow, de-icing salts, temperature fluctuations, and they undergo a significant amount of cyclic loading (Bader, 2008).

Cyclic loading of metallic structures such as bridges leads to fatigue cracks, and in turn when the cracks propagate, the structural system accumulates damage thereby leading to serviceability loss and/or eventual collapse. These failures can be prevented by appropriate maintenance scheduling and repair. An optimal maintenance strategy for metallic structures under fatigue is presented, which works with reliability metrics redefined within the framework of imprecise probabilities. The effects of uncertainties are expressed in terms of probabilities of failure, repair, and expected costs of operation. A welded connection between a web stiffener and girder's flange of a bridge is presented to illustrate and to discuss the suggested approach as well as its applicability. The proposed optimal

maintenance strategy is implemented in OpenCossan; the open source engine of COSSAN software for uncertainty quantification and risk management. The initial crack length is modelled as lognormal variable with imprecision of the mean value and defined standard deviation: LN ([0.5, 3], 0.4) using Reliability- Based Optimization method. The optimal inspection time is obtained between 1.5 x 10^6 to 1.8 x 10^6 load cycles based on the initial crack and total costs of operation.

Reliability metric definition within an appropriate or suitable framework that can determine a maintenance strategy which is both robust with respect to uncertainties and optimal from an economical viewpoint would be most applicable for reliability assessment in an overall optimization of very complex problems. So, before a reliability-based optimization can be performed methods to estimate the reliabilities must be accessible.

Reliability estimation is limited to first order reliability methods (FORM) for component and systems reliability evaluation in Enevoldsen and Sorensen, 1994. Augusti et al., 1998 pioneered the problem of maintenance optimization at the network level proposing a technique for the comparison and ranking of several maintenance plans. An efficient reliability analysis method for durability of structural components subjected to external and inertial loads with time-dependent variable amplitudes is presented in Yu et al. (1998). Reliability-based design optimization (RBDO) involves evaluation of probabilistic constraints, which can be done in two different ways, the reliability index approach (RIA) and the performance measure approach (PMA). For the concave performance function in PMA, a new RBDO methodology was developed integrating hybrid mean value HMV method with a proposed response surface method, which is specifically developed for reliability analysis and optimization in Youn et al. (2003).

Frangopol, 2010 reported the state-of-the-art and state-of-practice on maintenance optimization for individual bridges. In recent time Peeta et al. (2010) proposed an efficient technique for the optimal allocation of limited funding among the bridges of a highway network, considering also the effect of uncertainty, but disregarding

correlations and aging. Gao et al. (2010) presented a remarkable framework for the optimization of the maintenance interventions on pavements of a transportation network. Bocchini and Frangopol (2011) proposed a methodology for the optimal scheduling of the maintenance interventions at the bridge network level, including uncertainty, correlation, and deterioration. Matsumura et al. (2013) reported in his work about the debate on how to treat the uncertainties involved, various technical approaches that has been studied - including probability theory, Dempster–Shafer evidence theory and possibility theory - and that due to limited data usually available for identifying epistemic uncertainty, there is a tendency to treat epistemic uncertainty conservatively in design, e.g., worst case scenarios and upper bounds of 95% confidence interval. These conservative treatments, however, may lead to substantial performance losses.

From the initial developments imprecise probabilities have emerged into several application fields in engineering with structured approaches. The largest application field appears as reliability assessment, where imprecise probabilities are implemented to address sensitivities of the failure probability with respect to the probabilistic model choice (Beer et al., 2013). This contribution therefore proposes robust maintenance strategy for metallic engineering structures and systems under fatigue, which works with reliability metrics redefined within the framework of imprecise probabilities.

7.2.1 Fatigue Modelling

The whole Section 4.2 of Chapter 4 has been designated for fatigue crack modelling. Fatigue is the process of progressive localized permanent structural change occurring in a material subjected to conditions which produce fluctuating stresses and strains at some point or points and which may culminate in cracks or complete fracture after a sufficient number of fluctuations as defined by ASTM. Fatigue occurs when a material is subjected to repeat loading and unloading. If the loads are above a certain threshold, microscopic cracks will begin to form at the stress concentrators such as the surface, persistent slip bands, and grain interfaces (Kim

and Laird, 1978). Eventually a crack will reach a critical size, the crack will propagate suddenly, and the structure will fracture. The shape of the structure will significantly affect the fatigue life; square holes or sharp corners will lead to elevated local stresses where fatigue cracks can initiate.

The entire fatigue process involves the nucleation and growth of a crack or cracks to final fracture. In this contribution, Region 2 of the growth of a crack is considered only (see Fig. 4.3), simply because the stress intensity factor at the tip of the crack is too low to propagate a crack at threshold region, and little fatigue crack growth life is involved in fracture region, since it does not contribute significantly to the fatigue life, it is ignored. Likewise, Mode I crack displacement or extension is used in modelling fatigue degradation phenomenon (as shown in Fig. 4.2), it is the most common one, and particularly the combination of Modes II and III often turn into Mode I cracks.

Paris law which is the most widely used fatigue crack growth model is adopted. The Paris law connects the crack growth rate with the amplitude of stress intensity factor through a simple power function which makes the engineering application more easily. The finite element method in which the global FEA (Finite Element Analysis) model, 2D FEA model, and 3D FEA model is applied in estimating stress intensity factors is also employed.

In summary, the damage due to fatigue is addressed using a fracture mechanics approach (Anderson, 1991; Paris and Erdogan, 1963). The crack propagation is simulated by integrating appropriate laws that describe the crack growth. Crack growth rate is obtained by applying the Linear Elastic Fracture Mechanics concepts. Finite Element Analysis as one of the available numerical methods is applied for estimating Stress Intensity Factors (Wang et al. (1997)). Life estimations for fatigue crack growth and damage tolerance design are made by using the following important information: The stress intensity factor, the fracture toughness, the applicable fatigue crack growth rate expression, the initial crack size, and the final or critical crack size. The life estimation is made by adopting Paris-Erdogan's law as the applicable fatigue crack growth rate expression, and the stress intensity factor

modified in Fisher et al., 1989 as elaborated in Eq. (4.7) to (4.12). Here, Paris law is denoted (Eq. (4.7)) as

$$\frac{da}{dN} = C.\Delta K(a)^M$$

In Eq. (4.8), the Stress Intensity Factor, K is

$$K = F_e.F_s.F_w\sigma.\sqrt{\pi.a}$$

The Fatigue Life is therefore expressed in Eq. (4.12) as:

$$N = \int_{a_i}^{a_f} \frac{1}{C(\Delta K(a))^M} da \quad \text{(Cycles)}$$

7.2.2 Maintenance Scheduling and Repair

7.2.2.1 Maintenance Scheduling

The repair event consists in the removal of one or more cracks, and this event takes place based on the outcome and quality of the inspection. The under listed four (4) events are taken into consideration simultaneously in scheduling the maintenance activities, viz.:

- Event A: is the performance for non-detected cracks that cause no failure.

This event is described as a function of probability of detection, the critical crack length, and the crack length size during the second inspection (i.e. after first inspection, $g_R \geq 0$). When the critical number of cycles is more than the number of cycles at the time of inspection, this obviously shows the structure is safe.

- Event B: is the performance for non-detected cracks that cause failure.

An event where function of probability of detection, the critical crack length, and the crack length size during the first inspection is considered. $g_R \geq 0$

- Event C: is the performance of repair - where all cracks are detected and repaired.

The performance function of repairs is based on detection probability and the chance of detection. This is discussed in section 7.2.2.2. The following conditions necessitate repair activities. Crack is detected when the performance function of

repairs is in the failure region ($g_R \leq 0$), at this region crack is detected and must be repaired. Also, when the measured crack length size is larger than the critical crack length (g_F=a_c-$a > 0$). The aforementioned conditions must occur simultaneously to ascertain repair actions. Another possibility is to simulate the target condition by taking the minimum between the two conditions and comparing it to unity (see e.g. (Valdebenito et al., 2010). g_R= min (a_c-a, $POD - \theta$). When the critical number of cycles does not exceed the number of cycles at the time of inspection, this obviously shows the structure will fail and needs repairs ($N^c < N_{INSP}$).

- Event D - Performance of Failure: where all cracks are detected that causes failure.

This event is mainly based on or considered as a function of the crack lengths both at the time of inspection and as critical. Likewise, failure occurs when the given criteria take place: When the performance function of failure is in the failure region ($g_F \leq 0$) or (g_F=a_c-$a \leq 0$); when crack is detected (g_R=0); and when the critical number of cycles exceeds the number of cycles at the time of inspection ($N^c > N_{INSP}$).

where g_F and g_R are performance values for failure and repair respectively, N^c and N_{INSP} are critical number of cycles and the number of cycles at the time of inspection respectively. a_c is the final or critical length of crack, a is the measured crack length, while POD and θ are probability of detection and chance of detection respectively.

7.2.2.2 Inspection and Repairs

Fatigue crack growth under cyclic loading and/or unloading like other resistance deterioration/degradation due to defect size growth are seldom inspected with non-destructive inspection tools; whereby optimal inspection and maintenance schedules could be selected when the reliability analysis of the quality of inspection tools and maintenance criteria is well considered. According to Zheng and Ellingwood (1998), in-service inspection and assessment of fatigue damage are necessary for managing risk in an aging structure and for scheduling maintenance

or repair. State-of-the-art non-destructive evaluation (NDE) techniques provide an opportunity to obtain data on fatigue crack growth in service without damaging the structure.

Since inspection activities may assess the damage incorrectly or may not even detect any damage at all based on the quality, a probability of detection (POD) associated with the non-destructive inspection techniques is assigned.

For this work, the POD is modelled (Zheng and Ellingwood, 1998; Staat, 1993) as:

$$POD = (1-p)\left(1-e^{-\lambda a}\right) \quad a \geq 0 \tag{7.1}$$

p is the probability of not detecting a large crack while λ is a constant depending on the specific NDI technique applied. The probability of detection is calculated based on two factors: the first one $(1-p)$ measures the probability of detecting a very large crack while the second factor $\left(1-e^{-\lambda a}\right)$ can be interpreted as a weight between 0 and 1 that depends on the crack length. This POD (a) is asymptotic to $(1-p)$ for large values of a; typically p would be on the order of 0.01- 0.05.

The chance to detect a crack when the inspection is performed (θ) is modelled as uniformly distributed random variable $\theta \sim$ U (0, 1).

Failure as considered in the context of this work is not that of the ultimate cause of all fatigue failures where a crack has grown to a point at which the remaining material can no longer tolerate the stresses or strains, and sudden fracture occurs. Neither is it fracture, the last stage of the fatigue process; which is the separation of a component or structure into two or more parts. But it is the monetary cost when bridges are closed or restricted due to repair actions.

7.2.3 Optimal Maintenance

In order to arrive at a safe and economic solution to an overall optimization problem without compromising the objective of acceptable level of safety being ensured and the economic efforts to be reasonable; and without misperception of the safety and economic level, all uncertainties inherent in the problem have to be

considered in a realistic manner and be processed with numerically efficient techniques (Enevoldsen and Sorensen, 1994; Gasser and Schuëller, 1997).

The total cost of operation is formulated and adopted as a deterministic substitute optimization problem in Enevoldsen and Sorensen (1994). Section 3.7 of chapter 3 explains the full details of the reliability based optimization framework employed here. The formulation as in Eq. (3.54) and (3.55) is:

$$\min_{N_I,t,e,d} C_T\left(N_I,t,e,d\right)=C_I\left(N_I,t,e.d\right)+C_R\left(N_I,t.e.d\right)+C_F\left(N_I,t,e,d\right)$$

$$s.t. \qquad \beta\left(T_L,N_I,t,e,d\right)\geq\beta_{\min}$$

A Monte Carlo simulation of the probabilities of repair and failure as an explicit function of the design variable (probabilities of repair and failure for times of inspection) and the fuzzy variable (initial crack length) has been used for solving the optimization. All other associated variables with the model, such as failure probability and total costs of operation, become fuzzy random variables and treated as so.

The initial crack length is modelled as lognormal variable with imprecision of the mean value and defined standard deviation: LN ([0.5, 3], 0.4) employing fuzzy sets theory. This has been analysed and discussed under the fatigue life of materials as an example of random variables that follow lognormal distribution, and the fatigue crack modelled as lognormal with mean imprecision values (Section 4.2.5 of Chapter 4).

The total cost of operation is the sum of expected cost of inspection, repair and failure. The inspection cost represents the expenditures on performing non-destructive inspection. This cost is an uncertain variable, because of the possibility of structure, system or components failing before inspection. In this work it is assumed that failure is a rare event, the probability of failure is far less than one $\left(P_F<<1\right)$, and hence it is deterministic and can be computed analytically.

The expected inspection cost is calculated as the product of the unit inspection cost corrected by the discount rate and the probability that inspection takes place. This expected cost is expressed in mathematical form, Eq. (3.57) as:

$$\text{Inspection Cost, } C_I = \frac{c_I(q)}{(1+r)^{T_I}}\left(1-P_F^T\right) \qquad (P_F << 1)$$

In this optimal maintenance strategy, the problem involves both random and fuzzy variables resulting from the probabilities of repair and failure thereby becoming imprecise probabilities. The evaluation of the expected cost associated with repair is quite challenging, as it involves the computation that is closely related with the evaluation of reliability; thus, methods of structural reliability have been applied in evaluating the expected costs.

The expected repair costs are modelled (see Eq. 3.58) as:

$$\text{Repair cost, } C_R = \sum_{i=1}^{N_I} C_{Ri}.P_{Ri}.\frac{1}{(1+r)^{T_I}}$$

The expected cost and reliability is estimated using Monte Carlo Simulation (MCS) with 10,000 samples and implemented in OpenCossan (Patelli, 2016).

Failure Cost

Failure here is when bridges are closed or restricted due to repair actions or penalty charged to the owner (in case of private). When considering whether to restrict lanes, close bridges temporarily, or construct a detour bridge, but the only costs are those to conduct the actual work (not fees or penalties charged by the government, in case of public)

7.2.4 Optimal Solution

Reliability and optimisation are invoked in a specific sequence of instructions for solution to this problem by designing the solution sequence to properly combine the methods. Firstly the reliability analysis is performed according to a predefined scheme of points - the assessment of several probabilities of failure and repair for combinations of time of inspection (i.e. design variable) and the mean value of the

initial crack length(i.e. fuzzy variable). The object RBOproblem in OpenCossan provides the natural environment for solving optimisation problems involving uncertain variables, in this case it reveals to be particularly effective in dealing with fuzzy variables. It embeds all the required tools and it allows directly calling the algorithms. Finally, the reliability-based optimization is performed - within the object RBOproblem by invoking the method optimize. This action returns an object containing the optimal solution.

7.2.5 Example Application

A welded connection between a web stiffener and girder's flange of a bridge as shown in Fig. 7.1 is presented to illustrate and to discuss the suggested approach as well as its applicability. The crack length is modelled as lognormal variable with mean value 1.5mm and standard deviation of 0.4mm^2. The initial crack length is an imprecise random variable with imprecision mean value, m= (0.5mm, 3mm). The critical crack length a_c is set as 15 mm. The parameters of the Paris-Erdogan law are taken as m =2.4 and C =2x10^{-10} mm/cycle (N/mm $^{1.5}$)$^{2.4}$ while the amplitude of the alternating stress applied is 30 MPa. The parameters associated with the POD are modelled such that p =0.02 and λ =0.1 mm. During one year of operation, a total of 2.4 x 10^6 load cycles are applied. The plate must endure a life period of 10 years, therefore the inspection time is chosen within the interval of 1.0 x 10^6 and 2.3 x 10^6 load cycles. The costs associated with inspection, repair and failure are set as C_I =70, C_R = 350 and C_F =2x10^5; which are all expressed in monetary units.

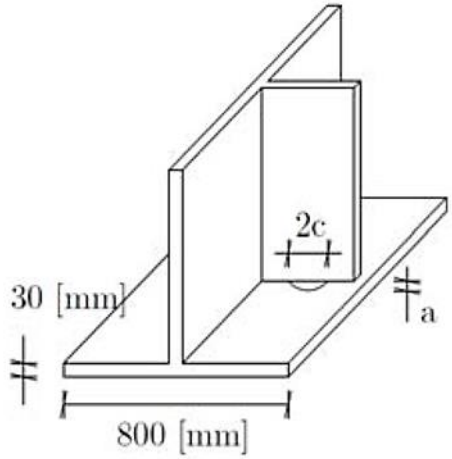

Figure 7.1a: A welded connection between a web stiffener and girder's flange of a bridge (Lukic and Cremona, 2001)

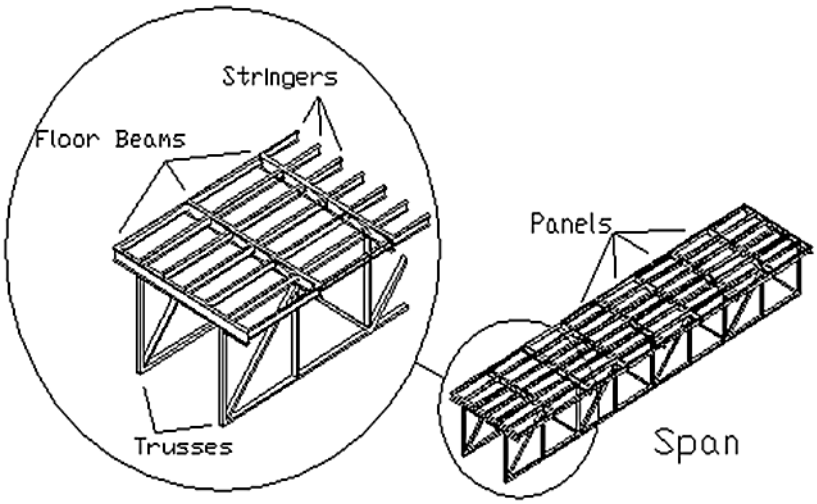

Figure 7.1b: A span of the southbound structure of the Winchester Bridge without the six inch (150mm) concrete deck (Paasch and DePiero, 1999)

7.2.5.1 Results and Discussion

Probability of failure increases for early inspection time (cracks too small for detection) and late inspection time (failure before inspection activity) in Fig. 7.2; also, probability of repair increases with the time of inspection as shown in Fig. 7.3. While sensitivities of the failure probability with respect to the probabilistic model choice is depicted based on the implementation of imprecise probabilities. The optimal inspection time is obtained between 1.5×10^6 to 1.8×10^6 load cycles based on the initial crack and total costs of operation, Fig. 7.6.

Figures 7.4 and 7.5 are the expected costs of repairs and failure as a function of the time of inspection and the initial crack length, respectively.

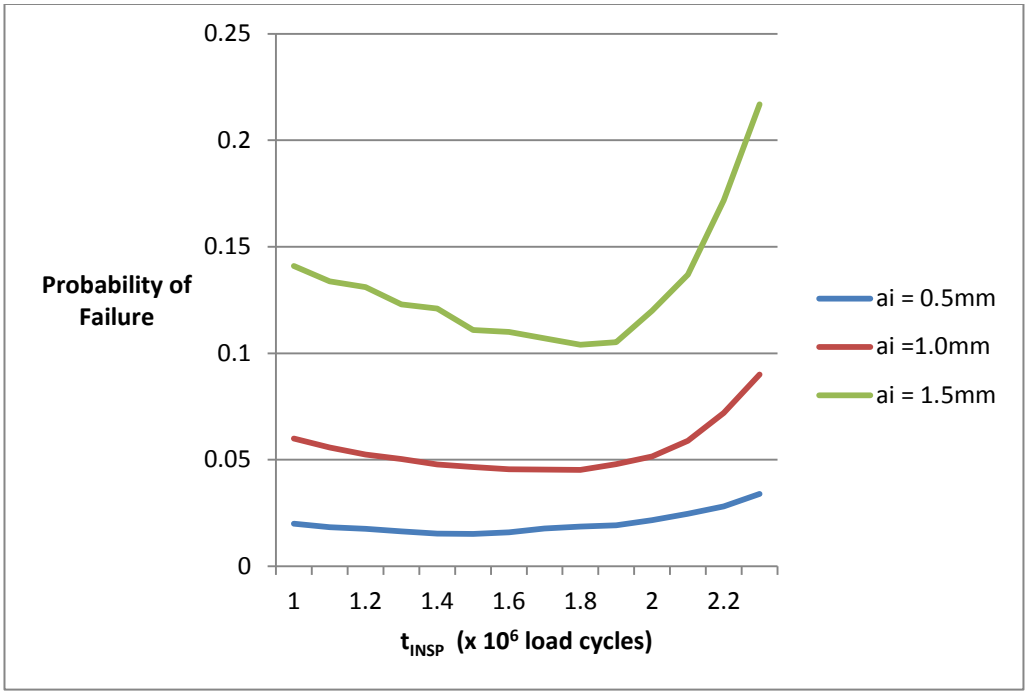

Figure 7.2: Probability of Failure as a function of expected value of initial crack length and time of inspection.

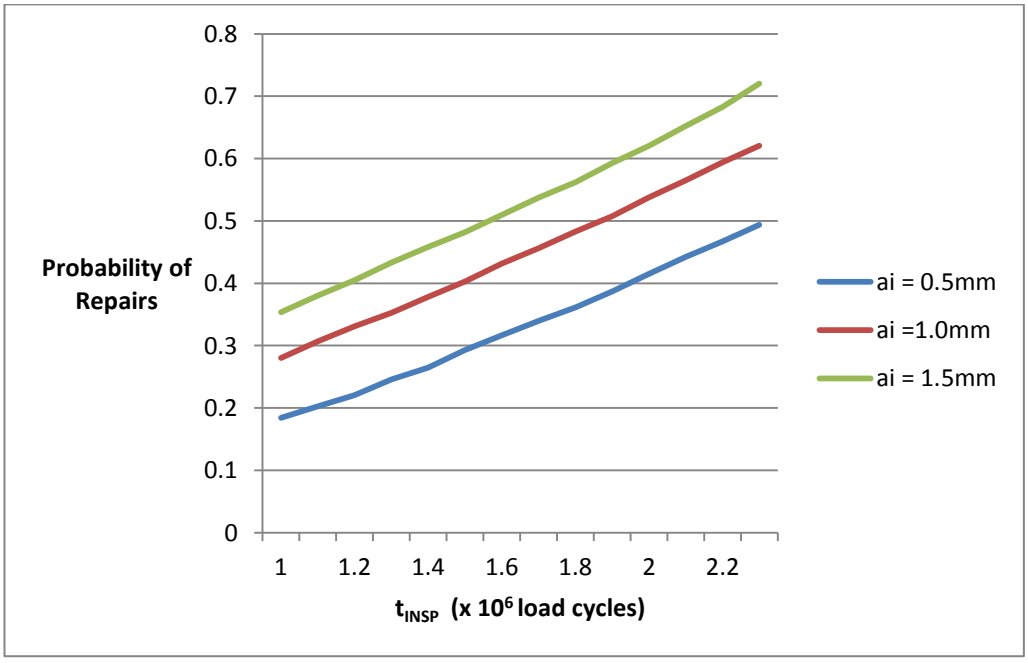

Figure 7.3: Probability of Repair as a function of expected value of initial crack length and time of inspection.

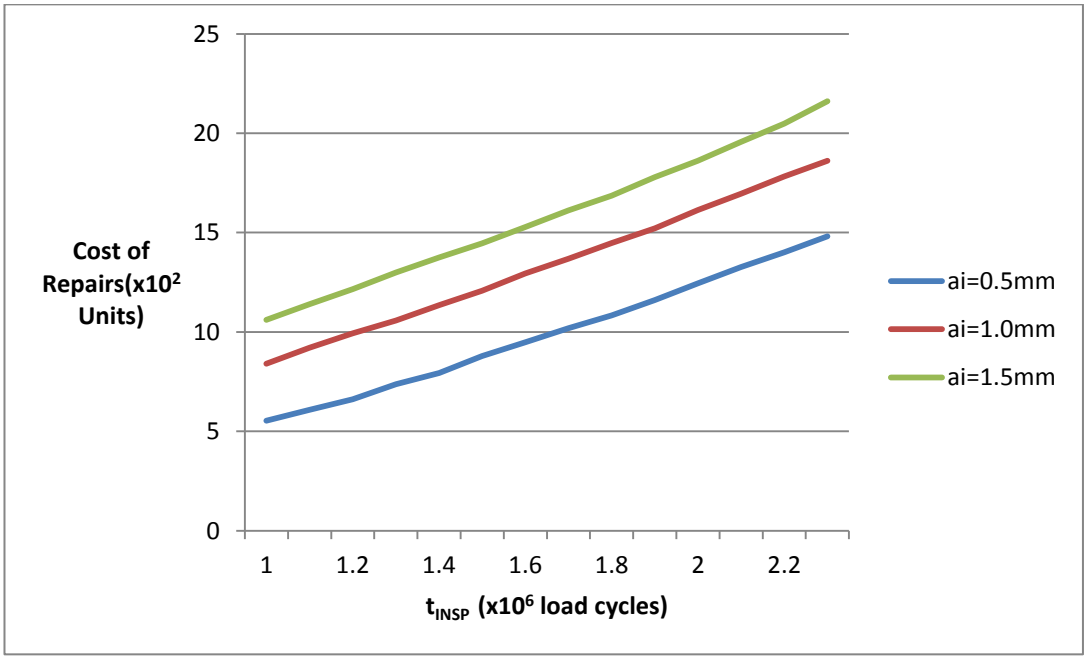

Figure 7.4: Expected Cost of Repairs as a function of the time of inspection and the initial crack length

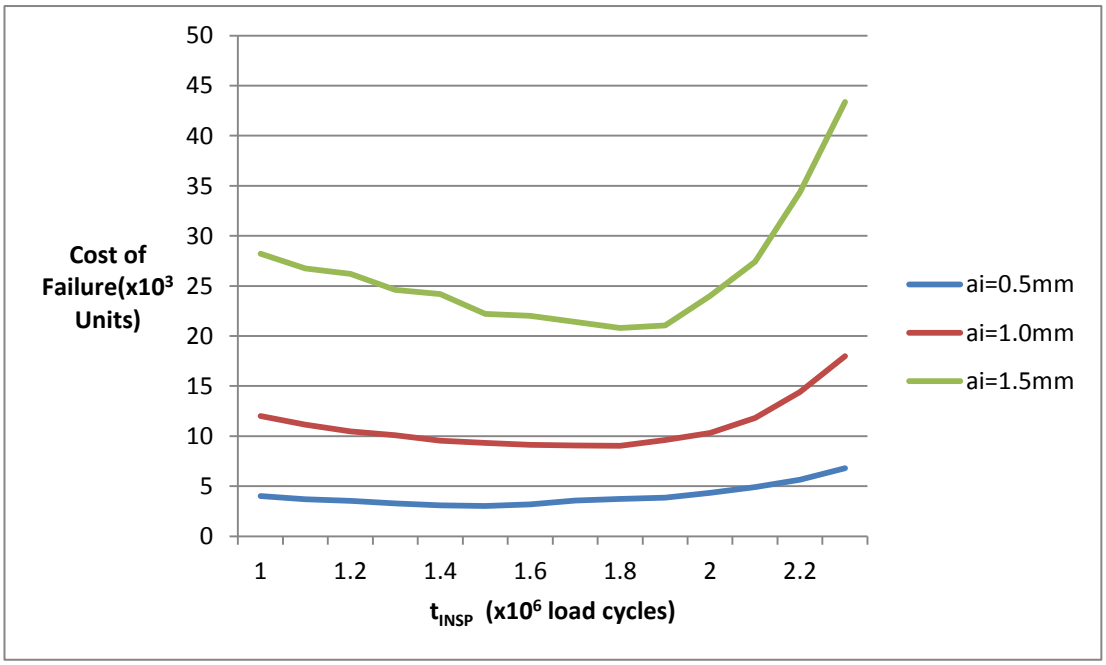

Figure 7.5: Expected Cost of Failure as a function of the time of inspection and the initial crack length

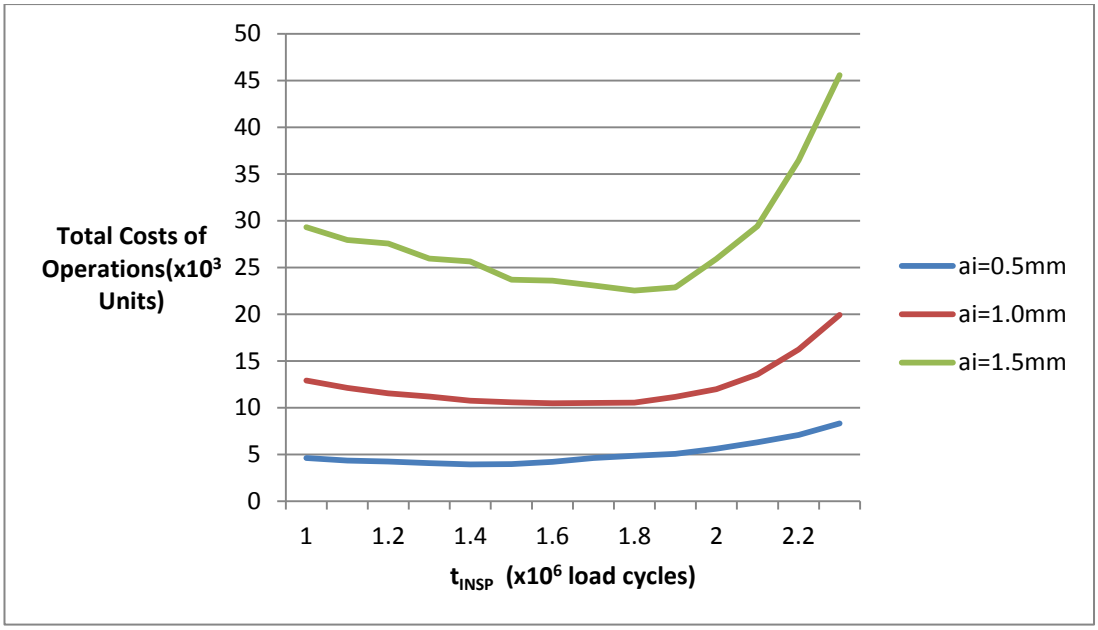

Figure 7.6: Expected Total Cost of Operations as a function of the time of inspection and the initial crack length

7.2.5.2 Limitations

Another numerical example to demonstrate the applicability of the proposed framework as well as the importance of considering the effects of uncertainty is shown using Winchester Bridge as described in Paasch and DePiero (1999), and shown in Fig. 7.1b. It is a bridge with bolted connections with cracks at the edges. Fatigue cracks as long as 4 inches (100 mm) have been found in the clip angles that connect the stringers to the floor beams, these cracks were typically found in the clip angles connecting the stringers to the floor beams at the ends of the spans, and some found in the interior clip angles. The cracks were located at the corner of the clip angle running vertically from the top of the clip angle down.

For the welded connection between a web stiffener and girder's flange of the bridge in the former example application, the suggested approach for optimal maintenance strategy works fine. But as simulations were run for Winchester Bridge of bolted connections with cracks at the edges, the results have always been "no crack lengths found at inspection".

7.3 Reliability-Based Optimization of Inspection Time Interval for Corroded Buried Pipelines

Non-destructive inspection tools such as magnetic flux leakage (MFL) and ultrasound (UTS) tools are generally used to identify the status of the system (e.g. corrosion defect). However, the inspection data are associated with imprecision and uncertainty due to the imperfect detection and measuring capabilities (i.e. the quality and ability of non-destructive inspection tools in detecting and sizing corrosion defect). In addition, variables such as the defect size, the corrosion growth rate and the failure pressure model used for predicting the remaining pressure strength of corroded pipeline; defect size; and corrosion growth rate are vital variables to be considered in the reliability analysis of corroded pipelines are also affected by uncertainty. To quantify these uncertainties, probability theory has been applied in assessing existing pipelines conditions. The classical probability theorem is used in dealing with uncertainties associated with pipelines reliability and maintenance, inspection time interval, and cost of operations; imprecision also, should be added to these uncertainties for a robust maintenance strategy. Likewise, the failure and maintenance criterion should be based on remaining pressure strength of corroded pipeline that depends on both depth and length of defects rather than maximum defect depth only; and in addition to this, combined simultaneous loadings on the corroded pipeline be given a proper consideration.

A framework with the concept and techniques from classical probability theory is employed for reliability estimates inculcating the impact of inspection and repair activities planned over the service life of a pipeline vulnerable to corrosion. The proposed approach is adopted to solve the optimal inspection interval and the repair strategy that would maintain adequate reliability throughout the service life of the pipeline.

Results obtained for typical pipelines are presented using illustrative numerical efficient algorithm, which serves as an example application to industry-size problems.

The scarcity of information associated with the condition of buried pipelines makes the maintenance of such system a challenging task. The inspection and monitoring of these pipelines is necessary in order to ensure their continued fitness for purpose, entails protection from any time-dependent degradation processes, such as corrosion, external interference and ground movement, either natural or man-made. This is necessary because pipeline failures have significant impact on the economic, environmental and social aspects of the society. Therefore, the proper assessment and maintenance of such structures are crucial; negligence will lead to serviceability loss and failure (Ahammed and Melchers, 1997).

A challenging task is the identification of optimal inspection interval time in order to reduce the overall inspection costs. For instance, areas needing repairs must be accurately pinpointed as to minimise excavations for verifications. This can be achieved in addition to non-destructive inspection tool that have the capability to deliver a consistently high-level of reporting pipeline features and defects (Caleyo et al., 2009; Hong, 1999). Likewise, early observations of failure mechanisms, and determination of the likelihood of failure in association with the pipeline must be handy.

The information obtained from in-line inspection data are imprecise due to the imperfect measurement of defect dimensions and the limited resolution of non-destructive inspection tools. To capture the variability of the data, combination of imprecise probabilities framework with the concept and techniques from classical probability approach is employed in this work for robust reliability analysis of pipelines. The proposed approach allows inculcating the impact of inspection and repair activities planned over the service life of a pipeline vulnerable to corrosion and combined loadings. This framework is applied to determine the optimal inspection interval and the repair strategy that would maintain adequate reliability level throughout the service life of the pipeline. The reliability analysis is performed adopting an efficient Monte Carlo procedure (Angelis et al., 2015) simulation, and implemented in the general purpose software OpenCossan (Patelli et al., 2014).

7.3.1 Pipelines Modelling

7.3.1.1 Corrosion models

The analysis of the future state of a pipeline, such as failure probability, residual strength, etc., is based on the predicted sizes of the defects which were detected during In-Line Inspection. The corrosion models for this work have been discussed in section 4.3 of chapter 4. Corrosion rates are assumed as constant values in Eq. (4.16) and (4.17):

$$d(t) = d_0 + v_d t$$

$$l(t) = l_0 + v_l t$$

The use of interval probabilities is adopted in modelling imprecision in the corrosion rates. Detailed description of this can be found in Chapter 3 Section 3.3.1. This becomes a necessity because the information available is not sufficient to formulate clear probabilistic models with substantial confidence. An interval (Beer et al. 2013) is a closed bounded set of real numbers [a, b] = {x: a ≤ x ≤ b}. Suppose A is an interval, and its end points are $\overline{A}$and $\underline{A}$, then $A = \left[\overline{A}, \underline{A}\right]$. So for n-dimensional interval vector, $(A_1, A_2, \ldots, A_n)$ if A is a 2-dimensional interval vector, then $A = (A_1, A_2)$, and for some intervals $A_1 = \left[\underline{A_1}, \overline{A_1}\right]$ and $A_2 = \left(\underline{A_2}, \overline{A_2}\right)$ such that $\underline{A_1} \leq a_1 \leq \overline{A_1}$ and $\underline{A_2} \leq a_2 \leq \overline{A_2}$.

The corrosion defect depth and length, as the most important variables in the failure pressure models were assigned an interval of 150 – 250 mm (defect length), and 0 - 100% as measured defect depth through the nominal wall thickness; representing epistemic uncertainty in the probabilistic procedures.

7.3.1.2 Combined Loadings

Oil pipelines are required to withstand circumferential and longitudinal stresses produced by operating pressure, external forces and influences, and differences in installation and operating temperature. The assessment of combined loadings for buried pipelines is enumerated in Chapter 4, Section 4. 8.

From Eq. (4.72), the circumferential stress due to internal/operating fluid pressure is estimated as:

$$\sigma_{cs} = P_{op} r / w_t \tag{7.2}$$

$$r = (D - 2w_t)/2 \tag{7.3}$$

P_{op} is operating pressure, r is radius of pipe, D is outside diameter of pipe and w_t is the pipe wall thickness.

The longitudinal stress is calculated as:

$$\sigma_{ls} = \mu\sigma_{cs} - \alpha E \Delta T + \sigma_{bs} \tag{7.4}$$

For buried pipelines under combined loadings, the longitudinal bending stress (see Eq. 4.73 and 4.78) is:

$$\sigma_{bs} = [(6k_m C_d \gamma B_d^2 E w_t r)/(E{w_t}^3 + 24k_d p r^3)] + Er\chi \tag{7.5}$$

The underground pipelines are subjected to both longitudinal and circumferential stresses and these are described as a function of the applied load with the aid of a mechanical model using von Mises equivalent stress expression. The mathematical expressions and formulations are in Eq. (4.79), (4.80) and (4.81).

$$\sigma_{es} = (\sigma_{cs}^2 + \sigma_{ls}^2 - \sigma_{cs}\sigma_{ls})^{0.5}$$

σ_{es}, σ_{cs} and σ_{ls} are von Mises equivalent stress, circumferential stress and longitudinal stress respectively.

7.3.2 Remaining Life of Pipeline

The assessment of the extra stresses induced by the corrosion defects in connection with the design failure pressure for the geometric parameters of a single surface corrosion defect is done by using the DNV-101 model. From Eq. (4.29) and (4.30) it is estimated in the form of:

$$p_f = 2w_t\sigma_f/(D - w_t)[(1 - d/w_t)/(1 - d/w_t M)] \tag{7.6}$$

$$M = \sqrt{\left(1 + 0.31(l^2/D.w_t)\right)} \tag{7.7}$$

where, p_f = failure pressure, d = corrosion maximum depth, D = pipe outside diameter, σ_f = flow stress, M = Folias' factor, and wt = pipe wall thickness.

The limit state function $G(x)$ for the effects of combined stresses/loadings is defined as the difference between the yield stress of the pipe material (SMYS) and the equivalent stresses σ_{es}, expressed mathematically in Eq. (4.86) as:

$$G(x)_1 = SMYS - \sigma_{es}$$

For the effect of stresses due to corrosion, we have the limit state function as the difference between the failure pressure (p_f) and the operating pressure of the pipe (P_{op}) to be:

$$G(x)_2 = p_f - P_{op} \tag{7.8}$$

Probability of failure (P_f) for the pipeline from Eq. (4.87) is written as:

$$P_f = P(G(x) \leq 0)$$

The failure of the pipe occurs when its resistance falls below the operating pressure, P_{op}. This is after treating the pipe section geometrical properties, corrosion growth rate, material properties, operating pressure and the defect dimensions as random variables to quantify the associated uncertainty in the pipeline system.

7.3.3 Pipeline Optimal Time of Inspection and Repairs

7.3.3.1 Inspections

Probability of detection is taken as the exponential probability distribution for the detectable depth. Consequently, the average depth of the detectable defects is the reciprocal of quality of the inspection tool. The probability of detection (Pandey 1998) is:

$$PoD = 1 - e^{-qd} \tag{7.9}$$

where d = defect depth, q = quality of inspection.

7.3.3.2 Repairs

The failure pressure safety factor often defines the repair criterion (Pandey, 1998); which is the ratio of the failure pressure (burst pressure) and the Maximum Allowable Operating Pressure (MAOP). A defect will be considered critical and needs to be repaired or removed from the pipeline if the safety factor for the given defect is lower than the threshold: $1.25 \leq SF_{p_f} \leq 1.5$.

$$SF_{P_f} = p_f / MAOP \tag{7.10}$$

7.3.3.3 Optimization formulation

In order to arrive at a safe and economic solution to an overall optimization problem without compromising the objective of acceptable level of safety being ensured and the economic efforts to be reasonable; and without misperception of the safety and economic level, all uncertainties inherent in the problem have to be considered in a realistic manner and be processed with numerically efficient techniques, see e.g. Enevoldsen and Sorensen, 1994. The total cost of operation from Eq. (3.54) and (3.55) as a deterministic substitute optimization problem is:

$$\min_{N_I,t,e,d} C_T(N_I,t,e,d) = C_I(N_I,t,e.d) + C_R(N_I,t.e.d) + C_F(N_I,t,e,d)$$

$$s.t.\ \beta = P_F(T)$$

7.3.3.4 Cost of inspection

The expected inspection cost is calculated as the product of the unit inspection cost corrected by the discount rate and the probability that inspection takes place, in Eq. (3.57) as:

$$C_I = \left[\left(c_I(q)\right)/(1+r)^{T_I}\right](1 - P_F^T)$$

7.3.3.5 Cost of repair

The expected repair costs modelled in Eq. (3.58) as:

$$C_R = \sum_{i=1}^{N_I} C_{Ri} \,.\, P_{Ri}/(1+r)^{T_I}$$

7.3.3.6 Cost of failure

The total capitalized expected costs due to failure are determined from in Eq. (3.59):

$$C_F = \sum_{i=1}^{N_I+1} C_F(T_F).\{P_F(T_F) - P_F(T_{F-1})\}/(1+r)^{T_I}$$

7.3.4 Example Application

In order to illustrate the application and the advantage of the proposed method, a real life pipeline is chosen for this analysis. Its parameters are listed in Table 7.1. The radial and longitudinal corrosion rates were assumed to be constant over the elapsed life of the pipeline; and the values are taken to be 0.5 mm/yr. for both.

The active corrosion defects are 3 mm and 200 mm for depth and length respectively. The pipeline outside diameter = 609.6 mm; wall thickness = 9.52 mm; and the operating pressure = 4.96 MPa. Other material properties of the pipeline are as follows: type is X52, yield stress is 358 MPa, and the tensile strength is 496 MPa. The parameter associated with the PoD: the quality of inspection is 3.262. The target lifetime of the pipeline is 50 years and the inspection time is chosen within the interval of 1 year and 25 years. The costs associated with inspection, repair and failure are set as multiplicative factor C_I = 0.018, C_R = 0.243 and C_F = 36.55, (see Table A-1 in Appendix; Gomes and Beck, 2014); these factors are multiplied by a unitary cost representing the cost of production and installation of one unit length of pipe, expressed in monetary units. The discount rate is taken as 0.05.

Monte Carlo simulation is employed to simulate the evolution of the system over the time considering inspections and reparation. Large number of system evolution histories is simulated. The simulation approach has been implemented into OpenCossan - the open source engine of COSSAN software for uncertainty quantification and risk management (Patelli et al., 2014). Monte Carlo simulation is also employed to calculate the failure probability. One thousand sets of random variables are generated and simulation repeated 400,000 times, varying the number of inspections from 1 to 25 in a time period of 25 years.

Table 7.1: Stochastic model used for the corroded pipeline (taken from Ahammed and Melchers, 1997)

Variable	Symbol	Unit	Pdf	Mean	CoV
Diameter	D	mm	N	609.6	0.02
Wall thickness	w_t	mm	N	9.52	0.02
SMYS	σ_y	MPa	N	358	0.10
MAOP	P_{op}	MPa	N	4.96	0.20
Young Modulus	E	MPa	N	$2.01x10^5$	0.033
Poisson coefficient	μ	-	N	0.3	0.023
Linear exp. coefficient	A	$1/^oC$	N	$11.7x10^{-5}$	0.01
Temperature differential	Δt	^oC	N	10	0.15
Ditch width	B_d	mm	N	760	0.10
Earth press. coefficient	C_d	-	LN	1.32	0.20
Deflection coeff.	k_d	-	LN	0.108	0.20
Soil unit weight	γ	N/mm^3	N	$18.9x10^{-6}$	0.10
Longitudinal curvature	χ	Rad/mm	N	$1.0x10^{-6}$	0.10
Multiplying constant	K	-	N	0.3	0.3
Exponential constant	N	-	N	0.6	0.2
Radial rate (Zhou,2010)	v_d	mm/yr	LN	0.5	0.10
Long. Rate (Zhou,2010)	v_l	mm/yr	LN	0.5	0.10

7.3.5 Results and Discussion

The total operation cost depends on the number of inspections in the remaining lifetime of the pipeline; time interval between inspections; qualities of inspection; and the number of repair actions based on the measured corrosion defect, and the resultant equivalent stresses from a combination of external loads on the pipe. This is performed adopting efficient Monte Carlo procedure simulation.

Figure 7.7 shows the repair criterion based on failure pressure safety factor threshold. The threshold is a typical values of $1.25 \leq SF_{p_f} \leq 1.5$ (see Eq. 7.10), this value is in agreement with the level of integrity established by actual pipeline hydro testing, and corresponds to the repair factor for a class 2 pipeline in Canadian code (CSA, 2007) as its safety factor adopted in design.

Once the pipe is buried, it is undesirable to dig it up for any reason. Pigs (i.e. magnetic flux leakage tools or ultrasonic tools) are sent through the buried pipe to perform inspections and clean the pipe. The pigs are carried through the pipe by the flow of the liquid or gas and can travel and perform inspections over very large distances. The pigs carry a small computer to collect, store and transmit the data for analysis. During each in-line inspection, based on the accuracy and detection ability of the inspection tool, some critical defects that are under-sized by the inspection method will be left unrepaired, while some subcritical defects that are over-sized by the inspection method will be excavated and repaired. The primary concern therefore is the interpretation of in-line inspection data considering uncertainties associated with defect dimensions, corrosion growth rate, operational loads, and pipeline material properties.

After the in-line inspection, all the collected data are processed to identify which defects are critical or not to the pipeline integrity. If the safety factor for a given defect is lower than the threshold, the defect will be considered critical, repaired and removed from the pipeline. A typical value of the failure pressure safety factor that is to ensure the same level of integrity as the actual hydro testing of the pipeline is 1.25.

Figure 7.7 shows a general probabilistic analysis for reliability assessment to determine the optimal inspection interval based on the repair criterion that would maintain adequate reliability throughout the pipeline service life. Once the reliability is performed and the probability of failure with time is known, the operator/maintainer has options to manage the present and future integrity of the pipeline.

In Fig. 7.8, the unit cost of failure irrespective of the amount does not seem to have any effect on the total cost, when the number of inspections is between 20 and 25 times. Likewise, increase in numbers of inspections increases the total cost for every increment on the unit cost of failure.

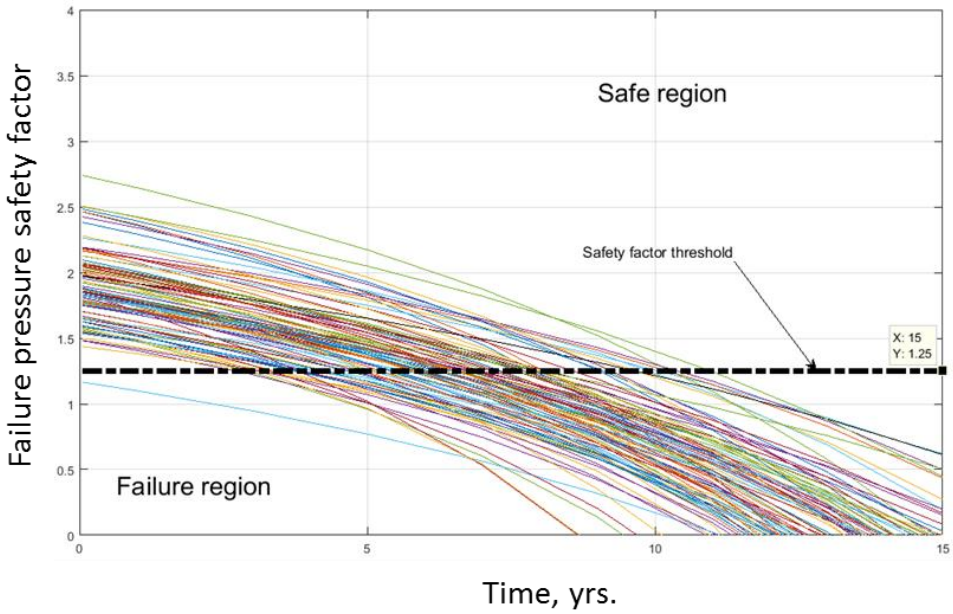

Figure 7.7: Repair criterion based on failure pressure safety factor

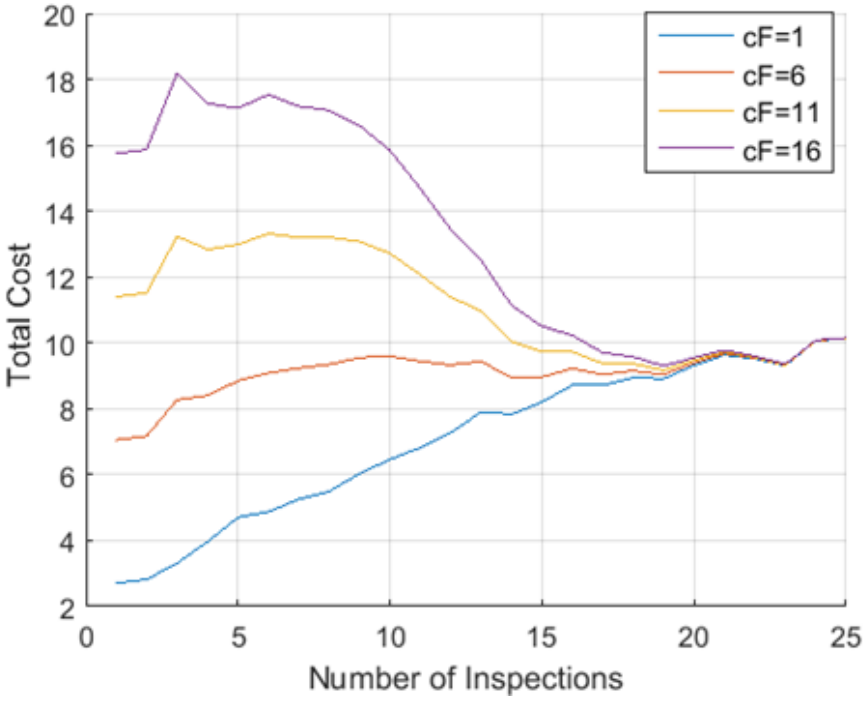

Figure 7.8: Total cost of operation as a function of varying units of failure cost

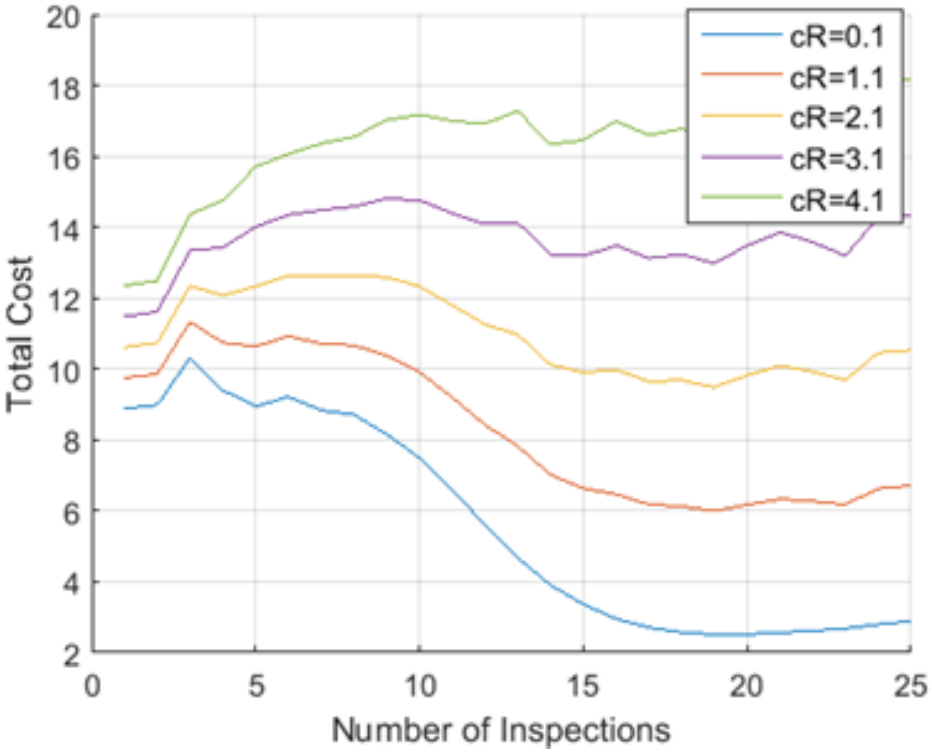

Figure 7.9: Total cost of operation as a function of varying units of repair cost

The total cost reduction with increasing number of inspections in Fig. 7.9 is as a result of the expenditure in carrying out inspections and eventual repairs by varying the number of inspections from only one (1) in 25 years to twenty five (25) inspections in a time period of 25 years. For instance, when the total numbers of five (5) inspections are carried out in a time period of 25 years, the total cost of operation is higher for each unit cost of repairs than when twenty (20) different inspections are carried out in a time period of 25 years. This analysis is to aid regular scheduled inspections that can validate corrosion rates and allow to better plan for maintenance situations.

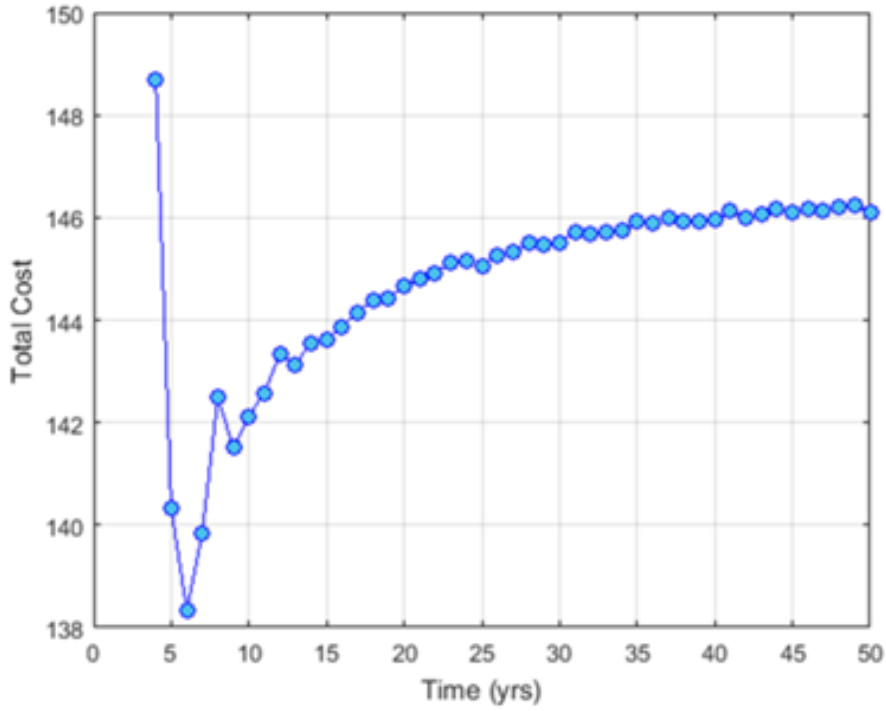

Figure 7.10: Total cost of operation as a function of time

The total cost of operation associated with inspection, repair and failure are set as multiplicative factor (see Table 5.4 and Table A-1.1 in the Appendix). These factors are multiplied by a unitary cost representing the cost of production and installation of one unit length of pipe, expressed in monetary units.

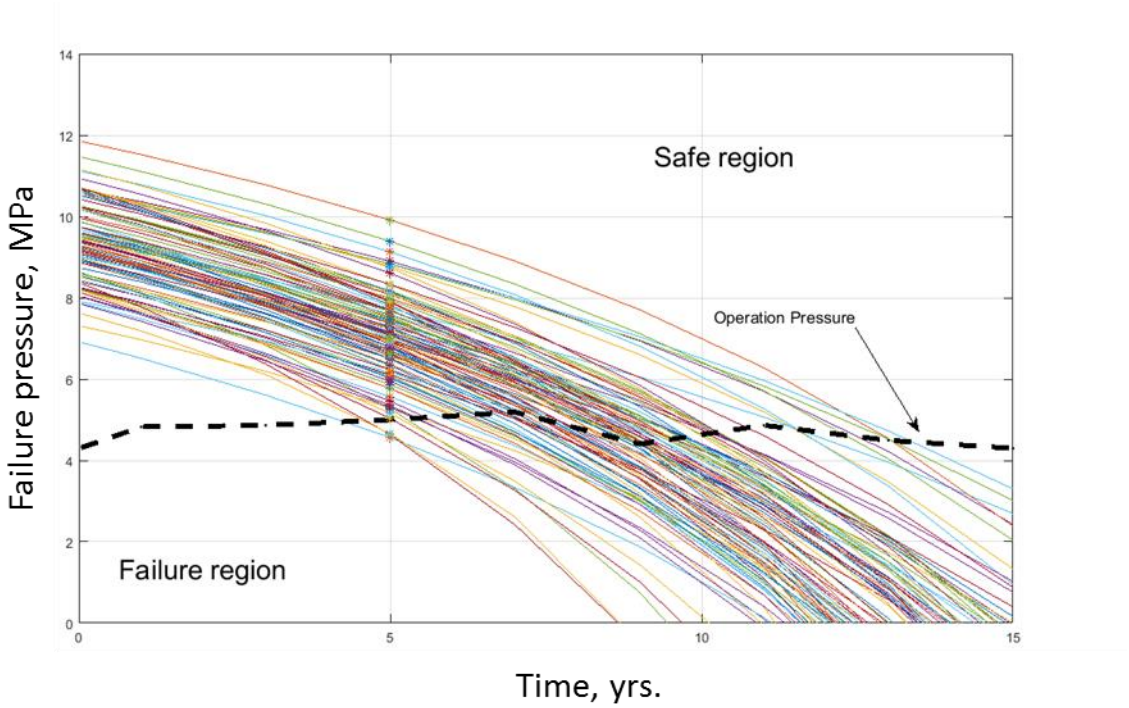

Figure 7.11: Repair criterion based on failure pressure

Fig. 7.10 shows the total operation cost as a function of time. As the inspection time intervals increase, a large influence on the total cost is seen at the beginning, which later increases and remains constant as from 35years of the pipeline lifetime.

The repair criterion based on failure pressure shown in Fig. 7.11. The operating pressure, which is the standard level of pressure the pipeline system operates, and usually within a fairly narrow range of tolerances; fluctuates as the pipe aged. This indicates that the operating pressure in the system at some times has enough pressure to be operational, and at some other times, either the system is not pressurized yet, or there is a problem preventing full pressure, such as a leak or a shortage of oil/gas. This is a pointer to an underlying issue that needs to be addressed, and it should be evaluated to learn more about the malfunction, thereby constituting a maintenance outcomes. The operating pressure might have been varied depending on temperature (i.e. due to the effects thermal stresses) and the effects of one or combinations of variable compressive axial load, transverse load, moment, etc. Likewise, since the density of the oil/gas is a function of the operating pressure, it is a good indicator to measure their flow. Based on the operating pressure, when the failure pressure is considered against the age of the

pipeline, results for the example application presented herein shows an optimum inspection time interval of about ten (10) years (i.e. between 8 to 10 years).

Early inspection schedules result in small or no defect detection for reparation, while late schedules of inspections will amount to failure before inspection. Pipeline structural systems, though usually protected from excess pressures and temperatures by safety devices, but these devices can fail to function due to time-related degradation and/or maintenance. Hence minimization of the maximum failure probability between the times of inspections will normally yield an optimal inspection time. Corrosion defects in a typical pipeline material will grow by ductile tearing prior to failure as the pressure increases, thereby resulting into a phenomenon known as pressure reversal.

7.4 Summary

In conclusion, the time at which inspection is carried out is so fundamental in the overall effectiveness of an optimal maintenance strategy; or else, even though expensive, is a waste if inappropriate scheduling is done.

The proposed methodology in the metallic bridge could be extended in order to consider several inspections, instead of a single inspection. Likewise, numerical framework for both welded and bolted connections with cracks at the middle and at edges can be written and cast into software solutions. This is a possibility of future work and recommendation for the research work that could be extended to other engineering structures and systems.

A probabilistic framework for reliability estimation of optimal inspection and maintenance schedule selection for buried pipelines under uncertainty using efficient Monte Carlo procedure has been proposed and employed in this work. A real life pipeline is presented to demonstrate the robustness and efficiency validation of the approach. The optimal pipeline inspection time allows the minimization of expenditures incurred when conducting maintenance activities, and at the same time keeping the pipeline in safe operation mode. The probabilistic framework presented is well suited for use to determine the optimal inspection

interval and the repair strategy that would maintain adequate reliability throughout pipeline service life due to its simplicity, general applicability and singular reliability estimation for the whole optimization procedures.

8. Conclusions and Recommendations

8.1 Concluding Remarks

This thesis is concerned with the realistic consideration and quantification of uncertainties of diverse inherent features and magnitude which is a key issue in ensuring a faultless life of engineering structures and systems despite fluctuations and changes of structural and environmental parameters and conditions. Imprecise probabilities theories are an extension of classical probability theory with clear operational and behavioural interpretations, and as a general uncertainty model, these have been adopted in this thesis to characterise and quantify the uncertainty. The presented approach of imprecise probabilities has emerged into several application fields in engineering with structured approaches. The largest application field appears as reliability assessment, where imprecise probabilities are implemented to address sensitivities of the failure probability with respect to the probabilistic model choice. This has overcome the drawbacks in classical probabilistic methods with the consideration of an entire set of probabilistic models in one analysis, thereby making imprecise probabilities framework to provide mathematical basis for dealing with problems which involve both classical probabilistic and non-classical probabilistic information. The issue of load combination in engineering structures and systems by considering them as having stochastic nature is solved using Markovian approach through modelling of the loads with Markovian description.

Maintenance of structures which remains a big challenge owing to the multi-dimensional variations as a result of sudden or gradual decrease of strength of the structures and infrastructures are critical for the functionality of our environmental, societal and economical life. This has been considered as an optimisation problem. Overall, an applicable numerical approach for comprehensive robust design and a methodology for designing robust maintenance strategies for engineering structures and systems subject to varying load under severe uncertainty. All these

are achieved via the use of both probabilistic (classical probability) and imprecise probabilistic (non-classical probability) approaches, and the combination of both approaches to minimize the consequences of unexpected events, and decision margins for subsequent design revisions.

8.2 Concluding Summary

The detailed conclusions from the present work are as follows:

In the method of assessing reliability of arctic above-ground oil field collection and main pipelines where application of the imprecise probabilities (e.g. p-boxes, probability bounds, and intervals), Markovian approach, and combination of both approaches for reliability analysis of the oil pipelines with surface corrosion defects subjected to a combination of loads has been employed. In order to design new arctic pipelines or reassessing the "future" reliability of existing pipeline systems, the necessity to modify design wind loads due to global climate change has to be taken into direct consideration.

In order to estimate the design wind loads, a quantitative analysis of the trend of the wind speed in time has been performed, its goal being finding the change of the climate mean and variance of the wind extremes for a particular geographic region.

As demonstrated in Chapter 6, one of the most convenient ways to achieve this goal is by using the imprecise probabilistic approach.

Its application to study wind speed evolution in long term calendar time due to climate change as related to the above ground pipeline reliability by using a set of wind load models is given and reported in chapter 6. Results of this study show the utility of the imprecise probabilistic approach and provided the much needed robustness with respect to the probabilistic model choice; and as one of the generalized methods, it permits overcoming the simplifications and assumptions that cannot be justified to compensate for lack of data, imprecision and vagueness in modelling.

The results of this contribution could help engineers and pipeline operators in achieving a better design of future pipelines, more accurate risk analysis and providing a better pipeline life cycle cost estimate.

The imprecise probability approach could also be useful in planning the next inspection and repair time interval when scheduling pipeline maintenance, when drafting the life cycle of arctic pipelines.

The specifics of the developed Markovian approach for reliability analysis are that it splits the task of evaluating the reliability into two independent tasks namely:

- Constructing admissible areas in load space, and
- Assessment of the probability of escape of the vector load from the admissible region. In this formulation, the dimension of the problem is not the product of the number of defects on the number of loads in combination, but just the number of loads, which allows overcoming the curse of dimensionality.

When considering analysis and design of maintenance strategies for corroded above ground and/or buried pipelines: The deterministic procedures are very simple with capability of being applied on pipelines, but cannot deal with uncertainties in the input data. The degree of conservatism, as regards to the corrosion assessment is owned to safety factors introduced into the capacity equations or codes. The pipeline probability of failure increases with the increased measured relative corrosion defect, as well as the operation time as expected, in chapters 5 and 7. The probabilistic procedures are very useful in evaluating pipeline integrity because of the inherent uncertainties associated with corrosion growth rate, inspection tools, pipeline geometry, material properties and operating pressure. The probability of failure as a function of the expected values of the relative corrosion defect ($E[d]/E[w_t]$) shows that deterministic models such as the Shell-92 and the DNV-101 models are very conservative followed by Modified B31G model and the least in the B31G model. Take for instance, a small level of imprecision in the model parameter values (e.g. 1%), the results show that the Shell-92 and the B31G models give the highest and the lowest failure probabilities (for a relative corrosion level greater than 0.6) respectively. This is in accordance with results from literature obtained without considering imprecision (Caleyo et al., 2002). The uncertainty in the output predictions is dominated by the model

uncertainty. While for an imprecision level of 5% in the parameter values, the uncertainty due to the model parameters become comparable with the model uncertainty, in particular for small relative corrosion level, etc. Thus, considering the lower and upper probability bounds, DNV-101 and Modified B31G models could be quite relevant when dealing with unnecessary pipe repairs and for greater safe operating pressure in the pipelines. It will provide the operator with several options to manage both the present and future integrity of the pipeline at a minimum acceptable reliability level with limited resources.

The optimal pipeline inspection time allows the minimization of expenditures incurred when conducting maintenance activities, and at the same time keeping the pipeline in safe operation mode. The probabilistic framework presented is well suited for use in determining the optimal inspection interval and the repair strategy that would maintain adequate reliability throughout pipeline service life due to its simplicity, general applicability and singular reliability estimation for the whole optimization procedures. The only reliable procedure of making decisions for reparation or rehabilitation is the identification of the actual state of metallic pipelines through inspection. This will lead to reduction in unnecessary replacement of pipe within remaining useful life.

Finally, under the optimal maintenance strategy for metallic bridge structures with vague information: The probability of failure increases for early inspection time (cracks too small for detection) and late inspection time (failure before inspection activity). Also, probability of repair increases with the time of inspection as shown in chapter 7. While sensitivities of the failure probability with respect to the probabilistic model choice is depicted based on the implementation of imprecise probabilities. The time at which inspection is carried out is fundamental in the overall effectiveness of an optimal maintenance strategy; or else, even though expensive, is a waste if inappropriate scheduling is done.

The quantification of uncertainty as a measure of estimating the effect on the response metrics of interest, i.e. the model output is a very important task. Structural engineering problems are brimful with uncertainties. Uncertainties in

specifying material properties, geometric parameters, boundary conditions and applied loadings are unavoidable in describing real-life engineering structural systems. These problems are solved within the confines of models - either as a set of physical or probabilistic models – by modelling the uncertainties. In structural engineering, certainty for all practical purposes seems impossible to achieve, and decisions are to be made under some level of uncertainty. For a good prediction of the reliability of engineering structures and systems, mathematical idealisations/modelling and quantification is a prior requisite for realistic outcomes. The framework of imprecise probabilities provides a mathematical basis to deal with problems that involve both classical probabilistic and non-classical probabilistic information.

Imprecise probabilities as non-classical probabilistic models have not yet been exploited and/or applied to the same extensiveness compared with the classical probabilistic model. Even though the said models do not address all factors of interest and concerns without the agreement or participation of other models, but accrued to it is the potential and significance that is of valuable contribution as complimentary.

8.3 Future Works

Suggested work for possible future research is further exploits on non-classical probabilistic approaches both for reliability and maintenance of structures with focus on the treatment of uncertainties and imprecision involved in these activities.

For example, one of the possible ways to arrive at a general algorithm to estimate the reliability of buried pipeline structural system as an age long challenge is to consider employing non-classical probabilistic approaches in addressing the problem. More research work is required in the area of the inclusion of uncertainty and imprecision in models and parameters used in describing the analysis and assessment of engineering structures and systems. It is highly plausible that probabilistic models will be of great significance, particularly their development which could be interesting and demanding. Only such an approach can adjudge for the level of admissible risk, uncertainty and imprecision in design, construction, use,

and maintenance of structures; and also for the optimal allocation of economic resources that is available.

Some specific initial data needed for this methodology (for pipeline reliability) is regarded in every part of the world as "sensitive data" and pipeline companies are reluctant to provide it even for research reasons. This led to carving the scope of the dissertation to the available data. Having data (i.e. the in-line inspection results of a particular pipeline) about the sizes, location and the number of the (corrosion) defects of the pipeline, one can proceed from there and conduct two independent assessments of pipeline reliability and remaining life by using the generalised approach and the Markov approach.

Creating a mathematical model of the upheaval/subsidence phenomenon as a random function of time is another possible avenue of research area to pursue. This permits creating a sophisticated model of upheaval/subsidence of the soil underneath any structure/infrastructure, the one used for reliability analysis of an arctic above ground pipeline. The knowledge of the upheaval/subsidence for two adjacent supports of the arctic pipeline is very crucial. If the upheaval/subsidence is the same along the pipeline, there will be no kinematic forces influencing the pipeline, since there will be no bending of the pipe as it will move as a rigid body. Hence, we need to know the difference in the upheaval/subsidence between each pair of pipeline supports. This can be done by assuming hypothesis that the two adjacent pile supports are in different soils, which produce different upheaval/subsidence.

For fatigue in metallic structures, a possible suggestion is a series of Paris equation could be used to fit various regions of the crack growth curve thereby providing a method to treat and estimate the asymptote case in the general sigmoidal $da/dN - \Delta K$ behaviour. Alternatively, to combine Paris equation with any other equation that treats the asymptote case.

References

African Review of Business and Technology. (2016).

Ahammed, M. (1998). Probabilistic estimation of remaining life of a pipeline in the presence of active corrosion defects. *International Journal of Pressure Vessels and Piping, 75*, 321-329.

Ahammed, M., & Melchers, R. E. (1997). Probabilistic analysis of underground pipelines subject to combined stresses and corrosion. *Engineering Structures, 12*, 988-994.

Ait-Kadi, D., Jamali, M. A., & Artiba, A. (2002). Optimal periodic replacement strategies using new and used items. *Journal of Decision Systems*, 12 (1), 67-77.

American Society of Civil Engineers (ASCE). (2014). *2013 report card forAmerica's infrastructure http://www.infrastructurereportcard.org/a/e/bridge-repair-costs.* US: ASCE.

American Society of Civil Engineers (ASCE). (2006). *Minimum design loads for building and other structures. ASCE 7-05.* New York: ASCE.

American Society of Civil Engineers (ASCE) Committee on Fatigue and Fracture Reliability of the Committee on Structural Safety and Reliability of the Structural Division. (1982). Fatigue reliability 1-4. *J. Struct. Engrg. ASCE, 108*, 3-88.

Anderson, T. L. (1991). *Fracture mechanics: Fundamentals and applications.* Boca Raton, Florida: CRC Press.

Ang, A. H. S., & Tang, W. (1975). *Probability concepts in engineering planning and design. Basic principles, vol. 1***.** John Wiley.

Angelis, M., Patelli, E., & Beer, M. (2015). Forced Monte Carlo simulation strategy for the design of maintenance plans with multiple inspections. *ASCE-ASME J. Risk Uncertainty Eng. Syst., Part A: Civ. Eng., D4016001.*

ASME. (1991). *Manual for determining the remaining strength of corroded pipelines. A supplement of ASME B31G code for pressure piping.* New York: ASME.

ASME. (1995). *Manual for determining the remaining strength of corroded pipelines. A supplement of ASME B31G code for pressure piping.* New York: ASME.

Au, S. K., & Beck, J. L. (2001). Estimation of small failure probabilities in high dimensions by subset simulation**.** . *Probab Eng Mech, 16*(4), 263-277.

Augusti, G., Ciampoli, M., & Frangopol, D. M. (1998). Optimal planning of retrofitting interventions on bridges in a highway network**.** . *Engineering Structures, 20*(11), 933-939.

Aynbinder, A. B., & Kamershteyn, A. G. (1982). *Calculation of pipelines strength and stability: A reference guide.* . Moscow, Russia: Nedra.

Bader, J. (2008). Non-destructive testing and evaluation of steel bridges. *Ence 710,*

Barucha-Rheid, A. G. (1969). Elements of theory of Markovian process and their application. Moscow: Nauka. 511.

Battelle Columbus Laboratories. (1982). The Economic Effects of Fracture in the United States, National Bureau of Standards, U.S. Department of Commerce, Gaithersburg, MD, Special Publication 647-2, 1983.

Bazan, F. A. V., & Beck, A. T. (2013). Stochastic process corrosion growth models for pipeline reliability. *Corrosion Science, 74*, 50-58.

Beer, M. (2009). Fuzzy probability theory. *Encyclopedia of complexity and systems science* (vol. 6 ed., pp. 4047-4059). New York: Springer.

Beer, M., Ferson, S., & Kreinovich, V. (2013). Imprecise probabilities in engineering analyses. *Mechanical Systems and Signal Processing, 37*, 4-29.

Bjornoy, O. H., Cramer, E. H., & Sigurdsson, G. (1997). Probabilistic calibrated design equation for burst strength assessment of corroded pipes. *The Seventh International Offshore and Polar Engineering Conference, Honolulu, USA, Vol. IV,* pp. 160-166.

Bijen, J. (2003). Durability of Engineering Structures: Design, Repair and Maintenance. CRC Press.

Bocchini, P., & Frangopol, D. M. (2011). Uncertainty modeling in bridge network maintenance optimization. *ASCE, Vulnerability, Uncertainty, and Risk ICVRAM and ISUMA 2011* pp. 897-904.

Bolzon, G., Boukharouba, T., Gabetta, G., Elboujdaini, M., & Mekki Mellas, M. (12 May 2011). Integrity of pipelines transporting hydrocarbons: Corrosion, mechanisms, control, and management. *Technology & Engineering.* Springer science & business media.

Bulleit, W. M. (2008). Uncertainty in structural engineering. CE database subject headings: Uncertainty principles; structural engineering; structural design; probability; standards and codes. DOI: 10.1061/ (ASCE) 1084-0680(2008)13:1(24).

Burns Statistics. http//www.burns-stats.com/ Burns Statistics

Caleyo, F., Gonzalez, J. L., & Hallen, J. M. (2002). A study on the reliability assessment methodology for pipelines with active corrosion defects. *International Journal of Pressure Vessels and Piping, 79*, 77-86.

Caleyo, F., Valor, A., Venegas, V., Hernandez, J. H. E., Velazquez, J. C., & Jose Manuel Hallen, J. M. (2012). Pipeline Integrity—1: Accurate corrosion modeling improves reliability estimations. . *Ogj, 10*.

Caleyo, F., Velázquez, J. C., Valor, A., & Hallen, J. M. (2009). Markov chain modelling of pitting corrosion in underground pipelines. *Corrosion Science, 51*(9), 2197-2207.

Canadian Standard Association (CSA). (2007). *CSA Z662-07: Oil and gas pipeline systems.*

Chambers, J., Cleveland, W., Kleiner, B., & Tukey, P. (1983). *Graphical methods for data analysis.* Wadsworth.

Cosham, A., Hopkins, P., & Macdonald, K. A. (2007). Best practice for the assessment of defects in pipelines. *Corrosions Engineering Failure Analysis,* (14), 1245-1265.

de Angelis, M., Patelli, E., & Beer, M. (2015). Advanced line sampling for efficient robust reliability analysis *Structural Safety, 52*, 170-182.

Dekker, R. (1996). Applications of maintenance optimization models: A review and analysis. *Reliability Engineering and System Safety, 51*, 229-240.

Dekker, R., & Scarf, P. A. (1998). On the impact of optimisatiom models in maintenance decision making: The state of the art. . *Reliability Engineering and System Safety, 60*, 111-119.

Deodatis, G., & Spanos, P. D. (Eds.). (2004). *Special issue: Fourth international conference on computational stochastic mechanics. Probab Eng Mech 2004; 19.*

Dhillon, B. S. (2002). *Engineering maintenance: A modern approach.* Boca Raton London New York Washington, D.C.: CRC Press.

Ditlevsen, O., & Madsen, H. O. (1996). *Structural reliability methods.* Wiley.

DNV. (1999). *Corroded pipelines. Recommended practice RP-101, det norske veritas.* Elendom AS.: Det Norske Veritas.

DOD budget: Potential reductions to operation and maintenance program, United States general accounting office, Washington, D.C., 1996.

Elber, W. (1970). Fatigue crack closure under cyclic tension. *Engng. Fract. Mech., 2*, 37-45.

Eldred, M. S., Swiler, L. P., & Tang, G. (2011). Mixed aleatory-epistemic uncertainty quantification with stochastic expansions and optimization-based interval estimation. *Reliability Engineering and System Safety, 96*, 1092-1113.

Enevoldsen, I., & Sorensen, J. D. (1994). Reliability-based optimization in structural engineering. *Structural Safety, 15*, 169-196.

Faber, O., Hartmann, D., Niemann, H. J., & Weber, H. (1999). Analysis of loading and damage processes and reliability estimation for lifespan-oriented structural optimization. *ESREL 1999, Proc. European Safety and Reliability Conf., Munich Germany, EU.* pp. 539-544.

Ferson, S. (2002). *RAMAS risk calc 4.0 software: Risk assessment with uncertain numbers.* Boca Raton, Florida: Lewis Publishers.

Ferson, S., & Hajagos, J. G. (2004). Arithmetic with uncertain numbers: Rigorous and (often) best possible answers. *Reliab. Eng. Syst. Saf., 85*(1-3), 135-152.

Ferson, S., Kreinovich, V., Ginzburg, L., Myers, D. S., & Sentz, K. (2003). *Constructing probability boxes and Dempster–Shafer structures.* Albuquerque, NM: Tech. Rep. SAND2002- 4015, Sandia National Laboratories.

Ferson, S., & Long, T. F. (1995). Conservative uncertainty propagation in environmental risk assessments. Environmental toxicology and risk assessment. In J. S. Hughes, G. R. Biddinger & E. Mones (Eds.), (Third Volume, ASTMSTP 1218 ed., pp. 97-110) American Society for Testing and Materials, Philadelphia.

Fisher, J. W., Yen, B. T., & Wang, D. (1989). *Fatigue of bridge structure: A commentary and guide for design, evaluation and investigation of cracking.* No. ATLSS Report No. 89-02). Lehigh University, Bethlehem, Pennsylvania.

FOCUS. *"FOCUS", September 2007, (FHWA-HRT-07-017)*

Forbes, C., Evans, M., Hastings, N., & Peacock, B. (2010.). *Statistical distributions.* Willey.

Forman, R. G., Kearney, V. E., & Engle, R. M. (1967). Numerical analysis of crack propagation in cyclic-loaded structures. *Journal of Basic Engineering, 89*, 459-464.

Forman, R. G., & Hu, T. (1984). Application of fracture mechanics on the space shuttle, damage tolerance of metallic structures. In J. B. Chang, & J. L. Rudd (Eds.), *Analysis methods and applications* (ASTM STP 482 ed.). West Conshohocken, Pennsylvania: American Society for testing and materials.

Forman, R. G., Shivakuman, V., Mettu, S. R., & Newman, J. C. (November 1998). *Fatigue crack growth computer program "NASGRO" version 3.00* (Reference manual, JSC-22267B ed.). Houston, Texas: NASA Johnson Space Centre.

Frangopol, D. M. (2010). Life-cycle performance, management, and optimization of structural systems under uncertainty: Accomplishments and challenges. *Structure and Infrastructure Engineering,* Taylor & Francis.

Gao, L., Xie, C., & Zhang, Z. (2010). Network-level multi-objective optimal maintenance and rehabilitation scheduling. *Proceedings of the 89th Annual Meeting of the Transportation Research Board of the National Academies, TRB, Washington, DC, USA.*

Garg, A., & Deshmukh, S. G. (2006). Applications and Case Studies maintenance management: Literature review and directions. *Journal of Quality in Maintenance Engineering, 12*(3), 205-238.

Gasser, M., & Schuëller, G. I. (1997). Reliability-based optimization of structural systems. *Mathematical Methods of Operations Research, 46*(3), 287-307.

Gnedenko, B. V., Belyaev, Y. K., & Solovyev. (1965). Mathematical methods in reliability theory. (in Russian)Moscow: Nauka. 524.

Gomes, W. J. S., & Beck, A. T. (2014). Optimal inspection and design of onshore pipelines under external corrosion process. *Structural Safety, 47*, 48-58.

Grandt, J. A. F. (2004). *Fundamentals of structural integrity: Damage tolerance design and non-destructive evaluation.* Hoboken, New Jersey: John Wiley & Sons, Inc.

Hong, H. P. (1997). Reliability analysis with non-destructive inspection. *Structural Safety, 19*(4), 383-395.

Hong, H. P. (1999). Inspection and maintenance planning of pipeline under external corrosion considering generation of new defects. *Structural Safety, 21*, 203-222.

Huyse, L. (2001). Solving problems of optimization under uncertainty as statistical decision problems. *42nd AIAA Structures, Structural Dynamics and Materials Conference*, Seattle, WA, April 16-19, 2001.

Irwin, G. R. (1957). Analysis of stresses and strains near the end of a crack traversing a plate. *Journal of Applied Mechanics, 24*, 361-364.

Joint Committee on Structural Safety. (2000). *PROBABILISTIC MODEL CODE part 1 - BASIS OF DESIGN. JCSS-OSTL/DIA/VROU -10-11-2000, 12th draft*

Kareem, A. (1990.). Reliability of wind-sensitive structures. *J Wind Eng Ind Aerod, 33*, 495.

Kareem, A. (1999). Analysis and modeling of wind effects: Numerical techniques. In L. Larson Livesey (Ed.), *Wind engineering into the 21st century*. Balkema, Rotter-dam.

Kelly, A. (1978). *Management of industrial maintenance.* London: Newnes-Butterworths.

Kelly, A. (1984). *Maintenance planning and control.* London: Butterworths & Co.

Khan, L. R., & Tee, K. F. (2016). Risk-cost optimization of buried pipelines using subset simulation. *J. Infrastructural System, American Society of Civil Engineers, 130*, 125-131.

Kiefener, J. F., Maxey, W. A., Eiber, R. J., & Duffy, A. R. (1973). Failure stress levels of flaws in pressurised cylinders. *Progress in flaw growth and fracture toughness testing* (ASTM STP 536 ed., pp. 461-481) American Society for testing and materials.

Kim, W. H., & Laird, C. (1978). Crack nucleation and state I propagation in high strain fatigue- II mechanism. *Acta Metallurgica.,* 789-799.

Kiureghian, A. D., & Ditlevsen, O. (2009). Aleatory or epistemic? Does it matter? *Struct Saf, 31*, 105-112.

Klever, F. J., & Stewart, G. (1995). New developments in burst strength predictions for locally corroded pipes. *Shell Int. Res.*

Kong, J. S., Frangopol, D. M. (2003). Evaluation of expected life-cycle maintenance cost of deteriorating structures. *J. Struct. Eng., 129*(5), 682-691.

Kothamasu, R., Huang, S. H., & VerDuin, W. H. (2006). System health monitoring and prognostics – A review of current paradigms and practices. *The International Journal of Advanced Manufacturing Technology, 28*(9), 1012-1024.

Koutsourelakis, P. S., Kuntiyawichai, K., & Schuëller, G. I. (2006). Effect of material uncertainties on fatigue life calculations of aircraft fuselages: A cohesive element model. *Engineering Fracture Mechanics, 73*(9), 1202-1219.

Kumar, U. D. (1999). New trends in aircraft reliability and maintenance measures**.** *Journal of Quality in Maintenance Engineering, 5*(4), 287-295.

Kuzbozhev, A. S., Birillo, E. N., Vishnevskaya, N. S., & Berdnik, M. M. (2013.). *Beam transitions. Methods of calculation and reconstruction of the pipeline operating stage: A tutorial.* Russia: Ukhta, UGTU.

Latino, C. J. (1999). *Hidden treasure: Eliminating chronic failures can cut maintenance costs up to 60%, report*. Virginia: Reliability Centre, Hopewell.

Lee, O. S., Kim, D. H., & Choi, S. S. (2006.). Reliability of buried pipeline using a theory of probability of failure. *Solid State Phenomena, 110*, 221-230.

Leis, N., & Stephens, D. R. (1997). An alternative approach to assess the integrity of corroded line pipe. Part I current status and II alternative criterion. *Proceedings of the Seventh International Offshore and Polar Engineering Conference.* pp. 624-641.

Lukic, M., & Cremona, C. (2001). Probabilistic assessment of welded joints versus fatigue and fracture. *Journal of Structural Engineering, 127*(2), 211-218.

Madsen, H. O., Krenk, S., & Lind, N. C. (1986). *Methods of structural safety.* Prentice-Hall.

Matsumura, T., & Haftka, R. T. (2013). Reliability based design optimization modelling future redesign with different epistemic uncertainty treatments. *ASME Journal of Mechanical Design, 135 / 091006-1.*

McNeill, D., & Freiberger, P. (1993). *Fuzzy logic*. New York: Simon & Schuster.

Melchers, R. E. (2005), statistical characterization of pitting corrosion - part 1: Review. *Corrosion, 61*, 655-665.

Melchers, R. E. (1987). *Structural reliability, analysis and prediction.* New York: John Wiley & Sons.

Melchers, R. E. (1999). *Structural reliability analysis and prediction.* (2nd ed.). West Sussex, England: John Wiley & Sons.

Moller, B., & Beer, M. (2008). Engineering computation under uncertainty – capabilities of non-traditional models. *Computers and Structures, 86*, 1024-1041.

Moore, R. E. (1979). *Methods and applications of interval analysis.* Philadelphia: Siam.

Mustaffa, Z. (2014). Developments in reliability-based assessment of corrosion. In M. Dr. Aliofkhazraei (Ed.), *Developments in corrosion protection, ISBN: 978-953-51-1223-5, InTech, DOI: 10.5772/57488, 2014.* InTech.

National Association of Corrosion Engineers (NACE) International. (2002).

Newman Jr., J. C. (1998). The merging of fatigue and fracture mechanics concepts: A historical perspective. *Progress in Aerospace Sciences, 34*, 347-390.

Opeyemi, D. A., Patelli, E., Beer, M., & Timashev, S. A. (2015a). Reliability of arctic pipelines taking into account the global change of temperatures: Wind loads case study. *International Conference on Economic and Technical Aspects of Safety of Civil Engineering Critical Infrastructures. Yekaterinburg, Russia.*

Opeyemi, D. A., Patelli, E., Beer, M., & Timashev, S. A. (2015b). Reliability assessments and remaining life of pipelines subject to combined loadings using imprecise probabilities. Safety and reliability of complex engineered systems – Podofilini et al. (eds). Taylor & Francis Group, London, ISBN 978-1-138-02879-1, pp. 2789 – 2796.

Paasch, R. K., & DePiero, A. H. (1999). *Final report SPR 380-fatigue crack modeling in bridge deck connection details*

Pandey, M. D. (1998). Probabilistic models for condition assessment of oil and gas pipelines. *NDT and E International, 31*, 349-358.

Paris, P., & Erdogan, F. (1963). A critical analysis of crack propagation laws. *Journal of Basic Engineering (Transactions of the ASME), 85*, 528-534.

Patelli, E. (2016). COSSAN: A multidisciplinary software suite for uncertainty quantification and risk management**.** In R. Ghanem, D. Higdon & H. Owhadi (Eds.), *Handbook of uncertainty quantification* (pp. 1-69) Springer International Publishing.

Patelli, E., Broggi, M., Angelis, M., & Beer, M. (2014). OpenCossan: An efficient open tool for dealing with epistemic and aleatory uncertainties. *Vulnerability, Uncertainty and Risk. American Society of Civil Engineers,* pp. 2564-2573.

Patelli, E., Panayirci, H., Broggi, M., Goller, B., Beaurepaire, P., & Pradlwarter, H., (2012). General purpose software for efficient uncertainty management of large finite element models. *Finite Elements in Analysis and Design, 51*, 31-48.

Pedrycz, W. (1994). Why triangular membership functions? *Fuzzy Sets and Systems, 64*, 21-30.

Peeta, S., Salman, F. S., Gunnec, D., & Viswanath, K. (2010). Pre-disaster investment decisions for strengthening a highway network. *Computers and Operations Research, Elsevier, 37*(10), 1708-1719.

Pipeline operators' forum. (2009). Specifications and requirements for intelligent pig inspection of pipelines.

Pradlwarter, H. J., Schueller, G. I., Koutsourelakis, P. S., & Charmpis, D. C. (2007). Application of line sampling simulation method to reliability benchmark problems. *Structural Safety, 29*(3), 208-221.

Qian, G., Niffenegger, M., & Li, S. (2011). Probabilistic analysis of pipelines with corrosion defects by using FITNET FFS procedure. *Corrosion Science, 53*, 855-861.

Race, J. M., Dawson, S. J., Stanley, L. M., & Kariyawasam, S. (2007). Development of a predictive model for pipeline external corrosion rates. *Journal of Pipeline Engineering, 6*(1), 15-29.

Rackwitz, R. (2001). Reliability Analysis – a review and some perspectives. *Structural Safety,* 23, 365–395.

Radaj, D., & Sonsino, C. M. (1998). *Fatigue assessment of welded joints by local approaches.* Abington, England: Abington Publishing.

Ramulu, M., & Kobayashi, A. S. (2012). *Numerical and experimental study of mixed mode fatigue crack propagation. Handbook of fatigue crack propagation in metallic structures. Ed*. Newness: A. Carpinteri.

Report by the working party on maintenance engineering, department of industry, London, 1970.

Report on infrastructure and logistics, department of defence, Washington, D.C., 1995.

Riane, F., Roux, O., Basile, O., & Dehombreux, P. Simulation based approaches for maintenance strategies optimization. *Maintenance, 2009.*

RosHydromet. (2008). Assessment Report on Climate Change and Its Consequences in Russian Federation: Climate Change Impacts. Moscow: Federal Service for Hydrometeorology and Environmental Monitoring (RosHydromet).

Roy, S., Grigory, S., Smith, M., Kanninen, M. F., & Anderson, M. (1997). Numerical simulations of full-scale corroded pipe tests with combined loading. *Journal of Pressure Vessel Technology, Vol. 119 / 457.*

Schenk, C. A., & Schueller, G. I. (2005). *Uncertainty assessment of large finite element systems.* Berlin/Heidelberg: Springer; 2005.

Schmitt, G., Schütze, M., Hays, G. F., Burns, W., Han, E., Pourbaix, A., et al. (2009). Global needs for knowledge dissemination, research, and development in materials deterioration and corrosion control. *WCO,*

Schuëller, G. I., Gasser, M., Hartl, J., & Lener, G. (2001). Practical design procedures using reliability based optimization. *International Journal of Advanced Manufacturing Systems, 4*(1), 101-120.

Schueller, G., & Spanos, P. (Eds.). (2001). *Proceedings of the international conference on Monte Carlo simulation MCS 2000. Monaco: Swets & zeitlinger; 2001.*

SNIP 2.05.06-85*. (2000). *Building codes and regulations, Russian federation: Main pipelines: Approved by the USSR state 01.01.86.* . Moscow, Russia: Federal State Unitary Enterprise, Center of Design Products.

Sørensen, J. D. (2004). *Notes in structural reliability theory and risk analysis.* Aalborg:

SP 20.13330.2011. *Loads and effects. The updated edition of SNiP 2.01.07-85 *.*

Spangler, M. G., & Handy, R. L. (1982). *Soil engineering*. (4th ed.), Harper & Row, New York.

Staat, M. (1993). Sensitivity of and influences on the reliability of an HTR-module primary circuit pressure boundary. *Trans. 12th International Conference on Structural Mechanics in Reactor Tech., Vol. M. Amsterdam,*

Stamatis, D. H. (1995). *Failure mode and effect analysis: FMEA from theory to execution.* Milwaukee, Wisconsin: ASQC Quality Press.

Standard Recommended Practice RP 0169-92. (1992). *Control of external corrosion on underground or submerged metallic piping systems.* Houston: NACE.

Stangenberg, F., Breitenbücher, R., Bruhns, O. T., Hartmann, D., Hffer, R., Kuhl, D., et al (Eds.). (2009). *Lifetime-oriented structural design concepts.* Berlin, Heidelberg: Springer.

STO Gazprom 2-2.3-112-2007. (2007). *Guidelines for the assessment of the bearing capacity of pipeline sections with corrosion defects.* LLC "VNIIGAZ", LLC "Gazprom".

Su, C., & Zheng, C. (2013). Crack growth-based fatigue life prediction using spline fictitious boundary element method. *13th International Conference on Fracture, Beijing, China,*

Thoft-Christensen, P., & Baker, M. J. (1982). *Structural reliability theory and its applications.* Springer Verlag.

Timashev, S. A. (1982). *Reliability of large mechanical systems***.** Moscow: Nauka.

Timashev, S. A., & Bushinskaya, A. V. (2010). Practical methodology of preventive maintenance for pipelines. . *Proceedings of the 8th International Pipeline Conference, IPC2010, Calgary, Alberta, Canada. IPC2010-31197,* (IPC2010-31197)

Toorn, A. V. (1992). The maintenance of civil engineering structures, 2.pdf. Available at heronjournal.nl/39-2/2.pdf

Valdebenito, M. A., & Schuëller, G. I. (2010). Design of maintenance schedules for fatigue-prone metallic components using reliability-based optimization. *Computer Methods in Applied Mechanics and Engineering, 199*, 2305-2318.

Valor, A., Caleyo, F., Hallen, J. M., & Velazquez, J. C. (2012). Reliability assessment. *Ogj, 10*

Vasilyev, G. G., Kulikov, A. N., & Zemenkov, Y. U. D. (2007). *Operation of the equipment and gas industry facilities. In 2 volumes. Tutorial, 2007. 1216 p.*

Velazquez, J.C., Caleyo, F., Hallen, J.M., Romero-Mercado, O., & Herrera-Hernández, H. (2013). Probabilistic Analysis of Different Methods Used to Compute the Failure Pressure of Corroded Steel Pipelines. Int. J. Electrochem. Sci., 8, 11356 – 11370.

Viscusi, W. K., & Aldy, J. E. (2003). The value of a statistical life: A critical review of market estimates throughout the world. *J. Risk and Uncertainty*, 27, 5–76.

Walker, K. (1970). The effect of stress ratio during crack propagation and fatigue for 2024-T3 and 7075-T6 aluminum. *Astm Stp, 462*, 1-14.

Walley, P. (1991.). *Statistical reasoning with imprecise probabilities.* London. Chapman & Hall.

Wang, L. & Kareem, A. (2004). Modeling of nonstationary winds in gust-fronts. *9th ASCE Specialty Conference on Probabilistic Mechanics and Structural Reliability, PMC2004,* pp. 1-6.

Wang, L., Brust, F. W., & Atluri, S. N. (1997). The elastic-plastic finite element alternating method (EPFEAM) and the prediction of fracture under WFD conditions in aircraft structures, part I: EPFEAM theory. *Computational Mechanics, 19*(5), 356-369.

WeatherSpark. (2015). https://weatherspark.com/daily/28884/ Svalbard

Wen, Y. K. (2001). Minimum lifecycle cost design under multiple hazards. *Reliab. Eng. Syst. Saf.,* 73, 223–231.

Youn, B. D., Choi, K. K., & Park, Y. H. (2003). Hybrid analysis method for reliability-based design optimization. *ASME J. Mech. Des., 125*(2), 221-232.

Yu, X., Chang, K. H., & Choi, K. K. (1998). Probabilistic structural durability prediction. *Aiaa j., 36*(4), 628-637.

Zadeh, L. A. (1965). Fuzzy sets. *Information and Control, 8*, 338-353.

Zang, T.A., Hemsch, M.J., Hilburger, M.W., Kenny, S.P., Luckring, J.M., Maghami P., Padula, S.L., & Stroud, W.J. (2002). Needs and opportunities for uncertainty-based multidisciplinary design methods for Aerospace vehicles," NASA/TM-2002-211462.

Zhang, H., Mullen, R. L., & Muhanna, R. L. (2010). Interval Monte Carlo methods for structural reliability. *Structural Safety, 32*, 183-190.

Zheng, R., & Ellingwood, B. (1998). Role of non-destructive evaluation in time-dependent reliability analysis. *Structural Safety, 20*(4), 325-339.

Zhou, W., & Nessim, M. A. (2011). Optimal design of onshore natural gas pipelines. *Journal of Pressure Vessel Technology,* 133, 1-11.

Zhou, J., Rothwell, B., Zhou, W., & Nessim, M. (2006). Application of high-grade steels to onshore natural gas pipelines using reliability-based design method. *Proceedings of IPC2006, Sixth International Pipeline Conference*, ASME, Calgary, AB, Canada, Paper No. IPC2006-10058.

Zhou, W. (2010). System reliability of corroded pipelines. *International Journal of Pressure Vessels and Piping,* 87, 587-595.

List of Publications

Journal Papers

- **David Opeyemi**, Edoardo Patelli, Michael Beer and Sviatoslav Timashev: Imprecise Probabilistic Analysis and Robust Maintenance Strategies for Corroded Pipelines (submitted for review in International Journal of Pressure Vessels and Piping).
- **David Opeyemi**, Edoardo Patelli, Michael Beer, Bushinskaya A.V., and Sviatoslav Timashev: Reliability of Arctic Pipelines in the Space of Loads (submitted for review in Journal of Offshore Mechanics and Arctic Engineering).

Conference Papers

- **David Opeyemi**, Edoardo Patelli and Michael Beer (2014). Optimal Maintenance Strategy for Metallic Structures with Vague Information. ASCE-ICVRAM-ISUMA 2014: Second International Conference on Vulnerability and Risk Analysis and Management (ICVRAM 2014) & Sixth International Symposium on Uncertainty Modelling and Analysis (ISUMA 2014), 13^{th} – 16^{th} July 2014, University of Liverpool, Liverpool, UK.
- **Opeyemi D.A.,** Patelli E., Beer M. and Timashev S. A. (2015). Reliability of Arctic Pipelines Taking into Account the Global Change of Temperatures: Wind Loads Case Study. International Conference on Economic and Technical Aspects of Safety of Civil Engineering Critical Infrastructures, June 10-11, 2015, Ekaterinburg, Russia.
- **David A. Opeyemi**, Edoardo Patelli, Michael Beer and Sviatoslav A. Timashev. (2015). Comparative Studies on Assessment of Corrosion Rates in Pipelines as Semi-Probabilistic and Fully Stochastic Values.12th International

Conference on Applications of Statistics and Probability in Civil Engineering (ICASP12), Vancouver, Canada, July 12-15, 2015.

- **David Opeyemi**, Edoardo Patelli, Michael Beer and Sviatoslav Timashev. (2015). Reliability assessments and remaining life of pipelines subject to combined loadings using imprecise probabilities. 25th European Safety and Reliability Conference (ESREL 2015), 7^{th} – 10^{th} Sept., 2015, Zurich, Switzerland.
- **Opeyemi D. A**., Timashev S., Bushinskaya A., Patelli E. and Beer M. (2016). Method of Reliability Assessment of Arctic Pipelines in the Space of Loads. International Conference on Safety Problems of Civil Engineering Critical Infrastructures (SAFETY2016), 26-27 May 2016, Ekaterinburg, Russia.
- **D. A. Opeyemi**, E. Patelli, M. de Angelis, M. Beer and S.A. Timashev. (2016). Reliability-Based Optimization of the Inspection Time Interval for Corroded Pipelines. 6^{th} Asian-Pacific Symposium on Structural Reliability and its Applications, 28-30 May 2016, Shanghai, China.
- Timashev S.A., Bushinskaya A.V., **Opeyemi D**, Patelli E. and Beer M. (2016). Method of Two-sided Reliability Assessment of Arctic Pipelines in the Loads Space. Safety of Critical Infrastructures and Territories: VII All Russia Conference and XVII School of Young Scientists/Conference Proceedings and Abstracts. Yekaterinburg, Ural Branch Russian Academy of Sciences, 2016.
- Bushinskaya A.V., **Opeyemi D**, Timashev S.A., Patelli E. and Beer M. The Two-sided Estimate of the Reliability of Arctic Pipelines in the Space of Loads. 12th International Conference on Structural Safety and Reliability, ICOSSAR 2017, Vienna, Austria, August 6-10, 2017 (submitted).

Appendices

Appendix A

Table A-1.1: Summary of unit cost (Zhou and Nessim, 2011)

Cost item	Unit	Cost (CAD$)[a]	Reference
Bare pipe	$/tonne	1400	Zhou, et al. (2006)
Transportation and double-jointing	% bare pipe cost	66	
Welding		20	
In-line inspection	$/km	4000	
Corrosion defect excavation	$/defect	50,000	
Corrosion defect repair		5000	
Fatality	$/fatality	5,962,000[b]	Viscusi, et al. (2003)
Injury	$/injury	20,000[b]	
Property damage due to rupture-ignition	$/rupture	1,787,700	DOT database
Property damage due to rupture-no ignition	$/rupture	514,300	
Property damage due to large leak	$/large leak	457,800[b]	
Discount rate	%	5.0	Wen, 2001

[a]All absolute costs are in terms of 2006 Canadian dollars (CAD$).

[b]Costs that were originally given in US$ at years other than 2006 were converted to 2006 CAD$ by assuming an annual inflation rate of 2.0% and an exchange rate of 1.00 CAD$=0.85 US$.

Appendix A- 2.

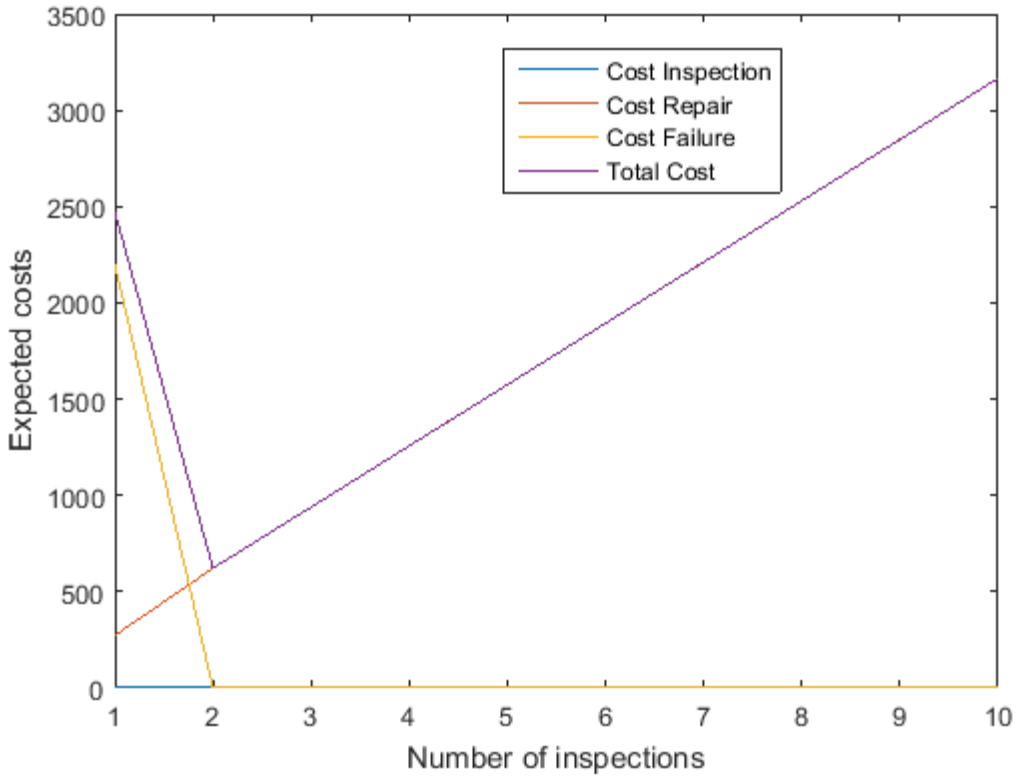

Figure A-2.1: Expected cost as a function of the number of inspections - considering 1 to 10 inspections in 20 years (Shell-92 model)

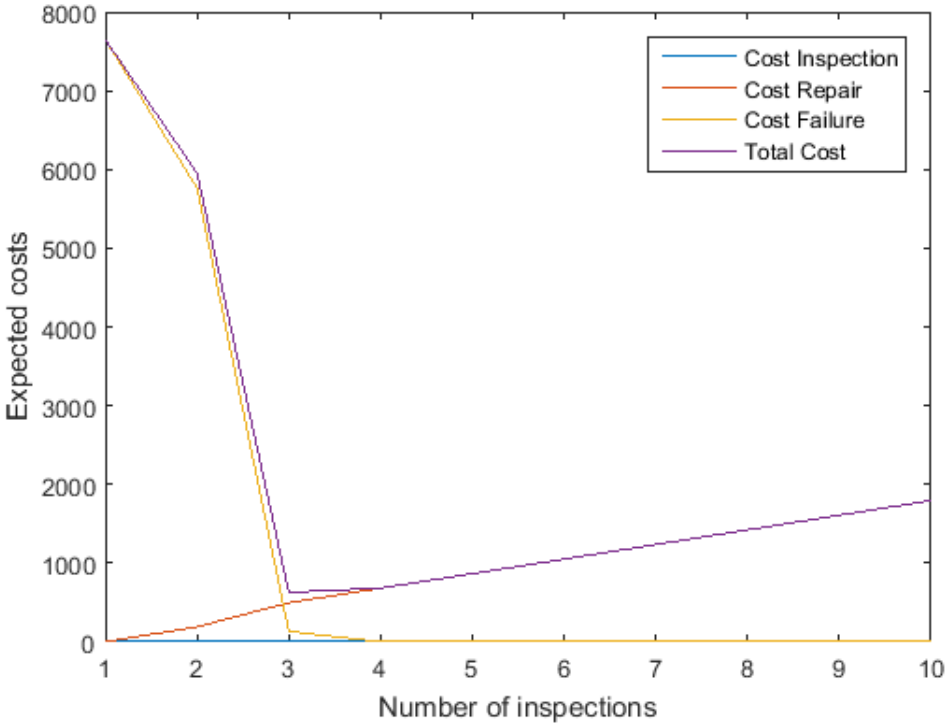

Figure A-2.2: Expected cost as a function of the number of inspections - considering 1 to 10 inspections in 50 years (Shell-92 model)

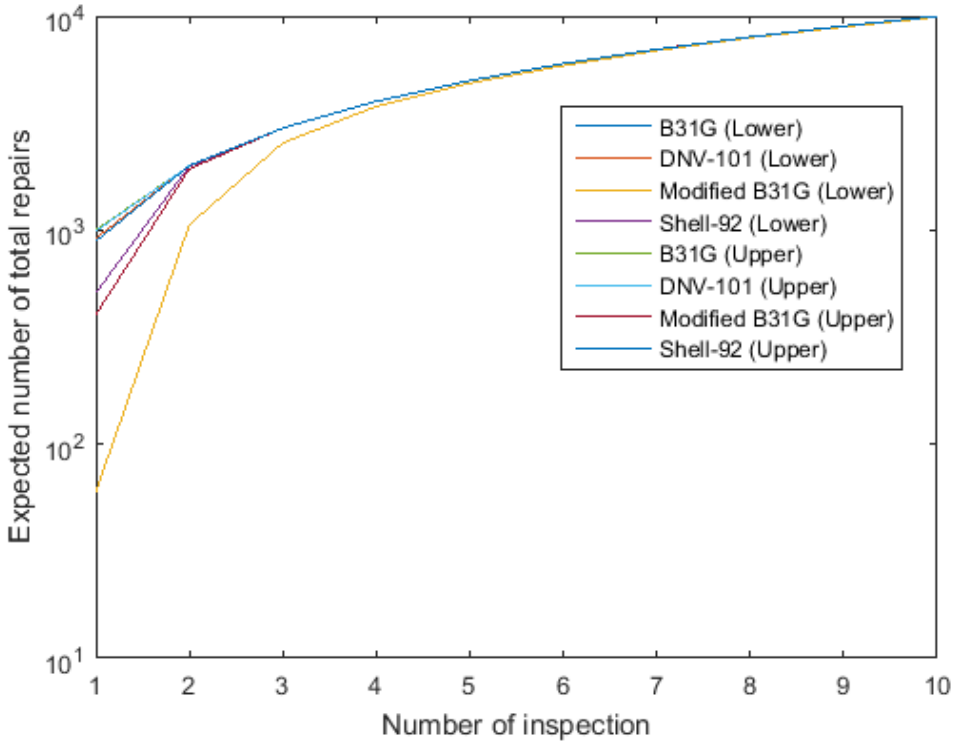

Figure A-2.3: Expected number of total repairs as a function of the number of inspections - considering 1 to 10 inspections in 20 years (B31G, DNV-101, Modified B31G & Shell-92 models)

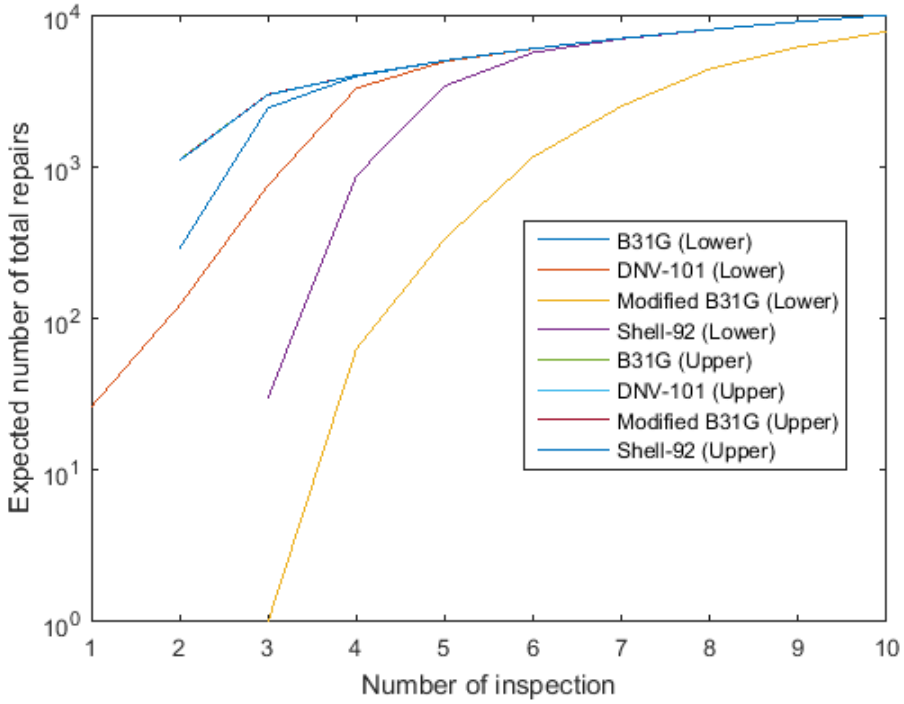

Figure A-2.4: Expected number of total repairs as a function of the number of inspections - considering 1 to 10 inspections in 50 years (B31G, DNV-101, Modified B31G & Shell-92 models)

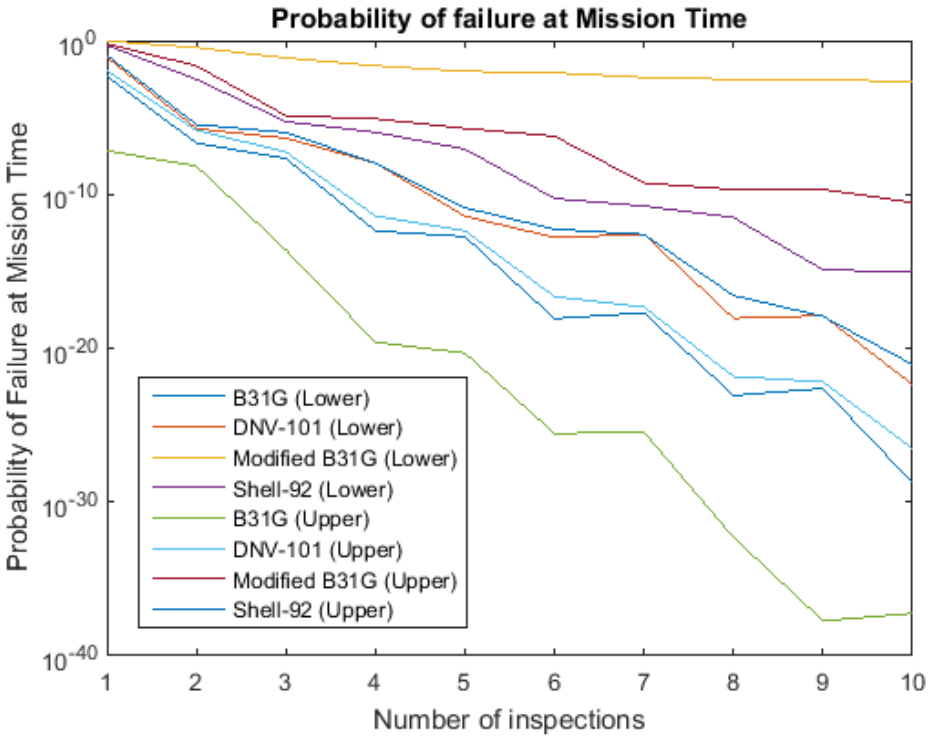

Figure A-2.5: Probability of failure at mission time as a function of the number of inspections - considering 1 to 10 inspections in 20 years (B31G, DNV-101, Modified B31G & Shell-92 models)

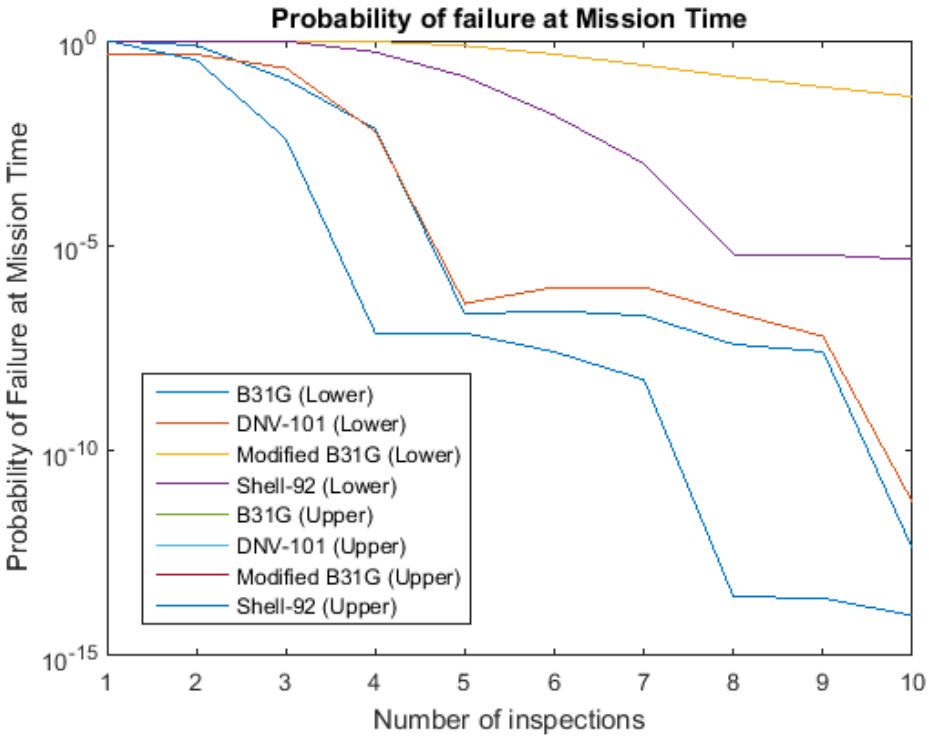

Figure A-2.6: Probability of failure at mission time as a function of the number of inspections - considering 1 to 10 inspections in 50 years (B31G, DNV-101, Modified B31G & Shell-92 models)

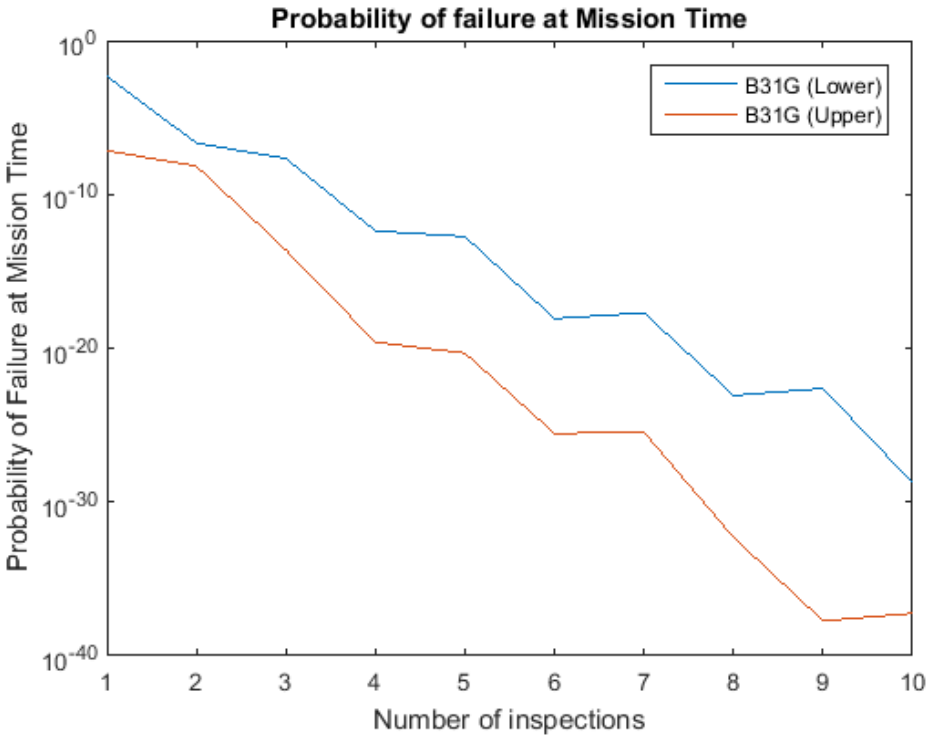

Figure A-2.7: Probability of failure at mission time as a function of the number of inspections - considering 1 to 10 inspections in 20 years (B31G model)

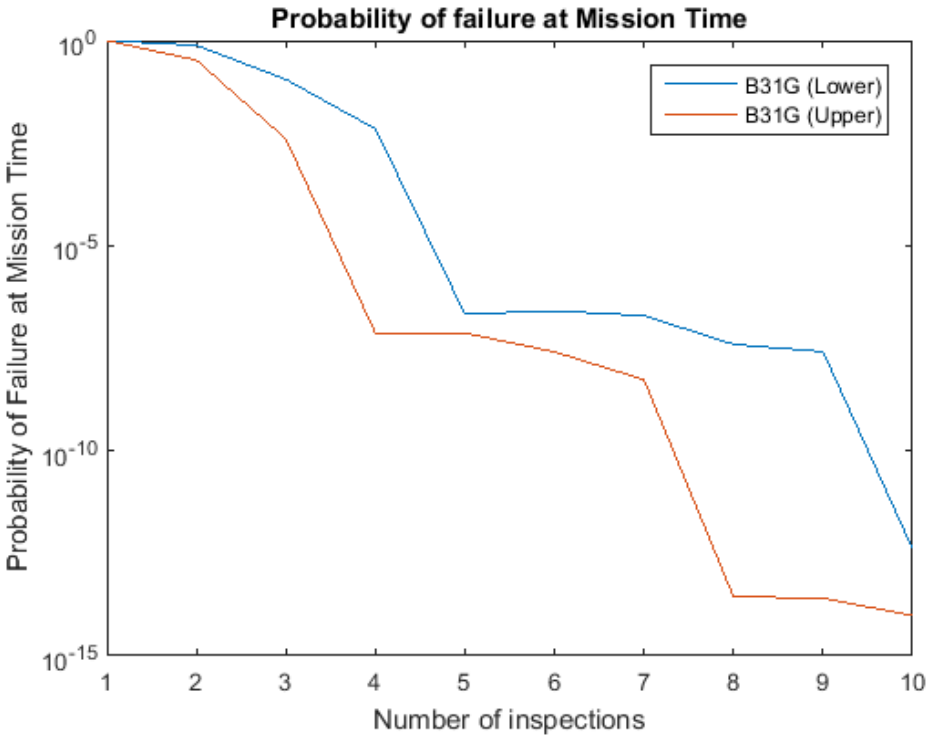

Figure A-2.8: Probability of failure at mission time as a function of the number of inspections - considering 1 to 10 inspections in 50 years (B31G model)

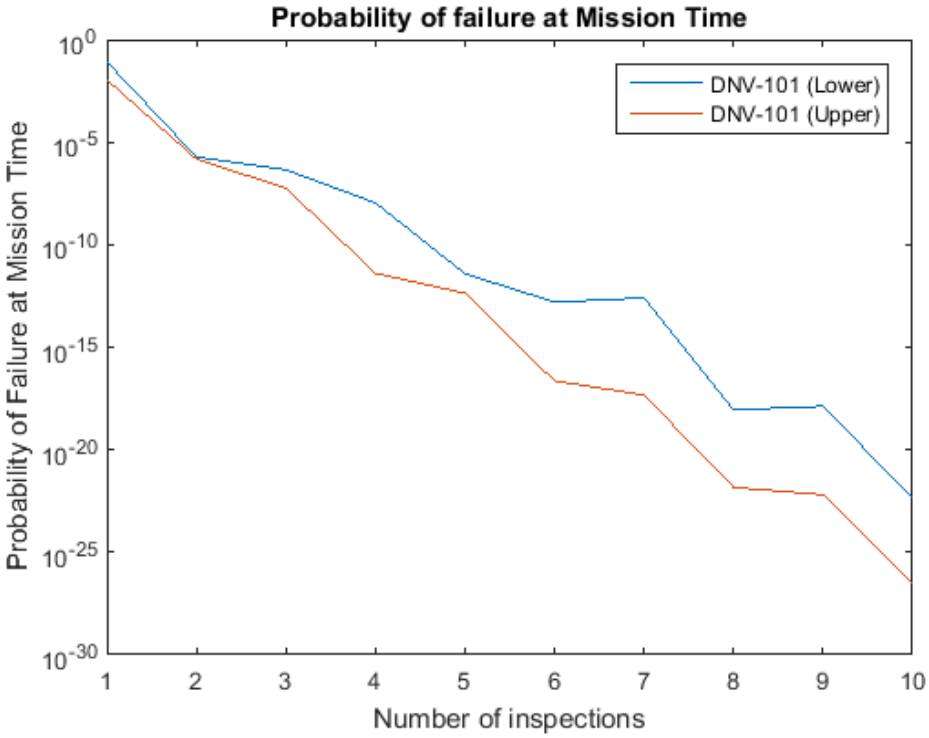

Figure A-2.9: Probability of failure at mission time as a function of the number of

inspections - considering 1 to 10 inspections in 20 years (DNV-101 model)

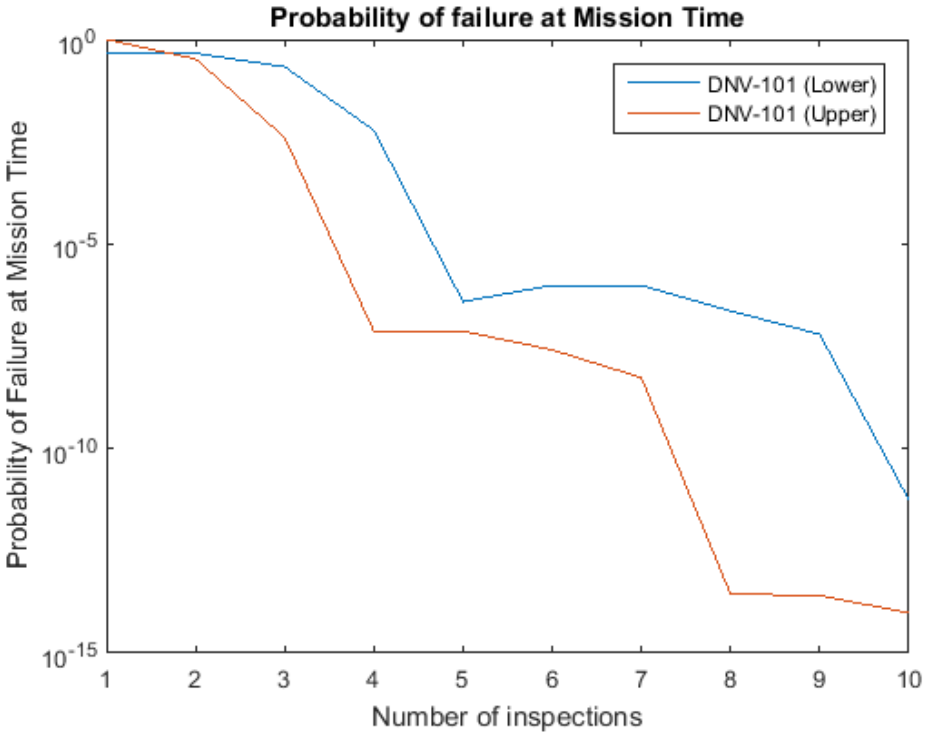

Figure A-2.10: Probability of failure at mission time as a function of the number of inspections - considering 1 to 10 inspections in 50 years (DNV-101 model)

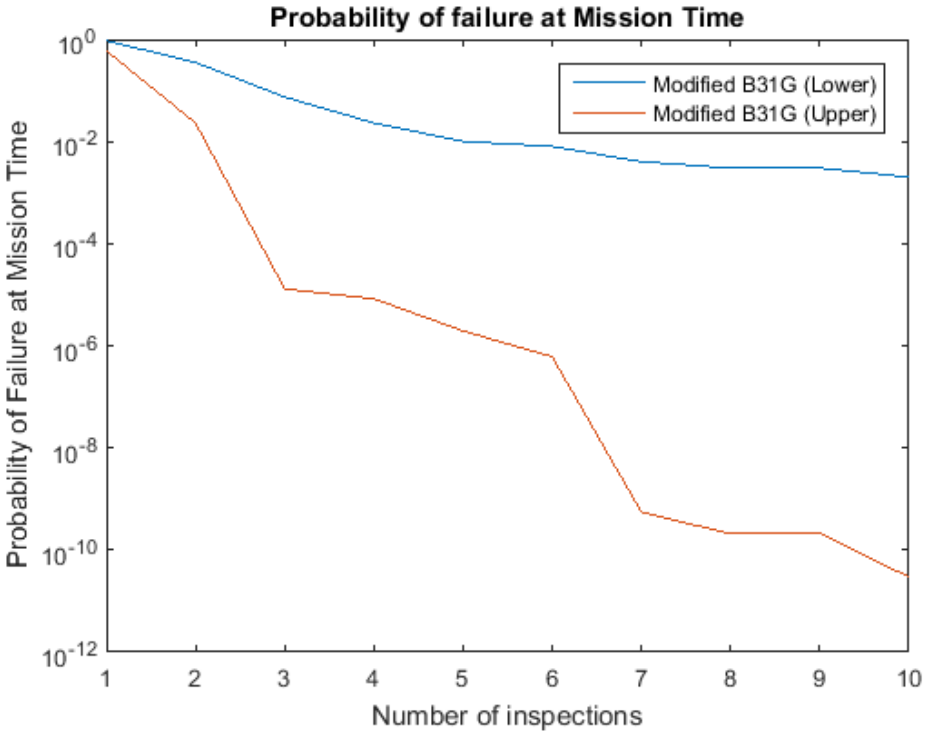

Figure A-2.11: Probability of failure at mission time as a function of the number of inspections - considering 1 to 10 inspections in 20 years (Modified B31G model)

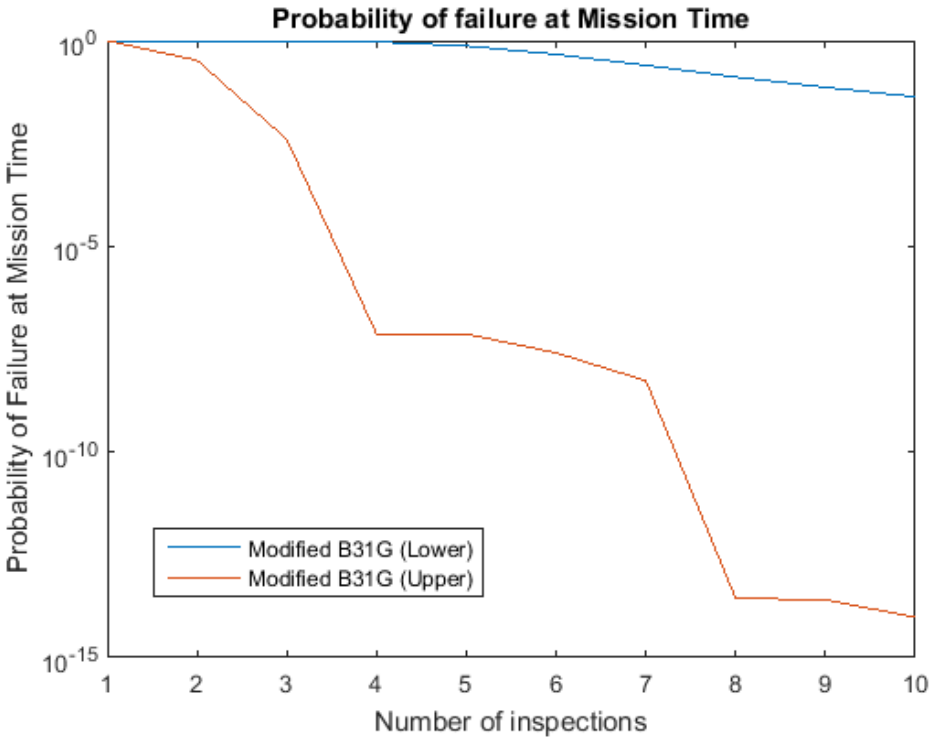

Figure A-2.12: Probability of failure at mission time as a function of the number of inspections - considering 1 to 10 inspections in 50 years (Modified B31G model)

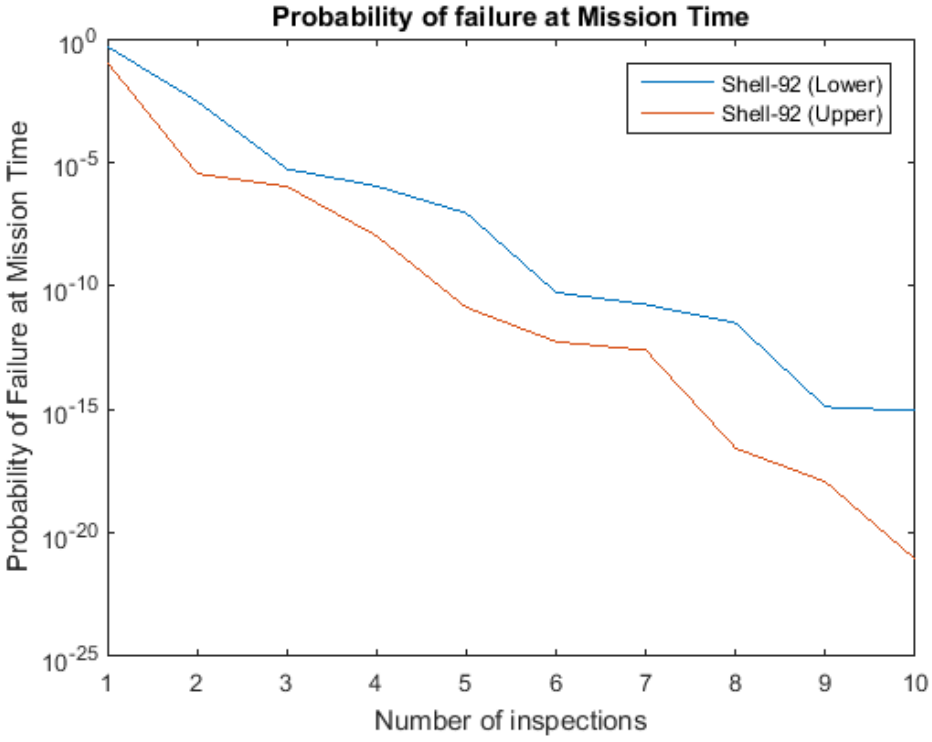

Figure A-2.13: Probability of failure at mission time as a function of the number of inspections - considering 1 to 10 inspections in 20 years (Shell-92 model)

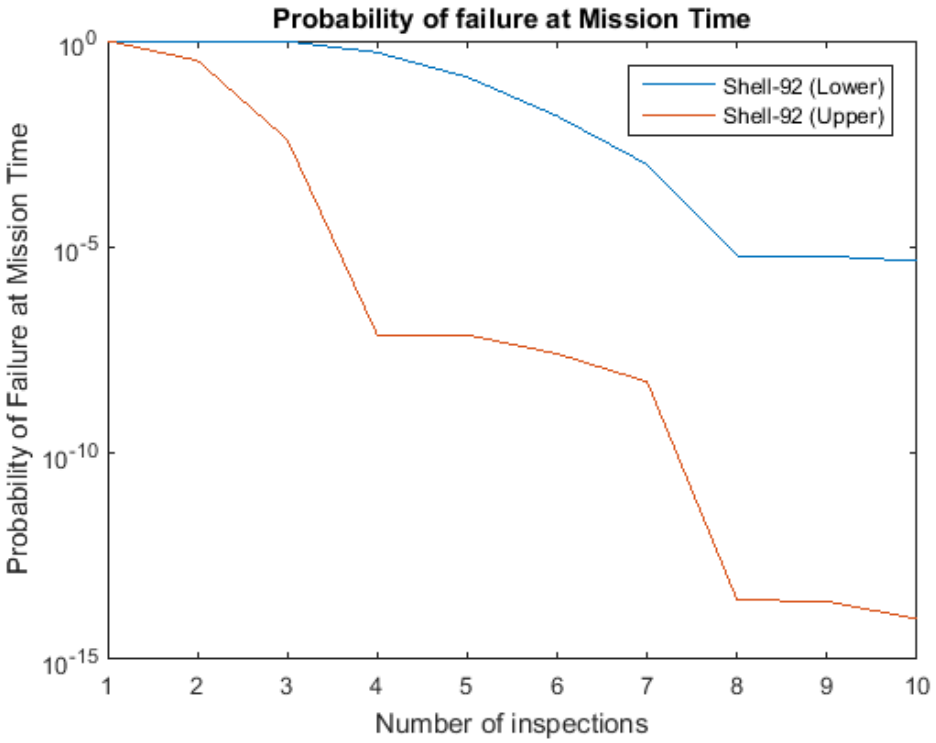

Figure A-2.14: Probability of failure at mission time as a function of the number of inspections - considering 1 to 10 inspections in 50 years (Shell-92 model)

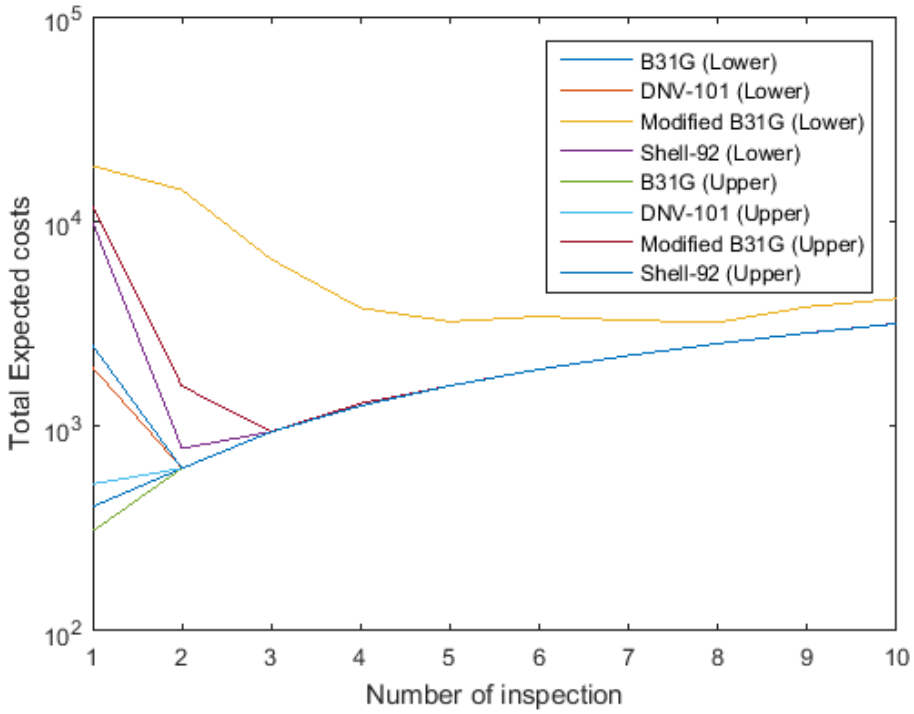

Figure A-2.15: Total expected cost as a function of the number of inspections - considering 1 to 10 inspections in 20 years (B31G, DNV-101, Modified B31G & Shell-92 models)

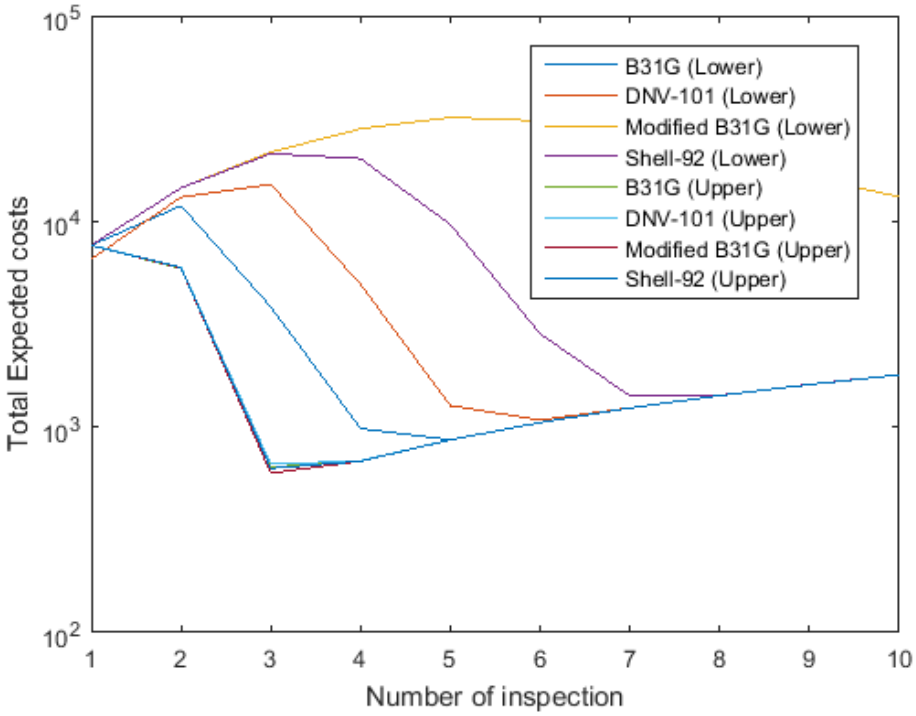

Figure A-2.16: Total expected cost as a function of the number of inspections - considering 1 to 10 inspections in 50 years (B31G, DNV-101, Modified B31G & Shell-92 models)

Appendix B

Wind data - Svalbard, Norway and Kotlas, Russia (WeatherSpark, 2015).

Table B-1: Maximum annual wind speed, m/s

Year	Svalbard, Norway	Kotlas, Russia
1950	unavailable or unreliable	9.003
1951	"	7.889
1952	"	7.526
1953	"	8.397
1954	"	7.683
1955	"	7.687
1956	"	6.11
1957	"	6.994
1958	"	5.97
1959	"	7.265
1960	"	7.077
1961	"	7.045
1962	"	7.04
1963	"	5.972
1964	"	6.817
1965	"	6.623
1966	"	6.25
1967	"	6.417
1968	"	6.538
1969	"	5.665
1970	"	7.042
1971	"	7.102
1972	"	7.462
1973	"	7.774
1974	"	10.258
1975	"	8.700
1976	"	8.581
1977	"	6.935
1978	"	8.409
1979	"	8.731
1980	"	6.724
1981	"	6.681
1982	"	6.269
1983	"	6.681
1984	"	6.889
1985	"	6.849
1986	"	7.387
1987	"	6.022
1988	"	6.600
1989	"	6.714
1990	17.467	6.032
1991	27.8	6.301

1992	22.6	6.183
1993	20.867	6.357
1994	21.6	6.14
1995	19.5	5.643
1996	25.7	5.678
1997	25.7	5.822
1998	20.6	5.065
1999	23.6	5.567
2000	19.5	5.581
2001	19.5	5.355
2002	19.0	6.301
2003	18.5	5.645
2004	22.6	5.433
2005	21.0	5.774
2006	25.0	5.323
2007	21.0	5.699
2008	19.549	5.156
2009	18.5	5.111
2010	20.6	5.473
2011	23.0	5.839
2012	19.0	5.011
2013	17.49	4.935
2014	19.03	5.086

Kotlas

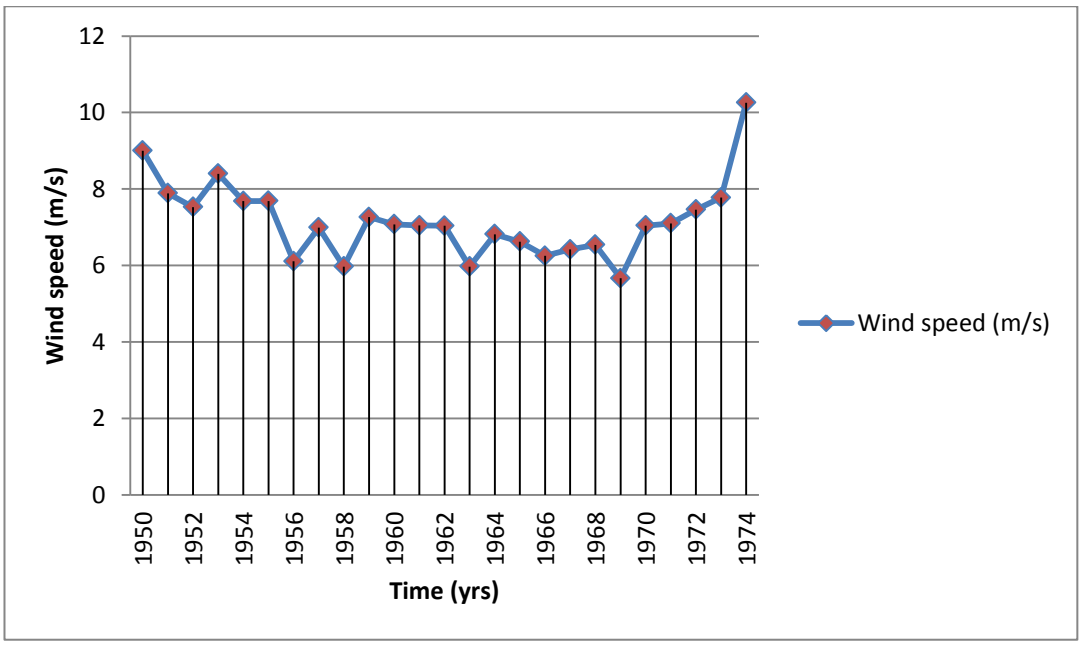

Figure B-1: Maximum measured wind speed over a period of 25 years - Kotlas, 1950 – 1974 (WeatherSpark, 2015)

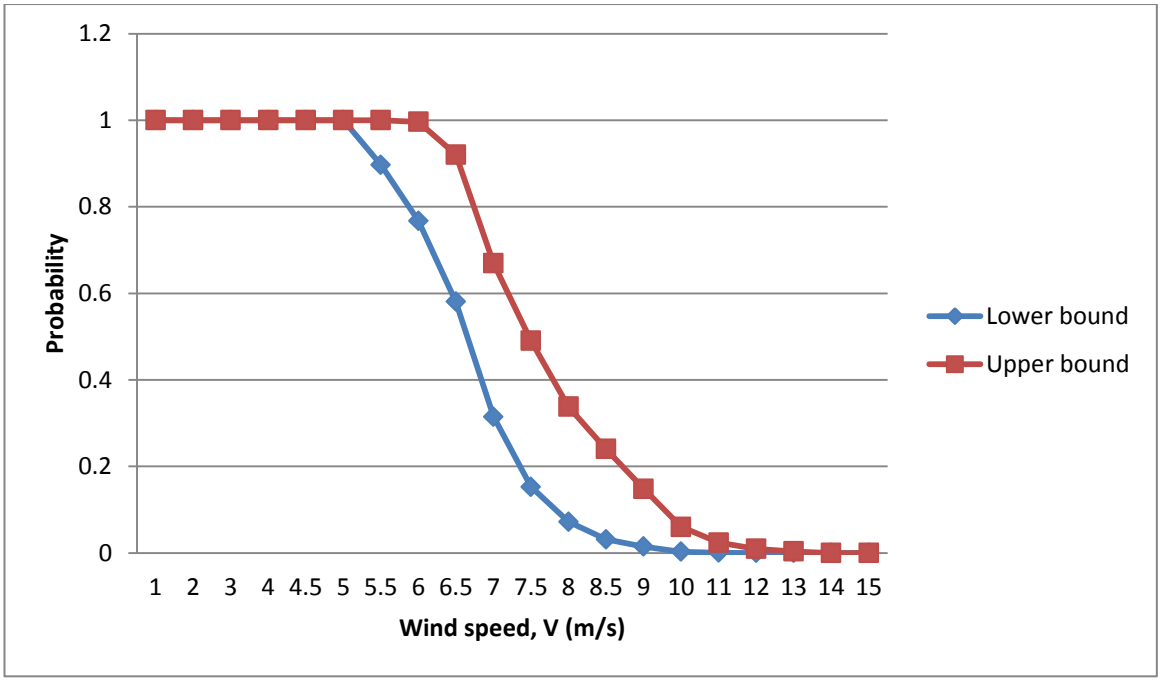

Figure B-2: Probability box for wind speed - Kotlas, 1950 – 1974 (WeatherSpark, 2015)

Table B-2: Wind speed data uncertainty characterization - Kotlas, 1950 – 1974 (WeatherSpark, 2015)

Wind speed (m/s)	Probabilities		Percentile
	Lower bound	**Upper bound**	**Level**
1	1.0000	1.0000	100
2	1.0000	1.0000	100
3	1.0000	1.0000	100
4	1.0000	1.0000	100
4.5	1.0000	1.0000	100
5	1.0000	1.0000	100
5.5	0.8970	1.0000	90 - 100
6	0.7674	0.9963	77 – 100
6.5	0.5805	0.9204	58 - 92
7	0.3147	0.6693	31 – 67
7.5	0.1527	0.4903	15 - 49
8	0.0721	0.3378	7- 34
8.5	0.0311	0.2402	3 - 24
9	0.0147	0.1480	1 - 15
10	0.0029	0.0603	0 - 6
11	0.0006	0.0239	0 - 2
12	0.0000	0.0093	0 - 1
13	0.0000	0.0036	0
14	0.0000	0.0000	0
15	0.0000	0.0000	0

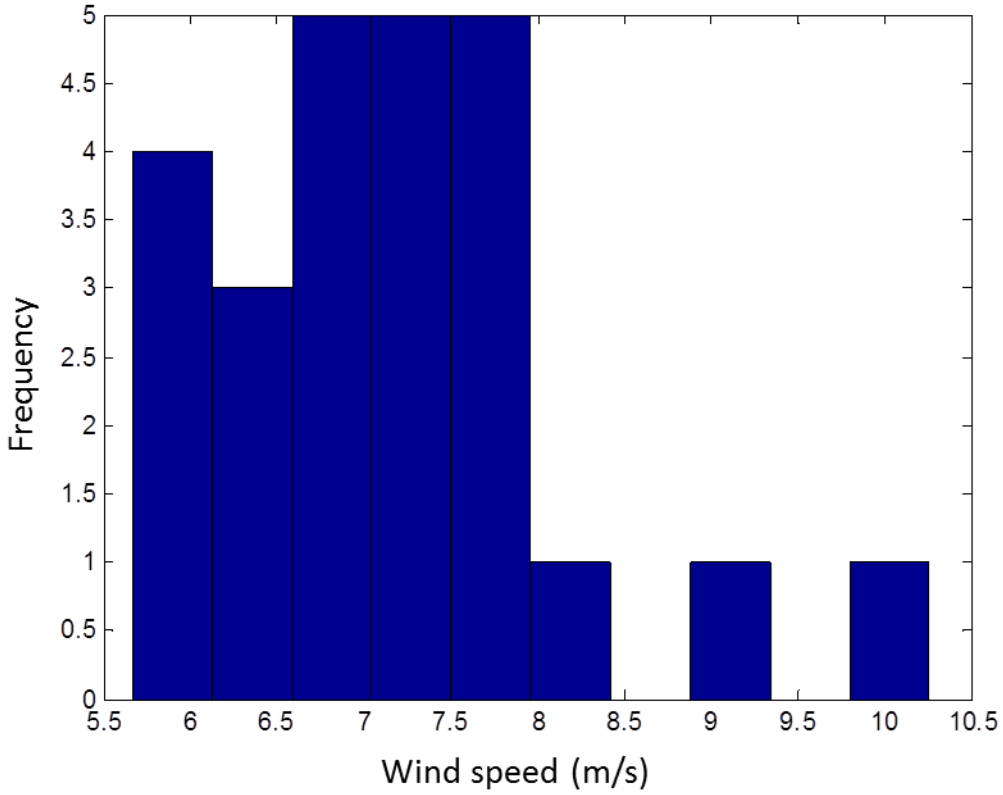

Figure B-3: Histogram - Kotlas 1950 –1974 (WeatherSpark, 2015)

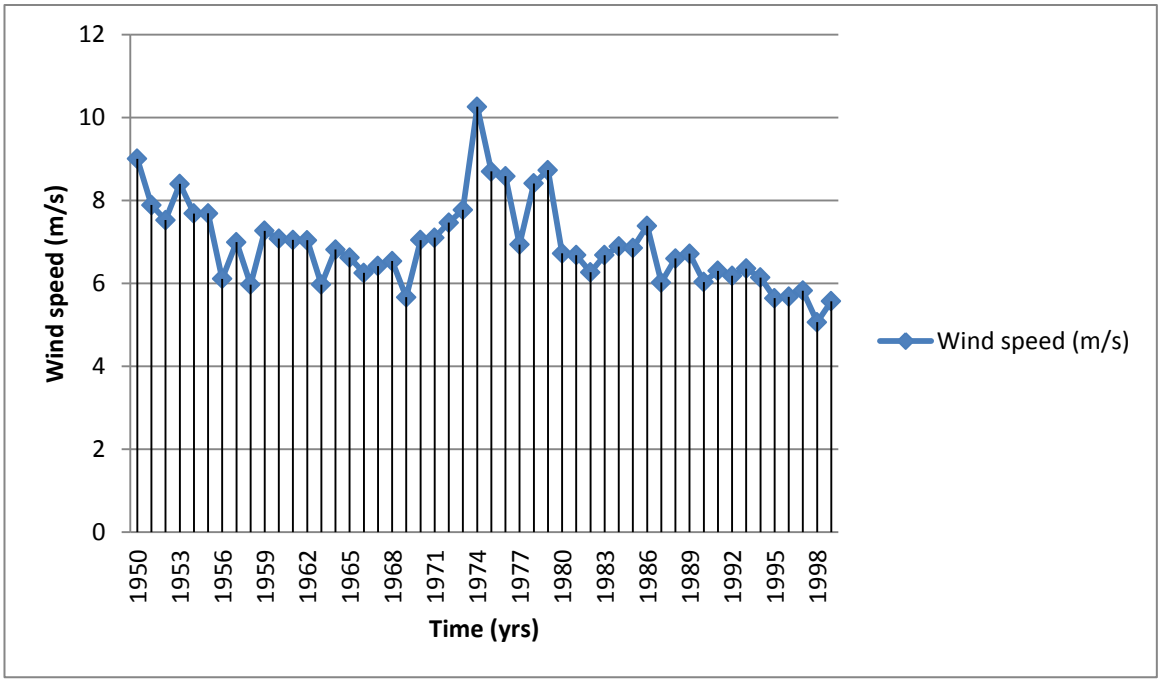

Figure B-4: Maximum measured wind speed over a period of 25 years - Kotlas, 1950 – 1999 (WeatherSpark, 2015)

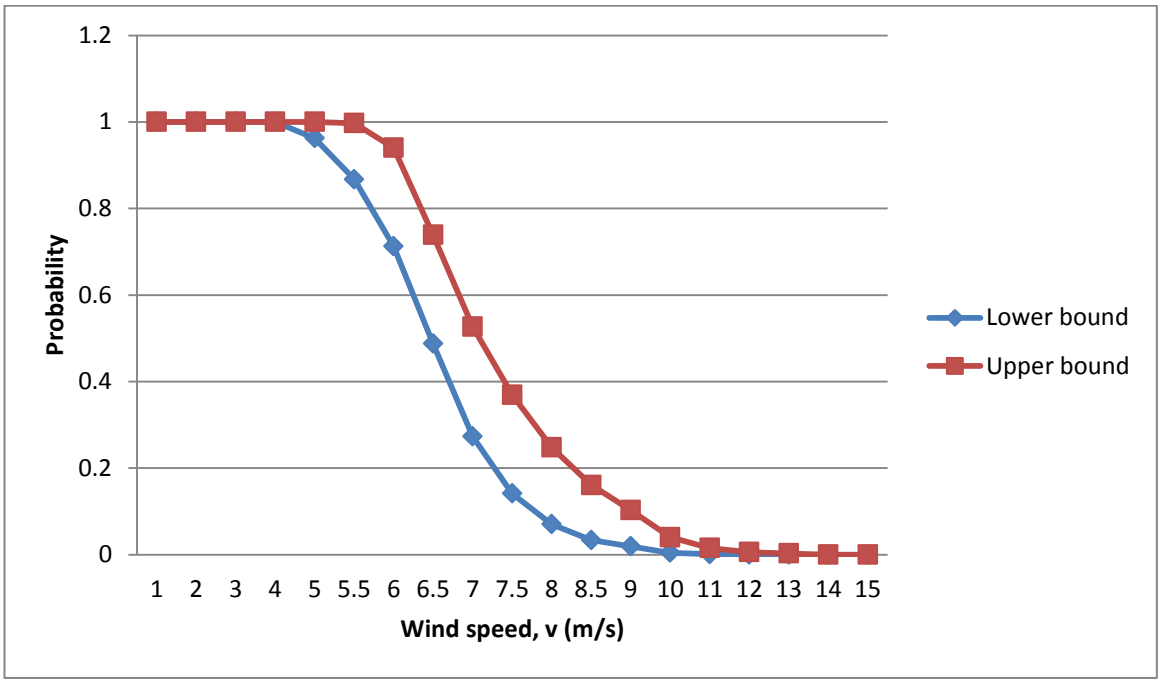

Figure B-5: Probability box for wind speed - Kotlas, 1950 – 1999 (WeatherSpark, 2015)

Table B-3: Wind speed data uncertainty characterization - Kotlas, 1950 –1999 (WeatherSpark, 2015)

Wind speed (m/s)	Probabilities		Percentile
	Lower bound	**Upper bound**	**Level**
1	1.0000	1.0000	100
2	1.0000	1.0000	100
3	1.0000	1.0000	100
4	1.0000	1.0000	100
5	0.9622	1.0000	96 – 100
5.5	0.8674	0.9972	87 – 100
6	0.7123	0.9400	71 -94
6.5	0.4873	0.7389	49 -74
7	0.2730	0.5265	28 -53
7.5	0.1411	0.3694	14 – 37
8	0.0700	0.2475	7 – 25
8.5	0.0334	0.1608	3 – 16
9	0.0190	0.1025	2 – 10
10	0.0044	0.0403	0 – 4
11	0.0009	0.0155	0 – 2
12	0.0000	0.0059	0 - 1
13	0.0000	0.0029	0
14	0.0000	0.0000	0
15	0.0000	0.0000	0

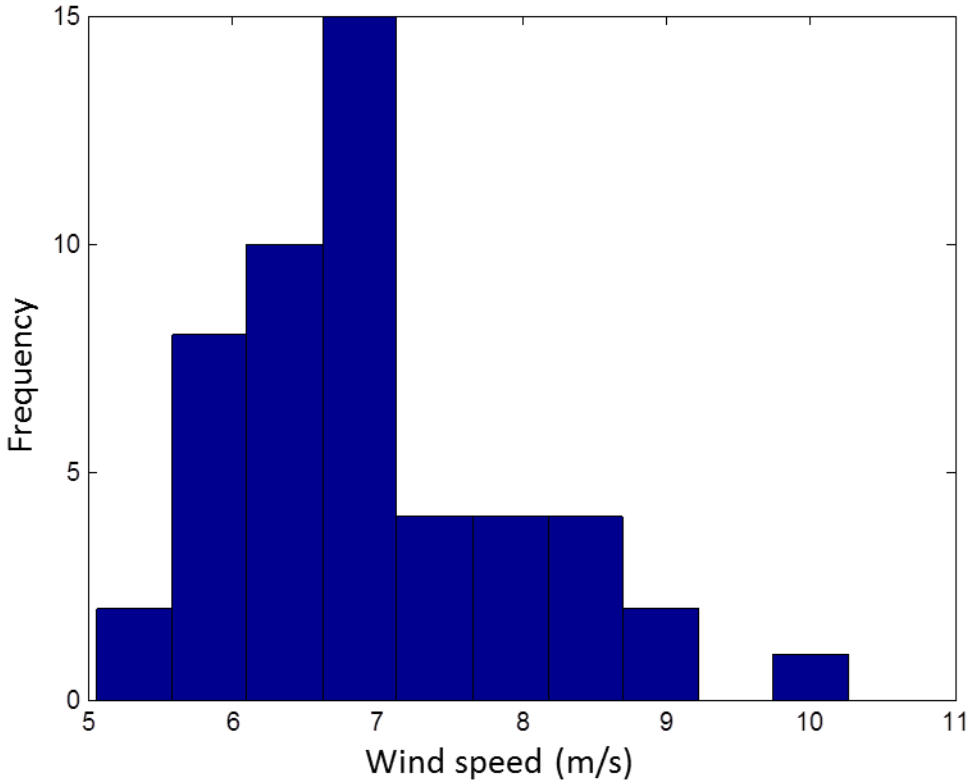

Figure B-6: Histogram – Kotlas, 1950 –1999 (WeatherSpark, 2015)

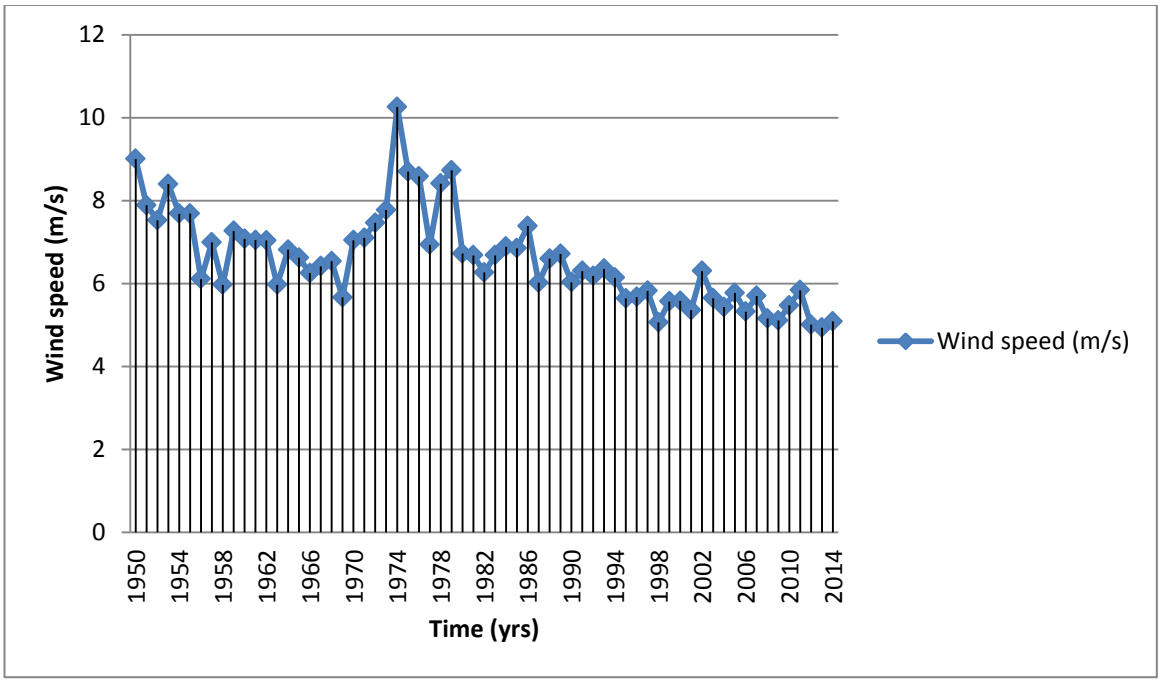

Figure B-7: Maximum measured wind speed over a period of 25 years - Kotlas, 1950 – 2014 (WeatherSpark, 2015)

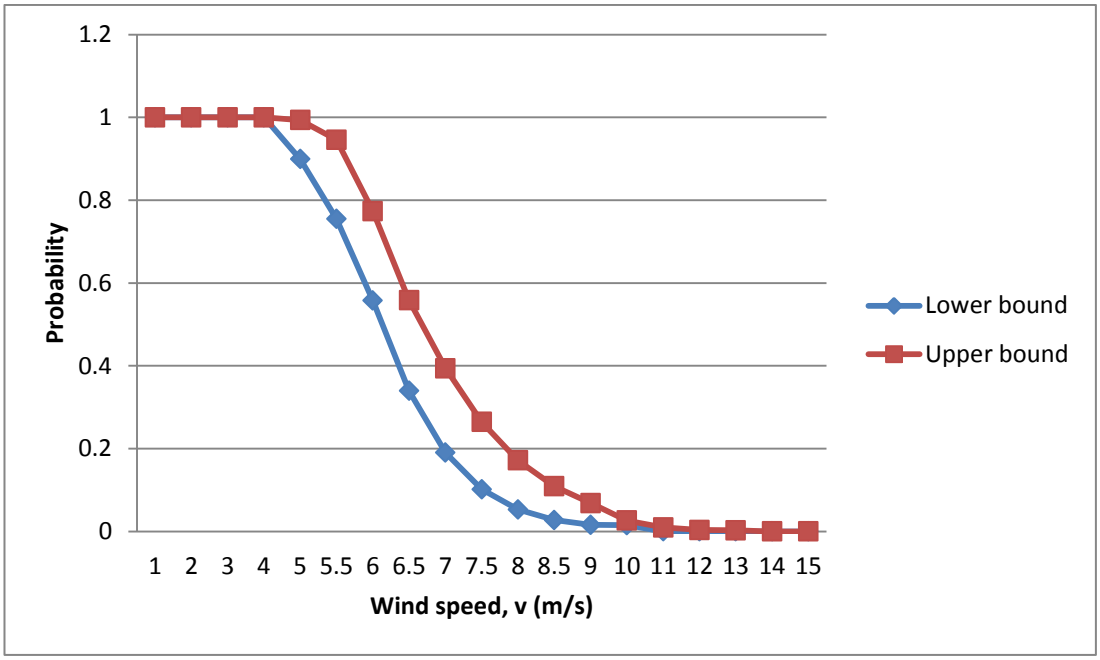

Figure B-8: Probability box for wind speed - Kotlas, 1950 – 2014 (WeatherSpark, 2015)

Table B-4: Wind speed data uncertainty characterization - Kotlas, 1950 –2014 (WeatherSpark, 2015)

Wind speed (m/s)	Probabilities		Percentile
	Lower bound	**Upper bound**	**Level**
1	1.0000	1.0000	100
2	1.0000	1.0000	100
3	1.0000	1.0000	100
4	1.0000	1.0000	100
5	0.8990	0.9933	90 - 100
5.5	0.7550	0.9460	76 – 95
6	0.5576	0.7736	56 - 77
6.5	0.3396	0.5581	34 – 56
7	0.1904	0.3941	19 – 39
7.5	0.1019	0.2646	10 – 27
8	0.0532	0.1718	5 – 17
8.5	0.0275	0.1092	3 – 11
9	0.0160	0.0685	2 - 9
10	0.0153	0.0264	2 - 3
11	0.0000	0.0100	0 - 1
12	0.0000	0.0038	0
13	0.0000	0.0029	0
14	0.0000	0.0000	0
15	0.0000	0.0000	0

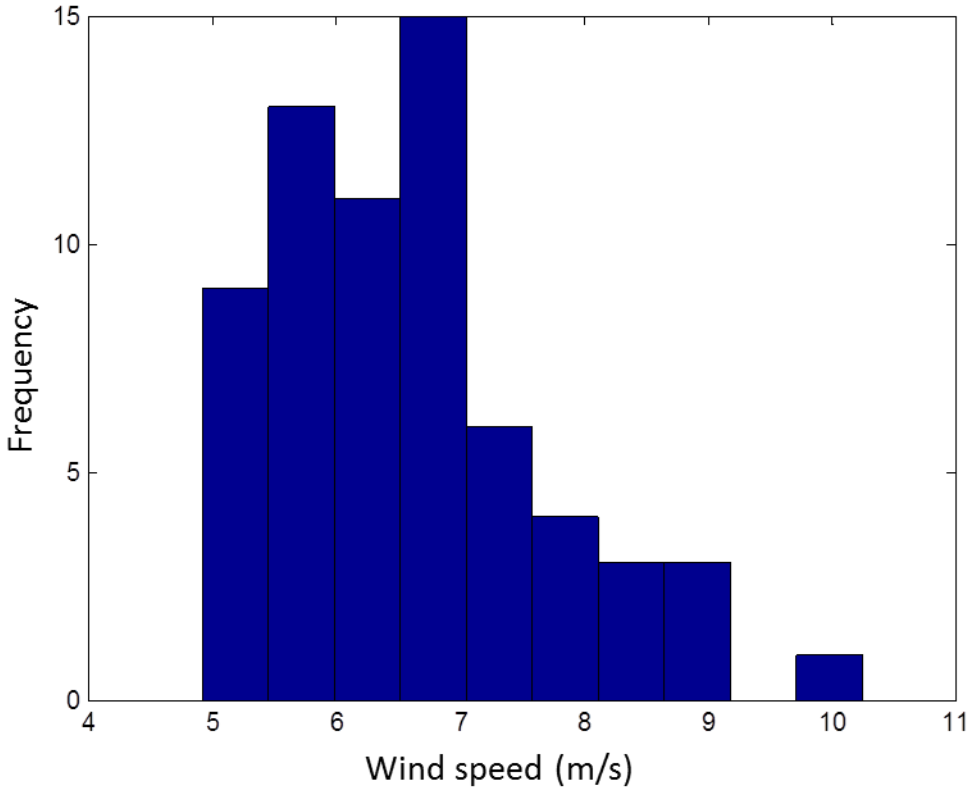

Figure B-9: Histogram – Kotlas, 1950 – 2014 (WeatherSpark, 2015)

Svalbard

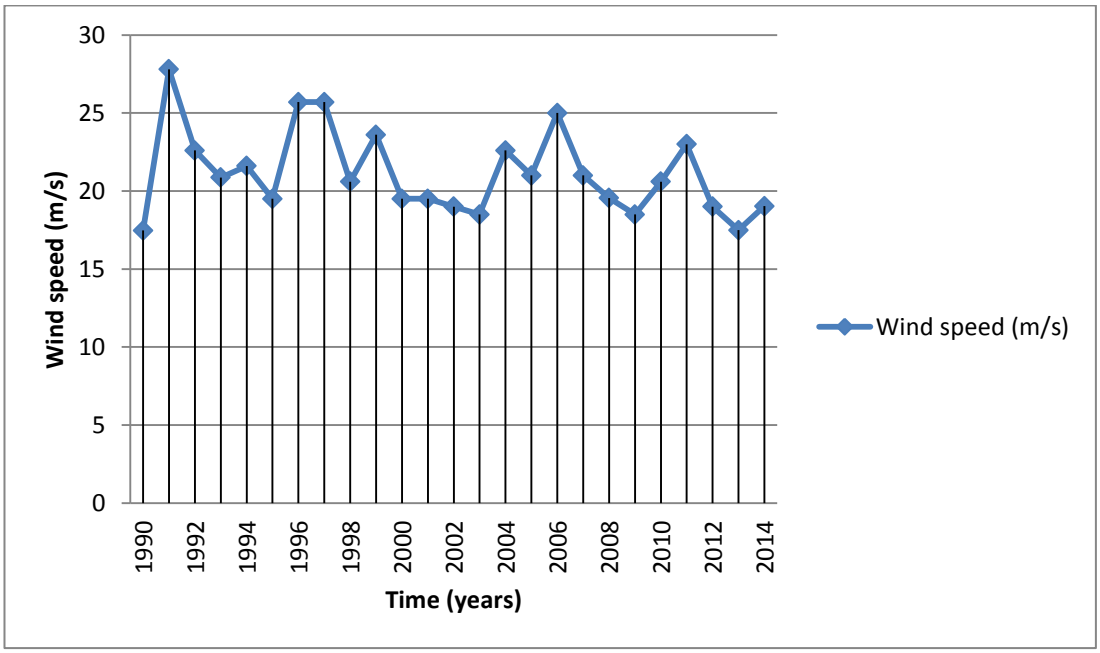

Figure B-10: Maximum measured wind speed over a period of 25 years - Svalbard, 1990 – 2014 (WeatherSpark, 2015)

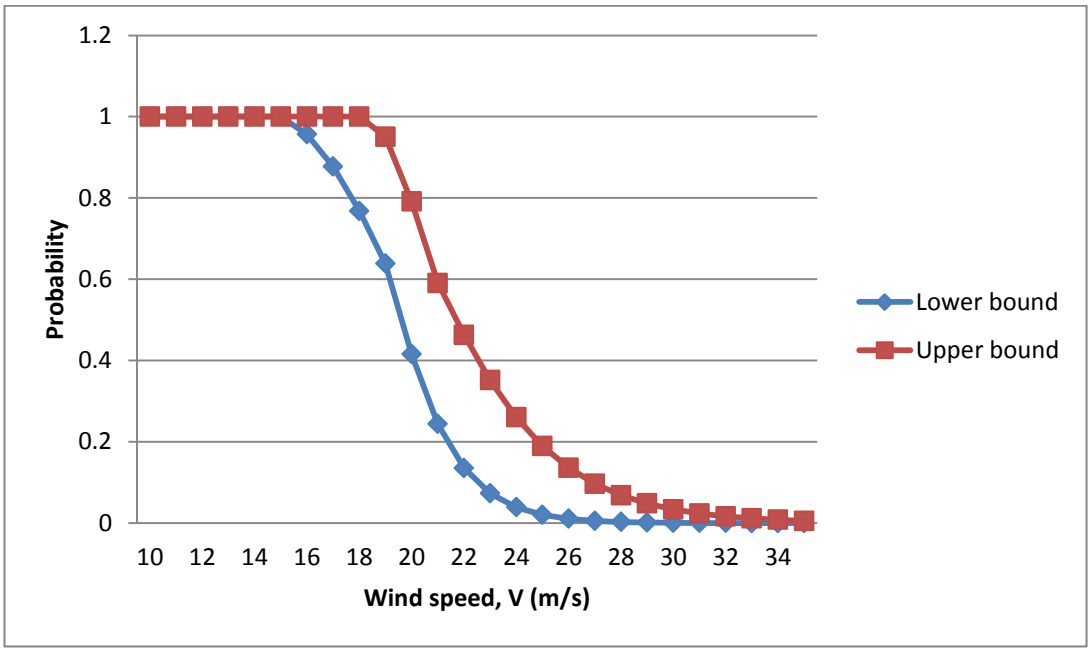

Figure B-11: Probability box for wind speed - Svalbard, 1990 – 2014 (WeatherSpark, 2015)

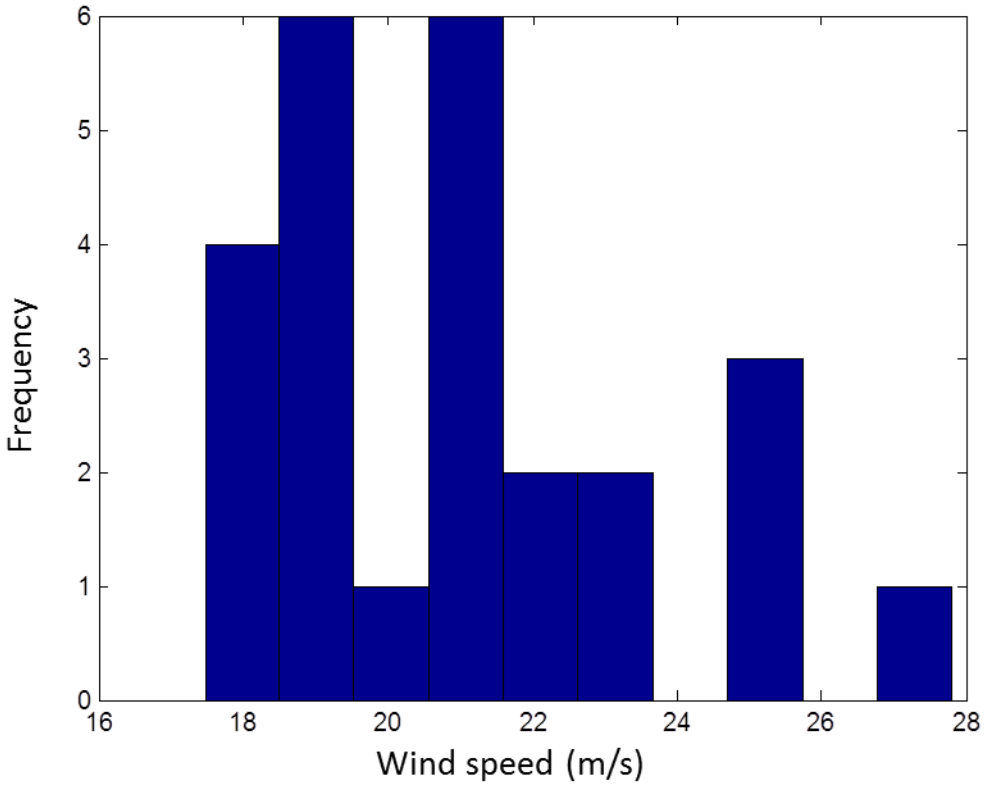

Figure B-12: Histogram – Svalbard, 1990 – 2014 (WeatherSpark, 2015)

Table B-5: Wind speed data uncertainty characterization - Svalbard, 1990 – 2014 (WeatherSpark, 2015)

Wind speed (m/s)	Probabilities		Percentile
	Lower bound	Upper bound	Level
10	1.0000	1.0000	100
11	1.0000	1.0000	100
12	1.0000	1.0000	100
13	1.0000	1.0000	100
14	1.0000	1.0000	100
15	1.0000	1.0000	100
16	0.9563	1.0000	96 - 100
17	0.8771	1.0000	88 - 100
18	0.7677	1.0000	77 - 100
19	0.6381	0.9505	64 - 95
20	0.4153	0.7911	42 - 79
21	0.2439	0.5906	24 -59
22	0.1355	0.4631	14 - 46
23	0.0731	0.3515	7 -35
24	0.0388	0.2604	4 - 26
25	0.0204	0.1894	2 - 19
26	0.0107	0.1361	1 - 14
27	0.0056	0.0968	0 - 10
28	0.0027	0.0685	0 - 7
29	0.0015	0.0482	0 - 5
30	0.0008	0.0338	0 - 4
31	0.0004	0.0237	0 - 2
32	0.0002	0.0165	0 - 2
33	0.0000	0.0116	0 - 1
34	0.0000	0.0081	0
35	0.0000	0.0056	0